

**THERMAL PERFORMANCE OF  
DIRECT-CONTACT WATER-AIR  
HEAT EXCHANGERS**

**Steven John Bluhm**

A thesis submitted to the Faculty of Engineering,  
University of the Witwatersrand, Johannesburg, in  
fulfilment of the requirements for the degree of  
Doctor of Philosophy.

**Johannesburg, 1990**



**ABSTRACT**

This work was carried out in response to the need for a simple engineering method for the thermal analysis of direct-contact air-water heat exchangers. A simple method of performance analysis is developed which is directly analogous and consistent with the fundamental approach used in conventional heat exchanger analysis and one in which the algebraic form of the overall equation and the grouping of each of the parameters are apparent.

The range of conditions considered are air and water temperatures of between 0 and 50 °C and barometric pressures ranging from 80 to 120 kPa. The air conditions considered range from completely dry to completely saturated with water vapour. Both air cooling and water cooling processes are considered.

Simple equations are developed to describe the change of energy state of the water and air stream as well as to describe the heat flow from an elemental wet area. The concept of sigma energy differences is used to describe the driving force for heat transfer from a wet surface (in place of enthalpy potential) as well as the change in energy state of the air stream. A specific heat term for air based on sigma energy is introduced making it possible to produce the overall performance equation from the algebraic manipulations. The performance equation does not require the identification of which fluid has the minimum thermal capacity and the NTU value is defined on a basis of the thermal capacity of the dry air stream.

In order to verify the performance equation a large experimental database was generated using a suite of direct-contact heat exchangers. Both air cooling and water cooling tests were carried out for otherwise identical situations. In addition the development and verification of the performance equation required the development of a comprehensive computer model for the simulation of counterflow direct-contact air-water heat exchangers. The program successfully models the real heat exchangers, and apart from the heat and mass transfer criteria, takes account of the fogging of the air stream. The performance equation is examined against 650 experimental and simulated sets of process conditions and appears to be satisfactorily accurate and versatile.

**ACKNOWLEDGEMENTS**

This thesis arises from work carried out as part of the research programme of the Environmental Engineering Division of COMRO (Chamber of Mines Research Organization)

The assistance of the following is acknowledged with sincere thanks.

- . Dr A W Whillier
- . Professor C J Rallis
- . Mr F H von Glehn
- . Mr T C W March
- . Mrs E J Stauch
- . Staff of COMRO

## CONTENTS

	Page
ABSTRACT	i
ACKNOWLEDGEMENTS	ii
LIST OF CONTENTS	iii
LIST OF APPENDICES	viii
LIST OF FIGURES	ix
LIST OF TABLES	xiii
NOMENCLATURE	xv
1 INTRODUCTION	1
1.1 Background	1
1.2 Objective and Scope	10
1.3 Layout of Thesis	11
2 FUNDAMENTAL MECHANISMS OF HEAT AND MASS TRANSFER BETWEEN WATER AND AIR AT AN ELEMENTAL SURFACE AREA	15
2.1 Introduction	15
2.2 Convective Heat Transfer at a Wet Surface	15
2.3 Radiant Heat Transfer	17
2.4 Convective Mass Transfer at a Wet Surface	18
2.4.1 Spalding's approach	19
2.4.2 Stagnant film approach	26
2.4.3 Comparison of the different approaches	30
2.4.4 Summary of the approach used in present study	31
2.5 Effect of Resistance to Heat Flow in the Bulk Water Phase	35
2.6 Total Heat Transfer	36
2.7 Supersaturation and Fogging of the Air Stream	37
2.8 Note on the Diffusion Coefficient of Water Vapour in Air	40
2.9 Note on the Prandtl, Schmidt and Lewis Numbers	46
3. A COMPREHENSIVE THEORETICAL MODEL FOR SIMULATING HEAT AND MASS TRANSFER IN A COUNTERFLOW DIRECT-CONTACT WATER-AIR HEAT EXCHANGER	49
3.1 Introduction	49
3.2 Basic Computer Model	50
3.3 Typical Examples of Simulated Data	57
3.4 Summary	59

	Page	
4	EXPERIMENTATION ON A COUNTERFLOW DIRECT-CONTACT WATER AIR HEAT EXCHANGER	62
4.1	Objectives of Tests	62
4.2	Description of Test Tower	63
4.3	Expected Uncertainty in Primary Measurements	69
4.4	Test Procedures	70
4.5	Measured Results	71
4.6	Energy Balance Criteria and Correction of Measured Data	72
4.6.1	General thermodynamic considerations and correction of inlet water tempera- ture for Joule Thompson effect	72
4.6.2	Energy balances for test data	75
4.6.3	Expected error in energy balance	76
4.6.4	Correction of data to create energy balance	78
4.7	Estimated Uncertainty in Final Results	80
4.7.1	Uncertainty in determination of heat transfer rate	80
4.7.2	Uncertainty in determination of mass transfer rate	80
5	VERIFICATION OF THE COMPREHENSIVE THEORETICAL MODEL AND EXAMINATION OF THE FUNDAMENTAL MECHANISMS OF HEAT AND MASS TRANSFER USING THE EXPERI- MENTAL DATA	93
5.1	Introduction	93
5.2	Selecting Best Value of $\alpha$ in the Heat and Mass Transfer Analogy for $(Pr/Sc)^2$	94
5.3	Validity of Correlation Equation for the Diffusion Coefficient	99
5.4	Simulation of Experimental Data and Determination of Overall Heat Transfer Coefficients	100
5.5	Validity of Supersaturation or Fogging Algorithm	101
5.6	Direct Comparison between the Overall Transfer Coefficient for the Evapora- tion Tests and that for the Conden- sation Tests	103
5.7	Summary	104

	Page	
6	A CRITICAL EXAMINATION OF THE ACCURACY AND LIMITATIONS OF THE MERKEL METHOD	112
6.1	Introduction	112
6.2	Merkel Method of Cooling Tower Analysis	113
6.3	Correlation of Experimental Data	120
6.3.1	Results in terms of $K_m A / m_w = a (m_w / m_a)^n$	120
6.3.2	Results in terms of $K_m A / m_w = a m_w^n m_a^m$	127
6.4	Assumptions and Limitations of the Merkel Equation	127
6.5	Summary	136
7	A SIMPLIFIED THEORETICAL MODEL (PERFORMANCE EQUATION) FOR SIMULATING HEAT AND MASS TRANSFER IN A COUNTERFLOW DIRECT-CONTACT WATER AIR HEAT EXCHANGER	144
7.1	Introduction	144
7.2	Development of an Improved Simplified Equation to Describe Total Heat Transfer from a Wet Surface	145
7.2.1	Effect of dry-bulb temperature changes on overall heat flow driving force	145
7.2.2	Sigma heat driving force	146
7.2.3	New improved total heat transfer approximation	152
7.2.4	Summary	157
7.3	Simplified Equations for the Change of Energy State of the Air and Water Streams	159
7.3.1	Energy balance equations across an element of direct-contact heat exchanger	159
7.3.2	Simplified energy balance equation	162
7.3.3	Simplified equation for the change of energy state of the air stream	163
7.3.4	Simplified equation for the change of energy state of the water stream	168
7.3.5	Summary	171
7.4	Development of Theoretical Performance Equation	172
7.4.1	Review of conventional (non direct-contact) heat exchanger practice	172
7.4.2	Development of a theoretical performance equation for the direct-contact case	179

	Page	
7.5	Refinement of Performance equation and Procedure for Selecting Parameter Values	187
7.5.1	Initial simplification of performance equation	188
7.5.2	Examination of parameters in performance equation for selected hypothetical conditions	191
7.5.3	Examination of parameters in performance equation v the experimental data	195
7.5.4.	Selection of appropriate sets of values of $(\alpha/\beta)_i$ , $[(\alpha/\beta)_{cavaf}^*]$ and $c_{aw}^*$	205
7.5.5.	Final specification of performance equation	209
8	VERIFICATION OF THE SIMPLIFIED THEORETICAL MODEL (PERFORMANCE EQUATION* BY COMPARISON WITH THE COMPREHENSIVE THEORETICAL MODEL AND EXPERIMENTAL DATA	233
8.1	Introduction	233
8.2	Overall Database	233
8.3	Comparison of Actual Performance Against that Predicted by Performance Equation	234
8.3.1	Quantification of accuracy	235
9	DISCUSSION AND CONCLUSIONS	238
9.1	Overall Performance Equation	238
9.1.1	General philosophy	238
9.1.2	Specification of performance equation	240
9.1.3	Issues related to unification of heat exchanger theory	243
9.1.4	Extrapolation beyond range of operating conditions	246
9.1.5	Equivalence with Merkel's method	247
9.1.6	Matching design characteristics of direct contact heat exchangers	249
9.1.7	Explanation of factor-of-merit method	258
9.1.8	Further research related to the overall performance equation	259
9.2	Additional Specific Conclusions	259
9.2.1	Heat transfer at a wet surface	260
9.2.2	Comparison of procedures for determining mass transfer	262
9.2.3	Effect of radiation in direct contact heat exchangers	262
9.2.4	Values of transport properties of water vapour-air mixtures	262

	<b>Page</b>
9.2.5 Heat and mass transfer analogy and value of the index, z	263
9.2.6 Supersaturation of the air stream	263
9.2.7 Comparison of transfer coefficients for evaporation and condensation tests	264
9.2.8 Comprehensive theoretical (computer) model	265
9.2.9 Unique experimental database	265
9.3 Concluding Statement	266
<b>APPENDICES</b>	<b>267</b>
<b>REFERENCES</b>	<b>377</b>

LIST OF APPENDICES	Page
APPENDIX A Equations used to evaluate the thermodynamic properties of moist air	267
APPENDIX B Estimation of the magnitude of radiant heat exchange	281
APPENDIX C Listing of computer program used to simulate the performance of counterflow direct-contact water-air heat exchanger	285
APPENDIX D Heat exchanger test facility	290
APPENDIX E Specification of spray nozzles used in test tower	302
APPENDIX F Specification of mist eliminator mesh used in test tower	306
APPENDIX G Specification of packing or fill used in test tower	310
APPENDIX H Expected uncertainty in the measurement of the energy balance	314
APPENDIX I Procedure for calculating heat balance and correcting data	317
APPENDIX J Direct comparison between the overall transfer coefficient for the evaporation tests and that for the condensation tests	319
APPENDIX K Accuracy of Merkel's equation when using sigma heat in place of enthalpy	343
APPENDIX L Procedure for calculating $\beta$ and its value for non-saturated air conditions	345
APPENDIX M Procedure for calculating $\alpha$ and its value for non-saturated conditions	349
APPENDIX N Procedure for calculating $\gamma$ and its value for non-saturated conditions	354
APPENDIX O Mathematical manipulation to produce performance equation for direct-contact case	359
APPENDIX P Generation of simulated database	363
APPENDIX Q Determination of the relationship $L = f(Z, N^*)$	375

## LIST OF FIGURES

Figure		Page
1.1	Growth in installed refrigeration capacity in South African gold mines	2
1.2	Range of moist air conditions being considered	13
1.3	Flow chart of logic	14
2.1	Simplified model showing a control volume at the water-air interface	22
2.2	Differences in the mass transfer rate as calculated by three different equations, the information is plotted as ratios using Method I as a base. The solid lines relate to Method II and the dashed lines relate to Method III	32
2.3	Differences in total heat transfer rate as calculated by three different equations, the information is plotted as ratios using Method I as a base. The solid lines relate to Method II and the dashed lines to Method III	33
2.4	Values of overall heat flow driving force for 25 °C water temperature and 100 kPa barometric pressure	38
2.5	Typical psychrometric chart	41
2.6	Diffusion coefficient for water vapour in air at 101,3 kPa	45
3.1	Model of counterflow tower for computer simulation	52
3.2	Control volume depicting the heat and mass transfer with and without fog formation	53
3.3	Flow diagram for computer model	56
3.4	Typical results from tower simulator (no fog)	58
3.5	Typical results from tower simulator (for fogging conditions)	60
4.1	Schematic of test cooling tower	64
4.2	Photographs of test cooling tower	65
4.3	Photographs of packing medium	67
4.4	Frequency distribution of measured error in heat balance	77
6.1	Typical process demand curves	116
6.2	Process demand curves for water cooling and air cooling for different pressures	117
6.3	Typical cooling tower packing characteristic curves	119
6.4	Correlation of test data with standard methods of characterization (Tests 1-32, spray only)	122

Figure		Page
6.5	Correlation of test data with standard methods of characterization (Tests 33-64, 12mm flute, 600mm ht)	123
6.6	Correlation of test data with standard methods of characterization (Tests 65-96, 12mm flute, 1200mm ht)	124
6.7	Correlation of test data with standard methods of characterization (Tests 97-120, 19mm flute, 600mm ht)	125
6.8	Correlation of test data with standard methods of characterization (Tests 121-160, 19mm flute, 1200mm ht)	126
6.9	Correlation between the Merkel enthalpy driving force and the true value	134
7.1	Distribution of errors involved in calculating the driving force for total heat flow while assuming saturated conditions	147
7.2	Schematic of adiabatic saturation process	150
7.3	Sigma energy of air for the range of conditions under consideration	151
7.4	Correlation of the new improved approximate equation against the exact formulation and distribution of error when $\beta = 1,096$	154
7.5	Values of $\beta$ for saturated air	158
7.6	Control volume of direct-contact heat exchanger with incremental heat and mass transfer	161
7.7	Value of $\alpha$ for saturated air	167
7.8	Value of $\gamma$ for water in contact with saturated air (note that these values are practically independant of changes in barometric pressure and water-air flow ratio)	170
7.9	Elemental section of a non direct-contact counterflow heat exchanger	173
7.10	Performance of non direct-contact counterflow heat exchangers ( $\Sigma$ vs NTU)	176
7.11	Performance of non direct-contact counterflow heat exchangers ( $\Sigma_w$ vs R)	178
7.12	Elemental section of a direct-contact counterflow heat exchanger	180
7.13	Values of the pseudo-specific heat term for different temperatures/pressures	184
7.14	a Hypothetical calculation A	192
	b Hypothetical calculation B	192
	c Hypothetical calculation C	193
	d Hypothetical calculation D	193
	e Hypothetical calculation E	194
	f Hypothetical calculation F	194

Figure		Page
7.15	a Experimental data Test No. 42	196
	b Experimental data Test No. 58	196
7.16	Values of $\alpha/\gamma$ for water in contact with saturated air, note that for all practical purposes these values are independent of barometric pressure	198
7.17	Values of the ratio ( $\alpha/\gamma$ ) for saturated air at 100 kPa	200
7.18	Values of $[(\alpha/\beta) C_{\text{avaf}}^*]$ for saturated air at 100 kPa	202
7.19	Plot of sigma energy content of air, depicting key values of the pseudo-specific heat term (100 kPa)	204
7.20	Values of L for varying water-air flow ratios and different values of the design characteristic $N^*$	208
8.1	Comparison of actual performance against predicted performance for full database (650 points)	237
9.1	Graphical representation of overall performance equation	241
9.2	Determination of pseudo-specific heat term	242
9.3	Graphical aid to determine value of ( $\alpha/\gamma$ )	248
9.4	Representation of overall performance equation with axes transposed to show equivalence with CTI curves	250
9.5	Representation of CTI curves with axes transposed to show equivalence with new performance equations	251
9.6	Experimental thermal characteristic of each packing geometry	256
9.7	Errors in approximate equations for heat transfer at a wet surface	261
A.1	Enthalpy of water vapour as a function of temperature	271
A.2	Thermal conductivity of air-water vapour mixtures	276
A.3	Viscosity of air-water vapour mixtures	279
B.1	Emissivity of air due to water vapour, valid for temperatures from 0 to 50 °C	282
J.1	Relationship between $Nu_A$ and the ratio of the film to bulk stream air density	331
J.2	Effect of the mass transfer driving force, $B$ , on the mass transfer coefficient (multiplying factor)	332
K.1	Accuracy of Merkel's equation when using sigma energy in place of enthalpy (correlation and distribution of error)	344

Figure		Page
L.1	Value of $\beta$ for 50 per cent relative humidity air at 100 kPa	346
L.2	Value of $\beta$ for dry air at 100 kPa	347
M.1	Value of $\alpha$ for 50 per cent relative humidity air at 100 kPa	350
M.2	Value of $\alpha$ for dry air at 100 kPa	351
N.1	Value of $\gamma$ for 50 per cent relative humidity air at 100 kPa	356
N.2	Value of $\gamma$ for dry air at 100 kPa	357

## LIST OF TABLES

Table		Page
2.1	Values of Prandtl (Pr) and Schmidt (Sc) numbers and the ratio $(Pr/Sc)^{2/3}$ for saturated air at varying temperatures and pressures	48
4.1	Grouping of test data	82
4.2	Measured results from full series of tests on experimental tower	83
4.3	Corrected results from full series of tests on experimental tower	88
5.1	Measured and simulated results for test Nos. 42 and 58	106
5.2	Balanced experimental data and the modelled information	107
6.1	Experimental data (including values of $K_{m,A}/m_w^*$ )	138
6.2	Statistics of correlations of test data with standard method of characterization	143
7.1	Comparison of simplified energy balance using enthalpies and that using sigma energy	211
7.2	Variation of the term J across and within the heat exchangers for each test	212
7.3	Performance of hypothetical heat exchanger under selected temperature conditions (barometric pressure 100 kPa)	217
7.4	Variations of the term $(a/\gamma)_i$ across and within the heat exchangers for each test	218
7.5	Variations of the term $[(a/\beta) \sigma_{avaf}^*]$ across and within the heat exchangers for each test	223
7.6	Representative values of the terms in the overall performance equation for each test	228
8.1	Statistics related to the difference between actual and predicted water efficiency	236

## LIST OF TABLES

Table		Page
9.1	Values of coefficients in Equation 9.9 for packing configurations	254
B.1	Comparison of the convective and radiative heat transfer coefficients	284
B.1	Expected uncertainty in the measurement of the energy balance	315
J.1	Representative values of the thermodynamic transport properties (mean values weighted by heat transfer for each of 100 segments of heat exchanger)	333
J.2	Coefficients of curve fitting for $Nu.A = f(Re, \dot{m}_w)$	338
J.3	Ratio of $Nu.A$ cold/hot for corresponding flow situations	339
J.4	Physical properties of water related to the formation of wet surfaces	342
P.1	Inlet temperature conditions used in generating simulated database	364
P.2	Simulated database	365

NOMENCLATURE

A*	cross-sectional area (m <sup>2</sup> )
A	area (m <sup>2</sup> )
a	constant or sigma energy content at 0°C (J/kg)
B	driving force for mass transfer (dimensionless)
B'	modified driving force for mass transfer (J/kg K)
b	constant
C <sub>min</sub>	thermal capacity of the fluid with the lower thermal capacity (W/K)
C <sub>max</sub>	thermal capacity of the fluid with the higher thermal capacity (W/K)
c	constant or thermal capacity (J/kg K)
c <sub>a</sub>	thermal capacity of pure air (1005 J/kg K)
c <sub>v</sub>	thermal capacity of water vapour (1840 J/kg K)
c <sub>w</sub>	thermal capacity of water liquid (4187 J/kg K)
c <sub>av</sub>	thermal capacity of air-water vapour mixtures (the <u>true</u> value of thermal capacity of moist air per mass of moist air) (J/kg K)
c <sub>ava</sub>	thermal capacity of air-water vapour mixture per mass of <u>dry</u> air (J/kg K)
c <sub>a</sub> *	pseudo-thermal capacity of saturated air defined through sigma energy (( $\Sigma - a$ )/t) (J/kg K)
c <sub>al</sub> *	pseudo-thermal capacity of saturated air at inlet wet-bulb temperature (J/kg K)
c <sub>aw</sub> *	pseudo-thermal capacity of saturated air at the water surface temperature (J/kg K)
D	diffusion coefficient (m <sup>2</sup> /s)
d	differential operator or characteristic dimension (m)
E	effectiveness of heat exchanger (dimensionless)
E <sub>w</sub>	water efficiency or water effectiveness (dimensionless)
E <sub>w</sub> *	water effectiveness for direct contact, based on wet-bulb temperature and pseudo-specific heat concept (dimensionless)
e	expected uncertainty in measurement
F	factor of merit (dimensionless)
G	multiplying factor in correcting experimental heat balances
g	gravitational acceleration (m/s <sup>2</sup> )

hb	heat balance
$h_c$	convective heat transfer coefficient ( $W/m^2 K$ )
$h_r$	radiative heat transfer coefficient ( $W/m^2 K$ )
$h_d$	convective mass transfer coefficient ( $m/s$ )
$i$	specific enthalpy ( $J/kg$ )
$i_a$	specific enthalpy of moist air ( $J/kg$ )
$i_{aw}$	specific enthalpy of saturated air at the water surface temperature ( $J/kg$ )
$i_{a\infty}$	specific enthalpy of moist air in the bulk air stream ( $J/kg$ )
$i_g$	specific enthalpy of water vapour ( $J/kg$ )
$i_l$	specific enthalpy of water liquid ( $J/kg$ )
$i_{fg}$	specific enthalpy of vaporization ( $J/kg$ )
J	grouping of terms in Equation 9.23
$J_1$	grouping of terms in Equation 9.5
$J_2$	grouping of terms in Equation 9.5
$J_3$	grouping of terms in Equation 9.21
$J_4$	grouping of terms in Equation 9.21
L	coefficient in Equation 7.74.
$K_m$	overall transfer coefficient ( $kg/s m^2$ )
$K_{1-13}$	constants or grouping of terms
k	thermal conductivity ( $W/m K$ )
$k_w$	thermal conductivity of water ( $W/m K$ )
$k_{av}$	thermal conductivity of moist air ( $W/m K$ )
$M_a$	mass of dry air in moist air sample ( $kg$ )
$M_v$	mass of water vapour in moist air sample ( $kg$ )
$\dot{m}'_a$	mass flow rate of air ( $kg/s$ )
$\dot{m}'_w$	mass flow rate of water ( $kg/s$ )
$\dot{m}_v$	mass transfer rate of water vapour ( $kg/s$ )
$\dot{m}_v'$	mass transfer rate of water vapour per unit surface area ( $kg/s m^2$ )
$\frac{\dot{m}_v}{\dot{m}_a}$	Reynolds flow or 'scrubbing action' flow which may also be considered as the mass transfer conductance ( $kg/s m^2$ )
$\dot{m}_f$	mass flow of water in the form of fog ( $kg/s$ )
m	constant, exponent in Equation 6.8
N	design characteristic or thermal size of non-direct contact heat exchanger based on air stream thermal capacity (dimensionless)
$N^*$	design characteristic or thermal size of direct contact heat exchanger based on air stream thermal capacity (dimensionless)
NTU	number of transfer units (dimensionless)
n	constant, exponent in Equations 6.7 and 6.8
p	barometric pressure (kPa)
$P_v$	water vapour pressure (kPa)
$P_{vs}$	saturated vapour pressure (kPa)
q	heat flow (W)
$\frac{q}{A}$	heat flow per unit area ( $W/m^2$ )
$q_c$	convective heat transfer (W)
$q_l$	latent heat transfer (W)

$q_t$	total heat transfer (W)
$q_r$	radiative heat transfer (W)
$R_a$	gas constant for air (287 J/kg K)
R	thermal capacity ratio (dimensionless)
$R^*$	thermal capacity ratio for direct contact heat exchanger (dimensionless)
T	absolute temperature (K)
$T_{ave}$	average temperature (K)
t	temperature ( $^{\circ}$ C)
$t'$	thermodynamic wet-bulb temperature ( $^{\circ}$ C)
$t_w$	water temperature ( $^{\circ}$ C)
$t_{ws}$	water surface temperature ( $^{\circ}$ C)
$t_{db}$	dry-bulb temperature ( $^{\circ}$ C)
$t_{wb}$	wet-bulb temperature ( $^{\circ}$ C)
U	overall heat transfer coefficient (W/m <sup>2</sup> K)
V	velocity of air stream (m/s)
W	mass of water vapour per unit mass of dry air, also known as humidity ratio or apparent specific humidity (kg/kg)
$W_v$	mass of water vapour per unit mass of moist air, also known as true specific humidity (kg/kg)
w	work rate (W)
X	error in simplified energy balance using enthalpy (J/kg)
Y	error in simplified energy balance using sigma energy (J/kg)
y	linear dimension (m)
Z	dimensionless logarithmic mean density factor or elevation (m)
z	constant, exponent in (Pr/sc) <sup>2</sup>

GREEK

$\alpha$	factor in determining change in energy of air stream based on sigma energy difference (dimensionless)
$\beta$	factor in determining total heat transfer from wet surface based on sigma energy difference (dimensionless)
$\gamma$	factor in determining change in energy of water stream (dimensionless)
$\epsilon_a$	air emissivity
$\lambda$	latent heat of vaporization (J/kg)
$\Sigma$	sigma energy content of air (J/kg)
$\Sigma_w$	sigma energy content of saturated air at water surface temperature (J/kg)
$\sigma$	Stefan Boltzman constant (W/m <sup>2</sup> K <sup>4</sup> )

$\rho$	density ( $\text{kg/m}^3$ )
$\rho_v$	density of water vapour ( $\text{kg/m}^3$ )
$\rho_a$	density of pure air ( $\text{kg/m}^3$ )
$\rho_{av}$	density of air-water vapour mixture ( $\text{kg/m}^3$ )
$\mu$	dynamic viscosity ( $\text{Ns/m}^2$ ) or Joule-Thompson coefficient ( $\text{K/Pa}$ )
$\mu_{av}$	dynamic viscosity of air water vapour mixture ( $\text{Ns/m}^2$ )
$\phi$	design factor (dimensionless)

SUBSCRIPTS

a	air
c	convective heat transfer
db	dry-bulb
f	film condition at average of water and air dry-bulb temperature
f*	film condition at average of water and air wet-bulb temperature
l	inlet or intermediate
l	latent heat transfer
o	outlet or overall
r	radiative heat transfer
rf	Reynolds flow
s	saturated conditions
t	mass transfer or total
v	water vapour
w	water
wb	wet-bulb
ws	water surface
$\infty$	bulk air stream condition

DIMENSIONLESS PARAMETER GROUPS

Le	Lewis number ( $\rho c D / k$ ) = $(Pr / Sc)$
Nu	Nusselt number ( $h_c d / k$ ) = $St / (Re \cdot Pr)$
Pr	Prandtl number ( $\mu c / k$ )
Re	Reynolds number ( $\rho V d / \mu$ )
Sc	Schmidt number ( $\mu / \rho D$ )
$St_h$	Stanton number for heat transfer data ( $h_c / \rho V c$ )
$St_m$	Stanton number for mass transfer data ( $k_f / \rho V$ )

## 1 INTRODUCTION

### 1.1 Background

The gold mines in South Africa use a considerable amount of refrigeration and air-conditioning equipment to provide acceptable environmental conditions in working places. On some 30 mines, the total installed refrigeration capacity exceeds 1 200 MW, with equipment installed both on surface and underground. This equipment is used to chill water, which is in turn used as coolant for ventilation air, and as service water in the mining operation to distribute cooling directly to the working areas(1,2,3).

Figure 1.1 shows the growth in the installed refrigeration capacity on South African mines in recent years, together with the manner in which this cooling is distributed. Of particular significance in this graph is the recent use of direct-contact air coolers which presently transfer some 450 MW of cooling to the ventilation air. A variety of designs are currently in use, ranging from conventional cooling-tower type packings to the more common spray chamber design in which the chilled water is sprayed vertically upwards in horizontal excavations through which the ventilation air flows(4,5). The cooling capacity of the individual units varies from 100 kW to in excess of 10 000 kW in some instances.

Rejection of the heat of condensation from the refrigeration machines is achieved with air-water heat exchangers. These exchangers are in the form either of evaporative condensers or, more commonly, shell and

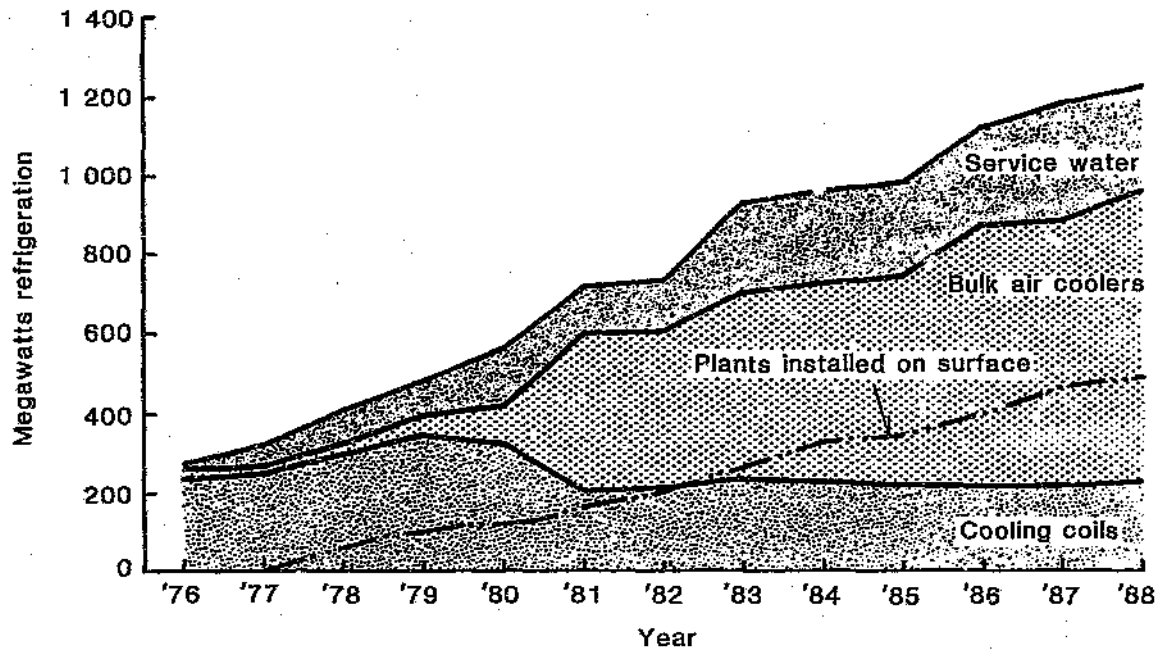


Figure 1.1 Growth in installed refrigeration capacity in South African gold mines

tube type condensers which are employed in conjunction with direct contact water-air cooling towers or spray chambers. With regard to the latter, surface installations use various designs of conventional packed cooling towers, while underground facilities use open vertical counter-flow spray towers or horizontal spray chambers.

Packed towers are also used in mine cooling systems as pre-cooling towers. When the cooling water is returned to surface from underground for re-cooling it is warmer than the ambient wet-bulb temperature and is pre-cooled in these towers before being refrigerated(6). Because of the high cost involved in refrigerating the water it is expedient to design and operate these pre-cooling towers at extremely close approach temperatures.

Thus, direct contact water-air heat exchangers are used extensively in the South African gold mining industry for many different applications, and therefore the process requirements vary widely. For example, a condenser heat rejection application may require the temperature of the inlet water underground to be as high as 50 °C with inlet air temperatures in excess of 30 °C and saturated, while on surface normal cooling tower operating conditions prevail. For air cooling applications, on the other hand, inlet water temperature is typically 10 °C but can be as low as 0 °C. Furthermore, detailed consideration is being given to the use of ice slurries in spray chambers(7). The temperature of the air to be cooled also varies widely from typically 30 °C saturated temperatures underground to dry winter conditions on surface. Another factor to consider in the underground operation of this equipment is the effect of fogging or supersaturation within the heat exchanger occurring because the inlet air is

close to saturation.

An important aspect which can affect the operation of direct-contact heat exchangers is barometric pressure. South African gold mines are situated at a relatively high altitude but are the deepest in the world, and this means that, depending on where the heat exchanger is situated, the barometric pressure may be as low as 80 kPa or as high as 120 kPa.

This wide range of thermodynamic conditions is important since most research and development work has been limited to warm water cooling towers at sea-level barometric pressure. Hence the empirical database for direct-contact water-air heat exchangers is strongly biased toward these conditions. Crude correction methods<sup>(8)</sup> are used to account for aspects such as changing barometric pressure and high supply water temperatures, and most of the empirical information which does exist is proprietary and of little assistance in the field to the practicing engineer. Furthermore, little work has been published on the performance of these heat exchangers when used to cool air rather than water.

Therefore, the basic approach to analysing the thermal performance of direct-contact air-water heat exchangers is that developed for cooling towers. This basic method is described in a number of standard texts<sup>(9,10,11)</sup>. In this approach, the total heat transfer from a wet surface, both sensible and latent, is considered to be proportional to a single driving force, namely, the difference between the enthalpy of the air and the enthalpy of saturated air at the water surface temperature; this relationship is known as the Merkel equation<sup>(12)</sup>. Equating the total heat flow described in this manner to the change of enthalpy

of the water stream and integrating between inlet and outlet states gives the standard cooling tower formulation:

$$\frac{K_m A}{\dot{m}_w} = \int \frac{c_w dt_w}{(i_{aw} - i_{as})} \quad (1.1)$$

The right-hand side of this equation is dependent on the process conditions imposed on the heat exchanger and therefore can be calculated when the inlet and outlet temperatures, the flowrates and the flow configuration are known. The left-hand side of the equation is determined by the design characteristics of the equipment and gives a measure of the capability of the heat exchanger.

The format of Equation 1.1 results from parallels being drawn to the relatively complicated mass transfer processes encountered in general chemical engineering. Historically, this approach has been used in preference to developing a method specifically for water-air heat exchangers. A good example of this point is reflected in the widespread use of symbols L and G for liquid and gas rather than symbols related to water and air. Direct contact water-air heat exchangers are so widely used in all industries that they warrant individual consideration rather than being dealt with simply as a subset of generalized chemical formulations.

The approach summarized by Equation 1.1 has a number of shortcomings. First, there is no fundamentally sound method for relating the left-hand side of the equation to the geometry of the heat exchanger and the flow, temperature and barometric pressure conditions imposed upon the unit. Second, the Merkel equation, while possibly acceptable for normal water cooling tower

conditions, is not accurate over a wide range of psychrometric conditions. Third, the mathematical relationship for calculating enthalpy from temperature measurements is not simple, and exact analytical solutions to the right-hand side of the equation have not been possible (numerical and graphical techniques are used). Fourth, whereas with water cooling towers the outlet air condition is of little concern, with air cooling applications (air conditioning as opposed to water cooling) it is important to determine both heat and mass transfer independently so that the air condition in terms of temperature and humidity can be determined. As a result of this and other complicating issues, most engineering methods of analysis are semi-empirical. With the widespread use of micro-computers, it is possible to build fairly rigorous models<sup>(13,14,15)</sup> which may be used to accurately predict performance. However, as Webb<sup>(16)</sup> notes, the cooling tower industry presently favours the approximate theory over the rigorous theory. This is the case in spite of the limitations mentioned above and is a fact which indicates the inherent need for a simple but accurate analysis tool.

The work described in this thesis was therefore carried out in response to the need for a simple engineering method of thermodynamic analysis for direct contact air-water heat exchangers. It is the contention of this work that a simple method of performance analysis can be developed for direct-contact heat exchangers, similar to that employed in conventional heat exchanger theory, which is a well-defined, easily learnt and widely used tool.

A number of other researchers have tackled the problem of unifying heat exchanger theory<sup>(23,24,25)</sup>. All methods are subject to the approximation of linearizing

the energy content of air as a function of temperature and all methods have difficulties in predicting thermal performance in a non-iterative manner from a knowledge of the inlet process conditions. The work of Webb(15,16,23) and co-workers has been of particular significance. Jaber and Webb(23) review past attempts to unify the heat exchanger theory and conclude that, notwithstanding the number of attempts that have been made, virtually all methods contain definitions that are flawed in the sense that they are inconsistent with the corresponding basic definitions used in conventional heat exchanger theory. They state '... the rash of NTU definitions reported in the literature have contributed little but a myriad of conflicting definitions'. The uniqueness of the solution described in the present work is the algebraic development of a performance equation in which it is not necessary to identify which fluid has the minimum thermal capacity ( $C_{min}$ ), the use of the concept of sigma energy and an NTU value which is based on the specific thermal capacity of dry air.

Historically, the first step in the present sequence of logic was the original development of the so-called factor-of-merit method by Whillier(17,18,19). This approach, although entirely empirical, drew on a number of the fundamental definitions of conventional heat exchanger theory. The method in its original form was used widely in the mining industry and showed a remarkable versatility. However, a number of shortcomings have been revealed in its application. The most important of these is that the form of the performance equation was empirical. There was no algebraic development from heat transfer basics which could lead to a fundamental understanding of the form of the equation and the trends that it described. This led to the fact

that performance trends cannot be understood and predicted from geometrical information from first principles and without a prior knowledge of the performance of a similar unit. Furthermore, the accuracy was often questioned, particularly when the performance of water cooling and air cooling installations were being compared. These limitations are equally applicable to the more standard (Merkel's approach) procedures described above.

Subsequent to Whillier's original work, this current research carried out by the author (5,20,22) led to a number of modifications and to the establishment of an initial relationship in which the empirical parameters could be more clearly understood and in which direct analogies could be drawn to conventional heat exchanger theory. The work described in this thesis presents the complete development of a method which is directly analogous and consistent with the fundamental approach used in conventional heat exchanger analysis and one in which the algebraic form of the overall equation and meaning of each of the parameters can be understood.

As mentioned earlier, the concept of sigma heat content is of importance to the hypothesis presented in this thesis and thus is worth introducing at this stage. A consideration of the adiabatic saturation process leads to the following energy balance equation for that process:

$$\Sigma = (i_a - W c_w t_{wb})_{in} = (i_a - W c_w t_{wb})_{out} \quad (1.2)$$

Since the adiabatic saturation process involves no overall net exchange of energy, it follows that the energy content of an air stream in such a process must

remain constant. The energy term which remains constant in the adiabatic saturation process is given by Equation 1.2. This term was given the name sigma heat by Carrier<sup>(31)</sup> in 1911, in order not to get it confused with total heat. (It was only after about 1940 that the term enthalpy was introduced in place of total heat<sup>(19)</sup>). Note that in this basic reference process the enthalpy of the air changes whereas the sigma energy remains exactly constant. Thus, if the sigma heat remains constant in any process involving changes in moisture content then it is certain that there has been no net heat transfer. It stands to reason that sigma energy should then be an important reference parameter. Furthermore, it has the added advantage that it is a unique function of wet-bulb temperature, at a given barometric pressure. (In fact it is the adiabatic saturation process that defines the thermodynamic wet-bulb temperature.)

In the 80 years since the concept of sigma energy was originally discussed by Carrier, it has not found wide use by air conditioning engineers and its development has not really progressed very far. This is surprising because it is a powerful concept. The usefulness of the sigma energy parameter was recognized by Whillier<sup>(17)</sup> and Bluhm<sup>(20)</sup> and has been fully exploited in this present work. It is shown later that, firstly, sigma energy differences are more accurate than the traditional enthalpy differences in approximating total heat transfer from a wet surface and, secondly, the use of sigma energy is more accurate than enthalpy in the typical approximate energy balance relationships between water and air streams.

## 1.2 Statement of objective and scope

Recognizing the limitations of the Merkel method, the primary objective of this work is to develop an improved and simple method for the thermal performance analysis of direct-contact water-air heat exchangers which may be used by the practicing field engineer in respect of design codes and procedures for thermal performance assessment.

Secondary objectives which are embodied in establishing the main goal are:

- . to develop a unified heat exchanger theory so that the general approach used for direct-contact heat exchangers will be similar to that employed in conventional heat exchanger theory;
- . to develop a comprehensive computer model for simulating heat and mass transfer in counterflow water-air heat exchangers;
- . to examine the supersaturation or fogging phenomena and develop a verified algorithm to describe its effects;
- . to establish the specific value of the index  $z$  in  $(Pr/Sc)^z$  in the Chilton-Colburn analogy between heat and mass transfer and determine the appropriate set of values for the diffusion coefficient of water vapour in air;
- . to establish the difference in the value of the overall heat transfer coefficient for water cooling (evaporation) and air cooling (condensation) in otherwise identical situations.

The scope of the work is such that the range of conditions considered are air and water temperatures of between 0 and 50 °C and barometric pressures ranging from 80 to 120 kPa. The air conditions considered range from completely dry to completely saturated with water vapour. Both air cooling and water cooling processes are considered. In the following chapters the moist air condition is defined by the combination of dry-bulb temperature, barometric pressure and wet-bulb temperature or true specific humidity. The overall range of moist air conditions under consideration are shown in Figure 1.2.

### 1.3 Layout of Thesis

The sequence of logic adopted in tackling this problem, as well as the layout of the thesis, is best described diagrammatically. Accordingly, a flow chart has been presented in Figure 1.3. Although the diagram is self explanatory it should be noted that:

- (i) there is no independent section related to a literature review. This is because the work has covered a wide range of topics, from fundamental issues to overall heat exchanger equations and it has been found appropriate to discuss the literature separately within the presentation of each topic.
- (ii) the direct comparison between the overall transfer coefficients for evaporation conditions and those for condensation conditions is regarded as a side issue to the main thrust of the work, namely the development of a new improved method of analysis of overall heat exchanger performance. However,

this aspect is considered to be an important issue and is discussed in detail in Appendix J.

It should also be noted that the Tables pertaining to a Chapter are generally to be found at the end of the Chapter.

It should be noted that the literature based on this general subject is extremely large, and it is not appropriate or pertinent to discuss each published item. However, some reading material, beyond the References discussed are listed in the Bibliography.

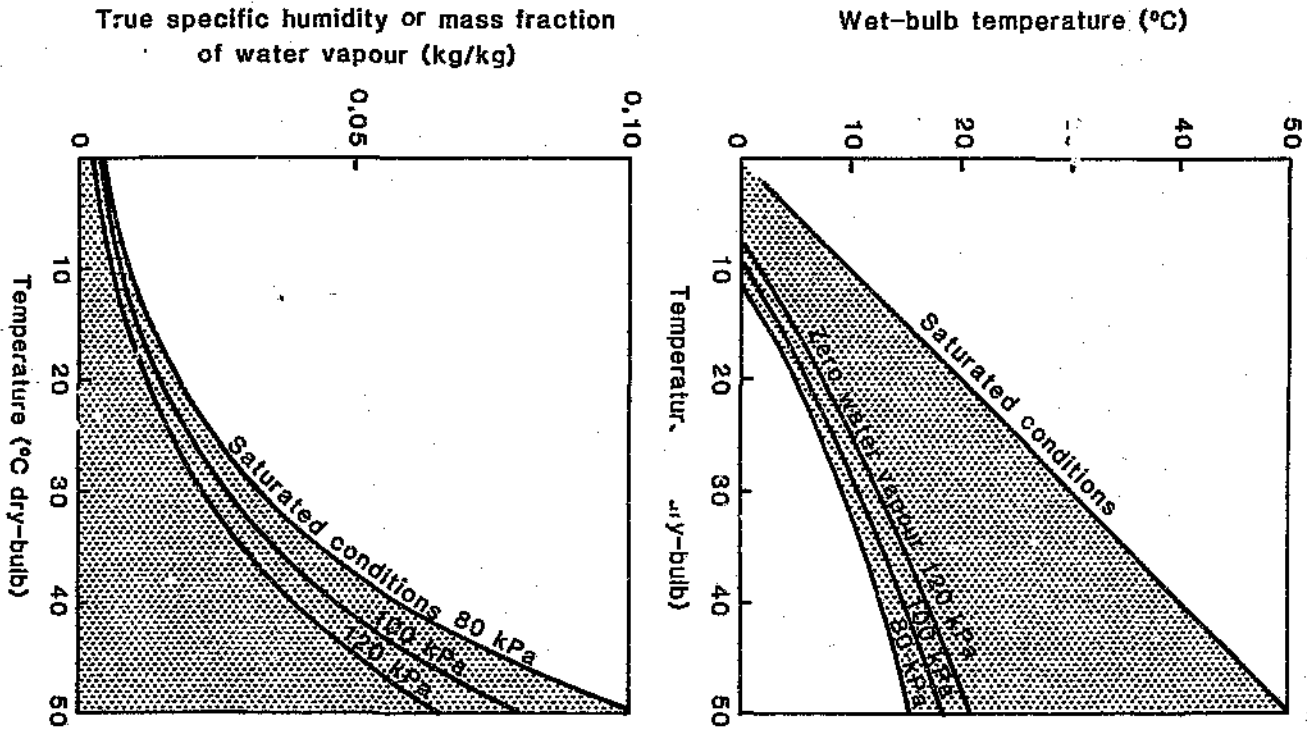


Figure 1.2 Range of moist air conditions being considered

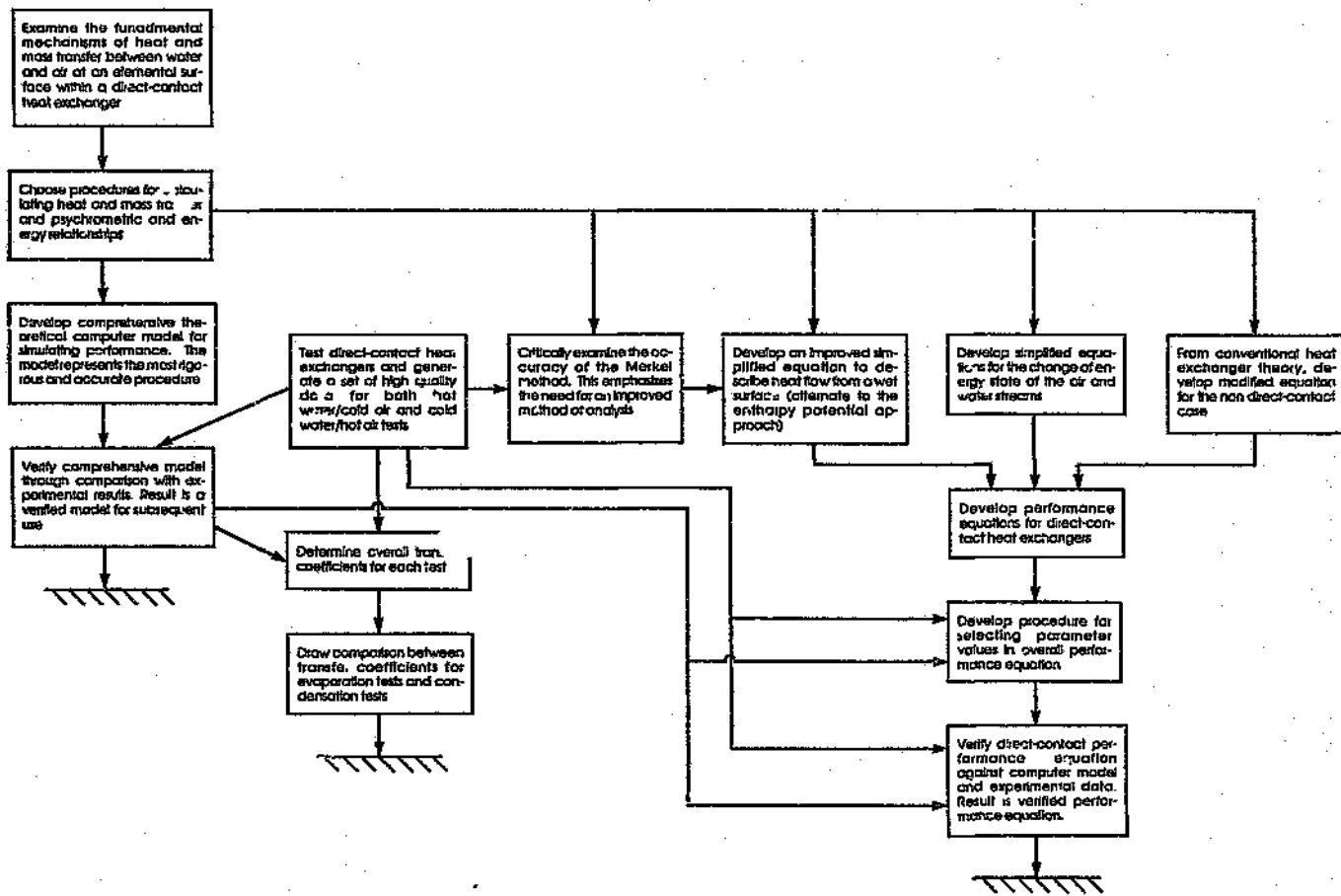


Figure 1.3 Flow chart of logic

## 2 FUNDAMENTAL MECHANISMS OF HEAT AND MASS TRANSFER BETWEEN WATER AND AIR AT AN ELEMENTAL SURFACE AREA

### 2.1 Introduction

This chapter examines the mechanism of heat and mass transfer between water and air. Most of these details are well known and are only dealt with briefly. Other aspects, such as the mass transfer formulations (both with respect to the transfer coefficients and driving force equations), the value of the diffusion coefficient, and the supersaturation of the air stream are covered in more detail. Some of the uncertainties that are involved at a fundamental level are highlighted and examined in subsequent chapters.

### 2.2 Convective heat transfer at a wet surface

The convective heat transfer to or from any surface, with or without moisture migration, is calculated by:

$$\dot{Q}_c = h_o (t_{ws} - t_{db}) \quad (2.1)$$

Note that the sign convention is that when heat flows from the water surface it is considered as positive.

The main pre-requisite of this calculation is a knowledge of the convective heat transfer coefficient. (Equation 2.1 defines this term.) This coefficient

depends, first, on the shape and size of the surface and on the velocity and direction of air passing over the surface and, second, on the thermodynamic transport properties of the air stream. Heat transfer literature<sup>(10,49)</sup> is replete with information for estimating heat transfer coefficients for a wide variety of situations. Most of the information on the film coefficient is of an empirical nature, and for the forced convection situation applicable to this study, the film coefficient is usually correlated in terms of the Nusselt, Reynolds and Prandtl numbers through an equation of the following form:

$$Nu = a Re^b Pr^c \quad (2.2)$$

Specific correlation equations and specific values of the film coefficient are considered later in examining experimental data for different heat transfer packing configurations. The values of the transport properties involved in Equation 2.2 are determined from the equations listed in Appendix A and are evaluated at the average of the water surface and bulk air stream temperatures.

The underlying premise is that the numerical value of the basic heat transfer coefficient is not influenced by any simultaneous moisture migration, such as when simultaneous evaporation or condensation takes place, provided that the mass transfer is not so great as to completely override the ordinary convective effects<sup>(46,67)</sup>. This basic premise is examined later where it is found that the effect of mass transfer on the transfer coefficients is inescapable.

### 2.3 Radiant heat transfer

Radiant energy is transmitted, absorbed and retransmitted by neighbouring wet surfaces. Within a direct-contact heat exchanger, where an approximately uniform distribution of air and water is likely to occur, it can be expected that neighbouring wet surfaces are at similar temperatures, and that the net radiant transfer between the wet surfaces would be low. In any event, of main concern is the heat transfer from the water stream to the air stream. The radiant component of this heat transfer occurs because the radiation between wet surfaces is transmitted through a non-luminous medium (air-water vapour mixture) which absorbs a small amount of the radiant energy.

An attempt has been made to quantify this component in Appendix B by comparing it in magnitude to the convective heat transfer. Three different configurations of direct-contact heat exchanger, which cover the range of possibilities, are considered. It is concluded that the value of the ratio of the radiative to convective heat transfer will always be less than 3 per cent and normally of the order of 0,5 per cent. The radiant heat transfer is small when compared to the sensible heat transfer, which itself is normally small when compared to the total heat transfer.

The radiant heat transfer between the air and water is invariably neglected in the analysis of cooling towers and other direct contact heat exchangers<sup>(58)</sup>. However, arguments similar to that presented in Appendix B, are seldom used to justify this. This mode of heat transfer has also been neglected in the present study.

## 2.4 Convective mass transfer at a wet surface

The latent heat exchange associated with the evaporation or condensation of water vapour at a wet surface is a major contributor to the total heat transfer. A study of the literature uncovered a surprising number of different approaches to the problem of quantifying mass transfer. Hence this subject is discussed in some detail here and a comparison made of the different published methods. The method eventually used in this study is that developed by Spalding<sup>(67,68)</sup> and advocated by a number of relatively modern texts<sup>(69,71)</sup>.

Convective mass transfer is conceptually treated in the same way as convective heat transfer. The basis is that, recognizing the complex nature of the transport processes close to the surface, an overall driving force for the transfer is defined between the bulk fluid and the surface condition and a transfer coefficient is used to describe the 'resistance' effect of the boundary layer in terms of a single parameter (the transfer coefficient in fact has the significance of a conductance).

The definitions involved in convective heat transfer are well established and a single universal approach is generally used. The same cannot be said for mass transfer. For instance, there are many different definitions of the key parameters involved, a good example being the varying definitions of the mass transfer coefficient.

Mass transfer processes are involved in many different industries and sciences. In solving the problems related to each discipline, each industrial group has

developed its own concepts and formulations independently. A good example of this is the large variety of units in use. Spalding(67) states that 'the subtleties of the science are such that conversion from one language to the other cannot be effected simply by multiplying by constants'.

All the different methods may be categorized in two groups and in essence there are two general approaches to studying mass transfer phenomena. The older and more traditional approach makes use of a model of a stagnant film (or Stefan flow(49)) and Fick's Law of one-dimensional diffusion. The other approach, described by Spalding(67), makes use of a model in which the air stream creates a 'scrubbing action' on the wet surface (Reynolds flow). Spalding in fact deliberately avoids introducing the mathematics of diffusion. According to Spalding neither model can be said to fit reality more closely than the other and the choice between them can be made on grounds of convenience. Both sequences of logic are presented below and a comparison is made. Spalding's approach has been used as the preferred procedure in this study.

#### 2.4.1 Spalding's approach

Spalding's approach is based on the simplified model shown in Figure 2.1 which depicts a small control volume situated at the interface between the water and air stream. This model of the transport process was first conceived by Reynolds(78) in 1874 as an aid to the understanding of convective heat transfer; Nusselt(55) then extended this logic to the convective mass transfer problem. Carrier(74) made use of a similar model specifically for the vaporization and

condensation of water, which he called the contact-mixture analogy.

The passing air stream has a scrubbing action and a certain flow rate of the bulk fluid enters the control volume. This scrubbing flow (or Reynolds flow),  $\dot{m}_{rf}$ , has the units of mass flow per unit surface area. The water vapour that is being transferred,  $\dot{m}_t$ , enters the control volume from the bulk water side of the interface. Both streams,  $\dot{m}_{rf} + \dot{m}_t$ , then leave the control volume. The properties and condition of this leaving air-water vapour mixture are those prevailing at the interface, which is assumed to be saturated at the surface temperature. (Note the sign convention is such that evaporation is positive.) The mass of water vapour must be conserved across the control volume, thus:

$$\dot{m}_t W_{\text{vss}} + \dot{m}_t = (\dot{m}_{rf} + \dot{m}_t) W_{\text{vws}} \quad (2.3)$$

The term,  $W_v$ , is the mass of water vapour per mass of air-water vapour mixture and is known as the true specific humidity or fractional mass concentration. Rearranging Equation 2.3 gives:

$$\dot{m}_t = \dot{m}_{rf} (W_{\text{vws}} - W_{\text{vss}}) / (1 - W_{\text{vws}}) \quad (2.4)$$

The scrubbing flow or Reynolds flow is in fact a fiction. A fluid-dynamic investigation would not be able to identify this stream in a real boundary layer and, as will be seen later, real flows exhibit deviations from this behaviour. However, having used a model in which the physical significance of the Reynolds flow is

apparent, it is also possible to consider the term,  $\dot{m}_{rf}$ , as a mass transfer coefficient. The right-hand side term in Equation 2.4 is then considered as the driving force and the equation can be expressed in the following form:

$$\dot{m}_t = \dot{m}_r B \quad (2.5)$$

The numerical values of the fractional mass concentration terms are usually small (e.g.  $W_v = 0,02$  for 25 °C saturated air at 100 kPa) and the denominator of the right-hand side terms of Equation 2.4 is close to unity. This leads to the following approximation, which is more recognizable as consisting of a transfer coefficient and a driving force.

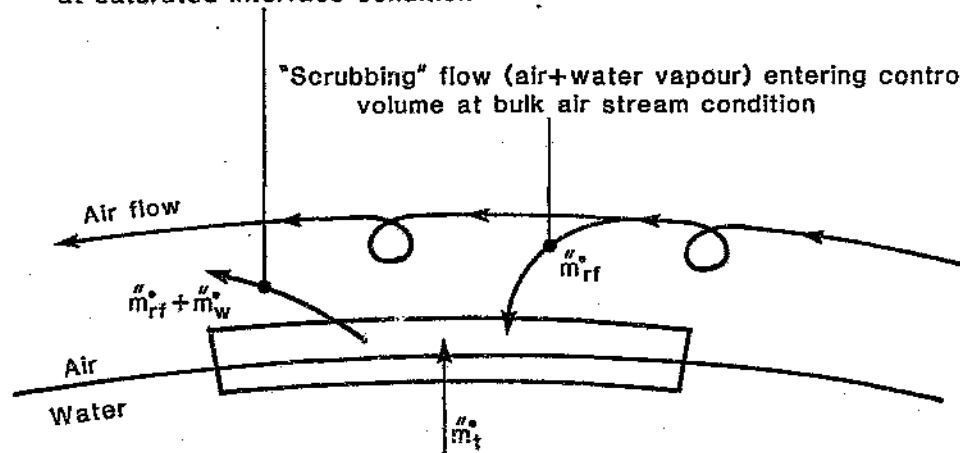
$$\dot{m}_t = \dot{m}_r ( W_{vws} - W_{v\infty} ) \quad (2.6)$$

This relationship is often treated as exact<sup>(11)</sup>, but this is only valid in the limit as  $W_{vws}$  tends to zero.

The pre-requisite of evaluating Equation 2.4 is a knowledge of the mass transfer coefficient,  $\dot{m}_{rf}$ . Unfortunately very few data exist on measurements made in specific mass transfer experiments. Because of this shortage, recourse is generally taken to the well known similarity with convective heat transfer, and the abundance of empirical correlations for convective heat transfer situations are used. Studies of the transfer processes taking place within the boundary layer have shown that the profiles of the vapour concentration (mass), temperature (heat) and velocity (momentum) are

Flow (air+water vapour) leaving control volume  
at saturated interface condition

"Scrubbing" flow (air+water vapour) entering control  
volume at bulk air stream condition



Water vapour entering control  
volume from bulk water stream

Figure 2.1 Simplified model showing a control volume  
at the water-air interface

similar. On the basis of this similarity, relationships between the heat transfer coefficient and the mass transfer coefficient have been developed. These relationships are known variously as the Modified Reynolds Analogy<sup>(10,75)</sup>, the Lewis Relationship<sup>(76)</sup> and the Chilton-Colburn Analogy<sup>(77)</sup>. In short, the mass transfer coefficient may be related to the heat transfer coefficient through the following equation:

$$\frac{h_m}{c_{\infty}} \frac{c_{\infty}}{h_c} = (Pr/Sc)^z \quad (2.7)$$

The relationship is essentially empirical but does have a reasonably sound theoretical basis for some simple geometries<sup>(67,79)</sup>. The value of Equation 2.7 is usually close to unity. Spalding presents a simple argument based on the steady flow energy equation applied across the control volume discussed earlier and shows that, in an idealized situation in the absence of a number of effects such as changes in kinetic and potential energy, Equation 2.7 is equal to unity. Note that in the present study this approximation is not made. Spalding points out that the index,  $z$ , in Equation 2.7 may vary between 0,50 and 0,75 depending on the specific flow situation and on the value of both the Prandtl number and the Schmidt number. He also stresses that there is no single value of the index which is always correct for all geometries and flow situations. It is one of the objectives of the present work to examine the value of this index and see if it changes for different heat exchanger geometries, or if it is affected by the direction of mass transfer or by different degrees of evaporation and condensation. This is discussed in detail later.

In the absence of any further information the recommendation is normally made that the value of 0,67 should be used. This was in fact the recommendation first made by Chilton(77) in 1934. A value of  $z = 0,67$  has been used in this present chapter to compare the different methods of estimating mass transfer rates.

The Prandtl and Schmidt numbers involve only the physical properties of the air and are evaluated at the average of water surface and free air stream temperatures. It should be recalled that the heat transfer coefficient was similarly defined and, furthermore, that the same 'film' condition must be applicable to the term  $c_{av}$  in Equation 2.7. Equations for calculating the transport properties and other thermodynamic parameters of moist air are given in Appendix A.

Strictly, Equation 2.7 is only applicable at relatively low mass transfer rates where the  $m$ 's migration has a negligible effect on the shape of the velocity, temperature or concentration profiles in the boundary layer. What actually constitutes a 'low' mass flow-rate is discussed later. Recall that one of the aims of the present study is to examine the effect of the direction of this mass flow (evaporation or condensation).

There is empirical and theoretical evidence(80,81) that the film transfer coefficient,  $\bar{h}_{rf}$ , is dependent, not only on the thermodynamic and transport properties through Equation 2.7, but also on the value of the driving force,  $B$  (in Equation 2.5). Spalding points out that this effect may be approximately accounted for by assuming that  $\bar{h}_{rf}$  varies proportionally to the following multiplying factor:

$$\bar{h}_{rf} \propto [ \ln (1 + B) ] / B \quad (2.8)$$

Spalding presents a theoretical derivation of this logarithmic correlation term from a simple analysis of a series of control volumes between the liquid and bulk air phase. The model is basically a series effect of what is shown in Figure 2.1. It should be noted at this stage, that the logarithmic correction term developed later in discussing the stagnant film approach is directly equivalent to the term given in Equation 2.8.

Some understanding of the meaning of 'low' mass transfer rates can now be discerned. A change in  $B$  from a value of zero to  $0,1$  would result in the value of the transfer coefficient varying by 5 per cent. Thus if variations of up to 5 per cent are acceptable, within the constraints of a particular calculation, the values of the driving force of less than  $B = 0,1$  would constitute a 'low' mass transfer situation. In this study the maximum value of the driving force is  $B = 0,1$  (for  $50\text{ }^{\circ}\text{C}$  water surface,  $0\text{ }^{\circ}\text{C}$  air and  $80\text{ kPa}$  barometric pressure). In the present work variations in the transfer coefficient (due to changes in the driving force) of 5 per cent are considered unacceptable and the logarithmic correction term is utilized. Whether this is in fact acceptable is discussed later when it becomes clear that the effect of mass transfer on the transfer coefficient is inescapable.

When the value of the driving force,  $B$ , is greater than zero, in the case of evaporation, the transfer coefficient decreases with an increase in the driving force. The opposite occurs in the case of condensation. Essentially, this is the only difference between the treatment of the mechanisms of evaporation and condensation. This issue is discussed in detail in Chapter 5 and Appendix J.

Based on Equation 2.8, Equation 2.5 can be re-written as:

$$\frac{\dot{m}_i}{\dot{m}_f} = \frac{\dot{m}_i}{\dot{m}_f} [ \ln (1 + B) ] \quad (2.9)$$

Equation 2.9 summarizes Spalding's approach as far as it affects this study; it is the equation used in the main body of this work. The value of the transfer coefficient,  $\frac{\dot{m}_i}{\dot{m}_f}$ , is calculated through Equation 2.7. Thus, finally:

$$\frac{\dot{m}_i}{\dot{m}_f} = \left( \frac{h_o}{c_{av}} \right) \left( \frac{Pr}{Sc} \right)^z \ln \left( \frac{1 - W_{\infty o}}{1 - W_{\infty s}} \right) \quad (2.10)$$

Rewriting this equation in a form similar to Equation 2.5 produces:

$$\frac{\dot{m}_i}{\dot{m}_f} = h_c B' \quad (2.11)$$

where,

$$B' = \left( \frac{1}{c_{av}} \right) \left( \frac{Pr}{Sc} \right)^z \ln \left( \frac{1 - W_{\infty o}}{1 - W_{\infty s}} \right) \quad (2.12)$$

#### 2.4.2 Stagnant film approach

The stagnant film approach is more traditional than Spalding's approach. In it, the mechanics of molecular diffusion are used to describe the behaviour of convective mass transfer. Fick's Law of diffusion is

considered as a starting point, and in its simplest form is expressed as:

$$\dot{m}_i = D (-) d\rho/dy \quad (2.13)$$

The density gradient,  $d\rho/dy$ , is normal to the surface and the negative sign indicates a mass transfer in the direction of decreasing concentration. This formulation gives rise to a mass transfer coefficient and driving force being defined as:

$$\dot{m}_i = h_d ( \rho_{vws} - \rho_{v\infty} ) \quad (2.14)$$

Note that in this form the structure of the defining equations for convective heat transfer and mass transfer are identical. Compare the following two heat transfer equations (Equations 2.15 and 2.16) to their analogous mass transfer counterparts (Equations 2.13 and 2.14). (These four equations do not really represent laws of nature but are rather definitions of the diffusion coefficient, mass transfer coefficient, thermal conductivity and the heat transfer coefficient.)

$$\dot{q}_c = k (-) dt/dy \quad (2.15)$$

$$\dot{q}_c = h_c ( t_{ws} - t_{\infty} ) \quad (2.16)$$

However, there is an important difference between heat and mass transfer and as a result a logarithmic correction factor is required when drawing analogies between

mass transfer and heat transfer. This difference and the development of the correction factor are now described.

Consider moist air above a water surface: there is a continuous gas phase above the surface and the total pressure (sum of the partial pressures of the air and water vapour) can be considered to be continuous. The Gibbs-Dalton law applies and any concentration gradient and diffusion of water vapour infers a concentration gradient and diffusion of air in the opposite direction. Herein lies the difference between the treatment of heat transfer and that of mass transfer as there is no equivalence to this in convective heat transfer. Thus, when evaporation takes place the air component would diffuse toward the water surface. The surface is impermeable to air and hence a bulk velocity away from the surface must exist so that the net transportation of air is zero. The bulk flow exactly offsets the diffusion and hence the air may be considered to be 'stagnant'. The bulk flow not only transports air but also water vapour away from the surface.

The net mass flow of air is zero and hence:

$$\rho_a V = D \, d\rho_a/dy \quad (2.17)$$

where  $V$  is the bulk velocity away from the surface.

The total mass transfer of water vapour is then:

$$\dot{m}_i = \rho_v V + D \, (-) \, d\rho_v/dy \quad (2.18)$$

Using Equation 2.17 this may be written as:

$$\dot{m}_i = D (\rho_v / \rho_a) d\rho_a/dy + D (-) d\rho_v/dy \quad (2.19)$$

Integrating across the boundary layer (thickness  $y$ ) and making use of the perfect gas laws produces:

$$\dot{m}_i = (DZ/y) (\rho_{vws} - \rho_{vco}) \quad (2.20)$$

where  $Z$  is a dimensionless logarithmic mean density factor for the 'stagnant' air and is given as:

$$Z = \left( \frac{p}{R_a T_{ave}} \right) \frac{\ln (\rho_{aco} / \rho_{aws})}{(\rho_{aco} - \rho_{aws})} \quad (2.21)$$

Note that this is the corresponding equivalent of the logarithmic correction term presented earlier in discussing Spalding's approach.

A comparison of Equations 2.20 and 2.14 infers that:

$$h_d = DZ/y \quad (2.22)$$

Referring now to heat transfer information and specifically making use of the Chilton-Colburn analogy<sup>(77)</sup>, the mass transfer coefficient can be related to the heat transfer coefficient by:

$$h_d \rho_{av} c_{av} / h_c = Z (Pr/Sc)^{2/3} \quad (2.23)$$

Substituting into Equation 2.14 gives:

$$\frac{\dot{m}_1}{\dot{m}_s} = \left[ Z \left( \frac{h_0}{C_{av} \rho_{av}} \right) \left( \frac{Pr}{Sc} \right)^{2/3} \right]_{\text{film}} (P_{vws} - P_{v\infty}) \quad (2.24)$$

Note that all the transport properties are determined at the film condition.

Equation 2.24 summarizes the 'stagnant' film approach. Equations of this type are found in a number of texts and are the more 'rigorous' versions of what normally follows. By using the perfect gas laws, the density terms in Equation 2.24 can be transformed to partial pressure terms. Also the term,  $Z$ , is approximately equal to unity and thus Equation 2.24 is often simplified to:

$$\frac{\dot{m}_1}{\dot{m}_s} = 0,622 \left( \frac{h_0}{C_{av}} \right) \left( \frac{Pr}{Sc} \right)^{2/3} \left( \frac{P_{vws} - P_{v\infty}}{P} \right) \quad (2.25)$$

The constant 0,622 is the ratio of the molecular mass of water vapour to that of air.

### 2.4.3 Comparison of the different approaches

#### Mass transfer

The different methods, as summarized by Equations 2.10, 2.24 and 2.25, are referred to here as Method I (Spalding approach), Method II (stagnant film approach) and Method III (simplified stagnant film approach), respectively. Comparisons of these methods for the full range of temperature conditions are shown in Figure 2.2. The values are presented as ratios using

the values from Method I as the base, namely  $\dot{m}_{tII}/\dot{m}_{tI}$  and  $\dot{m}_{tIII}/\dot{m}_{tI}$ . Generally, the answers given by these three equations agree to within 10 per cent; however, the differences can be as much as 16 per cent. (Note at this stage that a value of the index  $z = 0,67$  is used but the acceptability of this is examined later.) Only the case where the barometric pressure is 100 kPa has been presented since the situation is much the same for the other barometric pressures.

#### Total heat transfer

The differences in the total heat transfer when evaluated by the three different methods is of more importance to this study than the mass transfer alone. The total heat transfer is the sum of the convective and latent heat transfer (see later) and is given by:

$$\frac{\dot{Q}_t}{\dot{Q}_t} = h_c ( t_{ws} - t_{db} + \lambda B' ) \quad (2.26)$$

The terms  $q_{tI}$ ,  $q_{tII}$ ,  $q_{tIII}$  correspond to Methods I, II and III for calculating the mass transfer. Comparisons are shown plotted in Figure 2.3. The values are plotted as ratios using the value from Method I as a base. Again, the values given by the three different methods generally agree to within 10 per cent and, as stated previously, only the case where the barometric pressure is 100 kPa is presented.

#### 2.4.4 Summary of method used in present study

Based on Spalding's approach the mass transfer rate of water vapour is calculated through:

$$\frac{\dot{m}_t}{\dot{m}_t} = \frac{\dot{m}_t}{\dot{m}_t} [ \ln ( 1 + B ) ] \quad (2.27)$$

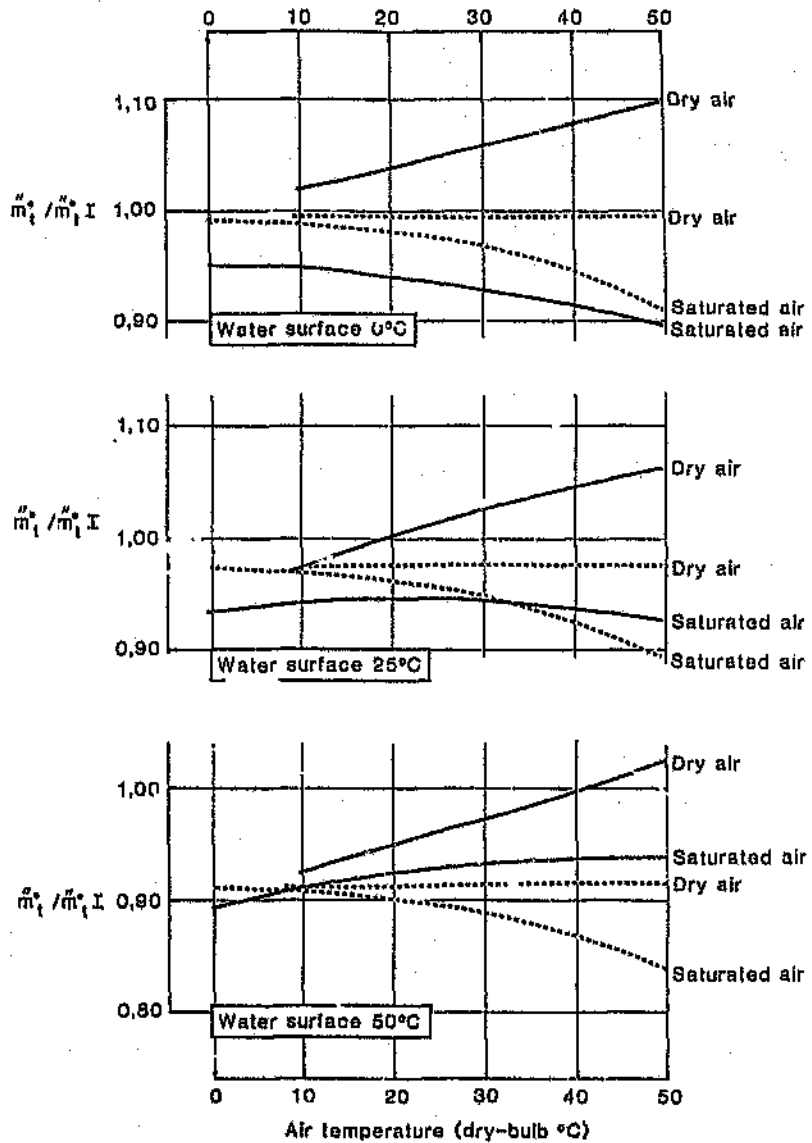


Figure ..2 Differences in the mass transfer rate as calculated by three different equations, the information is plotted as ratios using Method I as a base. The solid lines relate to Method II and the dashed lines relate to Method III

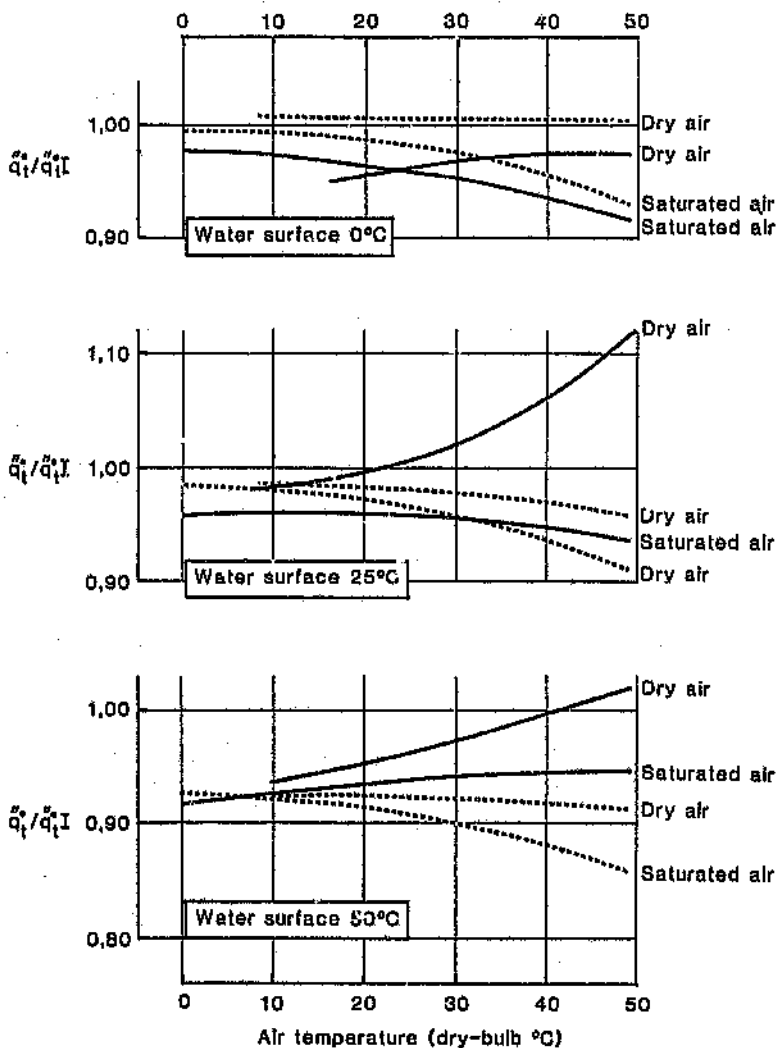


Figure 2.3 Differences in total heat transfer rate as calculated by three different equations, the information is plotted as ratios using Method I as a base. The solid lines relate to Method II and the dashed lines to Method III.

$$B = (W_{vws} - W_{v\infty}) / (1 - W_{vws}) \quad (2.28)$$

The term,  $\dot{m}_{rf}$ , can be considered as a mass transfer coefficient with the units  $\text{kg/s m}^2$ . The term,  $W_v$ , is the mass of water vapour per mass of moist air; it is known as the fractional mass concentration of water vapour or the true specific humidity. The subscript,  $ws$ , refers to the zone directly adjacent to the surface of the water; it is assumed that this moist air is saturated with water vapour and has the same temperature as the water surface. Equations for calculating the mass concentration of water vapour are given in Appendix A. Note that the sign convention is such that evaporation is considered as positive.

Based on the well known similarity between convective heat and mass transfer phenomena, the mass transfer coefficient is related to the heat transfer coefficient through:

$$\dot{m}_{rf} c_{av} / h_c = (\text{Pr}/\text{Sc})^z \quad (2.29)$$

The index,  $z$ , has values between 0,50 and 0,75. The applicability, for cooling tower packing, of the normally assumed  $z = 0,67$  is examined later. Combining the above equations:

$$\dot{m}_{rf} = h_c B' \quad (2.30)$$

where  $B'$  is the modified driving force for mass transfer defined as:

$$B' = \left( \frac{1}{c_{av}} \right) \left( \frac{\text{Pr}}{\text{Sc}} \right)^z \ln \left( \frac{1 - W_{v\infty}}{1 - W_{vws}} \right) \quad (2.31)$$

## 2.5 Effect of resistance to heat flow in the bulk water phase

The total heat flow from the water surface to the bulk air stream may now be quantified. It is evaluated by adding the effects of the sensible heat flow and latent heat flow due to mass transfer. But no consideration has yet been given to the flow of heat from within the layer of water or drops of water to the water surface.

The thermal resistance of the liquid phase is difficult to determine either theoretically or empirically. Fortunately the resistance to heat flow within the water mass is small. This is because of the dynamic nature of the thin film of water flowing over the irregular surface of packing media as well as the size and dynamic nature<sup>(83)</sup> of the water droplets involved. Webb<sup>(16)</sup> quotes a typical value of a water film heat transfer coefficient (defined between bulk water temperature and surface temperature) of  $2\ 300\ \text{W/m}^2\ \text{K}$  for cooling towers. This value is determined from equations given by Ganic<sup>(82)</sup>. By comparing this term to typical values of the overall mass transfer coefficient, Webb concludes that the overall transfer coefficient would not be affected by more than a few per cent by ignoring the water phase thermal resistance.

In most work of this nature it is normal to ignore this resistance and assume that the water surface temperature is in fact that of the bulk water mass<sup>(23)</sup>. This is the approach which has been adopted in the present study, but it must be noted that the analysis is such that this resistance is implicitly included within the overall transfer coefficient.

## 2.6 Total heat transfer

Associated with the mass transfer of water vapour is the change in enthalpy of the vapour as it changes phase and temperature. The latent heat change by itself is negligibly different from the total change in enthalpy provided the latent heat content is evaluated at the water surface temperature<sup>(46)</sup>. The heat flow due to mass transfer is given by:

$$\dot{q}_l = \dot{m}_l \lambda \quad (2.32)$$

The total heat flow is the sum of the convective and latent heat transfer rate, giving:

$$\dot{q}_t = h_o ( t_{ws} - t_{db} + \lambda B' ) \quad (2.33)$$

Since the resistance to heat flow offered by the water stream is to be ignored, the total heat transfer from the water to the air is given by Equation 2.33 with the water surface temperature,  $t_{ws}$ , replaced by the water stream temperature,  $t_w$ . This equation is repeated below:

$$\dot{q}_t = h_o ( t_w - t_{db} + \lambda B' ) \quad (2.34)$$

The term in brackets can be considered as the driving force for the total heat transfer. It is a function of barometric pressure, air temperature, moisture content and water surface temperature. Some typical values of the driving force term (having the units of

temperature °C) are shown in Figure 2.4. A water temperature of 25 °C and a barometric pressure of 100 kPa have been chosen merely for illustrative purposes.

Note that the value of the driving force is almost independent of dry-bulb temperature for a constant wet-bulb temperature. This important observation is applicable to the full range of conditions being considered. It indicates that the driving force may be evaluated in terms of a function that is dependent on wet-bulb temperature and barometric pressure only. This is examined in more detail later.

## 2.7 Supersaturation and fogging of the air stream

The effect of fogging is important in the operation of heat exchangers situated underground in mines since the inlet air is invariably close to saturation.

Supersaturation occurs when a water vapour-air mixture exists at a temperature below its saturation value. At the same time the air is supersaturated the vapour may be considered subcooled. Under these conditions small drops (0,1 to 40  $\mu\text{m}$ ) are normally formed by condensation of the vapour<sup>(60)</sup>. Under certain circumstances a degree of supersaturation is possible without fog formation, but in most industrial processes there are sufficient nuclei present to assume that once the temperature is below the saturation temperature fog will occur<sup>(60,61)</sup>. (Turbulence also minimizes the degree of saturation required for fogging<sup>(62)</sup>).

Fog droplets are extremely small and once formed would pass through the heat exchanger packing in the air stream. (This is in keeping with observations made on

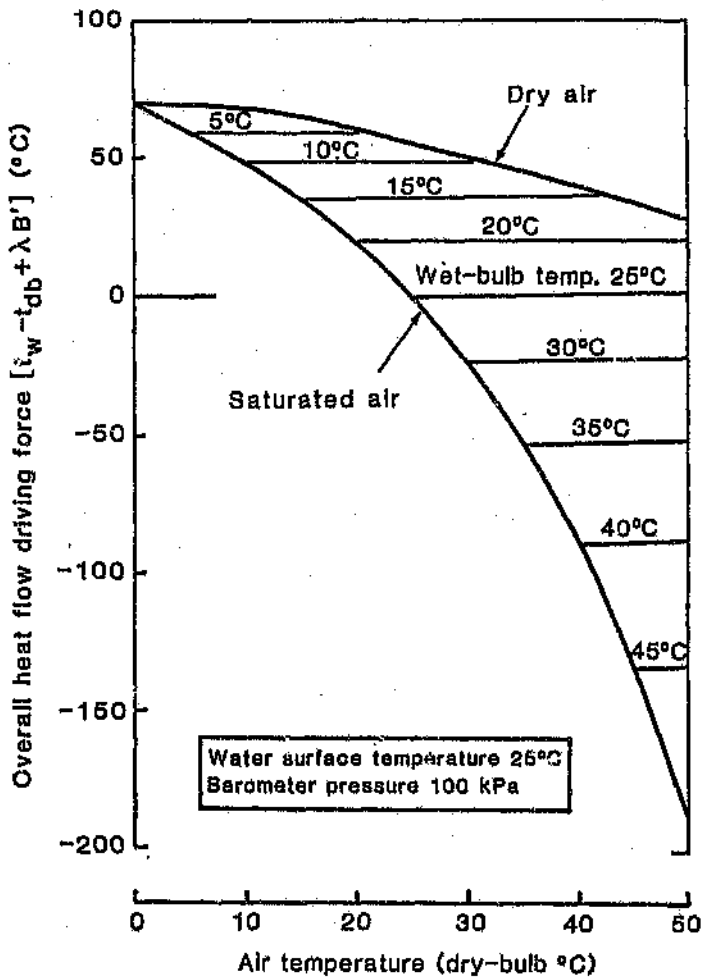


Figure 2.4 Values of the overall heat flow driving force (°C) for 25 °C water surface temperature and 100 kPa barometric pressure.

condensers, where once fog is formed it passes out of the unit to the demisters<sup>(63)</sup>.) In the specially constructed test heat exchangers described later, special demister pads were used to capture this carry-over of fog droplets.

The fogged air stream is a homogeneous mixture of saturated moist air and small liquid water drops, with the two components in thermal equilibrium. Chisholm<sup>(60)</sup> discusses the effects on fog formation and the existence of fog on the heat and mass transfer driving forces and the associated transfer coefficients. He concludes that the effects are negligible and that the treatment of the heat and mass transfer processes remains unchanged. Hence, the earlier formulations should apply even in the presence of fog. The validity of these simplifications is examined later in comparing modelled data against experimental information.

When saturated air comes into direct contact with a water surface at a different temperature the process change of the air is such that supersaturation occurs. This is the case whether the water is being heated or cooled.

Process changes of an air stream due to direct contact with a wet surface are dictated by the temperature of the water surface and the condition of the air. The process change of the air stream is often described by the ratio of enthalpy to moisture change. With saturated air the value of the ratio is such that the process will always tend to create supersaturated conditions. This can be appreciated by examining the process changes on a psychrometric chart. The value of the enthalpy-moisture ratio closely approximates that found by drawing a straight line on a psychrometric chart between the air condition and saturated

air at the water temperature. This is not surprising since the Reynolds flow model reduces to a hypothetical mixing of a small part of saturated air at the water temperature with the main stream air. Saturated air may be represented by point A on Figure 2.5 and the water surface condition by points B or C depending on whether the water is hotter or colder than the air. Line AB can be considered to be the direction of the process change in the air stream for the hot water condition and line AC that for the cold water condition. Note that both lines fall above the saturation line. The region above the saturation curve represents fogged conditions of moist air. Thus, when saturated air comes into direct contact with a water surface at a different temperature, the process change of the air is such that supersaturation or fogging occurs; this is the case whether the water is being heated or cooled.

The effect of fogging on the overall performance of a heat exchanger is small. However, as seen later, it is surprising just how high a proportion of the total mass transfer can result as fog. In modelling heat exchanger performance it is necessary to take account of the fog in order to maintain the balance of mass flow of water and water vapour.

## 2.8 Note on the diffusion coefficient of water vapour in air

A literature search has surprisingly shown that several reputable heat and mass transfer texts present different values of the diffusion coefficient for water vapour in air (see Figure 2.6). As a result, this aspect has been examined in some detail here, first from the point of view of existing literature and later

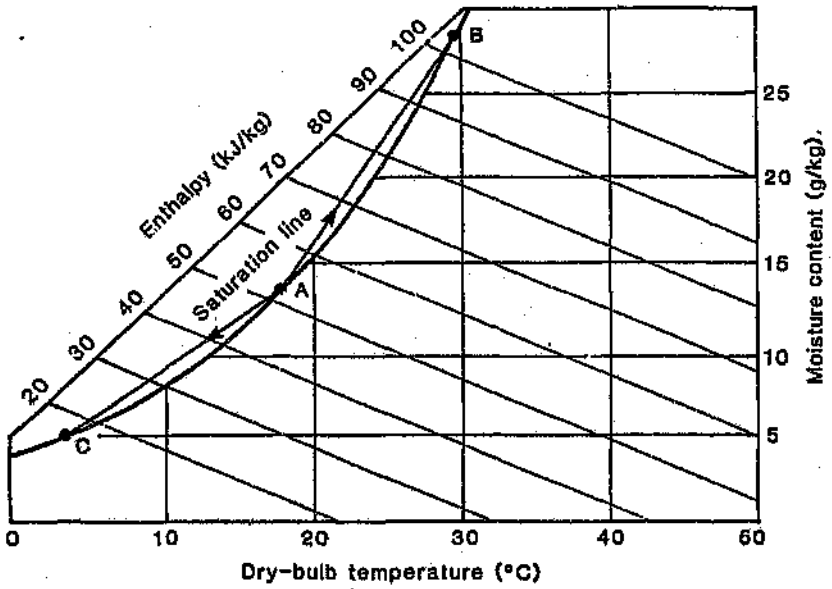


Figure 2.5 Typical psychrometric chart

in comparing modelled data against experimental information.

Based on the kinetic theory of gases Maxwell<sup>(31)</sup> in 1868 proposed that the diffusion coefficient is independent of the mixture composition of the diffusing gases. Experimentation has shown a maximum composition dependence of a few per cent, but this dependence is negligible for the conditions being considered here<sup>(35)</sup>. Also on the basis of the kinetic theory of gases, Maxwell proposed that the diffusion coefficient is related to temperature and pressure by:

$$D = K_0 T^{3/2} / p \quad (2.35)$$

where  $K_0$  is a constant depending on the molecular structure of the diffusing gases.

Numerous derivations and modifications to this original equation have been proposed. All the modifications are essentially related to the value of the constant,  $K_0$  and of the index,  $3/2$ . Gilliland<sup>(30)</sup> in 1934 considered the experimental database that was available at the time and, for water vapour and air, suggested:

$$D = 4,22 \times 10^{-7} T^{1.50} / p \quad (2.36)$$

This is the relationship recommended by Kern<sup>(27)</sup>.

A consideration of further data some years later by Fuller et al<sup>(32)</sup> led to what is termed an optimized

Gilliland equation<sup>(26)</sup>,

$$D = 1,19 \times 10^{-7} T^{1,75} / p \quad (2.37)$$

This is the relationship recommended by Reid and Sherwood<sup>(33)</sup> and by Perry & Chilton<sup>(26)</sup>.

Mason and Monchick<sup>(34,35)</sup> presented further experimental data in 1965. Based on this they made empirical adjustments to the theoretical constants involved in the equation of state for real gases. They then recalculated the diffusion coefficient values and tabulated this information for air temperatures up to 300 °C at a pressure of one atmosphere. These values are recommended by the US National Bureau of Standards<sup>(35)</sup> and by ASHRAE<sup>(10)</sup>. Accepting the inverse relationship with pressure, the following equation has been fitted (by the author) to this data:

$$D = 1,676 \times 10^{-7} T^{1,884} / p \quad (2.38)$$

This is the equation used in the present study.

Sutherland<sup>(37)</sup> in 1898 proposed a slightly different form of the original theoretical equation which he modified to produce:

$$D = K_1 T^{2,5} / ( p ( K_2 T + K_3 ) ) \quad (2.39)$$

With this form of equation in mind, Spalding<sup>(38)</sup> analysed the data that was available at the time (1946)

and showed that for water vapour-air mixtures, the data is correlated well by:

$$D = 1,64 \times 10^{-6} T^{2.5} / ( p ( 1,8 T + 441 ) ) \quad (2.40)$$

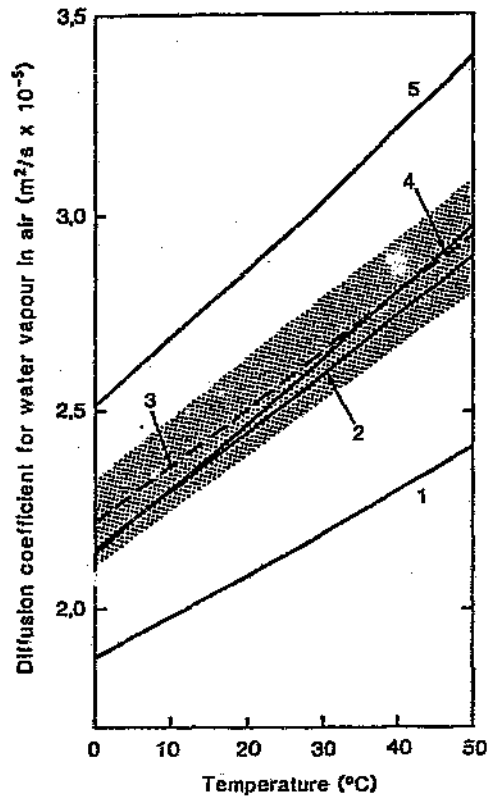
This equation is recommended by both Sherwood and Pigford<sup>(36)</sup> and by ASHRAE<sup>(10)</sup>. (Note that the ASHRAE handbook makes two separate recommendations; they are not, however, significantly different.)

It is interesting to note that Eckert and Drake<sup>(50)</sup>, in their widely used text book, present the following equation for water vapour diffusing in air, which gives considerably higher values than the other correlations. Unfortunately, the original source of this equation is not clear.

$$D = 0,99 \times 10^{-7} T^{1.81} / p \quad (2.41)$$

Figure 2.6 shows a plot of this variety of equations (Equations 2.36, 2.37, 2.38, 2.40 and 2.41). There are surprisingly large discrepancies. However, the more recent work and the correlations quoted in the more specialized texts (lines 2,3 and 4 in Figure 2.6) agree fairly well.

Equation 2.38 (line 3 in Figure 2.6) has been used in this study, since this correlation appears to be the best possibility. However, apart from the disagreement of the various correlation equations, there is also a large scatter in the data originally used in each case (see, for instance, Sherwood and Pigford<sup>(36)</sup>).



- 1 Equation 2.36 Gilliland<sup>(30)</sup>, Kern<sup>(27)</sup>
- 2 Equation 2.37 Reid & Sherwood<sup>(33)</sup>,  
Perry & Chilton<sup>(28)</sup>
- 3 Equation 2.38 Mason & Monchick<sup>(35)</sup>,  
Ashrae<sup>(1)</sup>
- 4 Equation 2.40 Sherwood & Pigford<sup>(36)</sup>,  
Ashrae<sup>(1)</sup>
- 5 Equation 2.41 Eckert & Drake<sup>(50)</sup>

Figure 2.6 Diffusion coefficient for water vapour in air at one atmosphere pressure (101,3 kPa)

Although it is impossible to quantify accurately, it is intuitively expected that the diffusion coefficient predicted using Equation 2.38 is probably within the bounds of  $\pm 5$  per cent, shown as the shaded area in Figure 2.6.

## 2.9 Note on the Prandtl, Schmidt and Lewis numbers

The Prandtl and Schmidt numbers are used to correlate experimental data for heat and mass transfer. They are defined as:

$$Pr = \mu c_{2v} / k \quad (2.42)$$

and

$$Sc = \mu / \rho_{2v} D \quad (2.43)$$

It should be noted that in this application the relevant specific heat term is the true thermal capacity of the air-water vapour mixture per unit mass of this mixture, and the density term applicable is the true density of air-water vapour mixture (see Appendix A).

As discussed earlier, this study is concerned with the value of these properties at the saturated 'film' condition(25). Values of Pr and Sc have been calculated (using the equations presented in Appendix A) for different temperatures and pressures and are given in Table 2.1.

The ratio,  $(Pr/Sc)^2$ , is used to relate heat transfer coefficients to their mass transfer counterparts. Values of this term for  $z = 0,67$  are also given in

Table 2.1. (The value of this term is sometimes called the Lewis number; there are, however, differing opinions in the literature as to the exact definition of the Lewis number.)

For the range of conditions being considered, Pr has a mean value of 0,725 with a range from 0,718 to 0,746, Sc has a mean value of 0,611 with a range from 0,602 to 0,630, and the ratio  $(Pr/Sc)^{0,67}$  has a mean value of 1,120 with a range from 1,113 to 1,129. Although there is relatively small variation in these values, rather than using constant average values, the full equations (as listed in Appendix A) have been used to calculate these parameters in the main body of the work.

Table 2.1 Value of Prandtl (Pr) and Schmidt (Sc) numbers and the ratio  $(Pr/Sc)^{2/3}$  for saturated air at varying temperatures and pressures

		TEMPERATURE (°C)						
		0	10	20	30	40	50	
BAROMETRIC PRESSURE (kPa)	80	Prandtl No. Pr Schmidt No. Sc $(Pr/Sc)^{2/3}$	0,722 0,602 1,129	0,720 0,604 1,124	0,721 0,608 1,120	0,724 0,613 1,117	0,732 0,620 1,117	0,746 0,630 1,119
	100	Prandtl No. Pr Schmidt No. Sc $(Pr/Sc)^{2/3}$	0,721 0,602 1,128	0,719 0,604 1,123	0,719 0,607 1,120	0,721 0,611 1,117	0,727 0,617 1,116	0,737 0,626 1,115
	120	Prandtl No. Pr Schmidt No. Sc $(Pr/Sc)^{2/3}$	0,721 0,602 1,128	0,719 0,604 1,123	0,718 0,605 1,120	0,719 0,610 1,116	0,723 0,615 1,114	0,732 0,623 1,113

### 3 A COMPREHENSIVE THEORETICAL MODEL FOR SIMULATING HEAT AND MASS TRANSFER IN A COUNTERFLOW DIRECT-CONTACT WATER-AIR HEAT EXCHANGER

#### 3.1 Introduction

In recent times, there have been a number of computer models (14,104) developed for direct-contact air water heat exchangers. However none of the existing models make use of the complete set of equations given in Chapter 2 or explicitly account for supersaturation.

The aim of this chapter is to develop a computer model that can undertake a fully comprehensive analysis of heat and mass transfer in a counterflow direct-contact heat exchanger. The algorithms used represent the best possible procedures and none of the simplifying assumptions that are so often used in cooling tower theory are employed. The model represents a comprehensive and accurate analytical tool and, as such, should be considered as an independent product of this research which may find application in other research in the future.

In the present work this simulator plays an important role in achieving a number of the objectives. First, the model is used to examine the fundamental heat and mass transfer relationships by comparing simulated information based on these relationships with real data. As a result it is possible to comment on the value of the index in the heat and mass transfer analogy as well as on the applicability of the procedure used to describe the fogging phenomena. Second, the simulator is used to investigate the value of the various groups

of parameters that are identified in the development of the overall performance equation. As a result, it is possible to evaluate the changes of these parameters within the heat exchanger and not simply at the end states. Third, the simulator is used to generate performance data against which the proposed overall performance equation can be checked.

### 3.2 Basic computer model

The underlying assumptions in the model are that the air and water flows are evenly distributed (which infers that the entire surface area of fill is equally wetted and experiences the same air velocity) and also that for a single operating condition (flowrates, inlet temperatures and pressure) a single value of the convective film coefficient is applicable across the entire heat exchanger.

The model determines the overall heat and mass transfer in a direct-contact heat exchanger from a knowledge of the product of the convective film coefficient and the surface area of contact, the inlet air condition, the inlet water temperature, the dry air mass flowrate and the inlet water flowrate. This is achieved by dividing the heat exchanger into small sections and then solving the applicable differential equations numerically and sequentially from inlet to outlet conditions. The inlet and outlet stations and the control section are shown in Figure 3.1.

It was shown in Chapter 2 that supersaturation and the formation of fog occurs under some circumstances and it is assumed that:

. fog appears instantaneously with supersaturation;

- . heat and mass transfer formulations and transfer coefficients remain unchanged by fogging;
- . air, water vapour and fog exist as a uniform mixture at a uniform temperature; and
- . fog droplets pass through the heat exchanger packing in the air stream but are captured in the demister pads.

The equations governing the heat and mass transfer within the control volume (see Chapter 2) are:

$$\Delta q_i = h_c (t_w - t_{db} + \lambda B') \Delta A \quad (3.1)$$

$$\Delta m_i = h_c B' \Delta A \quad (3.2)$$

With reference to Figure 3.2, for the situation when supersaturation does not occur, a mass balance across the control volume produces:

$$m_{w0} = m_{w1} - \Delta m_i \quad (3.3)$$

$$W_0 = W_1 + \Delta m_i / m_a \quad (3.4)$$

An energy balance across the control volume will reduce to an enthalpy balance (see Chapter 4) producing:

$$\Delta q_i = m_a (i_{a0} - i_{a1}) \quad (3.5)$$

$$\Delta q_i = m_{w1} c_w t_{w1} - m_{w0} c_w t_{w0} \quad (3.6)$$

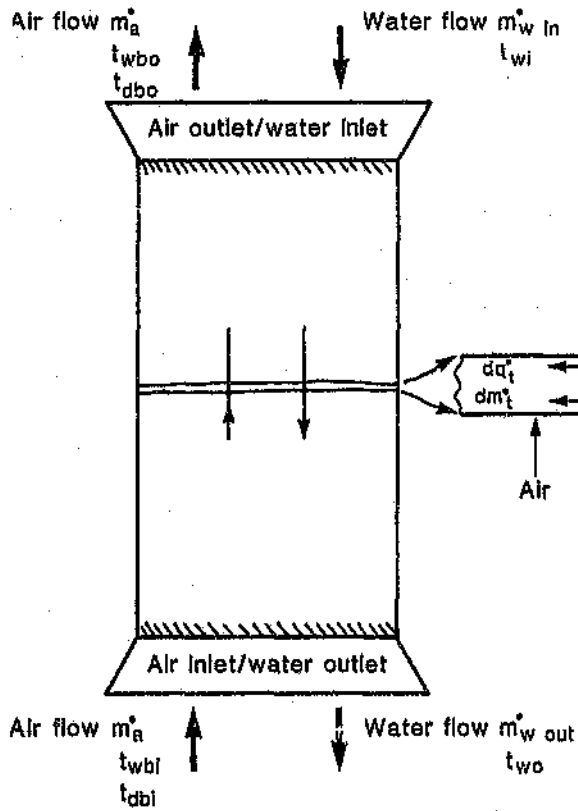


Figure 3.1 Model of counterflow tower for computer simulation

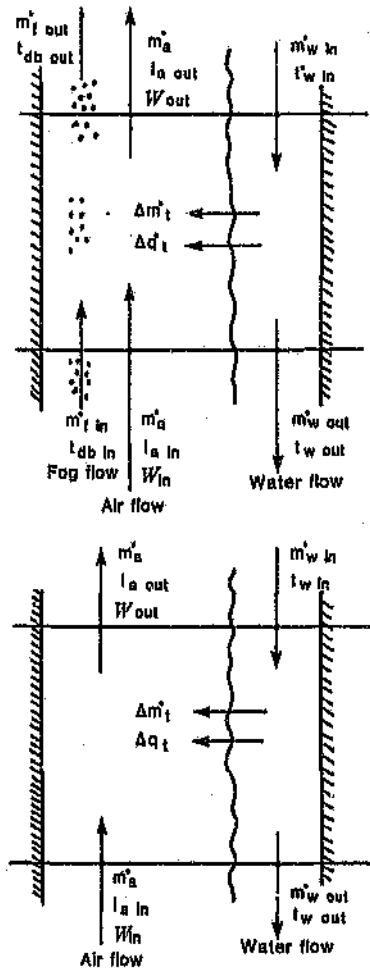


Figure 3.2 Control volume depicting the heat and mass transfer with and without fog formation

For the situation where supersaturation occurs, the mass and enthalpy balances become:

$$m'_{wo} = m'_{wi} - \Delta m'_t \quad (3.7)$$

$$W'_o = W'_i + (\Delta m'_t - \Delta m'_f) / m'_a \quad (3.8)$$

$$m'_{fo} = m'_{fi} - \Delta m'_f \quad (3.9)$$

$$\Delta q'_t = m'_a (i_{ao} - i_{ai}) + c_w (m'_{fo} t_{ao} - m'_{fi} t_{ai}) \quad (3.10)$$

$$\Delta q'_t = m'_{wi} c_w t_{wi} - m'_{wo} c_w t_{wo} \quad (3.11)$$

Recall, that once fogging has occurred, the air-water vapour component is treated as saturated. The water droplets in the form of fog do not remix with the main water stream in the heat exchanger but move from section to section resulting in an accumulation as the fogged air moves through the heat exchanger. However, at the air outlet side the fog is stripped from the main air stream in the demisters and then remixes with the main incoming water stream.

For any particular set of conditions these equations can be solved numerically and progressively for each section of the heat exchanger. The heat exchanger is divided into sections of equal surface area (or height). The calculation is iterative since the inlet boundary conditions for the air and water are known at opposite ends of the heat exchanger. The calculation

starts at the air inlet side. To initiate the calculation, the outlet water temperature and outlet water mass flowrate are estimated. All the relevant conditions at the air inlet/water outlet boundary of the first section are thus specified. The temperatures are assumed to be applicable throughout that section and Equations 3.1 and 3.2 are used to determine the heat and mass transfer within the section. The mass and enthalpy balance equations are then used to calculate the air conditions entering and the water temperature and flow leaving the following section. The calculation progresses through the heat exchanger arriving at the water inlet/air outlet end. The calculated inlet water temperature and inlet water flowrate are then compared to the specified input values and the estimated outlet water temperature and flowrate updated. A simplified flow diagram of this logic is shown in Figure 3.3 for the set of circumstances where the model is being used to determine the  $h_c A$  value, the heat and mass transfer at each strip, the amount of fogging that takes place and the water and air conditions w.r. in the heat exchangers from a knowledge of the inlet and outlet conditions.

It was found that sufficient accuracy could be achieved by dividing the heat exchanger into 200 sections. The calculation process converges after six iterations (typically) with a tolerance of 0,005 °C on the inlet water temperature and 0,05 g/s on the inlet water mass flowrate.

The barometric pressure is assumed to vary linearly between inlet and outlet conditions. Although variations in the air pressure, of the magnitude involved in this study, are of secondary importance, account was taken of the air pressure differential across the heat exchanger. This is to ensure that the simulated end

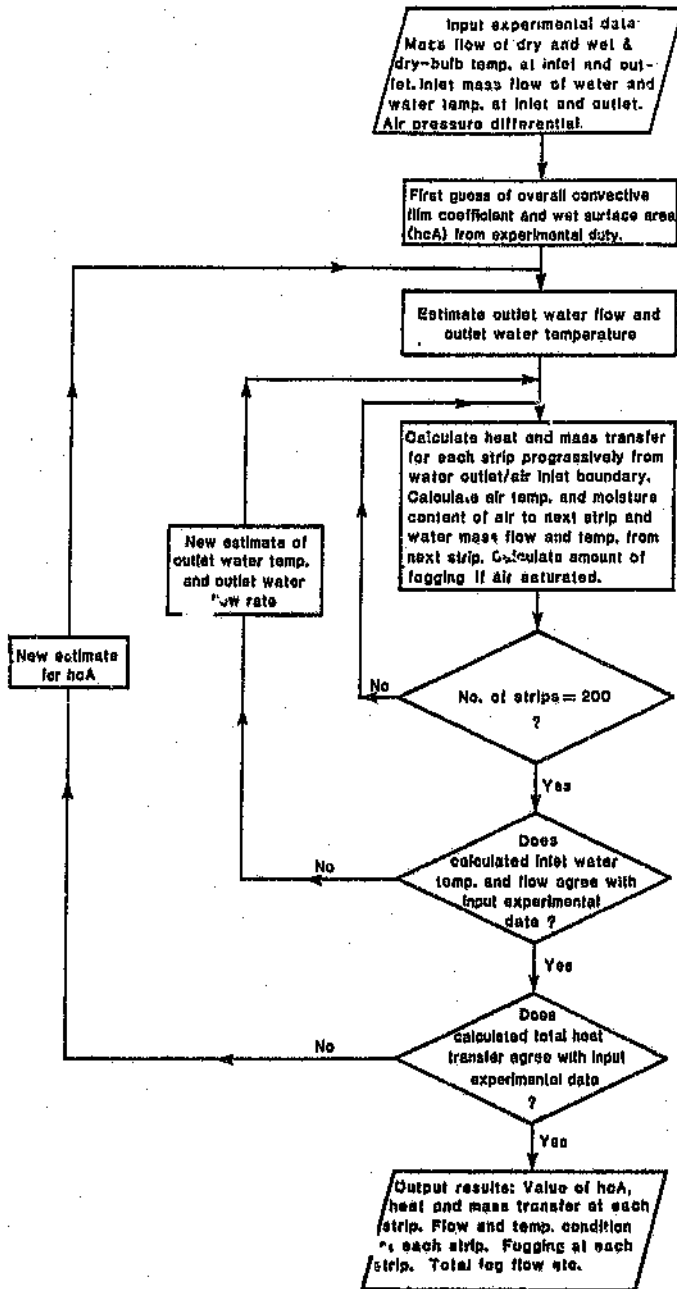


Figure 3.3 Flow diagram for computer model.

states of the fluids are directly comparable to the measured data described in Chapter 4.

A full listing of the program is given in Appendix C.

### 3.3 Typical examples of simulated data

Two typical examples of the simulator output are given below. In the first example supersaturation or fogging does not occur but in the second example it does.

In the first example a supply water flowrate of 5,80 kg/s at a temperature of 8,46 °C is used to cool an air flowrate of 4,88 kg/s from an initial air condition of 28,04 °C wet-bulb and 33,04 °C dry-bulb temperature. The air pressure at inlet is 83,66 kPa and the pressure drop across the heat exchanger is 160 Pa. The overall transfer coefficient of the heat exchanger is 7,841 kW/K. (This operating condition corresponds to Test No. 42 described in Chapter 4.) The simulator may be used to calculate the outlet air condition, the outlet water flowrate and temperature, and any intermediate value of all the parameters related to the heat and mass transfer. Some results are shown plotted in Figure 3.4. In this particular example it can be seen that the heat and mass transfer per section of heat exchanger increases almost linearly between the water inlet and outlet. It is also interesting to note that the latent heat contribution to the total heat flow varies between 60 and 70 percent. These are not general conclusions but simply apply to this example.

For the second example a supply water flowrate of 5,73 kg/s at a temperature of 39,03 °C is cooled by an air flowrate of 5,38 kg/s with an initial condition of 11,11 °C wet-bulb and 16,01 °C dry-bulb temperature.

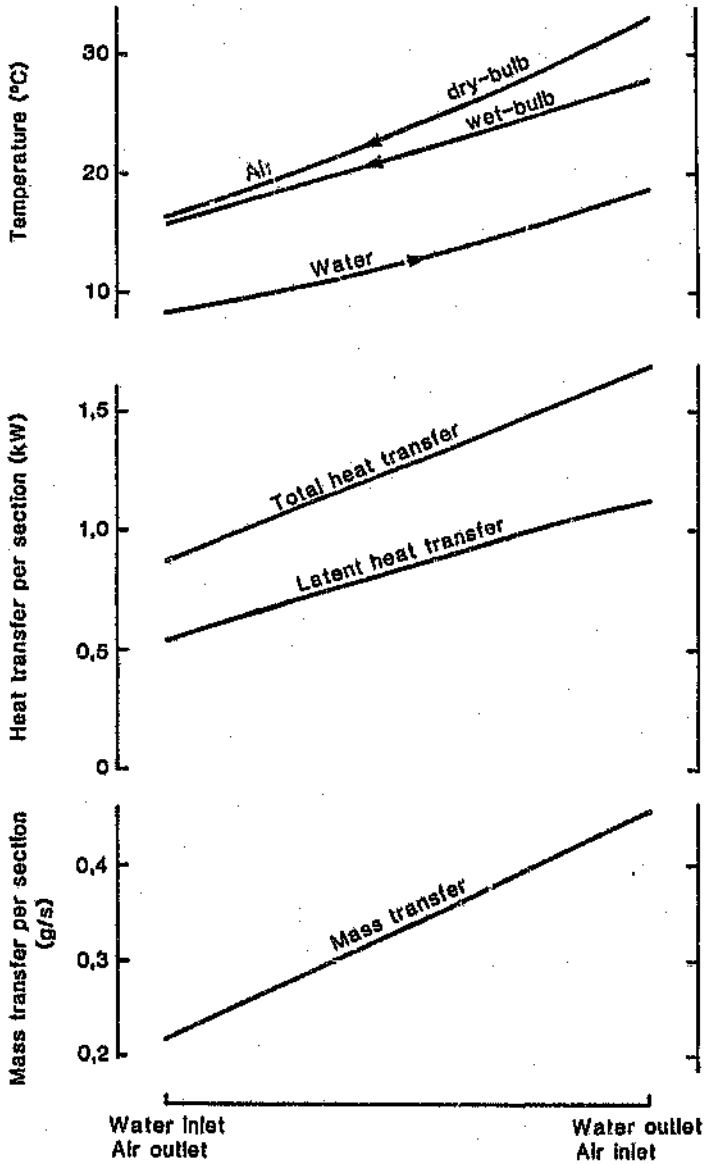


Figure 3.4 Typical results from tower simulator (no fog)

The air pressures are the same as in the first example. The overall transfer coefficient of the heat exchanger is 8,721 kW/K. (This operating condition corresponds to Test No. 58 described in Chapter 4.) Again the simulator can be used to calculate all the relevant parameters both at the end states and within the heat exchanger. Some results are shown in Figure 3.5. Take note of the commencement of fog formation once the air becomes saturated.

### 3.4 Summary

This chapter has described a computer model, based on Spalding's approach to heat and mass transfer at a wet surface, for simulating the performance of direct contact counter flow heat exchangers. From a knowledge of the value of the parameter,  $h_c A$ , all internal and end state conditions may be predicted given the inlet flow, inlet temperature and air pressure conditions. The model is verified in Chapter 5 where it is concluded that it produces an extremely accurate simulation of the test heat exchangers.

The simulator thus allows the study of the heat and mass transfer from the end state point of view as well as on a 'microscopic' scale in which the fundamental heat and mass transfer processes can be examined. For example, the value of the diffusion coefficient and the value of the index in  $(Pr/Sc)^Z$  from Equation 2.7 will be examined using this model in conjunction with experimental data (see Chapter 5). Another example is: the use of the comprehensive computer model to investigate changes in the overall performance parameters within the heat exchanger (see Chapter 7) and thus select appropriate values of these parameters for use in the performance equation.

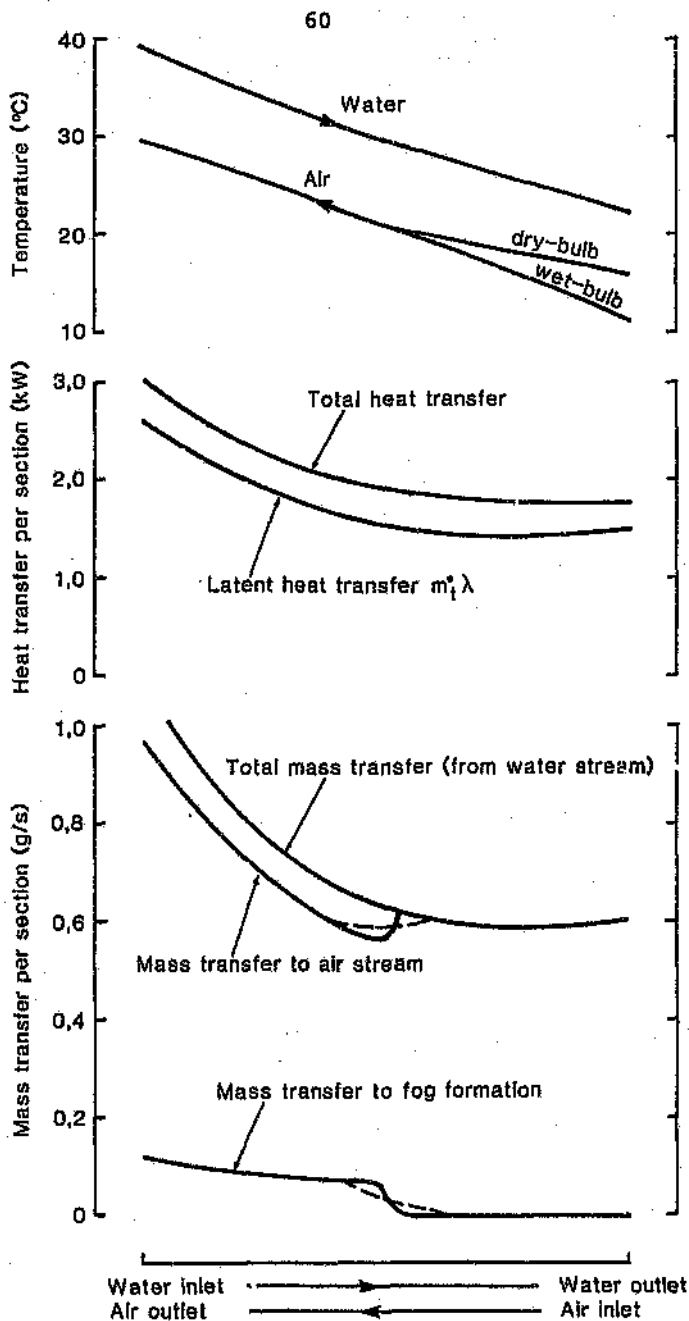


Figure 3.5 Typical results from tower simulator (for fogging conditions)

The model accounts for the possibility that supersaturation or fogging of the air stream will occur. This model is unique in this aspect and, as will be seen later, highly successful in modelling this and all the other phenomena involved. Although this computer simulator can be considered as an independent product of this research that will be useful to other researchers, it must also be considered as a means to an end. The simulator is used throughout this thesis as a tool to achieve the main objectives.

The generation of a large experimental database is now described (see Chapter 4). Using this experimental data, the verification of the computer simulator is then considered (see Chapter 5).

#### 4. EXPERIMENTATION ON A COUNTERFLOW DIRECT-CONTACT WATER AIR HEAT EXCHANGER

##### 4.1 Objective of tests

The objective of these tests was to measure mass and heat transfer rates for varying air and water temperature conditions and different heat exchange packing geometries. An experimental heat exchanger tower was constructed and tested for different flow and geometric conditions with widely varying air and water temperatures. The range of designs and process conditions covered all the typical applications.

The aims of the tests were two-fold. First, a sound set of overall performance data was needed in the development and checking of the new overall heat exchanger performance equations. Second, it was necessary to provide data which would enable a comparison of the performance of the various configurations with either evaporation or condensation and allow a fundamental examination of the combined heat and mass transfer phenomena with both evaporation and condensation.

Special emphasis was placed on experimental accuracy when designing the apparatus and conducting the tests. Detailed attention was given to quantifying the experimental error to ensure that the overall conclusions drawn are both statistically real and significant. To the best of the author's knowledge, these data (as a set) are unique.

## 4.2 Description of test heat exchangers

The tests were carried out in the Heat Exchanger Test Centre of COMRO (Chamber of Mines Research Organization). The facility makes use of a heat pump (250 kW) which provides a source of both hot and cold water. An air circuit provides a flow of air which is conditioned to a pre-selected temperature and humidity by using the hot or cold water from the heat pump. A water circuit simultaneously provides cold or hot water to the heat exchanger under examination. Thus it is possible to conduct heat and mass transfer tests using hot air and cold water or cold air and hot water. In conjunction with the water storage facility it is possible to conduct tests with heat transfer rates of up to 1 000 kW. The barometric pressure at the test site was about 83,5 kPa. Further details of this sophisticated facility are given in Appendix D.

The test rig, which is essentially a counterflow tower, is shown in Figures 4.1 and 4.2. The tower is fabricated in steel. In order to minimize heat transfer through the walls of the tower, the walls were completely covered by a 50 mm thick layer of polystyrene insulation. For descriptive purposes, the test rig can be divided into three sections: the water distribution section, the packing section and the water sump/air inlet section.

The water distribution section contains a manifold with four nozzles spraying downwards. Each nozzle produces a square water distribution pattern which divides the cross-section of the tower into four equal squares. (The nozzles are Spraying Systems Co. type 1½H230SQ, producing a 70° spray angle, see Appendix E.) For a flowrate of 1 l/s through each nozzle the required water pressure is 35 kPa.

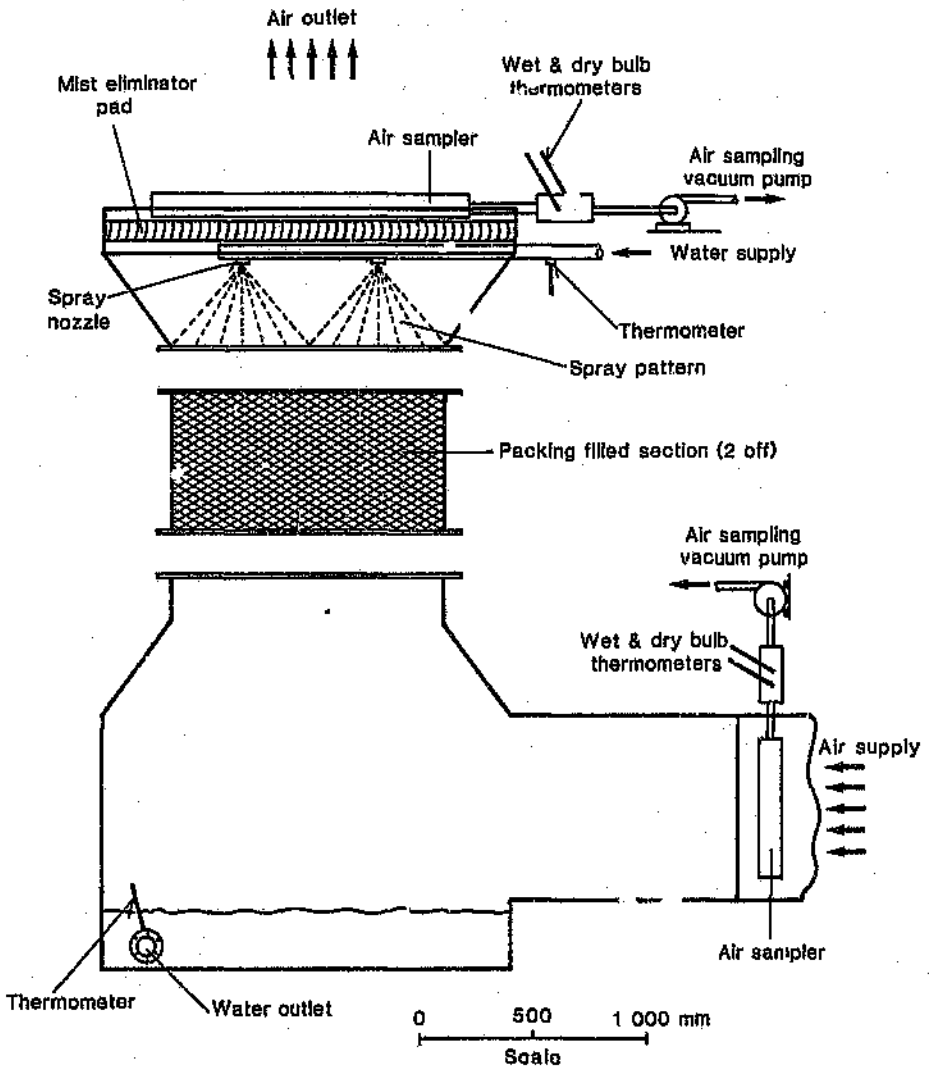


Figure 4.1 Schematic of test cooling tower

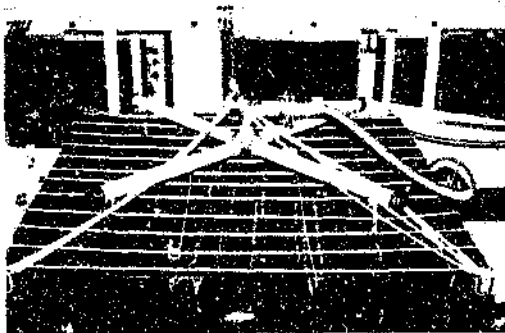


Figure 4.2 Photographs of test cooling tower

A mist eliminator pad is installed above the spray nozzles. The mist eliminator consists of interlaced plastic filaments in the form of a mat (Kimre Inc. type 16/96; see Appendix F ). Four layers of matting are used to create a pad about 100 mm thick which results in an extremely effective mist eliminator.

The packed section of the heat exchanger is made up of two modules, so that packing depths of both 0,6 m and 1,2 m can be examined. The packing medium consists of layers of corrugated PVC sheets joined together by adhesive resulting in a fluted type of fill. This type of heat transfer packing (supplied by Munters Euroform; see Appendix G) is probably the most commonly used cooling tower packing medium (both in South Africa and abroad). As shown in Figure 4.3, two different grades or flute sizes, 12 mm and 19 mm, were tested. The surface areas of the packings are  $243 \text{ m}^2/\text{m}^3$  and  $148 \text{ m}^2/\text{m}^3$  for the 12 mm and 19 mm Flute sizes respectively. The recommended minimum water loading for this packing is about 2.0 l/s per  $\text{m}^2$  while the maximum water loading is 8,3 l/s per  $\text{m}^2$ . For the test tower this corresponded to water flowrates varying between 2 and 12 l/s. The quoted operating range of air velocities is between 1,5 m/s and 4,5 m/s; for the test tower this corresponded to air volume flowrates of 2,2  $\text{m}^3/\text{s}$  to 6,5  $\text{m}^3/\text{s}$ .

The water sump/air inlet section is designed so that the inlet air flowrate is radically de-accelerated as it leaves the supply ducting at the base of the tower. This is in order to create an even distribution of air flow through the tower, which was subsequently confirmed by measurement.

Each test required the measurement of the air flowrate and air condition at the flow measuring station, the air condition into and out of the tower, the water



**19 mm  
FLUTE SIZE**

**12 mm  
FLUTE SIZE**

**MUNTERS  
PACKING**

Figure 4.3 Photographs of packing medium

flowrate to the tower, the supply water temperature, the water temperature leaving the packing section and the water temperature leaving the sump of the tower. The barometric pressure and the air pressure drop across the unit were also measured, although variations in these values are of secondary importance.

In the test facility the air flowrate is measured by determining the pressure drop across a set of flow nozzles designed to ASHRAE Standards<sup>(83)</sup>. The pressure drop across the nozzles was measured using a micromanometer. The exact air density at the measuring nozzles was determined through wet-bulb and dry-bulb temperature measurements and hence the mass flowrate of dry air could be determined. The uncontrolled air leakage in the downstream system was negligible.

The inlet air condition to the heat exchanger was determined by sampling the air flow through nozzles distributed across the ducting, by means of a small vacuum pump, and measuring the wet-bulb and dry-bulb temperatures. The outlet air condition was measured immediately above the mist eliminators. The air was sampled, through an arrangement of nozzles and a vacuum pump, and the wet-bulb and dry-bulb temperatures of the sampled air were then measured. In both cases the sampled air was drawn through a measuring section, made of 100 mm diameter tubing, which housed the thermometers. The air velocity over the damp wick of the wet-bulb thermometer was maintained at about 5 m/s. The small leakage of air from the main duct that this created was accounted for in subsequent analysis.

The water flowrate to the heat exchanger was measured using an orifice plate designed to British Standard 1042<sup>(64)</sup>. The pressure differential across the orifice plate was measured using a mercury manometer.

All temperatures were measured using carefully calibrated high precision mercury-in-glass thermometers. The temperature of the water being supplied to the heat exchanger was measured in a thermometer pocket mounted in the distribution manifold. Similarly, the temperature of the water leaving the heat exchanger was measured in the outlet drain pipe. This pipe was always full and the temperature indicated a representative mixed mean of the water in the sump.

The barometric pressure was measured using a standard Torricelli mercury barometer and the air pressure drop across the unit was determined using an inclined water manometer.

#### 4.3 Expected uncertainty in the primary measurements

Both the water and airflow rate measuring devices were designed according to standard codes which provide information for determining the uncertainties in these measurements. Through these routines it was estimated that the 'uncertainty' in the measurement of either flowrate was between one and two per cent. The water flow measurements were calibrated against readings using a tank and timer method and the 'uncertainty' of the orifice plate measurement was determined to be well within two percent. However, for the current analysis a value of two percent has been used for both the air and the water flowrates.

The term 'uncertainty' defines the range of values within which the true value will have a 95 percent probability of occurring<sup>(84)</sup>. If a normal distribution is assumed to represent the distribution of each of the random errors (see later), then the uncertainty

value is equivalent to two standard deviations.

The high quality mercury-in-glass thermometers used for all measurements have a resolution of 0,05 °C and, when calibrated against each other, all the thermometers read to within 0,05 °C over the full temperature range. The tests involved the measurement of steady state conditions; however, during any one test the temperatures might vary slightly. Based on this evidence the absolute maximum error in each of the temperature measurements has been estimated at 0,1 °C. Although this is a rough estimation the value of 0,1 °C is considered to have the same statistical meaning as the 'uncertainty' term discussed above (95 percent confidence limits, two standard deviations).

The ambient (or outlet) air pressure was measured using a standard Torricelli mercury barometer, the expected accuracy of which is estimated at 100 Pa. The pressure differential across the unit was measured to an estimated accuracy of 25 Pa with an inclined manometer.

#### 4.4 Test procedures

Each test involved a sequence of manual readings taken by the author and an associate. For each test the following steps were carried out:

- . the required flow and temperature conditions were set;
- . a period of 30 minutes was then used to allow steady state conditions to be established;
- . all the measurements were recorded repeatedly for a period of about 30 minutes, during which eight sets

- of measurements were taken;
- . the eight values of each parameter were then checked for consistency and a single representative value established, and
  - . the energy balance between the air and water streams was then checked for acceptability (see Section 4.6).

Two grade sizes of fill packing (12 mm and 19 mm flute size) were used and two depths of packing (600 mm and 1200 mm) were examined. Tests were also conducted with no packing. This was achieved by removing the packing modules and lowering the nozzle and mist eliminator section onto the water sump/air inlet section. Five different heat exchangers were thus examined. For each of these, a set of tests using cold water and hot air and another using hot water and cold air were carried out, giving a total of 10 series of data.

For each series of tests the water flowrate was varied from 3 to 12 l/s in four steps having values of 3, 6, 9 and 12 l/s. (Note that these are nominal values; the actual values varied slightly.) Also, the flowrate of the moist air was varied from 2 to 7 kg/s, again in four steps with nominal values of 2; 3,7; 5,3; and 7 kg/s. Thus, each series of tests comprised 16 sets of measurements.

#### 4.5 Measured results

The measured data are grouped into the 10 series of tests as shown in Table 4.1. All the measured results for each of the 160 tests are given in Table 4.2. The air density and mass flowrates quoted refer to the dry air component.

On average, the supply temperatures for the cold water/hot air tests were 10 °C water and 29/34 °C wet-bulb/dry-bulb air temperature; for the hot water/cold air tests they were 41 °C and 11/18 °C wet-bulb/dry-bulb respectively.

Throughout the tests the barometric pressure varied only slightly from 83,5 kPa.

#### 4.6 Energy balance criteria and correction of measured data

It is necessary to first consider some general thermodynamic criteria prior to correcting the measured data to create a heat balance.

##### 4.6.1 General thermodynamic considerations and correction of inlet water temperature for the Joule Thompson effect.

The heat flow through the walls of the heat exchanger was minimized by insulating the structure. It is estimated that for the worst set of conditions this heat flow would not be more than 0,5 kW. This is negligible and the overall system can be considered as adiabatic. The energy change of the air stream should then equal that of the water stream and any discrepancy would be due to errors of measurement.

The major energy changes are due to heat and mass transfer. However, the secondary energy effects such as kinetic energy, potential energy and pressure changes are considered below and a small correction to the inlet water temperature is introduced.

The steady flow energy equation is given below (note

that in order to account for the change in flowrate due to mass transfer, the mass flow term is included within the differential):

$$dq - d\dot{w} = d [ \dot{m} ( i + V^2/2 + gZ ) ] \quad (4.1)$$

In the thermodynamic sense a negligible amount of work is done by either stream. The kinetic energy change of the air stream between inlet and outlet is due to different duct sizes and air density. For the range of tests this energy change had a maximum value of 0,02 kJ/kg. The height of the at exchanger varied, but was on average of about 2 m; thus, the change in potential energy was also about 0,02 kJ/kg. These are both extremely small values and are regarded as negligible (incidentally, they tend to cancel each other out). Thus, the change in total energy content of the air stream is determined by the change in enthalpy alone. In calculating the enthalpy change, cognizance has been taken of the change in air pressure across the tower.

For the water stream it can again be argued that the change in kinetic energy between the inlet and discharge pipe is negligible as is the change in potential energy (which again is about 0,02 kJ/kg). Thus the change in the total energy content of the water stream is also determined by the change in enthalpy only. However, between the inlet and outlet measuring stations the water flows through the distribution nozzles where its pressure is suddenly reduced. The primary concern in this study is the heat and mass transfer in the heat exchanger; and it is convenient to divorce the thermodynamic effect of the nozzles from these effects and allow the results to be independent of

nozzle characteristics. (It is also convenient, standard and sufficiently accurate in studies of this nature for the water enthalpy to be considered as a function of temperature only.)

The nozzle water pressure is used to create a high velocity within the nozzle. This kinetic energy is subsequently dissipated in one way or another; for example, turbulence within the drops or kinetic energy being dissipated on contact with the packing. The thermodynamic details are complex, but between end states the overall process can be considered as essentially one of constant enthalpy. The Joule-Thompson coefficient<sup>(85)</sup> relates pressure and temperature changes through:

$$\mu = \left[ \frac{\partial t}{\partial p} \right]_h \quad (4.2)$$

The coefficient remains constant at a value of  $-0,24 \times 10^{-6} \text{ K/Pa}$ <sup>(86)</sup> for the range of temperatures under consideration.

The pressure-flow characteristic of the nozzles is given by:

$$\Delta p = 2,2 \dot{m}_w^2 \quad (4.3)$$

Thus the following temperature correction to the water is required:

$$\Delta T = 5,3 \times 10^{-4} \dot{m}_w^2 \quad (4.4)$$

This correction term is very small: for the full range of tests it varied between 0,005 and 0,076 K. However these effects have been accounted for and the measured inlet water temperatures have been corrected accordingly (the inclusion of the correction at the water inlet is not entirely correct but for ease of analysis this is where it is assumed to manifest itself). The values quoted in Table 4.2 incorporate this correction.

#### 4.6.2 Energy balance for test data

As shown above, the duty of the tower is determined by the change in enthalpy of either stream, and the cooling duty of the one stream should equal the heating duty of the other. The specific equations used for these calculations are:

$$dq_a = m_a (i_{a0} - i_{a1}) \quad (4.5)$$

$$dq_w = m_{w1} c_w t_{w1} - m_{w0} c_w t_{w0} \quad (4.6)$$

The duties for each stream have also been given in Table 4.2. As can be seen, the magnitude of the duty varied widely over the range of tests: from a minimum of 50 kW to a maximum of about 800 kW. The ratio of the air to water duty is given in the last column.

The error in the energy balance has been defined as the difference between the air and water duties divided by the mean value. These energy balance errors range between a minimum of -10 percent and a maximum of +8 percent. A perfect set of measurements would have a value of zero and

these errors can only be due to inaccuracies of measurement.

A frequency distribution of the heat balance error is given in Figure 4.4. The cold water/hot air tests and the hot water/cold air tests are shown independently. Clearly, there is no statistical difference in the error for the different temperature conditions (i.e. for tests with evaporation or condensation).

Correlations between the error and the airflow rate, the error and water flowrate, and the error and any mathematical combination of the two flowrates revealed no statistical foundation. However, there is a definite bias in the error to negative values. Even with this knowledge, a critical review of the test procedures and apparatus yielded no indication of the possibility of systematic errors. The possibility of the bias being caused by thermal storage effects in the system was examined and revealed no logical explanation. In fact, all possible avenues of explaining this bias were explored and no explanation was forthcoming.

The mean value of the absolute error is 4,1 percent (standard deviation 2,4 percentage points). The mean value of the actual error is -3,6 percent (standard deviation 3,1 percentage points). In the absence of any other evidence it has been concluded that the error in the heat balances are due to errors of measurements in each parameter and are to be treated as random.

#### 4.6.3 Expected error in energy balance

The error in the heat balance is calculated as a function of the primary measurements as:

$$\text{Error}_{hb} = f(m_a, m_w, t_{wb}, t_{db}, t_{wb}, t_{db}, t_{wb}, t_{db}, \Delta P) \quad (4.7)$$

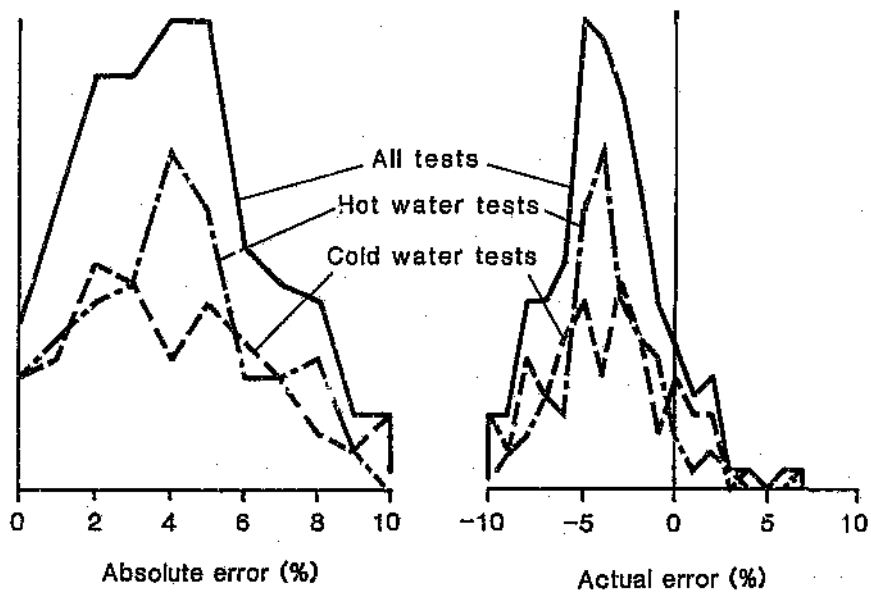


Figure 4.4 Frequency distribution of measured error in heat balance

The uncertainty in each of these measurements is given earlier. The propagation of the uncertainties in the calculation of this function and the estimation of the uncertainty in the heat balance may be calculated from standard procedures<sup>(84)</sup>, through:

$$\text{Error}_{hb} = \left[ \left( \frac{\partial hb}{\partial m'_a} e_{m'_a} \right)^2 + \left( \frac{\partial hb}{\partial m'_w} e_{m'_w} \right)^2 + \left( \frac{\partial hb}{\partial t_{wbl}} e_{t_{wbl}} \right)^2 \dots \right]^{1/2} \quad (4.8)$$

The expected uncertainty in the heat balance was calculated for numerous sets of conditions and was found to vary depending on the prevailing conditions. A limited number of these calculations are shown in Appendix H. The calculations indicated that the value varies between 3 and 6 percent but is most likely to be about 4 percent.

Hence the values of the error in the heat balance, as measured, were in accordance with what was predicted.

#### 4.6.4 Correction of data to create energy balance

In tests of this nature the measured data should be corrected so that an energy balance is created. This manipulation of the data is acceptable practice provided the correction policy is rigidly and consistently applied throughout the database. The measurements most susceptible to error are adjusted the most. From an overall statistical point of view, the accuracy of the data should be improved by this process.

It was indicated earlier that the errors would be

treated as random and that the errors in the flowrates have maximum values of about 2 percent and in the temperature measurements about 0,1 °C. The procedure adopted for correcting the measured data is as follows:

- . for each test, each of the flow and temperature measurements are corrected to some extent;
- . all corrections are such that each contribution improves the heat balance;
- . each flow measurement is corrected by  $2 \times G$  per cent and each temperature by  $0,1 \times G$  °C (the term  $G$  is a multiplying factor which would be applicable for one set of conditions; the value of  $G$  is determined iteratively on the basis of the heat balance);
- . the dry-bulb/wet-bulb temperature gap remains unmodified;
- . the measured values of the ambient air pressure and pressure differential are not modified.

The exact routine used to do these manipulations is listed in Appendix I. Because of the similarity between the measured and expected errors in the heat balance the value of the term,  $G$ , is seldom greater than unity.

The corrected results for each of the 160 sets are given in Table 4.3. This table is similar to Table 4.2 with differences due to the small adjustments required to make the air and water duty identical and the introduction of the column giving the mass transfer rate (based on changes in air moisture content). These corrected values are used in all further analysis.

#### 4.7 Estimated uncertainty in final results

The two primary results for each test are the heat transfer and mass transfer rates.

##### 4.7.1 Uncertainty in determination of heat transfer rate

As seen above, the uncertainty in the heat balance prior to correction of the data, both predicted and measured, is about 4 percent. The correction process improves this uncertainty. However the quantification of the improvement is impossible. Intuitively, it is felt that the uncertainty in the values of the total heat flow given in Table 4.3 is considerably better than 4 percent and is probably closer to half this value.

##### 4.7.2 Uncertainty in determination of mass transfer rate

The moisture transfer rate is determined by the change in humidity and the mass flowrate of the air. It was not feasible to measure the change in water flowrate between inlet and outlet of the unit and no water mass balance calculation was possible.

In estimating the uncertainty in the determination of the mass transfer rate, recourse had to be taken to the expected uncertainties in the primary measurements. The procedure followed was similar to the one used to determine the expected error in the heat balance (Section 4.6.3 and Appendix B).

Again, the expected uncertainty was calculated for numerous sets of conditions and was found to vary depending on the prevailing conditions. The value is typically 3 to 4 percent but may however be greater for large air flowrates and small heat transfer rates. The uncertainty in terms of mass transfer rate will always be less than 2,5 g/s and typically 1,5 g/s. These values may be considered as conservative since no cognizance is taken of the beneficial effect of correcting the data to create an energy balance.

Table 4.1 Grouping of test data

SERIES	TEST NO.	TOWER GEOMETRY		TEMPERATURE CONDITIONS
1	1 - 16	Spray only - No pack		Cold water / Hot air
2	17 - 32	Spray only - No pack		Hot water / Cold air
3	33 - 48	12 mm pack	600 mm deep	Cold water / Hot air
4	49 - 64	12 mm pack	600 mm deep	Hot water / Cold air
5	65 - 80	12 mm pack	1200 mm deep	Cold water / Hot air
6	81 - 96	12 mm pack	1200 mm deep	Hot water / Cold air
7	97 - 112	19 mm pack	600 mm deep	Cold water / Hot air
8	113 - 128	19 mm pack	600 mm deep	Hot water / Cold air
9	129 - 144	19 mm pack	1200 mm deep	Cold water / Hot air
10	145 - 160	19 mm pack	1200 mm deep	Hot water / Cold air

Test number	Air Pressure drop Pa	Water flow rate kg/s	Air mass flow rate (dry) kg/s	Air quantity m <sup>3</sup> /s	Density (dry air) kg/m <sup>3</sup>	Inlet water temperature °C	Outlet water temperature °C	Inlet wet-bulb temperature °C	Outlet dry-bulb temperature °C	Outlet wet-bulb temperature °C	Outlet dry-bulb temperature °C	Air Duty kJ/s	Water Duty kJ/s	
11	18	2.98	1.81	2.84	.99	11.70	15.96	33.69	37.00	28.45	28.80	32.5	-125.4	1.70
21	48	4.84	2.54	2.45	.97	4.72	15.89	33.88	41.45	21.43	23.30	148.1	-144.1	1.73
30	144	8.61	1.78	2.83	.98	7.64	11.40	32.88	41.38	15.89	18.89	192.6	-164.5	1.72
41	342	11.98	1.89	2.84	.98	7.38	16.68	32.88	41.89	12.38	13.18	187.4	-163.5	1.82
51	28	2.98	3.33	3.67	.91	11.78	15.95	36.13	32.78	27.53	27.88	56.4	-53.6	1.74
61	54	6.18	3.32	3.78	.90	6.82	12.61	27.73	37.44	21.68	21.44	144.4	-139.4	1.71
71	132	9.64	3.31	3.48	.88	6.95	12.78	27.85	37.35	15.75	15.98	216.1	-221.2	1.75
81	278	11.91	3.33	3.78	.90	7.38	11.91	27.88	37.18	13.48	14.48	234.8	-229.8	1.82
91	31	3.27	4.33	4.89	.98	8.31	13.88	27.88	38.88	24.78	26.68	78.8	-73.3	1.75
101	68	6.84	4.84	5.28	.92	4.83	12.98	24.97	32.78	28.13	21.77	131.7	-214.6	1.78
111	132	9.37	4.86	5.28	.92	7.88	12.48	24.88	32.85	15.28	16.28	212.7	-214.6	1.79
121	271	12.68	4.86	5.43	.91	11.89	14.88	27.48	34.28	18.88	21.48	247.2	-244.1	1.81
131	54	3.68	4.48	4.93	.93	8.38	13.58	26.95	32.48	24.88	26.78	83.7	-83.2	1.78
141	75	6.89	4.45	4.93	.93	7.87	14.25	25.95	32.25	24.25	22.28	144.4	-142.5	1.81
151	122	9.64	4.45	4.97	.92	7.23	13.98	26.78	33.88	17.18	18.18	244.3	-234.4	1.84
161	283	12.88	4.48	4.94	.93	8.83	13.58	25.48	32.85	14.85	15.25	241.8	-278.4	1.87
171	11	2.99	2.17	2.28	1.00	39.88	33.38	9.98	14.38	24.48	28.48	74.7	76.3	1.68
181	48	5.99	2.15	2.17	.99	43.12	33.82	11.48	18.88	31.48	32.58	294.3	213.8	1.76
191	148	8.97	2.14	2.16	.99	42.24	35.82	18.48	17.87	25.83	25.88	241.8	285.5	1.79
201	337	11.97	2.13	2.14	.99	42.45	36.93	18.48	17.58	27.38	27.38	286.4	271.3	1.78
211	28	2.99	3.78	3.78	1.00	38.88	32.18	9.48	15.95	17.88	18.48	83.4	87.4	1.75
221	51	5.99	3.68	3.68	.99	43.22	33.22	14.43	17.43	28.15	28.15	235.3	283.5	1.77
231	128	8.97	3.68	3.74	.99	42.34	32.74	14.35	17.48	31.48	33.48	388.1	374.8	1.82
241	276	11.99	3.67	3.67	1.00	42.85	33.97	18.88	18.78	35.43	35.43	442.2	431.4	1.80
251	34	2.98	5.28	5.28	1.00	43.48	34.22	18.47	17.12	17.42	17.93	122.2	122.3	1.69
261	68	3.99	5.28	5.28	1.00	41.38	34.83	18.47	17.82	24.83	24.83	281.3	272.4	1.83
271	121	8.99	5.24	5.28	.99	41.43	34.88	18.42	19.33	31.13	31.13	444.1	416.9	1.87
281	229	11.97	5.26	5.27	.99	41.45	31.35	11.47	19.88	22.83	22.83	589.3	528.5	1.86
291	33	2.99	7.81	7.81	1.01	41.42	34.72	9.38	14.33	15.98	17.88	138.3	143.3	1.73
301	75	5.99	7.83	7.81	1.00	41.49	27.35	18.53	17.45	23.27	23.27	316.4	317.6	1.79
311	122	8.99	4.99	7.81	1.00	41.48	23.68	11.38	19.23	28.17	28.17	471.2	433.8	1.82
321	282	11.99	7.84	7.81	1.00	41.45	27.73	19.38	17.88	36.43	36.58	597.4	612.4	1.86

Table 4.2 Measured results from full series of tests on experimental tower

Test number	Air Pressure drop Pa	Water flow rate kg/s	Air mass flow rate (dry) kg/s	Air quantity m <sup>3</sup> /s	Density (dry air) kg/m <sup>3</sup>	Inlet water temperature °C	Outlet water temperature °C	Inlet wet-bulb temperature °C	Inlet dry bulb temperature °C	Outlet wet-bulb temperature °C	Outlet dry-bulb temperature °C	Air duty kJ/s	Water Duty kW	
331	27	2.99	1.83	2.67	.981	9.78	28.89	33.25	37.45	26.78	21.49	125.1	1-137.9	.91
341	36	5.83	1.84	2.67	.981	9.79	15.87	32.28	37.58	15.58	14.18	158.5	1-144.8	.93
351	35	8.99	1.75	1.97	.981	9.18	15.98	32.88	34.85	11.98	12.27	144.5	1-133.7	.91
361	49	15.99	1.75	1.97	.981	9.88	13.87	32.95	37.23	12.95	13.32	151.4	1-132.4	.91
371	75	2.98	3.28	3.65	.981	9.72	23.33	31.28	34.78	22.85	22.88	131.3	1-148.5	.94
381	83	5.83	3.39	3.65	.981	8.95	17.82	29.78	35.88	19.27	19.88	212.2	1-224.8	.95
391	97	9.29	3.32	3.65	.981	7.85	13.78	29.27	33.98	12.68	13.58	238.8	1-238.8	1.00
401	114	11.99	3.31	3.67	.981	18.58	15.28	34.18	34.85	14.38	14.48	228.8	1-238.8	.94
411	147	2.98	4.81	5.27	.981	9.58	24.18	29.38	33.88	22.28	22.98	172.8	1-184.9	.96
421	164	5.83	4.84	5.27	.981	8.42	18.88	28.88	33.88	14.88	15.58	231.2	1-238.8	.97
431	188	9.29	4.23	5.28	.981	7.67	15.83	27.52	32.95	12.28	13.28	294.8	1-291.5	1.01
441	219	12.88	4.88	5.29	.981	12.78	17.45	24.85	33.85	15.33	15.88	231.5	1-238.8	.97
451	251	2.18	6.58	7.84	.981	9.68	24.88	27.67	31.78	21.73	22.68	185.8	1-188.5	.98
461	283	5.83	6.58	7.84	.981	7.92	28.34	24.82	31.88	15.73	16.98	382.7	1-318.8	.98
471	321	9.89	4.33	7.82	.981	11.99	19.38	23.95	32.58	14.97	15.33	287.4	1-281.4	1.02
481	369	11.97	4.32	6.99	.981	12.31	17.98	23.95	32.58	14.57	15.88	295.8	1-288.8	1.02
491	38	2.98	2.14	2.28	.981	42.88	27.38	12.38	19.23	31.78	31.78	187.4	1-245.6	.93
501	32	5.83	2.11	2.13	.981	39.42	29.43	12.18	17.43	34.85	34.95	233.8	1-247.9	.94
511	48	8.99	2.13	2.14	.981	41.85	33.37	11.75	18.43	38.88	38.98	293.9	1-242.6	.97
521	51	11.73	2.89	2.11	.981	42.88	36.48	12.15	19.47	37.45	37.45	274.2	1-293.2	.94
531	79	2.98	3.72	3.76	.981	43.85	22.64	11.78	18.98	28.85	28.88	235.9	1-244.9	.98
541	84	5.83	3.63	3.67	.981	39.32	23.68	11.78	17.82	32.28	32.28	334.6	1-331.4	1.01
551	89	8.99	3.72	3.73	.981	41.74	29.73	11.85	17.87	33.68	33.68	445.7	1-445.3	.96
561	114	11.73	3.44	3.68	.981	42.88	33.34	12.88	18.34	34.88	34.88	436.3	1-451.9	.97
571	135	2.98	5.39	5.82	.981	43.68	19.48	11.57	18.67	25.38	25.38	385.4	1-388.8	.99
581	144	5.83	5.29	5.28	1.00	34.12	22.34	11.29	14.18	29.58	29.58	486.2	1-422.5	.95
591	187	8.99	5.26	5.29	.981	38.64	23.53	11.79	18.44	32.18	32.18	479.5	1-514.9	.95
601	216	11.73	5.26	5.29	1.00	42.86	29.98	11.85	18.34	34.44	34.44	573.5	1-521.8	.92
611	258	2.98	7.82	7.81	1.00	43.85	14.72	11.15	18.44	24.44	24.44	346.3	1-348.1	.99
621	281	5.83	7.18	7.82	1.01	39.82	19.58	18.88	15.28	27.48	27.48	484.9	1-488.5	.96
631	318	8.99	7.81	7.88	1.00	37.74	23.84	11.88	18.27	31.83	31.83	422.3	1-443.7	.97
641	358	11.73	4.84	4.85	1.00	41.88	27.18	11.95	18.17	34.13	34.13	721.7	1-726.8	.96

Table 4.2 (Cont)

Measured results from full series of tests on experimental tower

Test number	Air pressure drop Pa	Water flow rate kg/s	Air mass flow rate (dry) kg/s	Air quantity m <sup>3</sup> /s	Wet air dry air	Inlet water temperature °C	Inlet air temperature °C	Inlet wet-bulb temperature °C	Inlet dry-bulb temperature °C	Inlet wet-bulb temperature °C	Inlet dry-bulb temperature °C	Air body °C	Water body °C	
451	46	2.94	1.92	2.15	.89	12.10	24.96	32.30	35.50	17.00	18.57	139.5	1-150.6	1.95
461	45	5.95	1.79	1.99	.89	9.62	17.06	33.60	33.25	11.20	12.60	173.3	1-167.7	1.33
471	52	6.91	1.74	1.99	.69	10.96	15.05	33.45	37.50	11.05	12.33	174.0	1-165.7	1.95
481	47	11.04	1.76	1.99	.69	16.31	14.17	33.30	34.70	11.45	12.16	174.0	1-164.0	1.95
491	110	2.94	3.33	3.66	.91	12.10	25.00	29.53	33.17	14.60	20.16	140.3	1-174.4	1.92
701	132	5.94	3.32	3.67	.91	9.62	24.10	34.20	34.15	12.10	12.50	253.7	1-266.6	1.96
711	152	6.99	3.32	3.67	.90	10.95	17.33	36.50	35.63	11.40	11.90	270.0	1-204.3	1.96
721	177	11.99	3.31	3.68	.90	8.55	14.42	36.00	35.43	10.60	10.30	286.3	1-299.9	1.95
731	231	2.94	4.91	5.32	.92	12.10	24.10	27.03	31.33	20.92	20.90	169.6	1-177.2	1.96
741	259	5.93	4.89	5.30	.92	9.62	21.35	27.73	31.97	13.10	13.50	270.0	1-290.2	1.97
751	294	6.90	4.87	5.28	.92	8.29	10.69	28.70	31.56	10.50	11.20	351.4	1-372.3	1.94
761	311	12.00	4.85	5.28	.92	8.16	15.50	28.95	32.73	9.95	10.53	343.0	1-374.2	1.97
771	302	2.99	4.83	7.03	.95	10.43	23.22	24.40	29.15	10.50	10.57	164.3	1-163.5	1.60
781	45	5.93	4.82	7.03	.94	8.72	21.03	25.33	30.60	14.15	14.43	207.0	1-207.4	1.60
791	504	6.97	6.56	7.03	.93	9.62	19.17	26.67	32.20	12.25	12.70	366.3	1-373.4	1.90
801	550	11.97	1.36	4.83	.93	9.20	16.06	27.89	32.45	11.50	12.00	379.4	1-383.7	1.99
811	47	3.02	2.14	2.17	.99	10.44	23.40	12.22	17.92	22.93	22.93	284.5	1-222.0	1.92
821	53	5.99	2.15	2.10	.99	12.10	20.71	11.65	19.10	20.45	20.43	324.2	1-337.0	1.91
831	59	6.90	2.12	2.15	.99	10.56	31.97	11.47	10.00	20.27	20.27	310.0	1-310.0	1.96
841	73	11.95	2.11	2.15	.98	11.75	33.27	13.40	20.45	10.27	10.27	327.0	1-346.5	1.96
851	128	3.01	3.65	3.60	.99	11.30	10.39	11.94	17.93	20.93	20.93	270.0	1-295.7	1.94
861	131	5.99	3.64	3.69	.99	12.32	23.83	11.10	10.65	24.57	24.57	443.0	1-094.2	1.94
971	150	6.99	3.63	3.60	.99	11.04	27.30	11.15	10.30	17.93	17.93	366.0	1-331.0	1.95
880	177	11.92	3.63	3.67	.98	11.93	31.23	13.17	20.00	20.20	20.20	527.4	1-537.2	1.95
891	220	3.01	5.27	5.29	1.00	11.30	15.53	11.67	17.72	22.40	22.40	317.0	1-335.3	1.99
901	251	5.99	5.27	5.29	1.00	12.10	24.10	11.25	10.43	23.07	23.07	333.0	1-377.0	1.96
911	294	6.99	5.20	5.29	1.00	11.49	23.73	10.97	10.31	20.13	20.13	442.9	1-443.5	1.96
921	343	11.95	5.23	5.30	.99	12.90	27.96	12.62	10.44	20.00	20.00	701.2	1-737.2	1.96
931	300	3.01	7.04	7.01	1.00	11.79	13.90	11.53	17.50	23.20	23.20	341.0	1-237.4	1.91
941	434	5.99	7.03	7.00	1.00	12.52	17.05	11.73	10.45	21.07	21.07	999.4	1-433.5	1.95
951	494	6.94	7.03	6.97	1.01	11.54	21.06	10.42	17.42	23.40	23.40	740.4	1-745.3	1.97
961	529	11.99	6.64	6.65	1.00	12.10	26.40	12.93	10.32	24.03	24.03	701.3	1-021.0	1.95

Table 4.2 (Cont) Measured results from full series of tests on experimental tower

Test number	Air Pressure drop Pa	Water flow rate kg/s	Air mass flow rate (dry) kg/s	Air quantity m <sup>3</sup> /s	Density (dry air) kg/m <sup>3</sup>	Inlet water temperature °C	Outlet water temperature °C	Inlet wet-bulb temperature °C	Inlet dry-bulb temperature °C	Outlet wet-bulb temperature °C	Outlet dry-bulb temperature °C	Air Ratio W	Water Ratio W	
979	19	2.73	1.99	2.15	.89	9.45	28.53	33.49	37.62	21.46	21.98	126.4	1-137.4	.92
981	22	5.91	1.88	2.12	.89	8.67	15.71	32.85	36.58	14.73	15.33	163.5	1-177.1	.92
991	26	9.81	1.89	2.12	.89	19.35	16.38	36.87	38.78	13.85	13.33	149.7	1-191.6	.98
999	42	11.74	1.99	2.15	.89	18.83	14.58	33.48	37.59	15.46	16.69	171.1	1-183.6	.93
9911	54	2.94	3.33	3.73	.93	9.55	22.68	31.16	37.25	22.28	25.87	156.2	1-181.8	.95
1021	68	6.89	3.31	3.78	.89	13.25	21.37	31.45	36.12	19.45	19.53	291.9	1-246.5	.92
1031	78	6.99	3.28	3.68	.89	12.25	18.68	31.48	36.53	16.48	17.83	238.8	1-221.7	1.00
1044	87	11.72	3.38	3.69	.89	18.88	16.83	31.88	36.55	16.59	16.98	243.6	1-257.5	.94
1054	114	2.93	4.98	6.39	.91	9.58	23.48	29.68	35.38	23.18	23.18	182.4	1-173.9	.97
1061	126	6.88	4.92	5.39	.91	9.17	19.28	29.55	34.58	17.58	18.55	245.8	1-267.1	.95
1074	148	8.87	4.88	5.27	.93	13.89	17.77	25.47	32.42	18.88	17.48	171.3	1-178.4	.98
1081	166	11.93	4.87	5.26	.93	12.38	16.38	23.88	32.53	16.53	17.28	189.4	1-198.8	.95
1091	221	3.83	6.87	7.43	.92	18.14	25.88	28.83	33.58	22.28	23.58	195.3	1-193.4	1.01
1101	238	5.98	6.81	7.13	.92	11.32	21.58	27.88	33.55	19.38	26.78	258.4	1-246.9	.99
1118	264	8.89	6.63	7.14	.93	11.24	19.83	26.78	33.27	16.88	18.28	286.8	1-285.3	.93
1128	302	11.98	6.67	7.13	.93	11.47	16.93	25.58	32.18	16.58	17.65	249.6	1-276.2	.98
1131	18	2.99	2.89	2.13	.98	11.48	28.83	12.75	28.48	36.28	36.28	157.9	1-173.5	.91
1141	22	5.98	2.11	2.14	.95	11.74	31.38	11.55	18.42	35.88	35.88	252.8	1-272.4	.95
1151	29	9.81	2.18	2.14	.98	11.81	33.85	12.73	28.43	37.32	37.32	274.8	1-283.6	.98
1161	42	11.98	2.18	2.14	.98	11.88	34.18	12.47	19.98	37.35	37.35	273.2	1-282.9	.97
1171	52	3.88	3.43	3.64	.99	12.81	24.38	11.82	18.48	27.32	27.32	239.3	1-239.3	.96
1180	68	5.98	3.43	3.68	.99	11.92	27.68	16.89	18.88	32.85	32.85	259.6	1-287.8	.93
1191	71	9.81	3.44	3.71	.99	16.43	36.23	12.85	19.88	34.43	34.43	391.4	1-302.8	.97
1201	89	11.91	3.43	3.78	.99	11.15	33.18	11.93	19.32	35.48	35.48	429.8	1-311.9	.95
1211	118	3.88	5.29	5.38	1.00	12.81	28.68	16.78	17.42	25.18	25.18	219.1	1-287.8	.98
1221	123	5.98	5.23	5.27	1.00	12.88	28.85	18.73	17.97	36.45	36.45	441.4	1-441.4	.95
1231	142	9.81	5.25	5.29	.99	39.95	27.32	11.47	19.32	32.33	32.33	489.9	1-495.1	.99
1241	167	11.93	5.24	5.29	.99	11.73	36.48	11.98	19.59	34.88	34.88	549.8	1-585.4	.94
1251	197	3.88	7.84	7.83	1.00	12.66	17.84	18.59	17.48	23.48	23.48	329.8	1-336.2	1.00
1261	221	5.98	7.85	7.81	1.01	12.82	21.28	16.28	17.43	29.98	28.78	527.3	1-536.8	.98
1271	253	9.81	7.82	7.82	1.00	39.48	24.17	11.18	18.85	36.73	36.73	587.7	1-594.3	.99
1281	271	11.92	6.91	7.79	1.00	11.78	27.67	11.48	19.38	33.28	33.28	617.6	1-731.3	.95

Table 4.2 (Cont) Measured results from full series of tests on experimental tower

Test number	Air Pressure drop Pa	Water flow rate kg/s	Air mass flow rate (dry) kg/s	Air humidity g/kg	Density (dry air) kg/m <sup>3</sup>	Inlet water temperature °C	Outlet water temperature °C	Inlet wet-bulb temperature °C	Inlet dry-bulb temperature °C	Outlet wet-bulb temperature °C	Outlet dry-bulb temperature °C	Air duty kJ/s	Water duty kJ/s	
1291	34	3.69	1.89	2.16	.98	16.81	21.68	31.77	33.25	27.93	16.37	139.3	1-168.3	1.93
1391	38	3.99	1.89	2.11	.99	9.42	16.78	32.35	35.18	31.64	12.87	174.5	1-168.2	1.93
1311	46	3.96	1.99	2.12	.98	1.46	14.83	32.45	33.58	18.85	11.93	182.5	1-175.2	1.94
1321	59	11.93	1.86	2.89	.89	12.83	15.48	32.83	34.49	14.29	13.68	166.8	1-175.4	1.95
1331	99	3.69	3.32	3.67	.98	16.83	25.35	36.53	33.95	29.22	26.52	172.4	1-187.4	1.92
1341	108	6.84	3.32	3.66	.91	9.32	19.37	36.19	32.89	13.15	17.35	244.1	1-236.1	1.95
1351	114	8.94	3.32	3.66	.90	9.84	16.58	36.83	31.95	11.45	12.83	273.5	1-204.5	1.97
1361	136	11.94	3.35	3.68	.91	11.29	16.33	29.78	32.72	13.43	13.78	235.1	1-237.1	1.92
1371	176	3.69	4.98	5.33	.92	18.73	25.43	28.32	32.42	29.53	24.95	182.1	1-199.2	1.96
1381	194	6.89	4.88	5.28	.92	9.32	28.89	28.18	34.59	14.15	14.58	285.4	1-235.4	1.97
1391	222	6.94	4.81	5.38	.91	9.34	17.78	29.22	37.59	12.27	12.88	349.8	1-321.2	1.96
1401	295	11.95	4.83	5.25	.92	18.95	16.95	28.29	32.87	13.33	13.68	295.5	1-345.9	1.98
1411	298	3.69	6.37	7.82	.94	16.91	25.13	26.28	34.13	24.87	24.52	182.5	1-183.3	1.96
1421	327	6.89	8.59	7.81	.94	9.48	21.84	25.57	28.82	14.78	15.89	318.2	1-319.6	1.98
1431	373	8.94	4.57	7.81	.94	9.01	13.73	25.88	34.62	12.65	13.85	349.2	1-319.4	1.98
1441	439	11.97	4.95	7.82	.93	18.68	17.87	26.94	31.89	13.29	13.85	356.2	1-347.2	1.97
<hr/>														
1451	35	2.98	2.16	2.13	.99	36.68	23.29	12.26	11.89	38.29	39.29	161.5	173.5	1.93
1461	39	6.85	2.89	2.12	.99	37.82	27.96	11.97	17.99	34.38	34.38	223.5	236.1	1.93
1471	46	9.83	2.16	2.12	.99	37.73	36.95	11.23	17.35	35.97	35.97	255.5	247.1	1.96
1481	59	11.99	2.86	2.89	.99	34.88	36.78	11.44	17.15	33.48	33.48	289.5	218.6	1.96
1491	98	2.98	3.61	3.67	.99	37.13	18.84	11.84	18.38	27.38	27.38	224.7	234.7	1.96
1501	182	6.84	3.65	3.69	.99	37.42	24.85	11.94	18.59	32.45	32.35	334.5	349.8	1.96
1511	183	9.82	3.66	3.69	.99	38.89	27.32	11.21	17.87	34.75	34.75	469.8	421.7	1.97
1521	137	12.89	3.65	3.68	.99	34.82	28.83	11.73	18.83	32.35	32.35	343.7	334.7	1.97
1531	173	2.99	5.25	5.29	1.00	37.47	15.93	11.64	18.17	25.18	25.18	245.4	235.7	1.96
1541	195	6.83	5.25	5.28	.99	37.72	21.81	11.94	18.55	38.43	38.43	423.5	434.2	1.98
1551	222	8.97	5.27	5.29	1.00	38.32	24.28	11.63	18.87	33.47	33.47	544.2	547.2	1.99
1561	261	12.88	5.29	5.31	1.00	34.25	25.25	11.71	18.39	31.36	31.36	453.5	458.1	1.97
1571	287	2.98	7.82	7.81	1.00	37.77	14.28	12.19	18.19	25.37	25.37	297.2	299.6	1.96
1581	328	6.84	7.82	7.81	1.00	37.82	18.45	11.99	18.39	28.75	28.75	486.5	542.3	1.97
1591	376	8.99	7.81	7.81	1.00	38.53	21.78	11.14	18.17	31.77	31.77	636.5	636.3	1.98
1601	444	11.98	7.89	7.86	1.00	33.79	23.17	11.46	18.29	29.87	29.87	548.2	549.8	1.98

Table 4.2 (Cont)

Measured results from full series of tests on experimental tower

Test number	Air pressure drop Pa	Water flow rate kg/s	Air mass flow rate (dry) kg/s	Air quantity m <sup>3</sup> /s	Supply (dry air) kg/s	Inlet water temperature °C	Outlet water temperature °C	Water wet-bulb temperature °C	Inlet dry-bulb temperature °C	Outlet wet-bulb temperature °C	Outlet dry-bulb temperature °C	Duty kWh	Mass transfer kg/s
11	10	2.97	1.81	2.84	.88	11.72	15.89	33.89	37.81	28.44	26.79	52.9	-14.4
21	48	5.89	2.17	2.49	.87	6.61	12.91	33.86	41.74	21.31	23.81	152.9	-43.6
31	144	8.76	1.81	2.86	.88	7.13	11.32	32.88	41.43	14.92	16.72	158.9	-42.7
41	342	12.63	1.79	2.83	.88	7.36	18.62	32.78	48.98	12.32	15.12	166.3	-44.8
51	29	2.96	3.37	3.72	.91	11.74	15.91	38.19	32.94	27.51	27.78	52.9	-13.3
61	54	6.93	3.39	3.70	.90	6.62	12.51	29.83	37.56	26.98	21.39	151.8	-36.3
71	132	8.93	3.35	3.72	.90	7.69	12.64	29.91	37.41	15.49	16.84	214.3	-38.8
81	276	11.97	3.32	3.68	.90	7.38	11.94	29.77	37.87	15.43	14.43	232.8	-48.6
91	31	3.25	4.34	4.83	.98	6.54	13.77	29.63	38.83	26.47	28.57	72.6	-14.7
101	68	5.98	4.88	5.22	.92	6.87	12.98	28.99	32.72	28.11	21.75	152.8	-38.1
111	132	9.35	4.87	5.26	.92	7.61	12.39	26.81	32.66	15.19	19.19	213.5	-57.1
121	271	12.71	4.33	5.82	.91	11.49	14.81	29.39	36.19	18.81	21.41	246.8	-58.8
131	54	2.99	6.47	6.97	.93	8.37	13.49	26.86	32.41	23.99	26.69	61.7	-16.1
141	75	6.61	6.43	6.91	.93	7.86	14.26	25.94	32.24	28.26	22.21	163.4	-37.7
151	123	5.88	6.39	6.91	.93	7.28	14.94	26.66	33.76	17.14	18.14	297.7	-61.2
161	283	14.92	6.92	6.98	.93	8.86	12.47	25.43	32.88	14.82	19.22	274.2	-73.3
171	11	2.98	2.28	2.21	1.09	38.98	33.22	9.88	16.28	26.42	28.42	75.4	26.9
181	48	5.92	2.17	2.28	.99	43.66	35.89	18.94	17.94	32.46	32.56	287.9	86.3
191	148	8.94	2.15	2.17	.99	42.23	38.54	18.58	17.88	33.85	35.99	283.2	87.2
201	337	11.92	2.14	2.15	1.09	42.43	36.95	19.66	17.55	37.32	37.32	288.3	93.4
211	28	2.96	3.74	3.74	1.09	38.75	32.15	9.35	15.99	17.95	18.45	85.9	36.1
221	51	5.94	3.59	3.71	.99	43.18	33.26	18.39	17.39	28.19	28.19	238.7	85.3
231	126	9.93	3.66	3.68	.99	42.38	32.67	18.38	17.71	33.57	33.57	386.4	127.8
241	276	11.92	3.69	3.69	1.09	42.32	34.86	9.97	16.75	35.46	35.46	446.8	146.4
251	24	2.98	5.28	5.28	1.09	43.48	34.22	18.87	17.12	17.62	17.93	122.2	48.5
261	68	6.84	5.23	5.24	1.09	41.35	34.88	16.12	17.57	24.78	24.78	274.9	93.7
271	121	9.16	5.13	5.18	.99	41.59	34.79	11.71	19.42	31.84	31.84	431.1	144.6
281	229	11.84	5.32	5.33	.99	41.48	31.48	11.62	19.63	32.88	32.95	517.9	172.7
291	55	2.96	7.15	7.09	1.01	41.57	38.78	9.32	16.47	16.84	17.86	146.4	53.8
301	75	3.97	7.85	7.83	1.08	41.48	29.36	19.82	17.44	23.28	23.28	316.1	107.7
311	122	9.83	6.96	6.98	1.08	41.58	29.66	9.48	19.25	28.15	28.15	487.6	158.5
321	282	11.84	7.13	7.18	1.08	41.39	29.79	18.44	17.74	38.31	38.36	599.2	197.9

Table 4.3 Corrected results from full series of tests on experimental tower

Test number	Air pressure drop Pa	Water flow rate kg/s	Air mass flow rate (dry) kg/s	Air quantity m <sup>3</sup> /s	Density (dry air) kg/m <sup>3</sup>	Inlet water temperature °C	Outlet water temperature °C	Inlet wet-bulb temperature °C	Inlet dry-bulb temperature °C	Outlet wet-bulb temperature °C	Outlet dry-bulb temperature °C	Duty h	Mass transfer g/s
331	27	2.82	1.88	2.13	1.08	9.84	28.67	33.38	37.88	28.57	21.27	131.2	-38.7
341	38	5.78	1.87	2.11	1.09	9.17	18.79	32.28	37.58	18.42	14.82	162.2	-45.5
351	38	8.86	1.78	2.91	1.09	9.28	13.87	32.99	36.76	11.87	12.16	171.9	-49.4
361	49	11.84	1.77	1.99	1.09	9.94	13.81	32.11	37.29	12.89	13.26	134.3	-43.1
371	73	2.85	3.33	3.72	1.06	9.81	23.25	31.28	36.28	21.97	22.72	154.9	-45.9
381	83	3.77	3.36	3.78	1.06	8.92	17.78	29.77	35.87	15.24	15.73	217.4	-39.8
391	97	7.22	3.33	3.66	1.01	7.85	13.69	29.28	33.91	11.99	13.49	238.5	-65.9
401	116	11.88	3.34	3.78	1.06	18.35	15.15	36.15	36.88	14.33	14.63	233.2	-62.2
411	147	2.87	4.86	5.33	1.01	9.64	24.84	29.36	33.88	22.14	22.84	177.4	-47.2
421	184	3.86	4.88	5.32	1.02	8.46	18.76	28.84	33.84	15.76	16.46	235.2	-67.1
431	188	9.32	4.82	5.24	1.02	7.66	15.84	27.81	32.94	12.21	13.21	293.8	-76.3
441	219	11.93	4.91	5.32	1.02	12.01	17.42	26.86	33.86	15.34	15.77	234.2	-87.3
451	251	2.89	6.37	7.07	1.03	9.63	24.78	27.69	31.89	21.73	22.58	188.1	-48.9
461	233	5.81	6.68	7.99	1.03	7.95	29.27	26.85	31.83	15.72	16.87	386.5	-88.8
471	321	9.83	6.51	6.98	1.03	11.95	19.33	25.98	32.47	15.86	15.36	284.8	-66.4
481	389	12.84	6.49	6.98	1.03	12.29	18.88	25.93	32.56	14.89	15.82	292.9	-88.6
491	38	2.92	2.21	2.25	1.08	42.78	27.41	12.19	19.24	31.81	31.81	194.8	84.7
501	32	5.72	2.14	2.17	1.09	39.33	29.74	12.89	12.58	35.84	35.84	239.3	78.4
511	48	9.92	2.15	2.18	1.09	41.88	33.41	11.71	11.41	38.84	38.84	287.4	97.1
521	51	11.36	2.12	2.14	1.09	41.99	36.48	12.87	18.41	37.83	37.83	288.9	93.4
531	79	2.84	3.74	3.78	1.09	43.82	22.83	11.67	18.75	28.81	28.81	258.6	86.9
541	84	5.74	3.71	3.73	1.09	39.44	23.88	11.62	16.94	32.28	32.28	342.7	111.2
551	99	8.78	3.77	3.88	1.09	41.48	29.82	18.98	17.98	35.78	35.78	434.6	138.4
561	114	11.63	3.68	3.72	1.09	42.83	33.35	11.95	18.25	36.83	36.83	442.9	146.3
571	153	2.97	5.48	5.43	1.09	43.59	19.61	11.56	18.66	24.31	26.31	386.9	183.8
581	164	5.73	5.38	5.37	1.08	39.83	22.39	11.11	16.81	29.89	29.89	411.5	131.9
591	187	8.76	5.35	5.38	1.08	38.56	23.65	11.62	18.32	32.18	32.18	491.5	162.5
601	216	11.45	5.48	5.42	1.08	41.93	36.83	11.72	18.17	34.73	34.73	595.5	194.7
611	258	2.98	7.83	7.82	1.08	43.95	16.73	11.14	18.39	24.61	24.61	347.4	118.9
621	281	5.74	7.21	7.12	1.01	38.89	19.57	18.73	15.13	27.67	27.67	428.3	121.3
631	318	8.88	7.89	7.88	1.08	39.89	23.85	11.83	18.22	31.88	31.88	433.2	200.8
641	358	11.38	6.96	6.93	1.08	41.81	27.17	11.88	18.38	34.22	34.22	737.4	245.6

Table 4.3 (Cont) Corrected results from full series of tests on experimental tower

Test number	Air pressure drop Pa	Water flow rate kg/s	Air mass flow rate (dry) kg/s	Air quantity m <sup>3</sup> /s	Density (dry air) kg/m <sup>3</sup>	Inlet water temperature °C	Outlet water temperature °C	Inlet wet-bulb temperature °C	Inlet dry-bulb temperature °C	Outlet wet-bulb temperature °C	Outlet dry-bulb temperature °C	W/W	Mass transfer g/s
651	48	2.87	1.96	2.28	.89	12.22	23.89	32.41	33.68	17.59	18.46	144.8	-42.9
663	45	3.04	1.61	2.83	.89	9.71	16.91	33.89	33.34	11.11	11.91	168.8	-54.9
673	52	4.81	1.78	2.81	.88	11.82	15.88	33.38	37.33	11.58	12.28	178.7	-52.2
689	67	11.73	1.78	2.81	.88	16.56	14.12	33.33	36.73	11.68	12.16	177.6	-51.7
691	118	2.87	3.48	3.75	.91	12.22	23.76	29.67	33.29	19.48	19.98	167.9	-47.2
769	132	5.87	3.36	5.71	.96	9.68	28.84	38.26	34.21	12.84	12.44	268.6	-72.4
711	152	8.98	3.38	3.73	.98	18.89	17.38	38.63	35.68	11.38	11.88	274.8	-74.8
721	177	11.86	3.38	3.72	.98	8.61	14.37	38.86	35.49	9.84	10.24	291.1	-79.8
731	231	2.91	4.47	5.38	.92	12.16	26.94	27.91	31.59	28.46	28.84	174.1	-46.4
741	259	5.69	4.93	5.34	.92	9.66	21.31	27.77	32.81	13.65	13.46	294.2	-78.3
751	294	8.83	4.94	5.37	.92	8.38	17.92	28.78	31.58	18.42	11.12	368.4	-169.4
761	341	11.91	4.88	5.32	.92	8.22	15.46	28.99	32.77	9.91	18.49	367.9	-168.3
771	382	2.99	6.64	7.82	.95	18.43	23.23	24.47	29.14	18.51	18.58	163.8	-35.7
781	436	5.93	6.62	7.83	.96	9.72	21.85	25.33	38.68	14.15	14.48	287.7	-71.2
791	484	8.92	6.59	7.87	.93	9.45	19.14	26.78	32.33	12.22	12.67	267.3	-62.3
881	556	11.94	6.38	6.85	.93	9.29	16.79	27.81	32.46	11.49	11.99	381.3	-96.7
811	47	2.94	2.28	2.23	.99	48.58	23.74	12.88	17.78	33.87	33.87	213.2	69.8
821	53	5.81	2.21	2.24	.99	42.27	28.86	11.58	19.83	39.38	39.38	348.3	114.2
831	59	8.78	2.15	2.18	.99	48.58	32.84	11.49	18.81	39.34	39.34	325.9	189.2
841	75	11.82	2.13	2.17	.98	41.78	38.32	13.33	23.48	48.32	48.32	332.8	112.1
851	128	2.95	3.72	3.75	.99	41.28	18.49	11.84	17.73	38.85	38.85	287.8	91.3
861	134	5.99	3.71	3.74	.99	42.43	22.98	11.11	18.58	36.64	36.64	473.9	157.9
871	156	8.76	3.71	3.74	.99	46.97	27.38	11.87	18.58	38.81	38.81	518.4	173.8
881	177	11.72	3.69	3.71	.98	41.83	31.31	13.89	19.92	39.28	39.28	548.6	181.7
891	229	2.99	5.31	5.33	1.00	41.34	15.87	11.83	17.88	27.52	27.52	332.8	189.2
981	259	5.99	5.33	5.37	1.00	42.43	28.17	11.18	18.56	33.94	33.94	566.8	189.1
911	294	8.76	5.36	5.37	1.00	41.42	23.81	18.89	18.25	36.21	36.21	668.8	222.8
921	343	11.88	5.32	5.37	.99	42.82	27.96	12.76	19.54	38.66	38.66	726.5	241.9
931	388	3.92	7.82	6.89	1.00	41.88	13.96	11.55	17.52	28.18	28.18	339.8	119.4
941	434	5.88	7.12	7.13	1.00	42.42	17.95	11.13	17.95	31.12	31.12	617.5	293.8
951	494	8.88	7.11	7.85	1.01	41.49	23.66	18.36	17.36	33.66	33.66	733.8	247.8
961	529	11.79	6.75	6.76	1.00	42.18	26.48	12.77	19.21	36.11	36.11	886.6	236.6

Table 4.3 (Cont) Corrected results from full series of tests on experimental tower

Test number	Air pressure drop Pa	Water flow rate kg/s	Air mass flow rate (dry) kg/s	Air quantity m <sup>3</sup> /s	Specific (dry air) kg/m <sup>3</sup>	Inlet water temperature °C	Outlet water temperature °C	Inlet wet-bulb temperature °C	Outlet dry-bulb temperature °C	Outlet wet-bulb temperature °C	Outlet dry-bulb temperature °C	Dry WB	Mass transfer g/s
978	18	2.66	1.94	2.28	.89	9.67	28.29	33.31	37.73	21.29	21.79	131.8	-38.7
981	22	5.79	1.92	2.16	.89	8.77	15.69	32.95	36.69	14.63	15.43	168.7	-49.4
991	29	8.98	1.98	2.13	.87	18.36	14.28	38.89	36.72	13.63	13.81	149.6	-46.6
1066	42	11.58	1.92	2.18	.88	16.87	14.43	33.47	37.37	15.33	15.93	174.7	-51.3
1019	64	2.89	3.38	3.78	.89	9.62	22.54	31.16	37.31	22.22	23.81	168.5	-42.9
1023	68	5.96	3.33	3.72	.89	13.38	21.34	31.48	36.65	19.42	19.62	203.5	-56.3
1031	79	9.13	3.23	3.62	.89	12.14	18.69	31.59	36.44	18.69	17.14	202.8	-65.3
1043	87	11.57	3.34	3.74	.89	16.94	15.96	31.87	36.62	16.48	16.91	247.9	-76.1
1051	114	2.91	4.93	5.42	.91	9.59	23.37	29.83	35.33	23.07	23.07	172.1	-42.5
1066	128	5.93	4.98	5.45	.91	9.23	19.14	28.61	34.56	17.44	18.49	231.2	-45.7
1075	148	8.93	4.91	5.29	.93	13.12	17.73	23.49	32.64	16.78	17.46	176.9	-38.7
1081	166	11.81	4.92	5.31	.93	12.43	16.23	23.93	32.58	16.48	17.23	192.2	-44.7
1091	221	3.64	6.85	7.41	.92	16.12	25.81	28.82	33.49	22.21	22.59	194.1	-45.4
1101	236	5.7	6.62	7.17	.92	11.33	21.49	27.81	33.56	19.25	20.78	239.7	-47.2
1111	265	8.9	6.79	7.23	.93	11.38	18.97	28.84	33.33	16.74	18.14	287.5	-71.3
1121	302	11.37	6.88	7.28	.93	11.37	16.83	25.68	32.28	16.28	17.45	268.6	-61.4
1131	16	2.99	2.13	2.19	.98	41.26	28.28	12.68	28.25	38.38	38.38	165.4	56.8
1141	22	5.94	2.16	2.19	.99	41.62	31.42	11.43	18.56	33.92	36.88	268.9	86.6
1151	29	8.98	2.13	2.17	.98	46.96	31.91	12.67	18.97	37.38	37.38	275.8	92.6
1161	42	11.88	2.12	2.16	.98	41.34	36.22	12.43	19.94	37.3	37.39	271.6	93.8
1171	52	2.97	3.67	3.76	.99	42.75	24.44	18.96	18.62	27.38	27.38	235.3	78.5
1181	60	5.84	3.74	3.77	.99	41.88	27.12	18.78	17.96	32.97	32.97	372.8	123.2
1191	71	8.94	3.69	3.74	.99	46.41	30.27	12.81	19.76	34.47	34.47	396.2	132.9
1201	89	11.74	3.78	3.75	.99	41.38	33.25	11.86	19.45	33.47	33.47	429.1	143.6
1211	110	2.98	5.33	5.34	1.00	42.76	28.84	19.66	17.38	29.14	29.14	283.9	95.3
1221	133	5.88	5.34	5.34	1.00	41.92	24.13	18.67	17.89	36.73	36.73	453.1	149.9
1231	142	8.98	5.27	5.31	.99	39.93	27.34	11.45	19.38	32.35	32.35	492.3	165.8
1241	167	11.78	5.35	5.39	.99	41.63	34.59	11.68	19.48	34.18	34.18	563.8	189.5
1251	197	3.88	7.96	7.93	1.00	42.65	17.88	18.58	17.48	23.68	23.68	338.8	112.2
1261	221	5.94	7.89	7.85	1.01	41.99	21.23	18.17	17.48	28.93	28.93	532.3	175.8
1271	233	8.98	7.84	7.84	1.00	39.38	24.19	11.88	18.83	38.77	38.77	591.5	197.9
1281	291	11.74	7.18	7.11	1.00	41.78	27.75	11.32	19.22	33.28	33.28	713.3	238.1

Table 4.3 (Cont) Corrected results from full series of tests on experimental tower

Test number	Air pressure drop Pa	Water flow rate kg/s	Air mass flow rate (dry) kg/s	Air quantity kg/s	Density (dry air) kg/m <sup>3</sup>	Inlet water temperature °C	Outlet water temperature °C	Inlet wet-bulb temperature °C	Inlet dry-bulb temperature °C	Outlet wet-bulb temperature °C	Outlet dry-bulb temperature °C	Duty kW	Mass transfer kg/s
1291 34	2.74	1.93	2.14	.90	10.91	21.98	31.87	32.35	17.83	18.27	135.6	-41.7	
1301 38	5.67	1.92	2.15	.89	9.82	16.68	32.45	33.28	11.59	11.97	179.7	-32.3	
1311 45	8.94	1.92	2.15	.90	9.83	13.96	32.52	33.37	18.58	11.48	186.6	-35.6	
1321 59	11.81	1.87	2.11	.89	12.88	15.43	32.68	33.45	13.15	13.59	168.6	-48.3	
1331 90	2.93	3.39	3.74	.90	16.95	25.21	34.63	34.97	29.18	28.48	586.3	-51.3	
1341 160	5.38	3.38	3.72	.91	9.48	19.29	36.18	32.88	13.97	13.58	238.3	-71.3	
1351 114	8.86	3.35	3.71	.90	9.89	16.46	36.87	34.89	11.41	11.99	278.9	-79.2	
1361 136	11.72	3.41	3.75	.91	11.37	16.24	29.87	32.91	13.36	13.69	243.3	-68.8	
1371 176	2.97	4.95	5.39	.92	16.99	25.59	28.38	32.48	26.47	28.89	188.8	-49.7	
1381 194	5.94	4.93	5.33	.92	9.37	28.73	28.15	38.33	14.18	14.43	298.2	-81.6	
1391 222	8.85	4.86	5.35	.91	9.39	17.73	28.27	37.33	12.72	12.63	314.7	-74.6	
1401 295	11.88	4.85	5.28	.92	19.88	16.92	28.31	32.78	13.38	13.77	381.3	-86.8	
1411 288	3.88	6.58	7.85	.94	19.91	23.12	26.39	38.46	28.86	28.33	183.8	-44.3	
1421 327	5.99	6.58	7.82	.94	9.41	21.79	26.58	28.83	14.89	13.87	318.9	-88.3	
1431 375	8.95	6.57	7.81	.94	9.88	18.73	26.88	36.42	12.65	15.83	339.9	-86.7	
1441 437	11.88	6.48	7.87	.93	18.72	17.83	26.94	31.94	13.16	13.81	388.8	-93.3	
1451 35	2.92	2.15	2.18	.99	36.88	23.31	12.18	18.49	38.31	38.31	147.4	88.5	
1461 39	5.93	2.14	2.18	.99	36.92	28.86	11.87	17.88	34.48	34.48	224.1	75.3	
1471 46	8.92	2.13	2.14	.99	37.67	31.81	11.17	17.29	36.83	36.83	259.9	85.4	
1481 59	11.88	2.88	2.18	.99	34.83	38.73	11.39	17.18	33.33	33.33	212.4	89.3	
1491 98	2.94	3.69	3.72	.99	37.87	18.87	16.57	18.23	27.37	27.37	229.9	76.7	
1501 162	5.97	3.79	3.74	.99	32.36	24.89	16.88	18.44	32.41	32.41	342.9	113.3	
1511 115	8.94	3.78	3.72	.99	38.83	27.36	11.17	17.83	34.79	34.79	415.1	138.9	
1521 137	11.91	3.68	3.71	.99	34.78	28.87	11.67	17.99	32.39	32.39	346.1	144.3	
1531 173	2.95	5.33	5.36	1.08	37.41	13.99	11.68	18.11	23.16	23.16	278.9	91.3	
1541 195	5.98	5.29	5.32	.99	32.88	21.85	11.98	18.51	28.67	28.67	429.8	142.1	
1551 222	8.95	5.38	5.31	1.08	38.29	24.28	11.11	18.85	33.49	33.49	543.6	179.6	
1561 261	11.89	5.34	5.36	1.08	34.21	25.29	11.67	18.26	31.34	31.34	499.7	151.9	
1571 287	2.94	7.11	7.14	1.08	37.71	14.34	12.84	18.94	23.43	23.43	294.6	106.2	
1581 328	5.98	7.89	7.88	1.08	37.77	18.58	11.85	18.25	28.88	28.88	493.8	163.9	
1591 374	8.93	7.87	7.86	1.08	38.51	21.82	11.11	18.14	31.81	31.81	643.4	212.9	
1601 444	11.87	7.89	7.87	1.08	33.78	23.17	11.46	18.28	29.87	29.87	548.9	181.8	

Table 4.3 (Cont) Corrected results from full series of tests on experimental tower

5           **VERIFICATION OF THE COMPREHENSIVE THEORETICAL  
MODEL AND EXAMINATION OF THE FUNDAMENTAL  
MECHANISMS OF HEAT AND MASS TRANSFER USING  
THE EXPERIMENTAL DATA**

5.1           **Introduction**

Chapter 4 presents empirical data from a series of tests on five direct-contact heat exchangers. For each heat exchanger both cold water/hot air and hot water/cold air tests were carried out. Chapter 3 presents a computer model which can simulate heat exchanger performance on the basis of a knowledge of the  $h_c A$  value and inlet flow and temperature conditions. This chapter investigates the computer simulation of the performance of the test heat exchangers so as to match the empirical data and thus check on verification of the comprehensive theoretical model.

In addition, this also enables important conclusions to be drawn regarding the areas of uncertainty in the fundamental heat and mass transfer formulations discussed in Chapter 2. Basically, four issues are examined. First, what is the best value of the index  $z$  in  $(Pr/Sc)^z$  in the analogy equation between heat and mass transfer? Second, what is the most suitable correlation equation for the diffusion coefficient? (Recall that there is conflicting information given in a number of reputable texts on values of the diffusion coefficient.) These two issues are not independent since the value of the diffusion coefficient is implicitly contained in the ratio  $(Pr/Sc)$ . Third, how successful is the numerical approach to fogging in modelling the real situation? The final question, is,

what is the difference in the value of the transfer coefficient for water cooling (evaporation) and water heating (condensation) in otherwise identical situations? This question is examined in detail in Appendix J by comparing the evaporation and condensation situations (for identical geometry and flow conditions).

## 5.2 Selecting best value of $z$ in the heat and mass transfer analogy for $(Pr/Sc)^{1/2}$

In Chapter 2 some of the fundamental aspects of heat and mass transfer were considered. The well known analogy, based on the similarity between convective heat and mass transfer, was drawn. This is now discussed in more detail.

The existence of the analogy was first shown by Nusselt<sup>(55)</sup> in 1916 (through the postulation of a Reynolds flow) and by Lewis<sup>(76)</sup> in 1922 who independently arrived at a similar conclusion. Since then a considerable amount of experimental work and numerous theoretical boundary layer studies have been carried out. This work has generally supported the contention that similar relationships may be used for the correlation of heat transfer and mass transfer data and has resulted in refinements which have made the analogy practically usable. For example, one of the best established experimental arrangements, similar in some ways to our present geometry, is turbulent flow in pipes and a considerable amount of related information is available. Deissler<sup>(53)</sup> surveyed the relevant data on heat and mass transfer and demonstrated that for the same Reynolds number, the heat transfer data and the mass transfer data fell on similar curves given by:

$$St_h = h_o / \rho V c = a Re^b Pr^z \quad (5.1)$$

$$St_m = \dot{m}_H / \rho V = a Re^b Sc^z \quad (5.2)$$

[The subscripts h and m to the Stanton number refer to heat transfer and mass transfer data correlations respectively.]

The two transfer coefficients are then related through:

$$\dot{m}_H C_{av} / h_o = (Pr/Sc)^z \quad (5.3)$$

The well accepted correlations for heat transfer data indicate that the value of z in Equation 5.1 should be 0,67. However, Deissler's<sup>(53)</sup> comparison of all the experimental data on turbulent pipe flow indicated that there are systematic deviations from Equations 5.1 and 5.2 that are related to the value of the Pr and Sc numbers. Spalding<sup>(67)</sup> points out that this observation merely signifies that the data cannot be represented totally in the simple form of Equation 5.1 and 5.2 with z = 0,67. In fact the indications are that z should be nearer to 0,5 when Pr is near unity and to 0,75 when Pr is large. To complicate matters even further, these data also indicate a dependency of the exponent z on Reynolds number.

Situations involving laminar boundary layer flow over a surface are also similar in some ways to our present geometry (compared to turbulent pipe flow they represent the other limit of possible flow regime). These flow situations are often amenable to detailed mathematical analysis, and theoretical boundary layer

studies(54) show that, for a uniform main stream velocity, the value of  $z = 0,67$  describes the trends well for Pr and Sc numbers greater than 0,5, but at smaller values the appropriate exponent changes to  $z = 0,50$ . (Unlike the turbulent pipe flow this is not influenced by changes in Reynolds number.) For the present study typical values of Pr and Sc are 0,73 and 0,61 respectively. Clearly no single value of  $z$  is always correct(67). Chilton and Colburn(77), more than fifty years ago, on the basis of relatively few data, recommended the exponent of  $z = 0,67$ . As a general recommendation this appears to have stood the test of time.

Based on the set of data generated as part of this present work, opportunity now exists to examine this issue from a fresh point of view. Advantage can be taken of the current set of data for both heat transfer and mass transfer measurements, for situations which are exactly relevant to the specific applications of cooling towers and direct-contact air coolers.

The experimental data is now examined and the applicable value of  $z$  calculated for each test. If  $z$  is considered to be a variable in Equation 5.3, then once the convective heat transfer coefficient is known, the value of the mass transfer coefficient becomes dependent on  $z$ , increasing with an increased value of  $z$ . Since both the heat transfer and the mass transfer were measured for each test it is possible to determine a unique value of  $z$  for each test.

This was done by using the computer model to simulate the experimental operating conditions for each test by adjusting the overall value of  $h_c A$  until the modelled total heat transfer was the same as the measured result, and then adjusting the value of  $z$  until the

modelled total mass transfer was the same as the measured result. This was done iteratively until both the measured heat transfer and the measured mass transfer were matched by the simulator. Hence unique values of  $h_c A$  and  $z$  were determined for each test. The matching was done to within a tolerance of 0,5 per cent for both the heat and mass transfer.

The set of calculated values of  $z$  were then examined statistically. Some of the calculated values of  $z$  were unacceptable from a statistical point of view and the 20 values furthest from the mean had to be discarded as meaningless. The remaining 140 values (about 90 per cent) were examined further and the statistical analysis of these data indicated a mean value of  $z$  of 0,65 with a standard deviation of 0,37. (This indicates that the appropriate value of  $z$  is not significantly different from 0,67.)

A similar statistical analysis was done to compare the cold water / hot air tests with the hot water / cold air tests. For the former, the mean value of  $z$  is 0,63 with a large standard deviation of 0,5 and for the latter the mean value of  $z$  is 0,67 (standard deviation, 0,05).

The mean value of  $z$  does not change significantly between the two sets of conditions and it appears that its value is not affected by the direction of mass transfer (i.e. evaporation or condensation). It is interesting to note that the standard deviation in the value of  $z$  is higher for the cold water/hot air tests than for the hot water/cold air tests. One possible explanation lies in the fact that, for the cold water/hot air tests, the ratio of latent to total heat transfer was considerably lower (56 per cent compared to 86 per cent). The modelled mass transfer rate would be

more sensitive to the value of  $z$  for the situation where the latent heat forms a smaller part of the total (recall that the model is initially forced to produce the measured total heat flow rate).

The values of  $z$  were examined for each set of tests corresponding to a different geometry. Recall that there were a total of five heat exchangers examined: one spray system and four packing arrangements. The mean value of  $z$  did not vary significantly for the different geometries. The values of  $z$  for different water and air flowrates were also compared and no statistical evidence of any trends or significantly different values of  $z$  were apparent.

Another way to examine this issue is to fix the value of  $z$  at 0,67 and use the computer program to simulate performance and predict the amount of mass transfer. A comparison of the measured and predicted mass transfer rates can be made and, if the correct value of  $z$  is being used, the simulated mass transfer and the actual mass transfer would be identical. The ratio of measured to simulated mass transfer was calculated. Of the 160 values, 140 were within three per cent of unity. The mean of the 140 values of the ratio is 1,0005 and the standard deviation 0,7 per cent. Again, a similar analysis was done for each of the different geometries, the different temperature conditions and the different flow conditions. No significant statistical deviation from a ratio of unity was observed for any of these groups of data. Clearly, a value of  $z = 0,67$  allows the mass transfer to be accurately modelled. However, the statistical significance of this sort of analysis should be considered. It may be argued that, since the simulator is being forced to give the measured total heat transfer by determining the relevant value of  $h_c A$ , the modelled mass transfer

rate would be insensitive to changes in  $z$ . In fact, the calculation of  $z$  in this manner would be trivial if the overall heat transfer was totally due to latent heat flow. In the present case the latent heat contribution varies from 56 per cent to a maximum of 86 per cent and hence the conclusions are considered real and significant.

From this section it can be concluded that for the range of situations under examination, the value of  $z = 0,67$  is indeed suitable. Its value is not affected by the direction of mass transfer (i.e. evaporation or condensation). Neither is it affected by the change in packing configuration. There was also no evidence that changes in Reynolds number, water flow (or air velocity) affected its value.

### 5.3 Validity of correlation equation for the diffusion coefficient

Having confirmed the value of  $z = 0,67$ , a brief comment can now be made on the selection of the correlation equation for the diffusion coefficient.

Recall that the dimensionless ratio,  $Pr/Sc$ , is directly proportional to the diffusion coefficient,  $D$ , and that  $Pr/Sc$  is typically equal to a value of about 1,2 (see Chapter 2). Thus, as a first order estimate, a 15 per cent increase in the selected value of the diffusion coefficient would be equivalent to changing the value of  $z$  in the previous analysis to 1,25. A 15 per cent decrease in the diffusion coefficient would be equivalent to having a value of  $z = 0,01$ .

Thus, direct parallels can be drawn to the previous section. Clearly, this reflects very well on the

choice of correlation equation for  $D$ . Although it is impossible to make a definite statement on the values of  $D$ , the exactness of the simulation for  $z = 0,67$  indicates an accurate choice of correlation for the diffusion coefficient. Certainly a combination of a value of  $z = 0,67$  and the chosen diffusion coefficient equation allow the experimental data to be accurately simulated.

#### 5.4 Simulation of experimental data and determination of overall heat transfer coefficients

Having established the above, the measured data can now be analysed further using the simulator. The computer program was used to simulate the experimental operating conditions by adjusting the input parameter,  $h_c A$ , until the simulated overall total heat transfer was the same as the measured result. This matching was done to within a tolerance of 0,01 per cent. Thus at this stage the model was forced to yield the measured total heat transfer but was left to its own devices in controlling the split between the latent and sensible components. The simulator predicted the mass transfer rate, outlet air condition, outlet water temperature, and outlet water flowrate. The amount of fogging was also quantified when the model predicted this to occur.

Table 5.1 gives specific examples to highlight the results for two tests, Nos. 42 and 58 (the same examples used earlier when discussing the output from the simulator). It should be noted that for Test 42, where the ratio of latent heat to total heat transfer was 65 per cent, the difference between the measured and predicted mass transfer was about 1 per cent. For Test 58, the difference between the measured and predicted mass

transfer was negligible. In this second case the simulator predicted a fog flow of about 7 per cent of the total mass transfer. Note also that in this case the ratio of latent to total heat flow was 83 per cent.

Table 5.2 presents all the experimental data and modelled information. This table is similar to Table 4.3 but now includes information on the modelled mass transfer rate, the ratio of latent to total heat flow, the amount of fogging predicted to have taken place within the heat exchanger, and the values of  $h_{cA}$ .

### 5.5 Validity of supersaturation or fogging algorithm

The algorithm used to model the supersaturation phenomena relies on a number of simplifications. These were discussed earlier in Chapters 2 and 3 and it was shown that the following appeared to be reasonable assumptions:

- . fog appears instantaneously with supersaturation;
- . heat and mass transfer formulations and the transfer coefficients remain unchanged by fogging;
- . air, water vapour and fog exist as a homogeneous mixture at a uniform temperature;
- . fog droplets pass through the heat exchanger packing as part of the air stream but are eliminated in the specially selected demister pads.

By comparing the modelled data with the measured data a comment can now be made on the validity of these simplifications. There are a total of 79 tests (out of

the 160) for which the simulator predicts that fogging occurred. These tests were mostly the ones in which hot water was being cooled by cold air (evaporation). However, the model was in no way constrained to this and fogging was also predicted for a few of the tests in which condensation took place.

The amount of fogging predicted to have taken place is listed in Table 5.2. It should be noted that a significant amount of the total mass transfer may eventuate as fog. Where substantial supersaturation did occur, the fogged flow was typically about 5 per cent, but in some instances it was as high as 9 per cent of the total mass transfer.

In order to judge the accuracy of the algorithm for fogging, a comparison can again be made between the measured mass transfer and that predicted by the simulator. Attention is focused now only on the tests in which fogging took place. The ratio of measured to simulated mass transfer rates for the 79 tests has a mean of 1,0003 and standard deviation of 0,19 per cent. Hence, the mass transfer rate in these tests is extremely well predicted and this reflects favourably on the algorithm used for fogging.

It is perhaps surprising just how high a proportion of the total mass transfer can result as fog; this must be considered as one of the specific findings of this study.

Clearly, the algorithm works well but it would be interesting to try to measure this fogged flow directly. In the series of tests described in the present work the mist eliminators were designed to strip the air completely of the fog droplets and this was achieved very effectively. Thus it was not possible to measure

the amount of fog directly. A further series of experiments to examine the fogging phenomena were initiated under the author's direction at a large surface mine air cooler<sup>(57)</sup> as well as at the heat transfer test facility at the University of Stellenbosch. However, no specific conclusions have yet been drawn.

#### 5.6 Direct comparison between the overall transfer coefficient for the evaporation tests and that for the condensation tests

As described above, values of the overall heat transfer coefficient,  $h_c A$ , were determined for each test and these are given in Table 5.2. The experimental test programme was structured so that, for the same flow and geometry conditions, equivalent tests were done for cold water/hot air conditions and hot water/cold air conditions. This allows the effects of these changes in temperature conditions and direction of mass transfer to be examined directly and in isolation to the flow and geometry variables.

This aspect of the investigation is considered a very important product of this research. However it must be regarded as a side issue to the main thrust of the work, namely the development of an improved method of analysis of overall heat exchanger performance. In order not to dilute the main arguments related to the primary goal, the detailed discussion of this issue has been incorporated as Appendix J. This does not detract from its general importance; Appendix J includes some novel observations, raises some important fundamental issues and identifies needs for further research. The reader is strongly advised to give this appendix due consideration.

## 5.7 Summary

The main conclusions from this empirical examination of the heat and mass transfer formulations are:

- . the best value of the index  $z$  in  $(Pr/Sc)^z$  in the analogy equation between heat and mass transfer is  $z = 0,67$ . This value, in conjunction with the chosen relationship for the diffusion coefficient, allows the experimental data to be accurately modelled;
- . the algorithm used to describe the effects of fogging within the computer simulator produces extremely accurate results;
- . the proportion of the total mass transfer that can result as fog can be as high as 9 per cent;
- . based on confirmation of the above, the computer program was used to simulate the experimental results and hence calculate values of the overall heat transfer coefficient,  $h_c A$ . These values are listed in Table 5.2;
- . the computer model was found to accurately predict the measured heat and mass transfer;
- . based on the comprehensive computer model and the unique set of data a direct comparison between the overall transfer coefficient for the evaporation tests and that for the condensation tests can be made. This is an important side issue of this research and is discussed in Appendix J.

It can be concluded that the development of the comprehensive theoretical model is successful. This simulator can be considered as an independent product of

this research that will be useful to other researchers. However as an engineering tool for the practicing field engineer it is unwieldy and over-sophisticated. Attention is now turned to using the simulator to develop a simplified method of performance analysis (see Chapter 7). Before this is done it is necessary to examine existing simplified methods and to highlight their limitations (see Chapter 6).

Table 5.1 Measured and Simulated Results for Test Nos. 42 and 58

	Test No. 42 No fog		Test No. 58 Fogging	
	Measured	Predicted	Measured	Predicted
Air flow rate (kg/s)	4,88	4,88	5,38	5,38
Inlet air temp (wb/db °C)	28,04/33,04	28,04/33,04	11,11/16,01	11,11/16,01
Inlet water flow rate (kg/s)	5,80	5,80	5,73	5,73
Inlet water temp (°C)	8,46	8,46	39,03	39,03
Overall heat transfer * (kW)	255,19	255,19	411,51	411,50
Overall mass transfer (g/s)	67,06	67,70	131,87	131,87
Outlet air temp (wb/db °C)	15,96/16,49	15,963/16,777	29,59/29,59	29,588/29,588
Outlet water temp (°C)	18,76	18,756	22,39	22,387
Fog flow leaving packing (g/s)	0,00	0,00	Unknown	8,64
Ratio Latent heat/Total heat transfer	65%		83%	

\* Note the simulation for prediction was controlled to match the measured value.

Test number	Air pressure drop Pa	Water film rate kg/s	Air mass flow rate (dry) kg/s	Inlet water temperature °C	Outlet water temperature °C	Inlet wet-bulb temperature °C	Inlet dry-bulb temperature °C	Outlet wet-bulb temperature °C	Outlet dry-bulb temperature °C	Daily m	Mass transfer (experimental) g/s	Mass transfer (modelled) g/s	Mass transfer (exp) g/s	Latent heat/Total heat kJ/kWh	Exp kJ/kWh
17 18	2.97	1.61	11.72	15.89	33.81	37.81	28.44	28.79	32.9		-14.4	-15.8	8.98	.74	.69
21 48	5.89	2.17	4.81	12.91	33.89	41.74	21.39	23.81	192.9		-43.4	-42.4	8.88	.69	2.18
31 144	8.76	1.81	7.13	11.32	32.88	41.43	16.92	16.72	188.9		-42.7	-41.8	8.88	.64	3.82
41 382	12.63	1.79	7.36	10.62	32.78	48.98	12.32	11.12	166.5		-44.8	-44.4	8.88	.64	3.82
51 28	2.96	3.37	11.74	12.91	36.19	32.94	27.51	27.76	92.5		-13.3	-13.8	8.88	.73	.88
61 54	4.85	3.39	4.12	12.51	29.83	37.56	28.98	21.36	131.8		-36.5	-39.5	8.88	.85	2.58
71 132	8.95	3.35	7.85	12.84	29.91	37.41	15.49	14.84	214.3		-35.8	-35.7	8.88	.84	4.68
81 278	11.97	4.32	7.35	11.94	29.77	37.87	13.43	14.43	232.8		-44.5	-44.2	8.88	.64	5.88
91 31	3.28	4.34	8.54	13.77	29.63	38.83	24.67	28.57	72.8		-14.7	-14.8	8.88	.63	1.85
101 49	3.98	4.85	6.87	12.88	28.99	32.72	28.11	21.75	152.8		-38.1	-39.3	8.88	.84	3.18
111 132	9.35	4.87	7.81	12.39	29.81	32.66	15.19	19.19	213.5		-37.1	-32.1	8.88	.68	5.86
121 271	12.71	4.88	11.48	14.81	29.59	34.19	18.81	21.41	244.8		-48.8	-43.1	8.88	.85	6.44
131 54	2.99	4.47	6.37	13.49	28.81	32.41	23.99	26.49	64.7		-16.1	-16.3	8.88	.62	1.23
141 78	4.81	4.43	7.64	14.26	25.94	32.26	28.26	22.21	183.4		-37.7	-44.7	8.88	.62	3.75
151 122	9.43	4.39	7.26	13.94	26.66	33.76	17.14	18.14	257.7		-41.2	-43.8	8.88	.81	4.49
161 243	11.93	4.32	8.84	13.47	25.43	32.88	14.82	19.22	374.2		-73.5	-65.4	8.88	.59	8.74
171 11	2.98	2.28	38.98	33.22	9.88	16.28	28.42	28.42	75.4		26.8	26.8	.88	.84	.69
181 48	5.92	2.17	43.66	35.88	18.94	17.94	32.46	32.56	297.9		68.5	68.4	3.62	.84	2.88
191 148	8.94	2.18	42.22	35.84	18.58	17.85	33.85	33.98	283.2		87.2	87.2	7.22	.85	3.19
201 337	11.92	2.14	42.43	36.95	18.64	17.56	37.32	37.32	288.3		95.4	95.4	4.58	.87	3.68
211 28	2.96	3.74	38.75	32.15	9.33	15.98	17.85	18.45	85.9		34.1	29.7	8.88	.84	.78
221 51	5.94	3.69	48.18	33.26	18.39	17.39	28.19	28.19	258.7		85.5	85.5	4.81	.85	2.41
231 128	9.83	3.44	42.38	33.67	18.38	17.71	33.57	33.57	381.4		127.8	127.8	9.46	.86	4.68
241 278	11.92	3.49	42.52	34.88	9.87	18.78	33.46	35.46	446.8		146.4	146.4	12.45	.86	5.49
251 34	2.98	5.28	43.48	34.22	18.87	17.12	17.62	17.95	122.2		46.5	43.2	8.88	.88	.88
261 48	4.81	5.23	41.33	36.88	18.12	17.87	24.78	24.78	274.9		93.7	93.7	3.38	.85	2.88
271 121	9.46	5.13	41.24	36.79	11.71	19.22	31.84	31.84	431.1		144.8	144.8	8.14	.84	3.28
281 228	11.84	4.32	41.48	31.48	11.42	19.83	32.88	32.95	517.4		172.7	172.9	116.94	.84	4.85
291 58	2.96	7.15	41.57	38.78	9.32	16.47	18.84	17.88	148.4		33.8	49.1	8.88	.84	1.21
301 78	5.77	7.87	41.48	29.34	18.32	17.44	23.28	23.28	316.1		187.7	187.7	7.28	.84	3.38
311 122	9.83	4.96	41.58	29.64	11.48	19.25	26.15	26.15	447.4		158.5	158.5	6.81	.85	5.23
321 282	11.84	7.13	41.39	29.79	18.44	17.74	36.31	36.36	599.2		197.9	196.1	112.58	.85	7.57

Table 5.2 Balanced experimental data and the modelled information

Test number	Air pressure dry Pa	Water flow rate kg/s	Air mass flow rate (dry) kg/s	Inlet water temperature °C	Outlet water temperature °C	Inlet wet-bulb temperature °C	Inlet dry-bulb temperature °C	Outlet wet-bulb temperature °C	Outlet dry-bulb temperature °C	Heat transfer (experimental) W/s	Heat transfer (modelled) W/s	Heat transfer (loop) W/s	Latent heat/total heat kg/s	h <sub>fg</sub> kJ/kg	
331	27	2.82	1.86	9.94	28.47	33.38	37.58	28.57	21.27	131.2	-38.7	-38.4	6.88	7.73	3.51
341	38	5.73	1.87	9.17	15.79	32.28	37.58	13.42	14.82	142.2	-45.5	-45.3	8.88	4.48	4.48
351	35	6.84	1.78	9.28	13.87	33.99	36.76	11.87	12.16	171.9	-49.4	-49.3	8.88	7.1	5.64
361	49	11.84	1.77	9.44	13.81	32.11	37.29	12.89	13.26	194.3	-43.1	-43.8	8.88	3.9	4.47
371	75	2.85	3.33	9.81	25.28	31.28	36.28	21.77	22.72	164.9	-45.4	-45.8	8.88	7.9	3.48
381	83	5.77	3.33	8.92	17.78	29.77	35.87	15.28	15.73	217.4	-58.9	-58.9	8.88	4.7	6.19
391	97	9.28	3.33	7.88	13.48	29.28	33.91	11.99	13.49	238.5	-45.2	-44.2	8.88	4.7	7.32
401	116	11.88	3.34	18.35	15.15	38.15	36.88	14.33	14.83	233.3	-42.2	-42.4	8.88	3.4	7.26
411	147	2.87	4.88	9.44	24.84	29.34	35.88	22.14	22.84	177.4	-47.5	-47.4	8.88	3.88	4.77
421	144	5.88	4.88	8.46	18.74	28.84	33.84	13.14	14.46	235.2	-47.1	-47.7	8.88	4.8	7.84
431	188	9.32	4.82	7.44	13.84	27.81	32.94	12.21	13.21	275.8	-74.3	-75.3	8.88	4.4	119.25
441	219	11.73	4.91	13.81	17.42	24.84	33.84	15.34	15.77	234.2	-57.3	-57.9	8.88	4.1	111.39
451	251	2.89	6.57	9.83	24.78	23.89	31.88	21.73	22.88	188.1	-48.8	-48.7	8.88	4.4	4.44
461	283	3.81	4.48	7.78	29.27	28.83	31.83	15.72	18.87	384.3	-68.9	-70.2	8.88	4.4	111.82
471	321	9.85	6.51	11.75	19.33	25.94	32.47	13.88	15.36	284.8	-44.4	-47.4	8.88	3.88	115.31
481	369	12.64	4.58	12.29	18.88	25.93	32.54	14.59	15.82	272.9	-48.8	-49.2	8.88	3.88	114.43
491	38	2.82	3.21	43.78	27.41	12.19	18.24	31.81	31.81	194.8	44.7	44.7	3.94	3.84	3.81
501	32	5.72	3.14	38.33	29.74	12.89	17.58	33.84	32.84	239.5	72.4	78.4	5.59	1.85	4.79
511	48	8.72	3.13	41.88	31.41	11.71	18.61	38.84	38.84	277.4	91.1	95.1	7.33	1.84	5.54
521	51	11.58	2.12	41.99	34.48	13.87	18.59	37.53	37.53	288.9	93.4	93.4	7.91	1.87	3.85
531	79	2.94	3.74	43.82	22.83	11.87	18.73	28.41	28.41	258.4	84.9	84.9	4.34	1.88	4.21
541	84	5.74	3.71	31.44	25.48	11.42	14.84	32.28	32.28	342.7	111.2	111.2	7.44	1.84	4.41
551	99	8.78	3.77	41.88	29.82	18.98	17.98	33.75	33.75	434.6	158.4	158.4	118.88	1.84	7.54
561	114	11.43	3.88	43.83	33.33	11.75	18.25	36.85	36.85	442.9	145.8	145.5	111.89	1.84	7.2
571	132	2.97	5.88	43.85	19.41	11.36	18.44	26.31	26.31	384.5	103.8	103.8	4.33	1.84	5.44
581	144	3.73	5.38	39.83	22.39	11.11	14.81	29.59	29.59	411.5	131.9	131.9	8.62	1.83	4.72
591	187	8.74	5.33	38.54	23.43	11.42	18.32	32.18	32.18	491.5	142.9	142.5	8.87	1.85	118.42
601	218	13.45	5.48	41.73	38.83	11.72	18.17	34.73	34.73	595.5	194.7	194.7	114.21	1.84	9.87
611	258	2.98	7.83	43.73	14.73	11.14	18.39	24.41	24.41	347.4	118.9	118.9	9.59	1.84	7.19
621	281	5.74	7.21	38.98	19.57	18.73	15.13	27.47	27.47	474.3	151.3	151.3	118.12	1.82	111.18
631	318	8.88	7.89	39.49	23.85	11.83	18.22	31.89	31.88	433.2	208.8	208.8	111.78	1.85	114.47
641	358	11.58	6.94	41.81	27.17	11.88	18.38	34.22	34.22	737.4	243.4	243.5	114.24	1.85	112.72

Table 5.2 (Cont)

Balanced experimental data and the modelled information

Test number	Air pressure drop Pa	Water flow rate kg/s	Air mass flow rate (dry) kg/s	Inlet water temperature °C	Outlet water temperature °C	Inlet wet-bulb temperature °C	Inlet dry-bulb temperature °C	Outlet wet-bulb temperature °C	Outlet dry-bulb temperature °C	July DB	Mass transfer (experimental) g/s	Mass transfer (modelled) g/s	Mass transfer (freq) g/s	Latent heat/total heat kWh/kWh
451	44	2.87	1.76	12.22	27.89	12.41	32.41	17.69	18.46	144.8	-42.9	-42.7	0.86	.72
461	45	3.04	1.81	9.71	16.91	33.89	33.34	11.11	11.91	188.8	-54.8	-54.2	.54	.74
471	52	4.41	1.78	11.62	15.68	33.36	37.33	11.58	12.28	175.7	-52.2	-51.7	0.89	.71
481	47	11.73	1.79	18.36	14.12	33.35	34.75	11.48	12.18	177.4	-51.7	-51.4	0.88	.71
491	116	2.87	3.48	12.22	25.74	29.67	33.29	19.48	18.98	147.9	-47.2	-47.5	0.86	.69
701	132	3.87	3.38	8.68	16.34	38.26	34.21	12.84	12.44	248.8	-72.4	-72.2	0.86	.69
711	152	8.98	3.35	18.89	27.89	38.33	33.88	11.33	11.85	276.8	-74.8	-74.5	0.86	.67
721	127	11.84	3.33	8.61	14.57	38.34	32.99	9.94	18.24	294.1	-79.4	-79.3	0.86	.68
731	231	2.91	4.97	12.16	24.64	27.91	31.39	28.44	28.84	174.1	-46.4	-47.3	0.86	.67
741	259	3.89	4.93	9.66	16.31	27.77	32.81	13.64	13.46	274.2	-78.4	-78.2	0.86	.65
751	294	8.83	4.94	8.38	17.62	28.78	31.38	18.42	11.12	348.4	-108.4	-99.4	0.86	.68
761	341	11.91	4.88	8.22	15.46	28.99	32.77	9.91	18.49	367.9	-109.3	-99.4	0.86	.67
771	382	3.99	4.44	18.43	23.23	29.47	29.14	18.91	18.58	163.8	-33.7	-38.3	0.86	.58
781	436	5.93	4.42	9.72	21.65	23.33	28.88	14.18	14.45	287.7	-71.2	-71.8	0.86	.61
791	584	8.92	4.39	9.45	19.14	24.11	32.33	12.22	12.47	349.5	-72.5	-72.3	0.86	.62
801	556	11.94	4.38	9.29	18.79	27.11	32.46	11.49	11.99	381.3	-73.7	-73.3	0.86	.62
911	47	2.94	1.29	16.58	23.74	12.88	17.78	33.87	33.87	213.2	49.8	49.8	4.43	.84
821	53	5.81	2.21	42.27	28.84	11.56	19.83	39.58	39.58	348.3	114.2	114.2	7.34	.84
831	59	8.78	2.15	16.58	32.84	11.46	18.81	39.34	39.34	325.9	189.2	189.2	7.43	.84
841	75	11.82	2.13	41.78	35.32	13.35	28.48	49.32	49.32	332.8	112.1	112.1	8.24	.87
851	129	2.95	3.72	41.28	16.49	11.81	17.73	38.85	38.85	28.11	94.3	94.3	3.83	.85
861	134	5.78	3.71	42.45	23.98	11.11	18.38	38.44	38.44	473.9	137.9	137.9	9.82	.86
871	158	8.78	3.71	46.97	27.38	11.87	18.38	38.81	38.81	318.1	173.8	173.8	10.88	.86
881	177	11.72	3.68	47.85	31.31	13.89	19.82	39.28	39.28	348.5	181.7	181.7	11.42	.87
891	229	2.99	3.31	41.54	15.57	11.83	17.68	27.82	27.82	332.8	189.2	189.2	4.97	.85
901	259	5.98	3.33	42.45	28.17	11.18	18.56	33.94	33.94	346.8	188.1	188.1	11.44	.86
911	294	8.78	3.34	41.42	23.81	15.88	18.25	34.21	34.21	448.8	222.8	222.8	11.48	.85
921	343	11.88	5.33	42.82	27.94	12.76	19.34	38.84	38.84	722.5	241.2	241.2	11.68	.86
931	388	3.82	7.82	41.84	13.94	11.33	13.82	25.18	25.18	358.8	119.4	119.4	7.53	.86
941	434	5.88	7.17	42.42	17.95	11.13	17.95	31.12	31.12	417.5	285.8	285.8	11.73	.85
951	494	8.88	7.13	41.49	21.44	18.34	17.34	33.44	33.44	733.8	247.8	247.8	11.21	.85
961	528	11.79	6.75	42.18	24.48	12.77	19.24	34.11	34.11	888.6	264.6	264.6	11.87	.86

Table 5.2 (Cont) Balanced experimental data and the modelled information

Test number	Air pressure drop Pa	Water flow rate kg/s	Air mass flow rate (dry) kg/s	Inlet water temperature °C	Outlet water temperature °C	Inlet wet-bulb temperature °C	Inlet dry-bulb temperature °C	Outlet wet-bulb temperature °C	Outlet dry-bulb temperature °C	Duty h	Mass transfer (experimental) g/s	Mass transfer (modelled) g/s	Mass transfer (reg) g/s	Latent heat/fluid heat kWh	h <sub>o</sub> °C
971	18	2.86	1.74	9.57	29.29	33.51	37.73	21.29	21.79	131.0	-58.7	-58.9	9.99	.73	2.37
981	22	5.79	1.92	8.77	15.48	35.95	36.68	14.43	15.43	168.7	-51.4	-48.8	9.99	.72	3.09
991	29	8.78	1.97	19.34	14.28	38.39	36.72	13.93	13.91	199.4	-48.4	-48.5	9.99	.67	4.93
1001	42	11.58	1.92	18.81	14.43	33.67	37.57	15.33	18.73	174.7	-51.3	-41.8	9.99	.72	4.11
1011	54	2.89	3.38	9.62	22.54	31.16	37.31	22.22	23.81	164.5	-42.9	-44.5	9.99	.68	3.45
1021	64	5.96	3.33	13.38	21.34	31.48	36.85	19.42	19.62	203.5	-45.3	-37.4	9.99	.68	4.61
1031	78	9.15	3.23	12.16	18.99	31.59	36.44	18.39	17.14	232.9	-45.3	-45.3	9.99	.78	4.61
1041	87	11.57	3.34	16.14	15.94	31.87	36.82	16.48	16.91	247.9	-48.1	-48.2	9.99	.78	4.61
1051	114	2.91	4.93	9.39	23.37	29.83	35.33	23.87	23.87	172.1	-42.5	-45.3	9.99	.65	4.99
1061	128	5.93	4.98	9.23	19.14	28.41	34.56	17.44	18.49	235.2	-45.7	-45.1	9.99	.65	7.15
1071	148	8.93	4.91	13.12	17.75	23.49	32.64	16.79	17.46	176.9	-38.7	-43.1	9.99	.56	8.43
1081	166	11.81	4.92	12.43	16.25	24.93	31.50	16.46	17.23	192.3	-44.1	-45.9	9.99	.59	7.96
1091	171	3.84	6.95	18.13	28.91	28.82	33.49	22.21	22.59	194.1	-45.4	-48.2	9.99	.64	6.49
1101	239	5.97	6.42	11.33	21.49	27.81	33.56	19.25	20.78	259.7	-47.2	-47.2	9.99	.64	8.82
1111	261	8.78	6.78	11.38	18.97	26.84	33.33	16.74	18.14	287.6	-47.3	-38.9	9.99	.61	11.17
1121	382	11.65	6.69	11.57	16.93	23.18	32.28	16.28	17.45	266.5	-41.4	-31.8	9.99	.89	11.77
1131	18	2.98	2.15	41.24	28.29	32.48	26.23	36.33	36.33	143.4	56.8	56.8	2.44	.86	2.35
1141	22	5.84	2.16	41.63	31.42	11.43	18.58	33.92	36.39	236.9	86.4	86.7	4.19	.84	4.89
1151	29	8.98	2.13	48.94	33.91	12.67	19.97	37.38	37.38	275.8	92.6	92.6	4.41	.87	4.74
1161	42	11.86	2.12	41.54	34.22	12.43	19.19	37.39	37.39	276.5	93.8	93.9	4.92	.87	3.99
1171	52	2.97	3.67	42.75	34.44	18.94	18.82	27.38	27.38	233.3	78.5	78.5	3.92	.85	3.31
1181	64	5.84	3.74	41.88	27.12	16.78	17.94	33.97	33.97	372.8	123.2	123.2	7.98	.85	5.92
1191	71	8.94	3.67	46.41	38.27	12.81	19.76	34.47	34.47	316.2	132.9	132.9	7.82	.86	4.61
1201	89	11.74	3.78	41.58	33.25	11.84	19.45	35.47	35.47	429.1	143.6	143.6	9.99	.86	4.82
1211	118	2.98	5.33	42.78	29.44	18.66	17.58	25.14	25.14	283.9	95.3	95.3	3.82	.85	4.64
1221	123	5.88	5.34	41.92	24.13	16.67	17.89	36.73	36.73	452.1	149.9	149.9	8.93	.85	7.58
1231	142	8.98	5.27	39.93	27.34	11.45	19.39	32.33	32.33	492.3	165.8	165.8	8.67	.85	6.56
1241	167	11.78	5.35	41.63	36.58	11.48	19.48	34.18	34.18	565.8	189.5	189.5	11.87	.86	8.21
1251	197	3.88	7.65	42.65	17.89	18.38	17.48	23.68	23.68	338.8	112.2	112.2	3.79	.85	4.81
1261	221	5.94	7.69	41.99	21.23	18.17	17.49	28.93	28.93	532.3	175.8	175.8	9.84	.85	9.73
1271	233	8.98	7.84	39.38	24.11	11.89	18.83	36.77	36.77	591.5	197.8	197.8	9.54	.85	11.61
1281	291	11.74	7.14	41.78	27.75	11.32	19.22	33.28	33.28	713.8	238.9	238.9	13.97	.86	11.33

Table 5.2 (Cont)

Balanced experimental data and the modelled information

Test number	Air pressure drop Pa	Water flow rate kg/s	Air mass flow rate (dry) kg/s	Inlet water temperature °C	Outlet water temperature °C	Inlet wet-bulb temperature °C	Inlet dry-bulb temperature °C	Outlet wet-bulb temperature °C	Outlet dry-bulb temperature °C	Power kW	Heat transfer (experimental) %	Heat transfer (modelled) %	Heat transfer (dry) %	Latent heat/total heat	h <sub>o</sub> h <sub>o</sub> /°C
1291	34	2.91	1.93	14.91	21.58	31.87	32.33	17.43	18.27	135.8	-41.7	-41.4	4.88	.74	3.23
1292	38	5.82	1.92	9.32	14.48	32.45	33.28	11.56	11.97	179.7	-52.3	-52.0	4.94	.71	4.33
1311	46	8.84	1.92	9.93	13.94	32.32	33.57	19.58	11.43	184.9	-53.4	-54.9	.63	.72	4.54
1320	59	11.81	1.87	12.88	13.43	32.48	34.85	13.15	13.33	184.8	-48.3	-48.2	4.88	.71	4.48
1331	69	2.93	3.39	18.73	25.21	36.85	34.67	29.18	26.48	189.3	-51.5	-52.1	4.69	.71	5.44
1341	69	5.94	3.38	9.49	19.29	36.11	32.68	15.87	13.56	236.3	-51.5	-51.2	4.69	.70	9.83
1351	114	8.84	3.33	9.89	14.44	36.87	34.89	11.41	11.99	278.9	-59.2	-58.7	4.69	.70	119.34
1361	134	11.72	3.41	11.37	16.24	29.87	33.81	13.34	13.84	243.3	-48.9	-48.7	4.69	.70	9.84
1371	174	2.92	4.93	18.78	28.38	32.48	34.47	28.47	28.89	184.3	-48.9	-48.9	4.69	.67	7.52
1381	194	5.94	4.93	9.37	28.78	28.15	34.53	14.48	14.43	298.2	-41.4	-41.3	4.69	.69	111.85
1391	222	8.85	4.84	9.39	17.73	28.27	37.33	12.22	12.43	314.7	-54.4	-54.9	4.69	.67	7.52
1401	253	11.88	4.85	18.78	14.92	28.31	32.78	13.39	13.77	301.3	-48.8	-48.4	4.69	.64	113.34
1411	288	3.89	4.58	18.91	25.12	24.29	39.64	28.84	28.51	183.8	-44.3	-44.3	4.69	.62	115.74
1421	327	5.94	6.46	9.41	21.74	24.58	29.83	14.49	15.87	318.9	-48.3	-48.2	4.69	.68	125.51
1431	373	8.93	4.37	9.84	18.73	24.88	38.62	12.43	13.85	339.9	-44.7	-44.4	4.69	.63	118.58
1441	439	11.88	4.48	18.72	17.83	24.94	31.84	13.18	13.81	348.8	-52.3	-52.7	4.69	.63	117.27
1451	35	2.92	2.15	34.58	23.31	12.15	18.89	24.31	24.31	167.4	83.5	83.5	2.53	.84	4.31
1461	39	5.93	2.14	34.92	28.44	11.87	17.88	34.44	34.44	229.1	73.3	73.3	4.44	.84	4.38
1471	46	8.92	2.13	37.67	31.81	11.17	17.29	34.83	34.83	289.9	83.4	83.4	5.88	.84	4.78
1481	59	11.88	2.08	34.83	38.75	11.39	17.18	33.53	33.53	212.4	81.3	81.3	4.28	.84	4.38
1491	68	2.94	3.49	37.67	18.87	11.57	18.23	27.37	27.37	228.9	76.7	76.7	3.23	.85	4.53
1501	182	5.97	3.78	37.36	24.89	11.88	18.44	32.41	32.41	342.9	113.3	113.3	4.81	.84	9.24
1511	115	8.94	3.78	38.63	27.34	11.17	17.83	34.78	34.78	413.3	134.9	134.9	6.93	.85	116.45
1521	137	11.91	3.48	34.78	28.87	11.67	17.99	32.59	32.59	348.4	114.8	114.5	5.81	.84	118.29
1531	173	2.93	5.33	37.41	13.99	11.48	18.11	25.14	25.14	278.4	91.3	91.3	3.74	.84	5.83
1541	185	5.98	5.29	37.68	21.83	11.89	18.51	34.47	34.47	429.8	142.1	142.1	7.88	.84	112.28
1551	222	8.93	5.38	38.29	24.28	11.11	18.85	33.49	33.49	543.5	179.4	179.4	4.73	.85	114.38
1561	241	14.89	5.34	34.21	25.29	11.67	18.24	31.34	31.34	459.7	151.9	151.9	4.59	.84	114.78
1571	287	2.94	7.11	37.71	14.34	12.84	18.84	23.43	23.43	294.8	166.2	169.2	4.32	.87	111.94
1581	324	5.98	7.89	37.77	18.58	11.85	18.23	28.88	28.88	495.8	183.4	183.4	8.89	.85	123.32
1591	378	8.93	7.89	38.51	21.82	11.11	18.14	31.81	31.81	443.4	212.4	212.4	11.93	.85	117.12
1601	444	11.97	7.89	33.78	23.17	11.44	18.28	29.87	29.87	548.9	181.8	181.8	7.87	.84	117.73

Table 5.2 (Cont) Balanced experimental data and the modelled information

## 6 A CRITICAL EXAMINATION OF THE ACCURACY AND LIMITATIONS OF THE MERKEL METHOD

### 6.1 Introduction

This chapter presents a detailed examination of the Merkel approach, which is otherwise termed the 'standard method' of cooling tower performance analysis. This method is used to analyse the experimental data and is shown to give a poor correlation. A fundamental assessment of the approach then highlights some of the inherent limitations of the method.

Two complementary issues are involved in designing heat exchangers and rating their thermal performance. The first is the description of thermal performance in terms of the imposed process conditions and an overall value of the design characteristic. (This first part is the main subject of this thesis.) Note, however, that this does not include a description of the design of the unit itself. The second part is a description of the design features related to the basic geometry and flow considerations which fix the nature and amount of contact surface provided and the thermodynamic properties of the fluid streams. These two parts are normally dealt with as two separate issues. It must be understood that in examining the accuracy of the Merkel method each of these parts has its own simplifications; it is thus difficult to assess independently the effects of each part on the overall inaccuracy.

## 6.2 Merkel method of cooling tower analysis

The Merkel or 'standard method' of cooling tower analysis is presented in many texts, the most common being the ASHRAE Handbooks(10,89), British Standard 4485(9) and the Cooling Tower Institute (CTI) procedures(59).

The basic Merkel approach to analysing the thermal performance of direct contact air-water heat exchangers was developed for water cooling towers. In 1925 Merkel(12) developed a simplified equation describing the total heat transfer from a wet surface. By making a number of approximations which, as will be seen, sacrifice accuracy, he showed that the sensible and latent heat transfer may be considered as a single overall process in which the driving force is approximated to the difference between the enthalpy of the saturated air at the wet-bulb temperature, and the enthalpy of the film of saturated air surrounding the water surface.

$$\dot{Q}_t = K_m ( i_{aw} - i_{a-wb} ) \quad (6.1)$$

This enthalpy driving force is the widely accepted basis for direct-contact water-air heat exchanger theory and most methods of predicting thermal performance are based on this approach. Merkel's sequence of logic and the development of the simplified equation is well covered in the literature(10,11,26,47). It is summarized below and discussed in more detail in Section 6.4.

Equating the total heat flow, described in terms of the enthalpy driving force, to the change of state of the

water stream (ignoring changes in water flow due to evaporation or condensation) and to the change of state of the air stream gives:

$$\begin{aligned} K_m (i_{aw} - i_{aes}) dA &= m'_w c_w dt_w \\ &= m'_a di_a \end{aligned} \quad (6.2)$$

This applies to any small element of surface area within a heat exchanger. The established practice is to assume that the overall coefficient,  $K_m$ , has an average and constant value across the entire heat exchanger. Integrating between inlet and outlet states, then, gives:

$$K_m A / m'_w = \int c_w dt_w / (i_{aw} - i_{aes}) \quad (6.3)$$

and

$$K_m A / m'_a = \int di_a / (i_{aw} - i_{aes}) \quad (6.4)$$

In normal practice, Equation 6.3 is invariably used. Note that the enthalpy of the entering air and the enthalpy of the air within the heat exchanger is considered to be equivalent to the enthalpy of saturated air at the wet-bulb temperature.

The practice is to integrate Equation 6.3 in combination with an energy balance equation; the standard procedure is embodied in the two equations below:

$$m'_a di_a = m'_w c_w dt_w \quad (6.5)$$

$$K_m A / m'_w = \int c_w dt / (i_{aw} - i_{aes}) \quad (6.6)$$

The right-hand side of Equation 6.6 is dependent on the process conditions imposed on the heat exchanger and therefore can be calculated when the inlet and outlet water temperatures, the inlet wet-bulb temperature, the ratio of the water-to-air mass flowrates and the barometric pressure are known. The mathematical relationship for calculating the integral is such that exact analytical solutions have not been possible; thus, numerical and graphical techniques have been used. Curves for certain selected design parameters have been made available by the Cooling Tower Institute (CTI) in a handbook that contains some 20 000 curves<sup>(59)</sup> and by Kelly<sup>(98)</sup>. Some typical examples are given in Figure 6.1. Obviously there are an infinite number of process conditions that could form a cooling specification.

These curves are only valid for water cooling duties at sea-level barometric pressure. Changes in barometric pressure and whether air or water is being cooled have a major effect on these curves. This is clearly shown in Figure 6.2 and demonstrates the first major weakness in this approach.

As mentioned earlier, the second part of predicting performance and designing heat exchangers is the description of the design features. The group of terms,  $K_m A / \dot{m}_w$ , on the left-hand side of Equation 6.6 is known as the 'characteristic' of a particular heat exchanger and is determined by the design features which fix the nature and the amount of contact surface provided, the relative velocity of the air stream to the water surface and the thermodynamic conditions of the air and water streams. It is extremely difficult to quantify this group of parameters by calculation from basic principles and its magnitude can only really be determined by experimentation, through Equation 6.6. Nottage and Boelter<sup>(91)</sup> attempted to calculate the

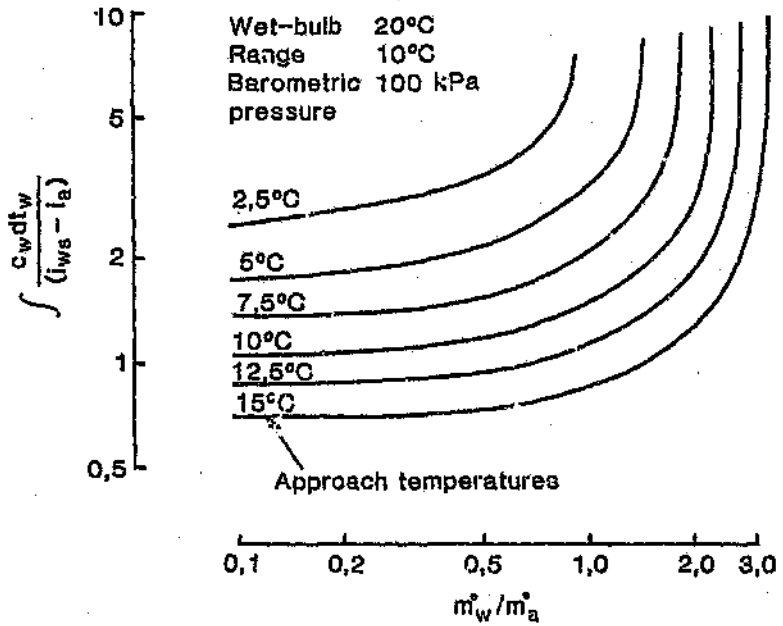


Figure 6.1 Typical process demand curves

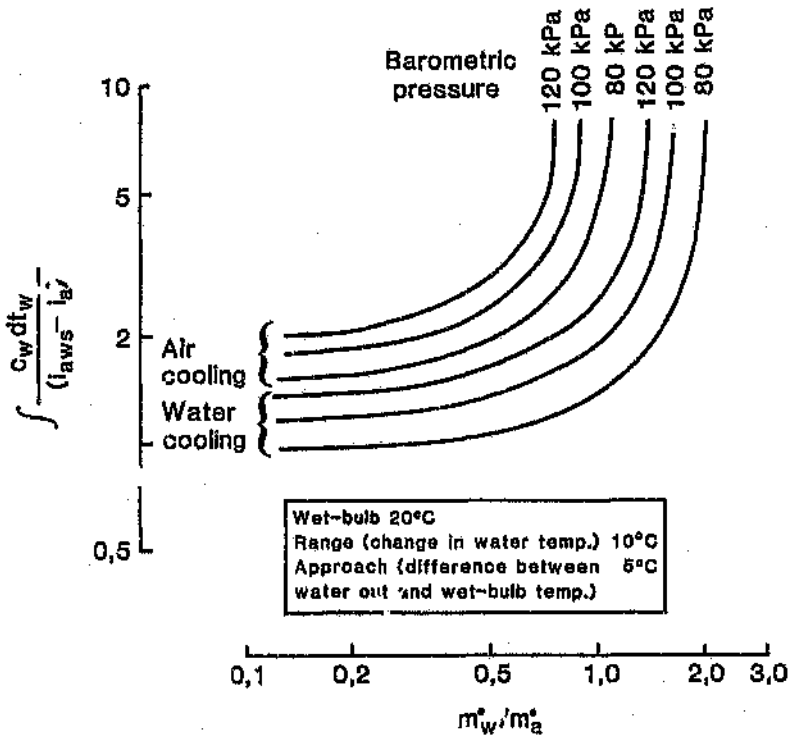


Figure 6.2 Process demand curves for water cooling and air cooling for different barometric pressures

effects of some design parameters for counterflow spray filled units, but did not advocate any general theory.

Bearing in mind that the value of the characteristic varies with water flow, air flow, inlet temperature conditions and barometric pressure, field engineers and manufacturers are faced with a major problem when predicting and representing performance for an entire range of conditions and equipment.

The approach is entirely empirical and representation usually takes the form of a series of plots correlating the characteristic  $K_m A / m'_w$  against the water-air flow ratio. The established procedure is to correlate empirical data in the following forms(24,92,93,102), although it must be noted that apart from dimensional analysis(93) there is no fundamental logic behind these correlations:

$$K_m A / m'_w = a (m'_w / m'_a)^n \quad (6.7)$$

$$K_m A / m'_w = a m'_w{}^n m'_a{}^m \quad (6.8)$$

The common but simplistic practice is to ignore the effect of temperature conditions, barometric pressure and even air velocity, and to use a single curve for each piece of equipment(24,89). A typical set of characteristic curves is given in Figure 6.3. This approach, in conjunction with the use of the Merkel equation leads to well known errors, particularly at high water temperatures above 40 °C(48,65).

A design selection obviously involves the choice of the

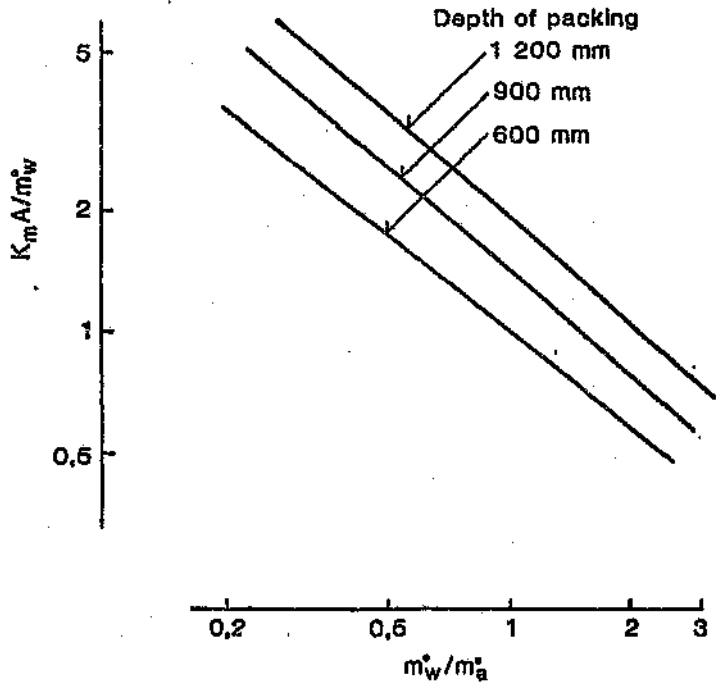


Figure 6.3 Typical cooling tower packing characteristic curves

required value of the characteristic to satisfy the desired process conditions as given, for example, in Figure 6.1.

The practical limitations of this method, particularly with regard to field application, are perhaps obvious. Furthermore, this approach is inaccurate and the present set of data are examined below in this manner as a demonstration.

### 6.3 Correlation of experimental data

The values of  $K_m A / m_w$  have been calculated numerically and are listed in Table 6.1 along with the other relevant test information.

#### 6.3.1 Results in terms of $K_m A / m_w = a (m_w' / m_a')^n$

The most commonly used correlation is given by:

$$K_m A / m_w' = a (m_w' / m_a')^n \quad (6.9)$$

The experimental results are shown in Figures 6.4.a to 6.8.a. Curve fitting routines have been used to determine the best values of  $a$  and  $n$  as well as the correlation coefficients, and these are given in Table 6.2. These values are generally in keeping with what was expected(92).

For the spray configuration with no packing (Test Nos. 1-32) there is clearly no correlation evident. In fact, the value of the exponent  $n$  tends to zero. However, for the sake of completion the information has

been plotted in Figure 6.4.a with a value of  $n = 1$ .

For the packed configurations some correlation exists, but it is poor. The absolute error in predicting  $K_m A / m'_w$  through this correlation is on average 12 per cent, with maximum values greater than 50 per cent. Recall that the uncertainty in the measured results was about 4 per cent in terms of total heat flow. So, clearly, this correlation is inaccurate. It must again be recalled that this approach is purely empirical and has no fundamental basis.

Why, then, has this approach been so widely adopted? The main reason is that there is not a large operating range over which industrial water cooling towers are normally used. However, for the present study the full range of operating possibilities in mining applications are being examined; hence the scatter.

It is interesting to note that from a statistical point no real difference can be identified for the hot water and cold water cases.

Although there is very little comparative data published, Kametani et al<sup>(105)</sup> tested a small counterflow packed tower for inlet water conditions of 40 °C and inlet air temperatures of 20 °C wet-bulb, 24 °C dry-bulb. This information they compared to the operation of the same tower with inlet water temperatures between 6 and 15 °C and inlet air temperatures of 24 °C wet-bulb and 29 °C dry-bulb. The correlation was done according to Equation 6.9. The index  $n$  was found to be the same (0,55) for both sets of conditions, however the value of the term,  $a$ , was found to be 10 per cent higher for the hot water application.

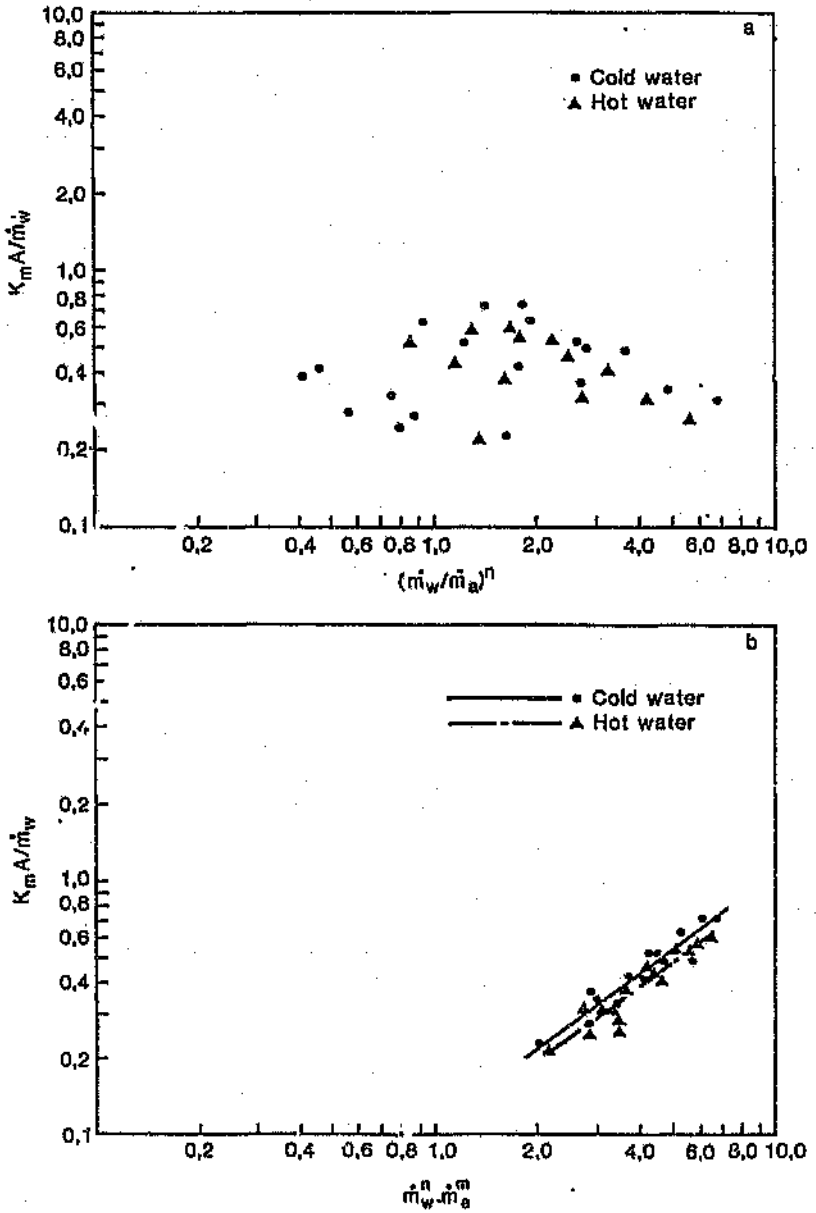


Figure 6.4 Correlation of test data with standard methods of characterization (Tests 1-32, spray only)

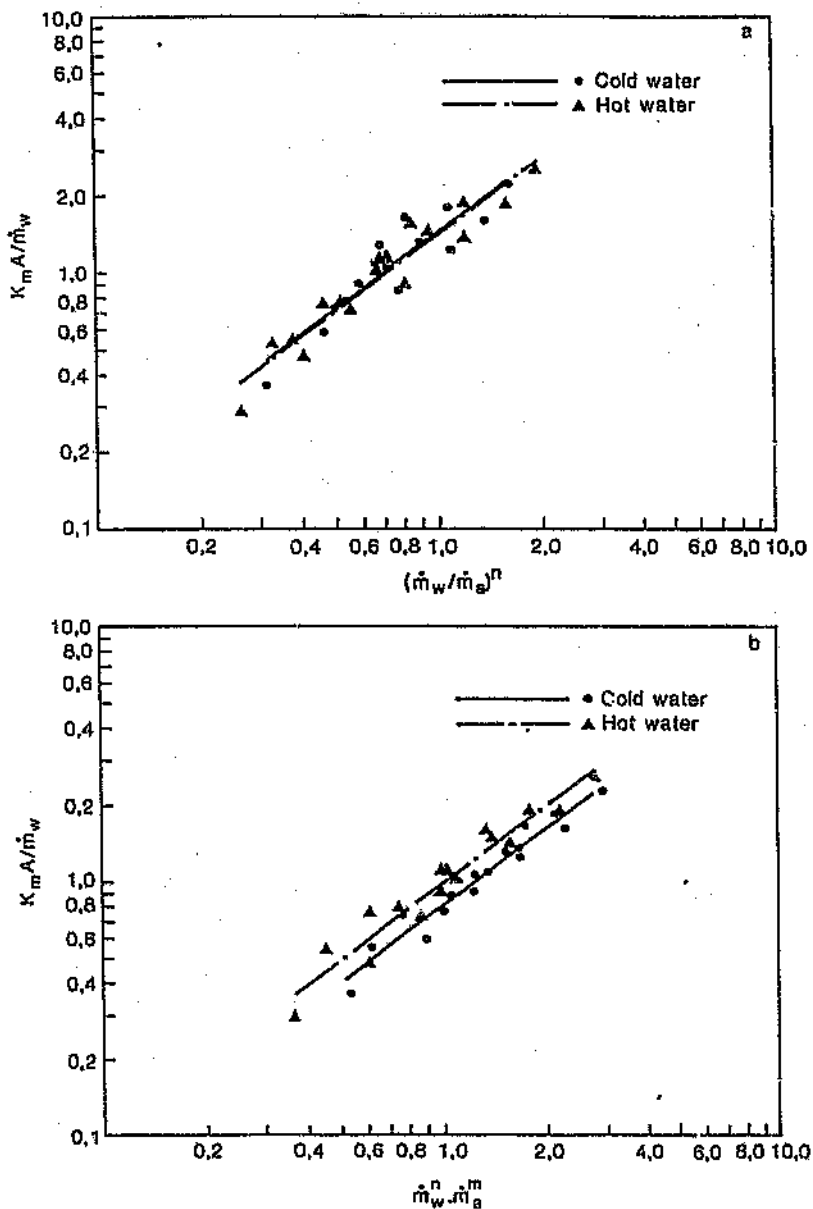


Figure 6.5 Correlation of test data with standard methods of characterization  
(Tests 33-64, 12mm flute, 600mm ht)

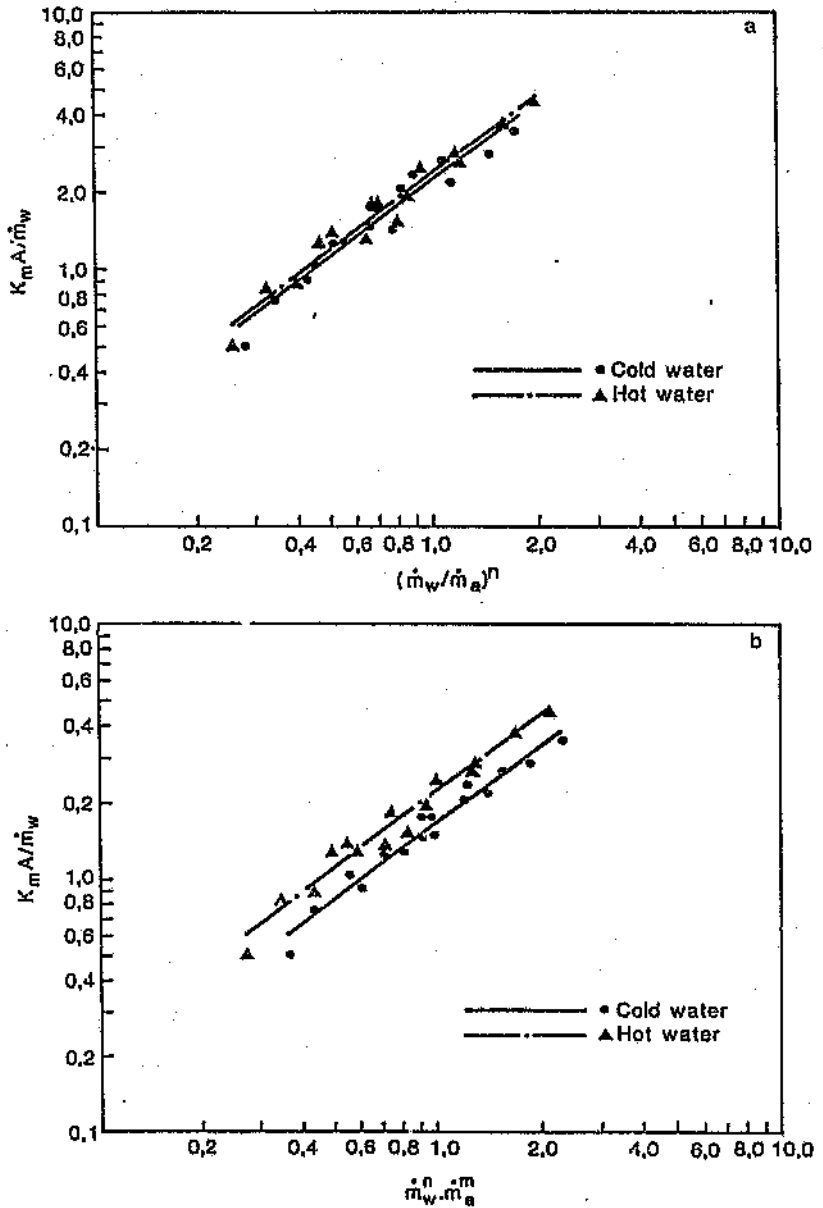


Figure 6.6 Correlation of test data with standard methods of characterization  
(Tests 65-96, 12mm Flute, 1200mm ht)

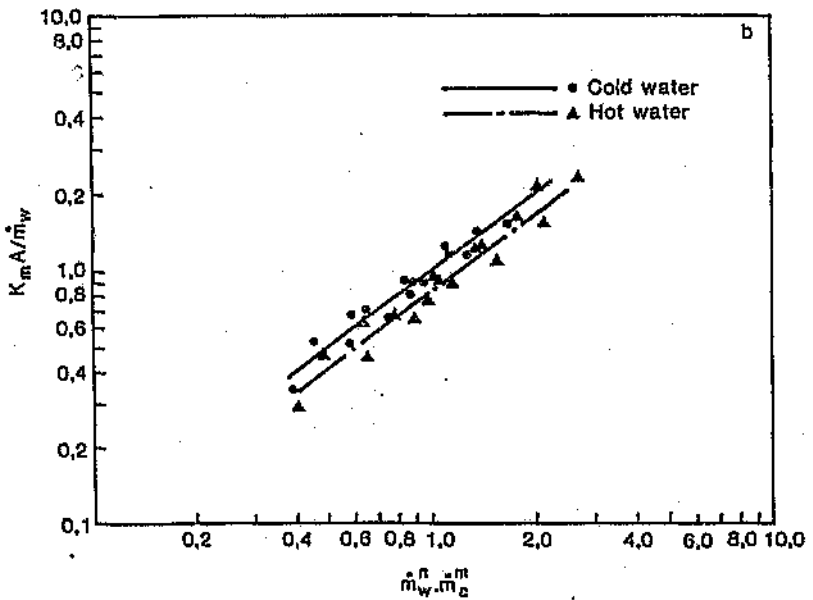
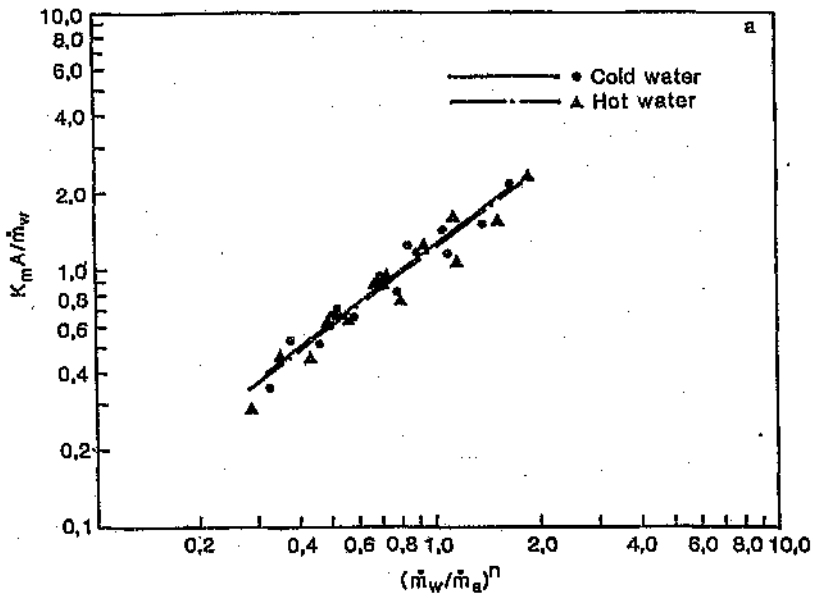


Figure 6.7 Correlation of test data with standard methods of characterization  
(Tests 97-120, 19mm flute, 600mm ht)

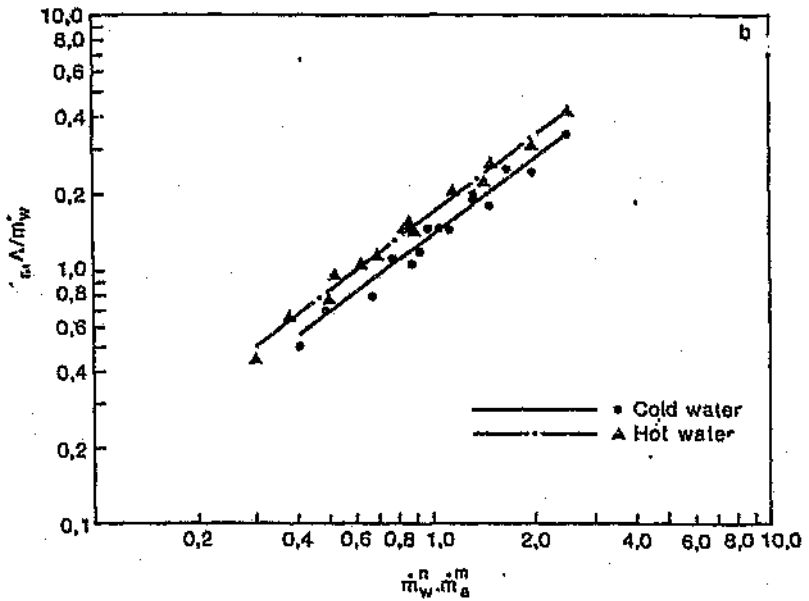
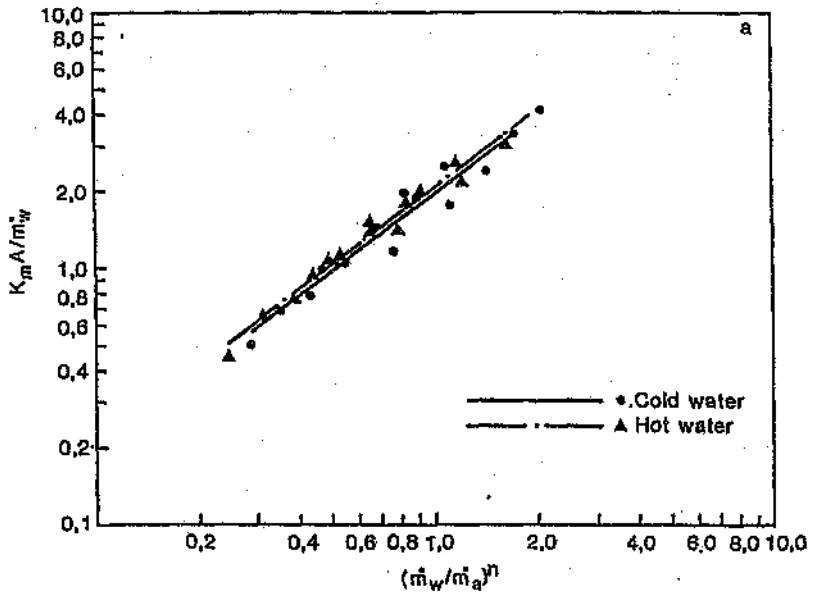


Figure 6.8 Correlation of test data with standard methods of characterization  
(Tests 121-160, 19mm flute, 1200mm ht)

### 6.3.2 Results in terms of $K_m A / m'_w = a m'_w{}^n \cdot m'_a{}^m$

To account for the effect of air velocities, the normal correlation (Section 6.3.1) is sometimes modified to the form:

$$K_m A / m'_w = a m'_w{}^n m'_a{}^m \quad (6.10)$$

A statistical analysis has been conducted on the data to determine the best values of  $a$ ,  $n$ , and  $m$ , as well as the correlation coefficients. These are summarized in Table 6.2. All the results are shown plotted in Figures 6.4.b to 6.8.b.

As was to be expected, the correlation for individual sets of tests has improved slightly. The absolute error in predicting  $K_m A / m'_w$  through these equations is, on average, 10 per cent, but with maximum values still greater than 50 per cent.

It is interesting to note that from a statistical point of view different correlations exist for the hot water and cold water cases. However, this reflects very badly on the widespread practice of using a single correlation for a wide range of thermodynamic conditions.

## 6.4 Assumptions and limitations of the Merkel equation

As mentioned earlier, Merkel's sequence of logic and the development of the simplified equation is well covered in the literature. However, the equations used in the present work are, as a set, probably unique (this is mainly due to the use of Spalding's approach

to mass transfer); hence the complete sequence of logic is examined below. Each of the assumptions involved are considered in term.

Merkel's approximation for total heat flow from a wet surface is given as(89):

$$\dot{Q}_t = K_m ( i_{aw} - i_{a\infty} ) = \left( \frac{h_c}{C_{a,v,a\infty}} \right) ( i_{aw} - i_{a\infty} ) \quad (6.11)$$

Describing this total heat transfer in terms of the basic heat and mass transfer formulations, in a relationship which may be considered as exact (or which at least presents the best possibility), gives:

$$\dot{Q}_t = h_c ( t_w - t_{db} + \lambda_w B' ) \quad (6.12)$$

Substituting for the mass transfer terms, this equation becomes:

$$\dot{Q}_t = h_c [ t_w - t_{db} + (\lambda_w / c_{a,v}) (Pr/Sc)^{2/3} \ln (1 + B) ] \quad (6.13)$$

where

$$B = ( W_{vw} - W_{v\infty} ) / ( 1 - W_{vw} ) \quad (6.14)$$

It is from the basic Equation 6.13 that Merkel's approximation can be developed through a series of seven sequential approximations. The first approximation to be considered is that since B is small compared

to unity (typically 0,06 with a maximum value of 0,11), then:

$$\ln (1 + B) = B \quad (6.15)$$

The typical and maximum errors in this approximation are 3 and 5,5 per cent respectively.

The second approximation is that since  $W_{vw}$  is small compared to unity (typically 0,02 with a maximum value of 0,10), then:

$$B = W_{vw} - W_{vo} \quad (6.16)$$

The typical and maximum errors in this approximation are 2 and 11 per cent respectively.

The third approximation is that the density of the air-water vapour mixture is not significantly different from the density of the pure air component alone.

Typically the difference is 2 per cent, but it can be as much as 11 per cent. Based on this assumption two further simplifications are possible. First, the true specific humidity terms ( $W_v$ ) may be replaced by apparent specific humidity terms ( $W$ ). Second, the thermal capacity of moist air per mass of moist air,  $c_{av}$ , may be replaced by the thermal capacity term of moist air per mass of dry air,  $c_{ava}$ .

The fourth approximation is that the ratio  $(Pr/Sc)^{2/3}$ , which is sometimes known as the Lewis Number, is unity. In reality the value is typically

1,12 (see Section 2.9) and does not vary significantly over the range of conditions being considered.

The fifth approximation is that the value of the latent heat of vaporization (at the water surface condition),  $\lambda_w$ , remains constant at 2501 kJ/kg irrespective of temperature changes. This value actually decreases by 5 per cent as the water surface temperature varies from 0 to 50 °C.

Equation 6.13 may now be written as:

$$\frac{h_c}{c_{af}} = h_o [ t_w - t_{db} + (\lambda/c_{avaf}) ( W_w - W_\infty ) ] \quad (6.17)$$

which may be rearranged to produce:

$$\frac{h_c}{c_{af}} = \left( \frac{h_o}{c_{avaf}} \right) [ ( c_{avaf} t_w + \lambda W_w ) - ( c_{avaf} t_{db} + \lambda W_\infty ) ] \quad (6.18)$$

The term,  $c_{avaf}$ , is the specific heat of moist air at the average of the water surface and air temperatures (film condition).

The sixth approximation is that both the specific heat of moist air at the bulk air condition and that of moist air at the water surface condition may be assumed to be equal to the specific heat at the film condition. Thus, it is assumed that:

$$c_{avac} = c_{avaw} = c_{avaf} \quad ( = c_{avf} ) \quad (6.19)$$

Over the range of conditions being considered,  $c_{ava}$  varies from 1005 to 1214 J/kgK. Bearing in mind that

an average condition is being considered, the maximum error in either of the specific heat terms at the water surface condition or the bulk air condition is 9 per cent, while a typical value is 2 per cent.

Equation 6.18 may now be written as:

$$\frac{q_t}{Q_t} = \left( \frac{h_o}{c_{avg}} \right) [ ( c_{avg} t_w + \lambda W_w ) - ( c_{avg} t_{db} + \lambda W_w ) ] \quad (6.20)$$

The specific heat of moist air is given by Equation A.10 which is repeated below:

$$c_{avg} = 1005 + 1.84 W \quad (6.21)$$

Substituting this and the value of (2501 kJ/kg) into Equation 6.20 produces:

$$\frac{q_t}{Q_t} = \left( \frac{h_o}{c_{avg}} \right) [ 1005 t_w + W_w ( 2501 + 1.84 t_w ) \times 10^3 - 1005 t_{db} - W_w ( 2501 + 1.84 t_{db} ) \times 10^3 ] \quad (6.22)$$

The enthalpy of moist air is given by Equation A.12 which is repeated below:

$$i_a = 1005 t_{db} + W ( 2501 + 1.84 t_{db} ) \times 10^3 \quad (6.23)$$

Thus, Equation 6.22 simplifies to:

$$\frac{q_t}{Q_t} = \left( \frac{h_o}{c_{avg}} \right) [ i_{aw} - i_{am} ] \quad (6.24)$$

The seventh and final approximation is that the enthalpy of saturated air at the wet-bulb temperature adequately describes the actual enthalpy content of the air as it flows through the heat exchanger. Typically the enthalpy difference in Equation 6.24 is likely to vary by less than 1 per cent because of this assumption. However, for dry air conditions with close approach temperatures this error could be large on the air entry side of heat exchangers.

Equation 6.24 then simplifies to:

$$\dot{Q}_t = \left( \frac{h_c}{C_{\text{AVAO}}} \right) [ i_{\text{AW}} - i_{\text{AOS}} ] \quad (6.25)$$

This is in fact the Merkel equation, which is normally written in terms of an overall transfer coefficient as:

$$\dot{Q}_t = K_m ( i_{\text{AW}} - i_{\text{AOS}} ) \quad (6.26)$$

Merkel's simplification involves a total of seven sequential approximations, each of which may have an error of about up to ± 10 per cent. Some of these errors are partially self-compensating. To estimate the overall inaccuracy of Merkel's basic simplification, a numerical approach has been used, and conclusions are drawn on a statistical basis. An assessment of the error in Equation 6.25 involves a comparison with the more accurate version, namely Equation 6.13 which, when rearranged in the same form as Equation 6.25, is written as:

$$\dot{Q}_t = \left( \frac{h_c}{C_{\text{AVAO}}} \right) [ C_{\text{AVAO}} ( t_w - t_{\text{db}} + \lambda B' ) ] \quad (6.27)$$

Thus, a statistical accuracy assessment simply involves the comparison between the driving force terms (the right-hand side term) in Equations 6.25 and 6.27. The statistical plane over which the error has been examined covers the full range of air and water conditions under consideration and was covered in steps of 10 kPa in barometric pressure and of 5 °C for each of the water and air temperatures except the wet-bulb temperature, which was covered in 1 °C steps because of the strong dependence of heat flow on this parameter. This amounted to a total of more than 10 000 sets of conditions.

The results are presented in the form of a correlation between the value of the enthalpy difference driving force and the real value of the driving force as calculated from the basic heat and mass transfer formulations. This plot is shown in Figure 6.9; each point on this figure corresponds to one set of conditions.

This figure gives an overall indication of the accuracy of Merkel's equation and the extent of the absolute errors involved. In order to give more information about the distribution of the inaccuracies, the distribution of the error as a percentage of the true value has also been presented in Figure 6.9. Two aspects should be noted. First, there is a bias toward negative errors (this means that the heat transfer predicted using an enthalpy difference would generally be higher than the true value). Second, the errors are not small and Merkel's equation departs significantly from the exact formulation; for example, if errors of  $\pm 3$  per cent are to be acceptable then only 50 per cent of all the conditions considered would qualify. The range of values covered the region where the driving force is zero and some of the larger errors may be attributed to the division by small numbers. However,

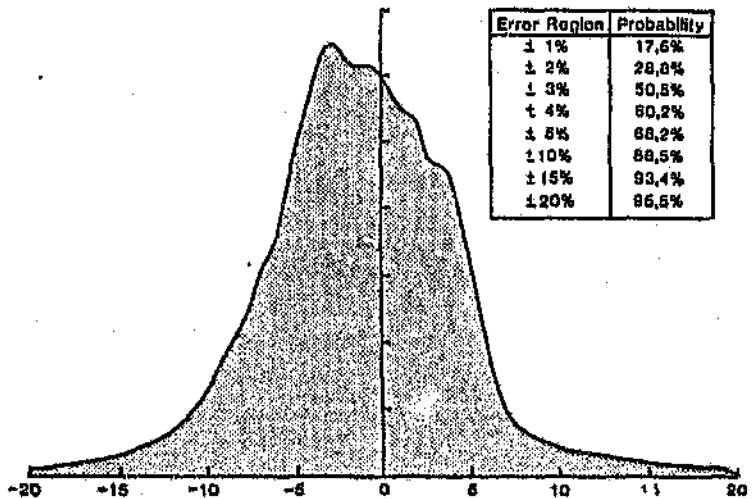
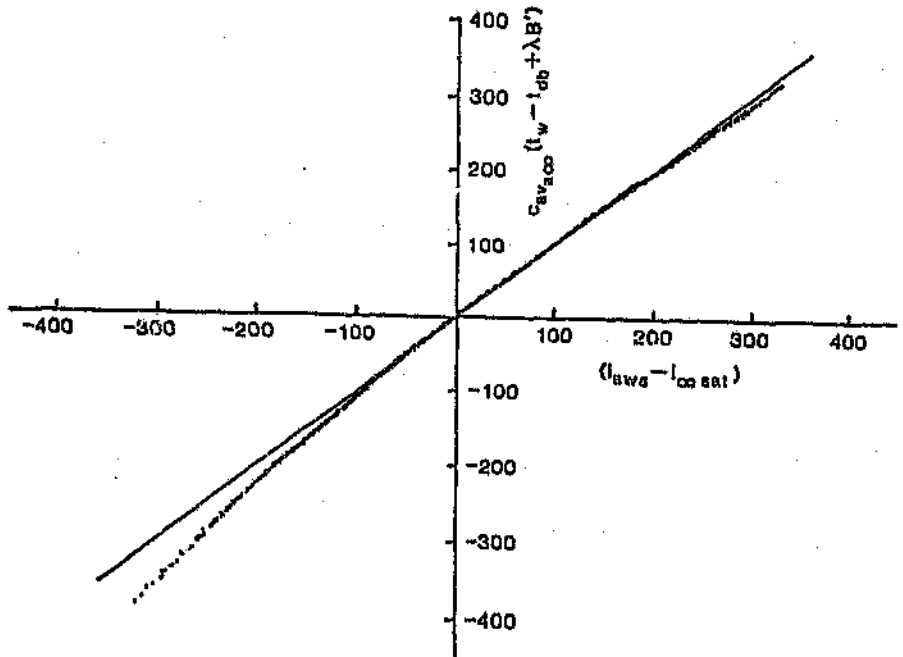


Figure 6.9 Correlation between the Merkel enthalpy driving force and the true value

all these large differences must not be considered insignificant. They in fact correspond to close approach conditions in a dry climate.

The numerous sets of conditions evaluated came from a simple and even distribution over the full range of conditions being considered; there was no weighting for conditions and processes that are more likely to occur than others. However, the conclusion that the Merkel equation is generally lacking in accuracy remains valid.

The manner in which Merkel's equation is used in practice deserves further examination and, with regard to the present argument, three points should be noted.

First, the value of the overall transfer coefficient  $K_m$  is given as  $h_c/c_{avac}$ , a fact that is seldom used in practice and a detail that is generally lost. (It is assumed that the transfer coefficient has an average and constant value throughout the entire heat exchanger.)

Second, Merkel's equation departs significantly from the exact formulation and, in practice, the empirical information is extrapolated to various conditions usually without taking account of the specific conditions prevailing when the 'characteristic' was originally established. The 'characteristic' value used through the Merkel equation is obtained from a correlation of experimental data and, in reusing this information, there would only be perfect agreement for process conditions identical to the original measurements. Extrapolation or interpolation to any other conditions would involve errors.

Third, associated with the Merkel equation and its subsequent use, is the fact that the energy balance equations ignore the effects of evaporation or condensation flowrates. The error involved in this assumption is typically 3 per cent, but can be considerably higher (see Section 7.3).

The real significance in the inaccuracy of Merkel's equation lies in how the overall heat transfer in a heat exchanger may be predicted (recall that the above is only applicable to an elemental surface area). This aspect is apparent from the analysis considered earlier where the performance of a full heat exchanger is examined. Clearly, any overall method of analysis based on the inaccuracies shown above will be inherently inaccurate.

A number of other detailed studies(13,70,94,95) aimed at quantifying the accuracy of the Merkel equation have been undertaken. Erens<sup>(90)</sup> concludes that all these studies are in general agreement with each other and that the error is typically between 10 and 15 per cent.

## 6.5 Summary

This chapter has examined the 'standard' cooling tower methods of analysis based on the Merkel equation, which are shown to give a poor correlation of the experimental data. The details of the development of the Merkel equation highlight the limitations of the approach and its lack of versatility in being able to deal with both water cooling and air cooling applications over a wide range of thermodynamic conditions.

The following chapter addresses the development of a

new and improved approximation to the total heat transfer relationship at a wet surface. This improved approximation is then used in the development of a new method for the overall performance analysis of direct-contact heat exchangers.

Test number	Air pressure drop Pa	Water flow rate kg/s	Air mass flow rate (dry) kg/s	Inlet water temperature °C	Outlet water temperature °C	Inlet wet-bulb temperature °C	Duty kW	hca W/°C	km/hw
11	16	2.97	1.81	11.72	15.89	33.81	52.9	.69	.25
21	48	5.89	2.17	6.81	12.91	33.89	152.9	2.15	.36
31	144	8.76	1.81	7.13	11.32	32.88	155.9	3.82	.34
41	342	12.83	1.79	7.36	16.62	32.78	166.3	3.82	.31
51	20	2.96	3.37	11.74	15.91	38.19	52.5	.80	.27
61	54	6.85	3.39	6.62	12.51	29.82	151.8	2.55	.42
71	132	8.98	3.35	7.88	12.64	29.91	214.3	4.68	.52
81	270	11.97	3.32	7.35	11.94	29.77	232.8	5.88	.48
91	31	3.25	4.34	8.54	13.77	29.63	72.8	1.85	.32
101	60	3.98	4.85	6.87	12.88	26.99	132.8	3.18	.52
111	132	9.35	4.87	7.81	12.39	26.81	213.5	5.86	.62
121	271	12.71	4.85	11.48	16.81	29.59	246.8	6.44	.49
131	54	2.99	6.47	8.37	13.49	26.86	64.7	1.23	.41
141	75	6.81	6.43	7.86	14.26	25.94	163.4	3.75	.62
151	122	9.88	6.39	7.28	13.94	26.66	259.7	6.49	.71
161	283	11.93	6.52	8.86	13.47	25.43	274.2	8.74	.72
171	11	2.98	2.28	38.98	33.22	9.88	75.4	.69	.22
181	48	5.92	2.17	43.86	35.88	18.94	287.9	2.88	.32
191	145	8.94	2.15	42.23	35.54	18.58	283.2	3.19	.31
201	337	11.92	2.14	42.43	36.93	18.66	288.3	3.68	.26
211	28	2.96	3.74	38.75	32.15	9.35	85.9	.78	.25
221	51	5.94	3.69	43.18	33.26	18.39	258.7	2.41	.37
231	128	9.83	3.66	42.38	32.67	18.38	384.4	4.68	.46
241	276	11.92	3.69	42.52	34.88	9.97	446.8	5.49	.41
251	34	2.98	5.28	43.48	34.22	18.87	122.2	.98	.28
261	60	6.84	5.23	41.35	38.88	18.12	276.9	2.88	.43
271	121	9.16	5.13	41.54	38.79	11.71	431.1	5.38	.54
281	229	11.84	5.32	41.48	31.48	11.82	517.9	6.88	.83
291	55	2.96	7.13	41.57	38.78	9.32	148.4	1.21	.39
301	75	5.97	7.85	41.48	29.36	18.52	316.1	3.38	.52
311	122	9.83	6.96	41.58	29.66	11.48	467.6	5.53	.57
321	282	11.84	7.13	41.39	29.79	18.44	599.2	7.57	.59

Table 6.1 Experimental data (including values of  $K_{m}/\bar{m}_d$ )

Test number	Air pressure drop Pa	Water flow rate kg/s	Air mass flow rate (dry) kg/s	Inlet water temperature °C	Outlet water temperature °C	Inlet wet-bulb temperature °C	dry bulb °C	h <sub>g</sub> kJ/kg	h <sub>o</sub> kJ/kg
331	27	2.92	1.89	9.84	29.67	33.38	131.2	2.51	.86
341	30	5.75	1.87	9.17	15.79	32.28	162.2	4.48	.73
351	35	8.98	1.78	9.29	13.87	32.99	171.9	5.06	.54
361	49	11.84	1.77	9.94	13.81	32.11	154.5	4.47	.36
371	75	2.95	3.33	9.81	23.25	31.28	164.9	3.68	1.24
381	83	5.77	3.35	8.92	17.75	29.77	217.4	6.19	1.84
391	97	9.28	3.33	7.65	13.69	29.28	238.5	7.32	.77
461	116	11.88	3.34	10.55	15.15	30.13	233.2	7.26	.59
411	147	2.87	4.86	9.64	24.84	29.36	177.6	4.77	1.68
421	164	5.88	4.88	8.46	18.76	28.84	285.2	7.84	1.31
431	188	9.32	4.82	7.66	15.84	27.51	293.8	10.25	1.86
441	219	11.93	4.91	12.81	17.42	26.86	234.2	11.39	.98
451	251	2.89	6.57	9.63	24.78	27.59	168.1	6.64	2.19
461	283	5.81	6.60	7.95	29.27	26.85	386.5	11.82	1.82
471	321	9.85	6.51	11.95	19.33	25.98	284.8	15.81	1.64
481	369	12.84	6.58	12.29	18.88	25.93	292.9	16.63	1.25
491	38	2.92	2.21	42.78	27.41	12.19	194.8	2.81	.98
501	32	5.72	2.14	39.33	29.74	12.89	239.5	4.79	.74
511	48	8.92	2.15	41.88	33.41	11.71	297.4	5.56	.53
521	51	11.56	2.12	41.99	36.48	12.87	286.9	3.85	.28
531	79	2.96	3.74	43.82	22.83	11.67	258.6	4.21	1.37
541	84	5.74	3.71	39.44	25.68	11.62	342.7	6.81	1.18
551	99	8.78	3.77	41.68	29.82	18.98	454.6	7.54	.77
561	114	11.63	3.68	42.83	33.35	11.95	442.9	6.22	.47
571	155	2.97	5.48	43.39	19.61	11.56	386.9	5.64	1.87
581	164	5.73	5.38	39.83	22.39	11.11	411.5	8.72	1.46
591	187	8.76	5.35	38.56	25.63	11.62	491.5	10.42	1.18
601	216	11.45	5.46	41.93	38.83	11.72	595.5	9.87	.72
611	259	2.98	7.83	43.95	16.73	11.14	347.4	7.49	2.53
621	281	5.74	7.21	38.95	19.57	18.73	478.3	11.18	1.98
631	318	8.88	7.89	39.69	23.85	11.83	633.2	114.47	1.95
641	358	11.58	8.96	41.81	27.17	11.88	737.4	112.92	1.82

Table 6.1 (Cont) Experimental data (including values of  $K_{m}A/m^2$ )

Test number	Air pressure drop Pa	Water flow rate kg/s	Air mass flow rate (dry) kg/s	Inlet water temperature °C	Outlet water temperature °C	Inlet wet-bulb temperature °C	Ruby °N	h <sub>ea</sub> W/°C	KmD/hm
651	46	2.87	1.96	12.22	23.89	32.41	144.8	4.44	1.44
661	45	5.8	1.81	9.71	16.91	33.89	188.8	6.75	1.83
671	52	8.81	1.78	11.82	15.88	33.58	179.7	8.32	.75
681	67	11.73	1.78	18.56	14.12	33.35	177.6	6.62	.58
691	118	2.87	3.48	12.22	25.76	29.67	167.9	6.62	2.16
781	132	5.87	3.36	9.68	28.84	38.26	268.6	11.28	1.74
711	152	8.99	3.35	18.89	17.38	36.63	274.8	12.69	1.25
721	177	11.86	3.35	8.61	14.37	38.86	291.1	12.83	.91
731	231	2.91	4.97	12.16	26.84	27.91	174.1	8.74	2.62
741	259	5.89	4.93	9.66	21.31	27.77	294.2	14.77	2.32
751	294	8.83	4.94	8.38	17.92	28.78	348.4	16.94	1.74
761	341	11.91	4.88	8.22	15.46	28.99	367.9	16.89	1.26
771	382	2.99	6.66	18.43	23.23	24.47	163.8	18.94	3.45
781	436	5.93	6.62	9.72	21.85	25.33	287.7	16.89	2.64
791	584	8.92	6.59	9.45	19.14	26.79	369.5	19.71	2.83
881	556	11.94	6.38	9.29	16.79	27.81	381.3	19.18	1.47
or									
811	47	2.94	2.28	48.58	23.74	12.88	213.2	4.78	1.53
821	53	5.81	2.21	42.27	28.86	11.58	348.	8.78	1.27
831	59	8.78	2.15	48.58	32.84	11.48	325.		.82
841	75	11.82	2.13	41.78	35.32	13.35	332.8		.58
851	128	2.95	3.72	41.28	18.49	11.84	287.8	7.84	2.61
861	134	5.98	3.71	42.45	23.96	11.11	473.9	11.65	1.81
871	158	6.76	3.71	48.97	27.38	11.87	518.4	13.86	1.37
881	177	11.72	3.69	41.85	31.31	13.89	546.6	12.44	.89
891	229	2.99	5.31	41.54	15.57	11.83	332.8	18.93	3.78
981	259	5.98	6.35	42.45	26.17	11.18	566.8	15.14	2.46
911	294	8.76	5.36	41.42	23.81	18.89	668.8	17.42	1.82
921	343	11.88	5.32	42.82	27.96	12.76	722.8	16.98	1.26
931	388	3.82	7.82	41.88	13.96	11.55	359.8	13.88	4.44
941	434	5.88	7.17	42.82	17.95	11.13	617.5	16.89	2.82
951	494	8.88	7.11	41.49	21.46	18.36	753.8	18.94	1.94
961	529	11.79	6.75	42.18	26.48	12.77	888.6	16.94	1.38

Table 6.1 (Cont) Experimental data (including values of  $K_{m,A}/m_{A1}$ )

Test number	Air pressure drop Pa	Water flow rate kg/s	Air mass flow rate (dry) kg/s	Inlet water temperature °C	Outlet water temperature °C	Inlet wet-bulb temperature °C	Duty kW	SCF M <sup>3</sup> /C	Kwh/Wh
971	18	2.86	1.94	9.57	26.29	32.51	131.8	2.37	.80
981	22	5.79	1.92	9.37	18.68	32.95	168.7	3.89	.65
991	29	8.98	1.98	18.36	14.28	38.89	149.6	4.93	.52
1001	42	11.50	1.92	18.89	14.43	53.67	174.7	4.11	.34
1011	54	2.89	3.38	9.42	22.54	31.16	168.5	3.48	1.15
1021	66	5.94	3.33	13.38	21.34	31.48	203.5	5.71	.91
1031	79	9.13	3.23	12.16	18.89	31.59	232.8	6.61	.69
1041	87	11.57	3.34	18.94	18.96	31.87	247.9	6.11	.51
1051	114	2.91	4.93	9.59	23.37	29.83	172.1	4.23	1.52
1061	128	5.93	4.98	9.23	19.14	28.61	281.2	7.15	1.17
1071	140	8.93	4.91	13.12	17.75	25.49	176.8	8.43	.91
1081	164	11.81	4.92	12.43	16.25	25.93	192.2	7.98	.65
1091	221	3.84	6.88	18.12	25.81	28.82	194.1	6.69	2.18
1101	238	5.97	6.62	11.33	21.49	27.81	259.7	8.82	1.42
1111	261	8.78	6.78	11.38	18.97	26.84	287.6	11.17	1.22
1121	362	11.65	6.88	11.57	16.83	25.68	268.6	11.77	.89
1131	18	2.98	2.15	41.26	28.28	12.68	165.4	2.35	.76
1141	22	5.84	2.16	41.62	31.42	11.43	268.9	4.88	.62
1151	29	8.98	2.13	48.96	33.91	12.67	275.8	4.74	.46
1161	42	11.88	2.12	41.54	36.22	12.43	276.6	3.99	.29
1171	52	2.97	3.67	42.75	24.44	18.96	235.3	3.31	1.87
1181	68	5.84	3.74	41.88	27.12	18.78	372.8	5.92	.94
1191	71	8.94	3.89	48.41	38.27	12.81	394.2	6.61	.66
1201	89	11.74	3.78	41.58	33.25	11.88	429.1	6.82	.45
1211	118	2.98	5.33	42.76	28.64	18.66	283.9	4.16	1.53
1221	123	5.88	5.34	41.92	24.13	16.67	453.1	7.58	1.22
1231	142	8.98	5.27	39.93	27.34	11.45	492.3	8.56	.88
1241	167	11.78	5.35	41.63	38.58	11.68	565.8	8.21	.63
1251	197	3.88	7.86	42.65	17.88	18.58	338.8	6.81	2.28
1261	221	5.94	7.89	41.99	21.23	18.17	532.3	9.73	1.58
1271	253	8.98	7.84	39.38	24.19	11.88	591.5	11.61	1.22
1281	291	11.74	7.18	41.78	27.75	11.32	713.8	11.35	.89

Table 6.1 (Cont) Experimental data (including values of  $K_A/d_p$ )

Test number	Air pressure drop Pa	Water flow rate m <sup>3</sup> /s	Air mass flow rate (dry) kg/s	Inlet water temperature °C	Outlet water temperature °C	Inlet wet-bulb temperature °C	Duty kWh	hcs W/°C	Kwh/hh
129	34	2.94	1.93	18.91	21.58	31.87	135.8	3.95	1.16
130	38	5.87	1.92	9.52	18.68	32.45	179.7	6.33	.99
131	46	8.84	1.92	9.83	13.96	32.52	186.8	4.56	.68
132	59	11.81	1.87	12.88	15.43	32.58	168.6	6.68	.58
133	98	2.93	3.39	18.95	25.21	38.65	188.3	5.44	1.76
134	188	5.98	3.38	9.48	19.29	38.18	258.3	9.83	1.44
135	114	8.86	3.35	9.89	16.46	38.87	278.9	18.38	1.88
136	136	11.72	3.41	11.37	16.24	29.87	243.3	9.88	.78
137	176	2.97	4.95	14.98	25.59	28.38	186.8	7.52	2.39
138	194	5.94	4.93	9.37	28.75	28.15	298.2	11.85	1.89
139	222	8.85	4.86	9.39	17.73	28.27	314.7	13.72	1.44
140	255	11.88	4.85	18.98	16.92	28.31	381.3	13.34	1.85
141	288	3.88	6.58	18.91	25.12	26.29	183.8	18.76	3.36
142	327	5.99	6.68	9.41	21.79	26.58	318.9	15.51	2.45
143	375	8.95	6.57	9.84	18.73	26.88	338	18.58	1.94
144	439	11.88	6.68	18.72	17.83	26.94	368.8	18.27	1.42
145	35	2.92	2.15	36.58	23.31	12.15	167.4	4.31	1.48
146	39	5.93	2.14	36.92	28.86	11.87	229.1	6.38	.94
147	46	8.92	2.13	37.67	31.81	11.17	289.9	8.98	.65
148	39	11.88	2.88	34.83	38.75	11.39	212.4	6.38	.95
149	98	2.94	3.69	37.87	18.87	11.57	229.9	6.33	2.18
150	182	5.97	3.78	37.38	24.89	11.88	342.9	9.26	1.44
151	115	8.94	3.78	38.83	27.36	11.17	415.1	18.65	1.86
152	137	11.91	3.68	34.78	28.87	11.67	348.1	14.29	.76
153	175	2.95	5.33	37.41	15.99	11.68	278.9	9.85	3.89
154	195	5.98	5.29	37.68	21.85	11.98	429.8	12.28	1.76
155	222	7.95	5.38	38.29	24.28	11.11	543.6	14.38	1.47
156	261	11.89	5.34	34.21	25.29	11.67	459.7	14.78	1.12
157	287	2.94	7.11	37.71	14.34	12.84	294.8	11.94	4.18
158	328	5.98	7.89	37.77	18.58	11.85	495.8	15.52	2.54
159	376	8.93	7.89	38.51	21.82	11.11	643.4	17.12	1.82
160	444	11.97	7.89	33.78	23.17	11.46	548.9	17.75	1.38

Table 6.1 (Cont): Experimental data (including values of  $K_{m,A}/K_{m,w}$ )

Table 6.2 Statistics of correlation of test data with standard method of characterization

TEST NOS	FLUTE	DEPTH mm	HOT/COLD WATER	$K_m A/m_w = a (m_w/m_a)^n$			$K_m A/m_w = a m_w^n m_a^m$			
				a	n	R <sup>2</sup>	a	n	m	R <sup>2</sup>
1- 32	SPRAY ONLY		B O T H			0,00	0,104	0,356	0,510	0,80
1- 16	SPRAY ONLY		C O L D			0,00	0,107	0,361	0,546	0,89
17- 32	SPRAY ONLY		H O T			0,00	0,095	0,346	0,521	0,90
33- 64	12	600	B O T H	1,403	-0,680	0,85	0,891	-0,555	0,841	0,93
33- 48	12	600	C O L D	1,416	-0,605	0,80	0,791	-0,441	0,814	0,95
49- 64	12	600	H O T	1,390	-0,777	0,89	0,972	-0,682	0,903	0,94
65- 96	12	1 200	B O T H	2,292	-0,731	0,93	1,895	-0,679	0,799	0,94
65- 80	12	1 200	C O L D	2,226	-0,677	0,92	1,639	-0,589	0,783	0,95
81- 95	12	1 200	H O T	2,354	-0,794	0,97	2,184	-0,774	0,821	0,97
97- 128	19	600	B O T H	1,201	-0,670	0,92	0,911	-0,594	0,766	0,95
97- 112	19	600	C O L D	1,220	-0,623	0,94	0,984	-0,563	0,698	0,97
113- 128	19	600	H O T	1,183	-0,725	0,91	0,809	-0,626	0,861	0,96
129- 160	19	1 200	B O T H	2,011	-0,744	0,94	1,493	-0,663	0,849	0,97
129- 144	19	1 200	C O L D	1,962	-0,680	0,91	1,338	-0,573	0,816	0,97
145- 160	19	1 200	H O T	2,052	-0,809	0,98	1,638	-0,750	0,889	0,99

## 7. A SIMPLIFIED THEORETICAL MODEL (PERFORMANCE EQUATION) FOR SIMULATING HEAT AND MASS TRANSFER IN A COUNTERFLOW DIRECT-CONTACT WATER-AIR HEAT EXCHANGER

### 7.1 Introduction

Having discussed the shortcomings of the established method of analysis, attention is now turned to the specific development of a new, accurate but simple performance equation. Up to this stage the thesis has concentrated on producing the tools needed to develop such a simplified theoretical performance equation. The verified comprehensive theoretical model, the carefully assessed bank of experimental data and the selected procedures for determining heat and mass transfer at an elemental wet surface, are now all used in the development of the new performance equation.

In order to achieve this there are two further requirements: first, a simplified equation to describe the total heat flow from a wet surface and, second, simplified equations to describe the change of energy state of the air and water streams.

These are developed in Sections 7.2 and 7.3; Section 7.4 then deals with the algebraic development of the performance equation; and Section 7.5 defines procedures for the selection of parameters within the performance equation.

## 7.2 Development of an improved simplified equation to describe total heat transfer from a wet surface

### 7.2.1 Effect of dry-bulb temperature changes on overall heat flow driving force

It was mentioned earlier that the value of the driving force for total heat transfer is almost independent of dry-bulb temperature for a constant wet-bulb temperature. Historically, in analysing the performance of direct-contact water-air heat exchangers, the effect of the dry-bulb temperature is usually ignored and the air is considered to be saturated at its wet-bulb temperature. This is required by virtue of Merkel's simplified equation, since it is impossible to identify the individual magnitudes of the sensible and latent heat transfer and, hence, to track the exact condition of the air through the heat exchanger.

The following analysis quantifies the error in calculating the total heat transfer from a wet surface while ignoring dry-bulb temperature variations. This has been done on a statistical basis by comparing the value of the driving force, when calculated for saturated conditions at the wet-bulb temperature, to the actual value over the range of conditions being considered. The statistical analysis was similar to that carried out to examine the error in the Merkel equation. Again, the range of conditions being considered was covered in steps of 10 kPa in barometric pressure and of 5 °C for each of the temperatures except the wet-bulb temperature, which was covered in 1 °C steps because of the strong dependence of heat flow on this parameter. This amounts to a total of more than 10 000 sets of conditions.

The results are presented in the form of a correlation graph between the value of the driving force, under saturated conditions, against its real value. This plot is shown in Figure 7.1 and gives some indication of the absolute errors involved. In order to examine the distribution of the errors, the error as a percentage of the true value has been considered and a distribution of these values is also presented in Figure 7.1. Errors of up to  $\pm 10$  per cent enclose about 90 per cent of the points while 46 per cent of the points have errors of less than  $\pm 1$  per cent. Again it must be argued that, since the range of values cover the region where the driving force is zero, most of the large percentage errors are due to division by a number close to zero. This is supported by the fact that the value of the absolute error increases as the driving force approaches zero.

It is concluded that the dry-bulb temperature is not a strong variable in describing the total heat flow from a wet surface. This indicates that the driving force may well be described in terms of  $\sigma$  parameter that is not a strong function of dry-bulb temperature. Such a parameter is the sigma heat content and this is examined further below. Note, however, that any parameter that is used to describe the driving force and that ignores dry-bulb variations at constant wet-bulb temperature could never have an accuracy better than that reflected in Figure 7.1.

### 7.2.2 Sigma heat driving force

Previous sections have shown that the use of the Merkel equation (or enthalpy driving force equation) can result in significant errors and that the driving force is not a strong function of dry-bulb temperature variations for the same wet-bulb temperature.

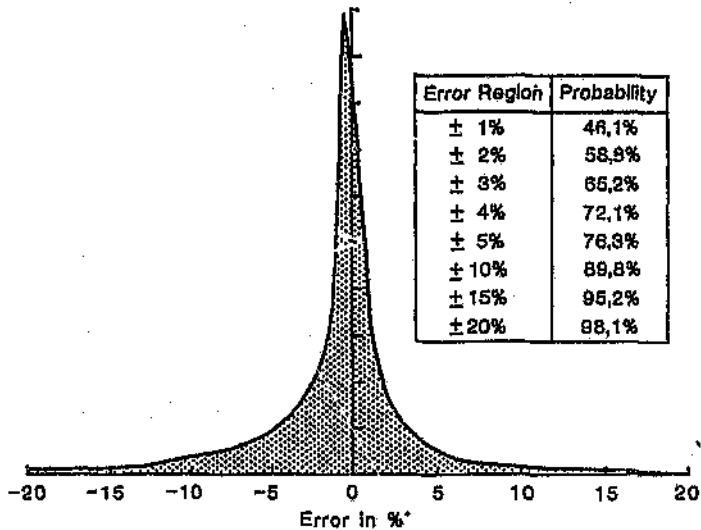
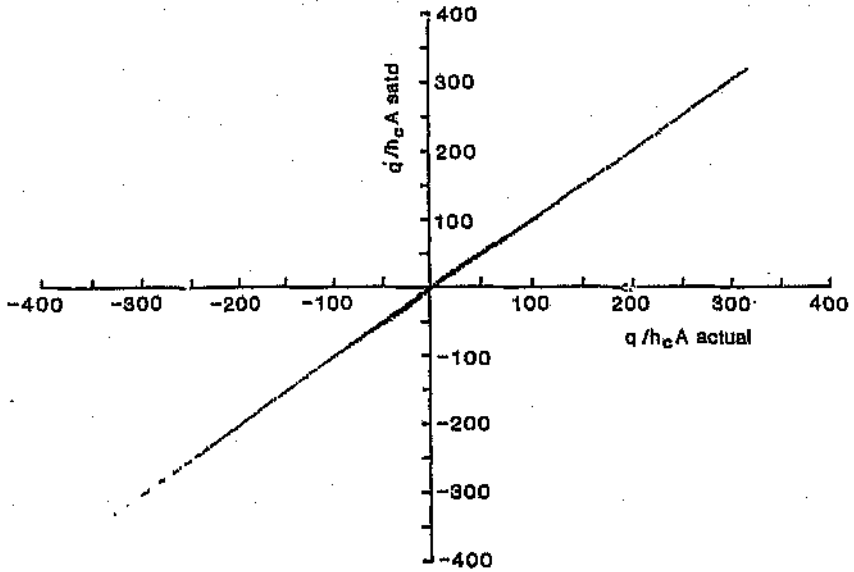


Figure 7.1 Distribution of errors involved in calculating the driving force for total heat flow while assuming saturated conditions

Sigma heat content is a parameter closely related to the enthalpy of moist air and differences in sigma heat between two air conditions will not be far different from enthalpy differences. Furthermore, the sigma heat is a unique function of wet-bulb temperature only (at a given barometric pressure).

Because of the importance of sigma energy to this present work, the basic logic behind the adiabatic saturation process and the sigma energy concept is discussed below. The concept of sigma heat content arises out of a consideration of the adiabatic saturation process. The adiabatic saturation process is shown schematically in Figure 7.2: on the basis of a unit flowrate of air and using the control volume surrounding the air stream, the steady flow energy equation produces:

$$i_{a0} = i_{a1} + m_1 i_g - m_1 i_{fg} \quad (7.1)$$

$$i_{a0} = i_{a1} + m_1 i_f \quad (7.2)$$

Applying a mass balance gives:

$$i_{a0} - W_0 i_f = i_{a1} - W_1 i_f \quad (7.3)$$

and hence

$$\Sigma = (i_a - W c_w t_{wb})_{in} = (i_a - W c_w t_{wb})_{out} \quad (7.4)$$

The energy term that remains exactly constant in the adiabatic saturation process is given in Equation 7.4. This term was called sigma heat by Carrier<sup>(31)</sup> in 1911, in order not to confuse it with total heat or enthalpy. The sigma heat content is the enthalpy of moist air minus the enthalpy of the water vapour content calculated as if the water vapour existed as liquid water at the wet-bulb temperature. Although the overall process is adiabatic, the enthalpy of the air remains only approximately constant. Thus, if the sigma heat (and not enthalpy) remains constant in the processes under consideration (involving changes of moisture content) then it is certain that there has been no heat transfer. By virtue of this fact, it stands to reason that sigma energy will be an important reference parameter, a fact which becomes clear later.

It should be noted that the sigma heat is a unique function of wet-bulb temperature at a given barometric pressure. (In fact the adiabatic saturation process defines the thermodynamic wet-bulb temperature.) The understanding afforded by the relationship between sigma energy and the wet-bulb temperature is extremely useful since it provides valuable insight in explaining the overall performance trends. This relationship is shown graphically in Figure 7.3.

Whillier<sup>(18)</sup> initially showed that a sigma heat difference may also be used to describe approximately the driving force for the total heat transfer from a wet surface. This logic is taken to its conclusion here and, as will be seen later, the sigma heat parameter is of considerable value to the hypotheses presented in this thesis.

What is also most important, is that sigma heat may be

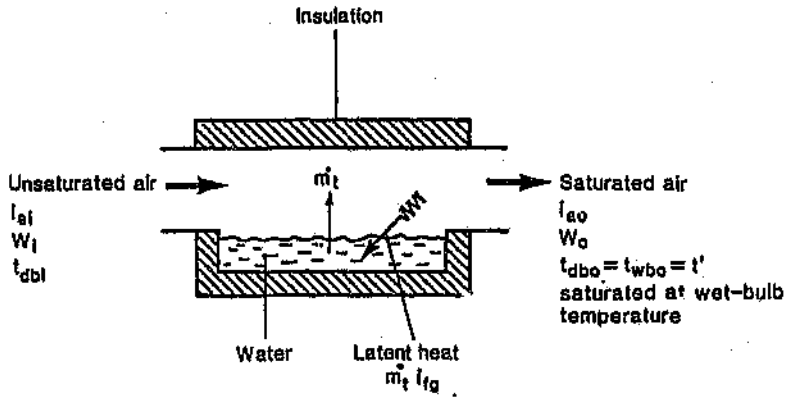


Figure 7.2 Schematic of adiabatic saturation process.

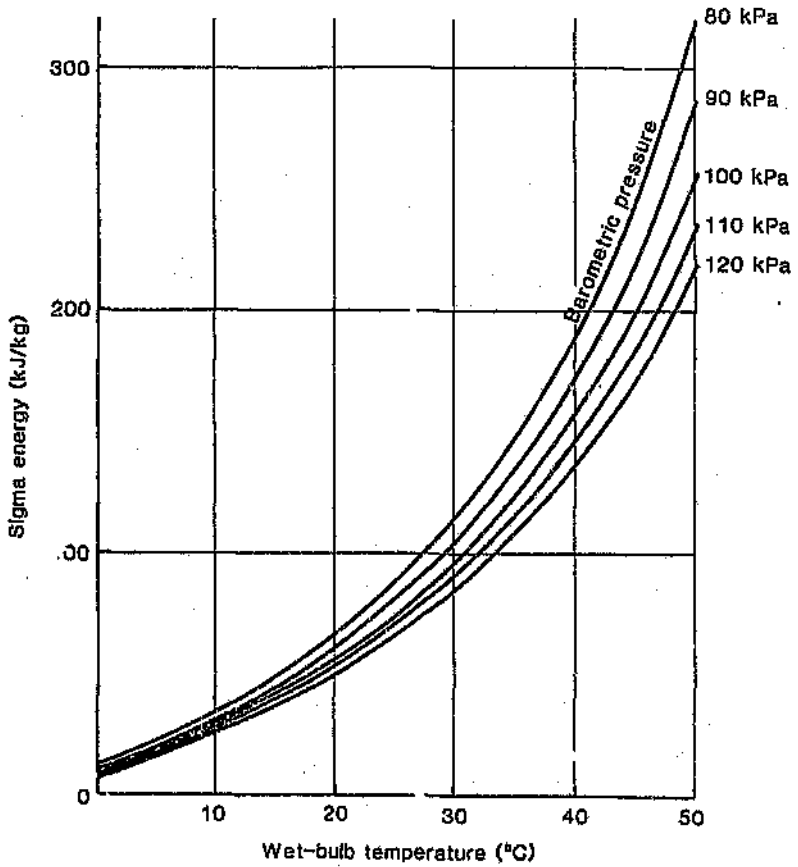


Figure 7.3. Sigma energy of air for the range of conditions under consideration

conveniently and accurately used to describe the overall energy balance between the water and air streams; this is discussed in Section 7.3.

### 7.2.3 New improved total heat transfer approximation

The exact equivalent of the Merkel equation when using sigma energy in place of enthalpy is given as:

$$\frac{\dot{Q}_t}{Q_t} = \left( \frac{h_c}{C_{avgcc}} \right) [ \Sigma_w - \Sigma_{\infty} ] \quad (7.5)$$

The accuracy of this equation has been studied in the same way Merkel's equation was examined earlier, and details are given in Appendix K. It is shown that Equation 7.5 is slightly more accurate than the Merkel equation (scatter is much less). Thus, the simple replacement of the enthalpy difference in the Merkel equation by a sigma heat difference effects a marginal improvement in the accuracy of the approximation.

The accuracy of the approximation to the total heat flow equation using the sigma heat concept may be further increased. A close examination of the development of the Merkel equation from the Spalding's mass transfer approach (see Chapter 6) indicates that the specific heat term used in Equation 7.5 would be better described in terms of the specific heat of the moist air calculated at the film condition. This observation, combined with the fact that the new sigma heat driving force appears to have some merit, led to the examination of the following approximation to the total heat transfer from a wet surface being examined:

$$\frac{\dot{Q}_t}{Q_t} = \left( \frac{h_c}{C_{avail}} \right) [ \Sigma_w - \Sigma_{\infty} ] \quad (7.6)$$

The film temperature referred to by  $F^*$  is not strictly speaking the mean of the air and water surface temperatures, but in keeping with making the right-hand side dependent only on wet-bulb temperatures, the temperature that has been used is the mean of the air wet-bulb temperature and the water temperature.

Recall that the 'exact' formulation for the total heat transfer is given by:

$$\dot{Q}_t = h_o ( t_w - t_{db} + \lambda B' ) \quad (7.7)$$

writing this in a form similar to Equation 7.6 gives:

$$\dot{Q}_t = \left( \frac{h_o}{C_{avgf^*}} \right) [ C_{avgf^*} ( t_w - t_{db} + \lambda B' ) ] \quad (7.8)$$

To assess the accuracy of the new approximation (Equation 7.6), the right-hand bracketed terms of Equations 7.6 and 7.8 have been compared. Again, this has been done statistically over the full range of air and water conditions under examination, using more than 10 000 sets of conditions. The results are presented in the form of a correlation plot between the two terms in Figure 7.4. This figure should be compared to Figure 6.9 which shows the accuracy of the original Merkel equation. Clearly, the spread in the data is reduced, but the data deviates more from the line of identity.

A linear regression analysis, forcing the fit through

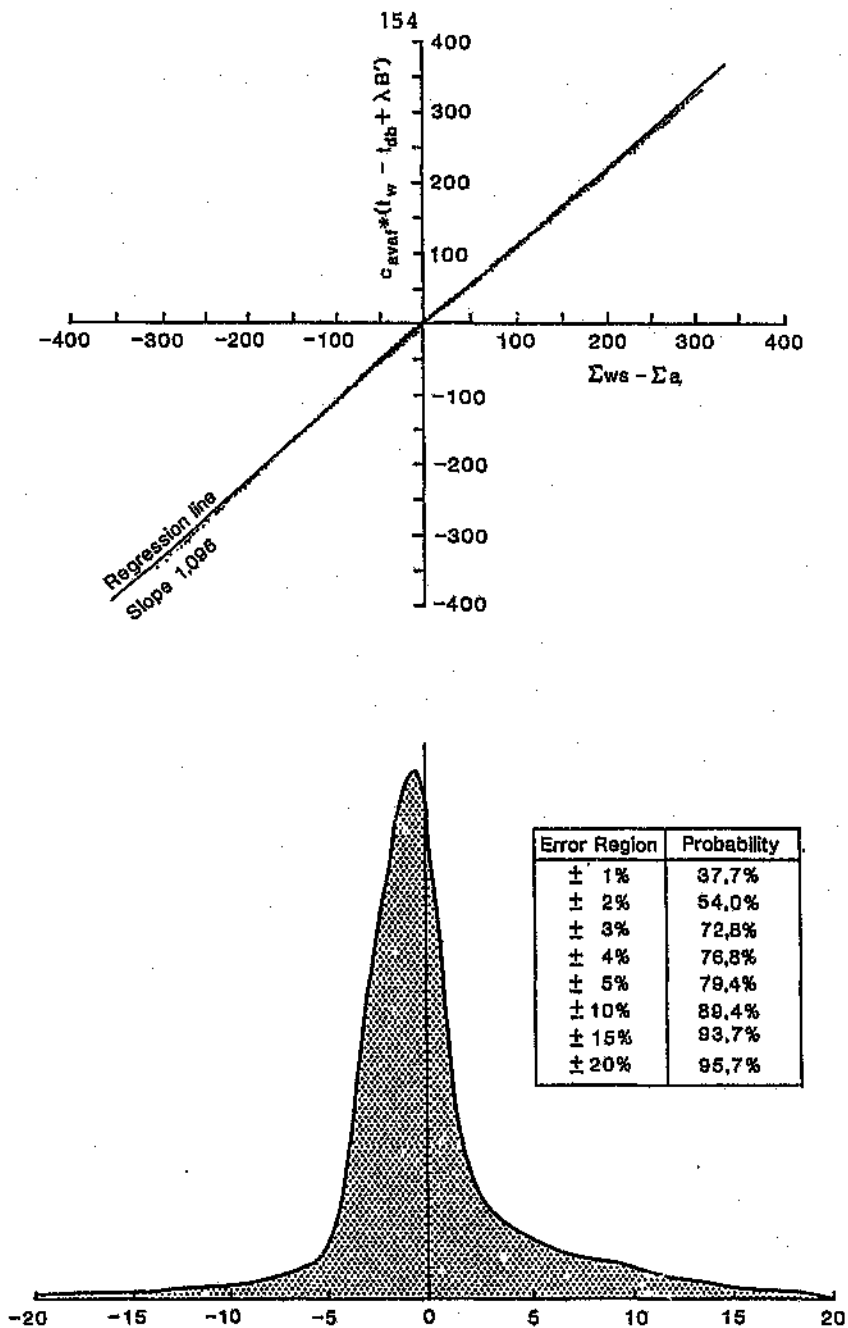


Figure 7.4 Correlation of the new improved approximate equation against the exact formulation and distribution of error when  $\beta = 1,096$

the origin, was conducted on the data shown in Figure 7.4. This produced the following correlation (regression coefficient 0,9998):

$$C_{\text{aval}} (t_w - t_{\text{db}} + \lambda B') = 1,096 (\Sigma_w - \Sigma_{\infty}) \quad (7.9)$$

The approximate equation for heat transfer at a wet surface may then be improved and stated as:

$$\frac{q_t}{C_{\text{aval}}} = \beta \left( \frac{h_c}{C_{\text{aval}}} \right) [\Sigma_w - \Sigma_{\infty}] \quad (7.10)$$

The accuracy of this equation has been examined with the term,  $\beta$ , having a value of 1,096; a distribution of the differences from the true values is also given in Figure 7.4. Clearly, the accuracy of this equation is considerably better than that of the Merkel equation. Equation 7.10 should be considered as a statement of a much improved approximation to the total heat flow formulation.

If the term,  $\beta$ , was to be considered as a constant in Equation 7.10, then over the full range of conditions the best estimate of it would be 1,096. However, in this present work the term has not been constrained to take on a single value. Where specific sets of conditions are being considered, more accurate values of the term may be calculated. This is done by equating Equation 7.10 to the exact formulation for total heat transfer (Equation 7.7) and thus defining the term, which would apply to a specific set of conditions, as:

$$\beta = \frac{C_{\text{aval}} (t_w - t_{\text{db}} + \lambda B')}{(\Sigma_w - \Sigma_{\infty})} \quad (7.11)$$

Note that this term is dimensionless, also that Equation 7.10 becomes exact if its value is calculated from Equation 7.11.

Note on the numerical value of the term,  $\beta$ .

The value of this term is always close to unity and is a function of the water surface temperature, the air dry-bulb temperature, the moisture content and the barometric pressure. The value of the term can be simply calculated using the relationships given earlier (further details are given in Appendix L).

Equation 7.10 is used to approximate total heat flow in the development of the overall performance equation in the rest of this study. As will be seen later the term,  $\beta$ , will be combined with another parameter to form the ratio  $\alpha/\beta$ . However, it is still of interest to see how the numerical value of the individual term,  $\beta$ , as calculated from Equation 7.11, varies over the range of conditions.

The term,  $\beta$ , is essentially the ratio of two driving force terms, the numerator (the more accurate) and the denominator (the approximation) and because the range of conditions under consideration covers the situation where these driving forces may be zero, its value may be between zero and infinity. The infinite case being when the air wet-bulb temperature is equal to the water temperature. This aspect, which is basically a mathematical instability, is worth noting at this stage, but it is shown later that this does not have any practical significance since unrealistic values only occur when the driving force for total heat transfer is unrealistically small.

Values of  $\beta$  for the situation where the air is saturated (which approximates closely to the general condition existing in a direct-contact heat exchanger) are presented in Figure 7.5. It can be seen that the value of the term for saturated air conditions varies between 1.06 and 1.14. Values of  $\beta$  for situations where the air is not saturated cannot be presented as concisely as those for saturated air. However, further information is given in Appendix L.

It should be noted that the values given by Equation 7.11 are applicable to a differential volume of direct-contact heat exchanger.

#### 7.2.4 Summary

This section commenced by showing that variations in the dry-bulb temperature do not affect the overall heat transfer driving force significantly. The sigma heat parameter is then introduced and it is noted that in an adiabatic saturation process it is the sigma heat content of the moist air, and not its enthalpy, that remains exactly constant. Furthermore, the sigma energy is a unique function of wet-bulb temperature only (at a given barometric pressure).

The development of a new approximation to the total heat transfer from a wet surface is then described. The new approximation is based on a sigma heat driving force difference and a more appropriate definition of the specific heat term for the mass transfer stream. The new approximation represents a significant improvement in accuracy over the widely used Merkel equation.

A specific conclusion of this chapter has thus far been the following relationship:

$$\frac{Q}{A} = \beta \left( \frac{h_0}{C_{\text{sat}}} \right) [ \Sigma_w - \Sigma_a ] \quad (7.12)$$

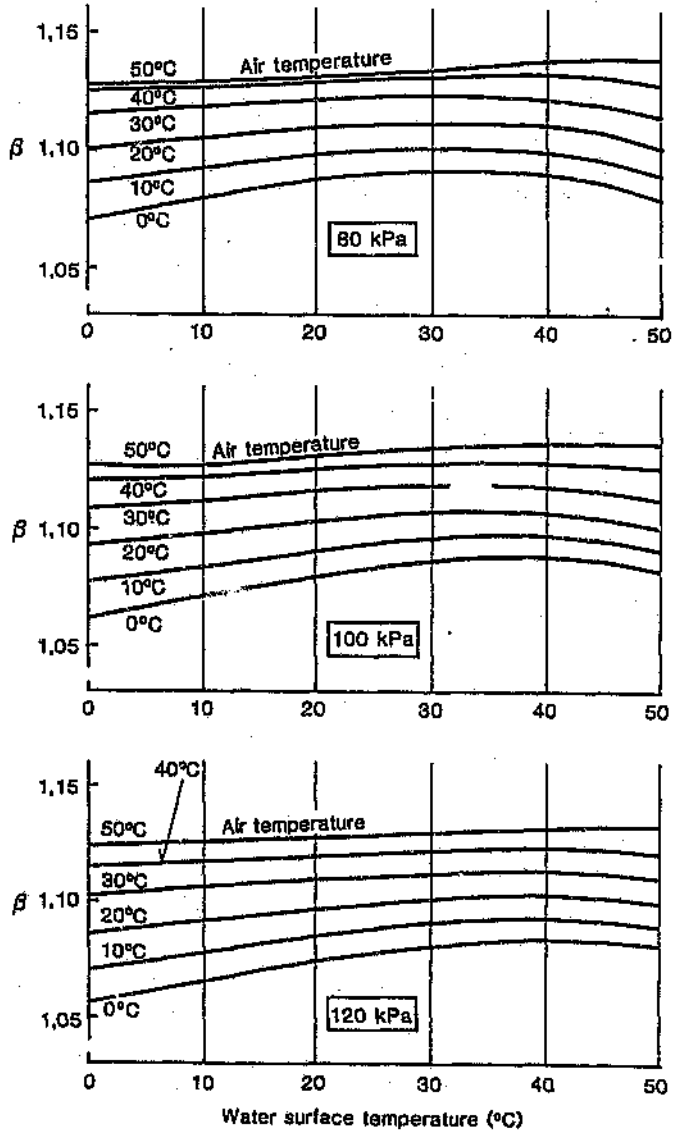


Figure 7.5 Values of  $\beta$  for saturated air

The concept of sigma heat is of considerable value to the hypothesis presented in this work, and as will be seen in Section 7.3, in addition to describing the heat flow driving force, it may also be used to describe the change in energy content of a moist air stream and thus describe the energy balance between the water and air streams.

### 7.3 Simplified equations for the change of energy state of the air and water streams

The rigorous forms of the energy balance equations for the air and water streams, across the element of a wet heat exchanger, are such that analytical manipulation is difficult and derivation of a useful overall performance equation impossible. This section discusses the development of simplified equations that are suitable for analytical manipulation and final solution.

#### 7.3.1 Energy balance equations across an element of direct-contact heat exchanger

The commonly used differential form of the energy flow equation is given below (note that the mass flow term is included within the differential to account for mass transfer).

$$d\dot{q} - d\dot{w} = d [ \dot{m} ( i + V^2/2 + gZ ) ] \quad (7.13)$$

When no work is being done and changes in kinetic energy and elevation can be neglected, as is applicable in this case, (for a detailed argument see Chapter 4), the equation is simplified to:

$$d\dot{q} = d ( \dot{m} i ) \quad (7.14)$$

For the air stream this solves to the usual form given below (note that the enthalpy is based on the flowrate of dry air which remains constant irrespective of any moisture transfer):

$$dq_a = \dot{m}_a di_a \quad (7.15)$$

For the water stream (in a constant pressure process) Equation 7.14 becomes:

$$dq_w = d(\dot{m}_w c_w t_w) \quad (7.16)$$

The thermal capacity of liquid water,  $c_w$ , may be considered to have a constant value of 4187 J/kg K. This value changes by less than 0,5 per cent over the range of temperatures being considered. Through Equation 7.16, the total change in enthalpy of the water stream (ignoring second order differential terms) is given by:

$$dq_w = \dot{m}_w c_w dt_w + d\dot{m}_w c_w t_w \quad (7.17)$$

Consider the small element of direct-contact counter-flow heat exchanger illustrated in Figure 7.6. Sensible heat is being transferred from the water surface to the air stream (defined as positive heat transfer). Water vapour is being transferred from the water surface to the air stream (defined as positive mass transfer). An enthalpy balance for the two streams, across the control volume produces:

$$\Delta q = \dot{m}_a (i_{a0} - i_{a1}) \quad (7.18)$$

$$\Delta q = \dot{m}_{w1} c_w (t_{w1} - t_{w0}) + \Delta \dot{m}_w c_w t_{w0} \quad (7.19)$$

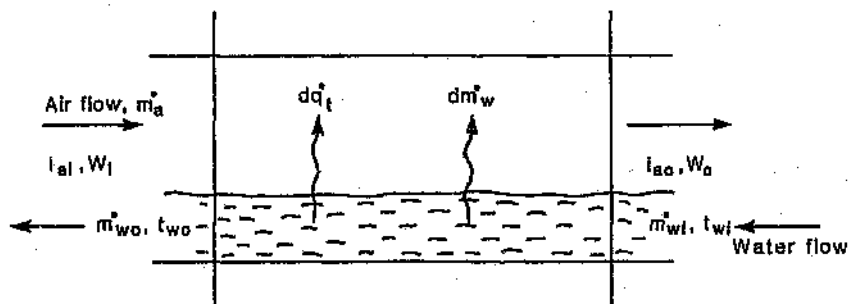


**Figure 7.6** Control volume of direct-contact heat exchanger with incremental heat and mass transfer

As discussed, under certain circumstances the air may become supersaturated and fogged and the form of these equations altered slightly. The fogging effect is considered in detail in Chapter 3 and fogged flow is accounted for in the computer model. This aspect does not effect the present argument.

### 7.3.2 Simplified energy balance equation

Combining Equations 7.18 and 7.19 produces the fully rigorous energy balance between the water and air streams.

$$\dot{m}_a (i_{a0} - i_{a1}) = \dot{m}_{w1} c_w (t_{w1} - t_{w0}) + X \quad (7.20)$$

where

$$X = \Delta \dot{m}_w c_w t_{w0}$$

In practice this equation is usually simplified by ignoring the term, X.

An improved alternative is to make use of sigma energy to describe the energy state of the air stream. Using sigma energy terms the full heat balance equation may be written as:

$$\dot{m}_a (\Sigma_0 - \Sigma_1) = \dot{m}_{w1} c_w (t_{w1} - t_{w0}) + Y \quad (7.21)$$

where

$$Y = \Delta \dot{m}_w c_w t_{w0} + \dot{m}_a c_w (W_1 t_{wb1} - W_w t_{w0})$$

The simplified form of this equation then ignores the term, Y.

The values of X and Y have been calculated for the full set of experimental data presented in Chapter 4. The relevant statistics of a comparison of X and Y are given in Table 7.1. Clearly an improved simplified energy balance equation would be given by Equation 7.21 with the term Y ignored.

$$m_a (\Sigma_0 - \Sigma_1) = m_{w1} c_w (t_{w1} - t_{w0}) \quad (7.22)$$

The above discussion demonstrates the advantage of using sigma energy in the simplified heat balance equation. However, for the present study the inaccuracy in using the simplified Equation 7.22 has not been ignored and as will be seen later a somewhat improved approach given by Equation 7.23 below is used in the present work.

$$m_{w1} c_w \Delta t_w = (\alpha/\gamma) m_a \Delta \Sigma \quad (7.23)$$

### 7.3.3 Simplified equation for the change of energy state of the air stream

There are a number of advantages for using changes in sigma heat content rather than changes in enthalpy to describe the overall energy change of the air stream. Apart from the improved accuracy in the simplified equation, there is a distinct advantage in using sigma heat rather than enthalpy, first, because the sigma heat of an air-water vapour mixture depends on the wet-bulb temperature and barometric pressure only, whereas enthalpy depends also on the dry-bulb temperature; and second, as was seen in Section 7.2, because the use of

a sigma  $\alpha$  at difference for the driving force in the simplified equation describing the total heat flow from a wet surface (Equation 7.12) constitutes a relatively accurate simplified approach.

In order to use sigma heat to describe the change of energy state of the air stream, the rigorous Equation 7.15 can be modified and written as:

$$dd_a = \alpha m_a dE \quad (7.24)$$

Equation 7.24 should not be considered as an approximation but rather as a definition of the term,  $\alpha$ . Inaccuracies only emerge when use is made of approximate values of the term. Note that this term is dimensionless and may also be expressed as:

$$\alpha = di_a / dE \quad (7.25)$$

Note on the numerical value of the term,  $\alpha$ .

The above definition is applicable to a differential control volume. As will be seen later,  $\alpha$  is combined with the term,  $\beta$ , in the ratio  $\alpha/\beta$  and another term,  $\gamma$ , in the ratio  $\alpha/\gamma$ . Use is also made of  $(\alpha/\gamma)_1$  and  $(\alpha/\gamma)_0$ , which are applicable across finite sizes of heat exchange surface. However, it is still of interest to see how the numerical value of the individual term varies over the range of conditions under consideration.

The enthalpy of an air-water vapour mixture can be expressed as a function of barometric pressure, dry-bulb temperature and wet-bulb temperature. Thus, for a constant pressure process an incremental change in enthalpy is given as:

$$di_a = (\partial i_a / \partial t_{db}) dt_{db} + (\partial i_a / \partial t_{wb}) dt_{wb} \quad (7.26)$$

Variations in wet-bulb and dry-bulb temperatures are not independent but will depend on the actual process involved.

The sigma heat content of an air-water vapour mixture is a function of barometric pressure and wet-bulb temperature only. For a constant pressure process an incremental change in sigma energy is given as:

$$d\Sigma = (\partial \Sigma / \partial t_{wb}) dt_{wb} \quad (7.28)$$

Because of the complexity of the form of the equations it is not possible to express the term,  $\alpha$ , as a simple analytical function. It is, however, a relatively simple matter to calculate numerically its value for different process changes of the air stream.

When saturated air comes into direct contact with a water surface and heat and mass transfer take place, the process change of the air stream is such that it becomes supersaturated and fogged. This is the case whether the water surface is being heated or cooled. Thus, once air is saturated in a direct-contact heat exchanger, it will remain saturated, assuming of course a fully mixed air condition and a uniform air-water

distribution. It was shown earlier that when fogging occurs the mechanisms involved can be accurately described by assuming the fog is carried along in the air stream in the form of small water droplets. Thus, the important issue in the present argument is that saturated air remains saturated and hence fogging per se does not affect the value of  $\alpha$ .

The value of the term for the situation where the air is saturated (which closely approximates the most commonly occurring conditions existing in a direct-contact heat exchanger) is dependent on the air temperature and pressure only since the air condition will remain saturated irrespective of the water temperature. Values of  $\alpha$  for air that is saturated are given in Figure 7.7. For these conditions the variation in  $\alpha$  with temperature is almost linear, varying from 1,01 at 0 °C to 1,11 at 50 °C. Note that the value for saturated air is always greater than 1,0. Further details and a listing of the computer program used to calculate these values is given in Appendix M. Values of this term for situations where the air is not saturated cannot be presented as concisely as those for saturated conditions. More information is given in Appendix M.

It should be noted that the values of  $\alpha$  given above are applicable to an infinitesimal differential volume of direct-contact heat exchanger. Consideration is given later to finite changes in process conditions.

The term,  $\alpha$ , is essentially the ratio of the two terms which describe a change in energy content; these changes in energy content may be positive, negative or zero. Thus, the value of  $\alpha$  may be between zero and infinity, the infinite case being when the process change of the air stream takes place at constant wet-bulb temperature. Typically the value of  $\alpha$  is close to

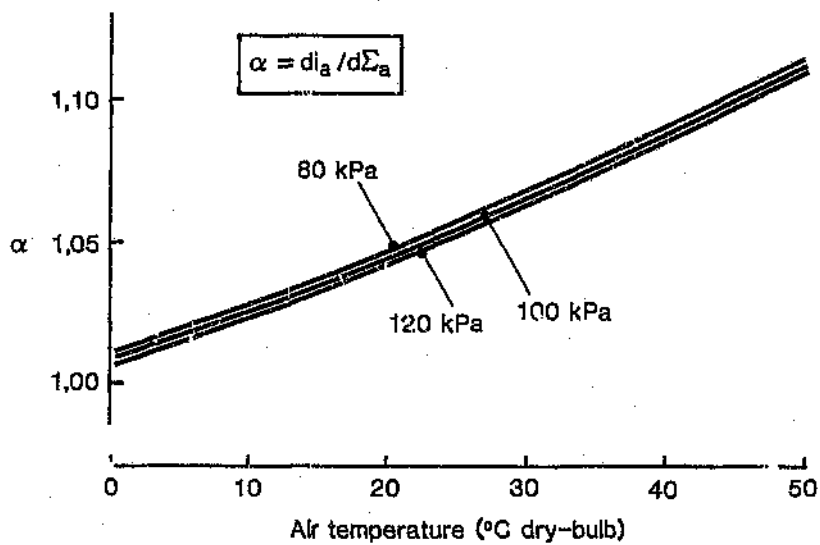


Figure 2.7 Value of  $\alpha$  for saturated air

unity, but the possibility of it having infinite or zero values should be noted. It will be seen later that this does not have any practical significance since unrealistic values occur only when the driving force for total heat transfer is unrealistically small.

#### 7.3.4 Simplified equation for the change of energy state of the water stream

Equations 7.17 and 7.19 describe the change of energy state of the water stream. The term on the far right-hand side of these equations accounts for the net evaporation or condensation that takes place. It represents only a small fraction of the total heat transfer and in most studies of this nature it is ignored and a simplified form of the equation is used. However, in the present study cognizance is taken of this term and the following simplified equation is used:

$$dq_w = \gamma m_w c_w dt_w \quad (7.29)$$

Equation 7.29 should not be considered as an approximation but rather as a definition of the term,  $\gamma$ . Inaccuracies occur only when approximate values of this term are used. Note that this term is dimensionless.

Note on the numerical value of the term,  $\gamma$ .

As will be seen later the term,  $\gamma$ , is combined in the ratio  $\alpha/\gamma$  and it is this ratio that is of significance in the subsequent analysis. Use is also made of two terms,  $(\alpha/\gamma)_i$  and  $(\alpha/\gamma)_o$ , which are applicable across finite sizes of heat exchange surface. However, it is

still of academic interest to examine the numerical value of the individual term,  $\gamma$ .

Through Equations 7.17 and 7.29 this term is given as:

$$\gamma = 1 + (\Delta m_w / m_w) \cdot (t_{wo} / dt_w) \quad (7.30)$$

Combining the basic relationships for heat and mass transfer with Equation 7.30 allows the term to be calculated from a knowledge of the water surface temperature, the condition of the air and the barometric pressure. This is discussed in Appendix N. It should be noted that fogging does not affect the value of  $\gamma$ .

It can be seen from Equation 7.30 that, as the term  $dt_w$  approaches zero, the value of  $\gamma$  tends to infinity. This fact is worth noting at this stage, but it will be seen later that this does not have any practical significance, since unrealistic values occur only when the driving force for total heat transfer is unrealistically small. The values of the term for the situation where the air is saturated are given in Figure 7.8. These values are practically independent of changes in barometric pressure and water-air flow ratio. The value of  $\gamma$  varies from 1.00 to 1.09 over the range of conditions, increasing with both air temperature and water temperature. Note that for saturated air the value will always be greater than 1.0, since  $dm_w$  and  $dt_w$  will always have the same sign.

Values of  $\gamma$  for situations where the air is not saturated cannot be presented as concisely as those for saturated conditions; however, further information is given in Appendix N.

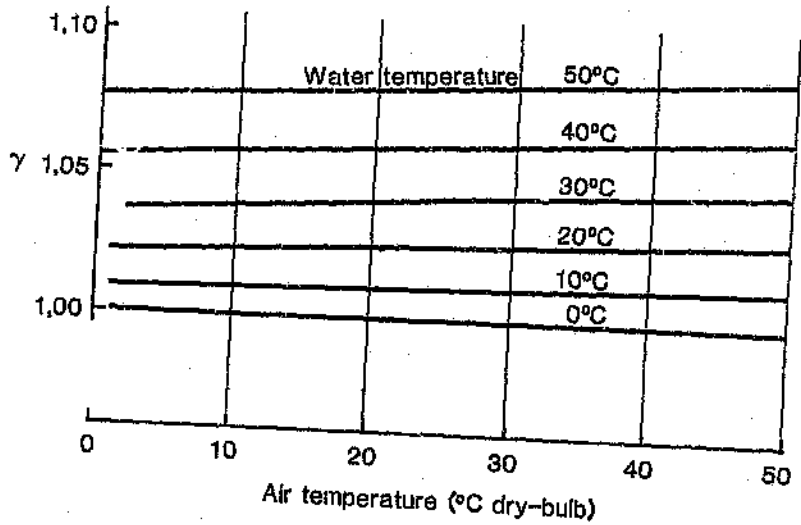


Figure 7.8 Value of  $\gamma$  for water in contact with saturated air (note that these values are practically independent of changes in barometric pressure and water-air flow ratio)

It should be noted that these values are applicable to a differential volume of the heat exchanger. Consideration is given later to representative values for finite changes in process conditions.

### 7.3.5 Summary

This section has defined simplified equations for describing the change of enthalpy of the air and water streams. The simplified equations for the air and water streams are given below:

$$dq_a = \alpha m_a d\Sigma \quad (7.31)$$

$$dq_w = \gamma m_w c_w dt_w \quad (7.32)$$

The two terms  $\alpha$  and  $\gamma$  are defined as:

$$\alpha = di_a / d\Sigma \quad (7.33)$$

$$\gamma = 1 + (dm_w/m_w) \cdot (t_w/dt_w) \quad (7.34)$$

The values of these terms are close to unity. Values for conditions where the air is saturated are presented here and further details for non-saturated conditions are given in Appendices M and N. Independently, the values of these two parameters are not relevant since they are combined with other parameters in subsequent manipulation.

The simplified form of the equations describing the changed energy state of the two streams is used in the next section, in combination with the simplified equation for the total heat transfer at a wet surface (see Section 7.2), to derive the overall direct-contact heat exchanger performance equation.

#### 7.4 Development of a theoretical performance equation

##### 7.4.1 Review of conventional (non direct-contact) heat exchanger practice

In a large proportion of heat exchangers there is no direct contact between the interacting fluids and the total thermal capacity of each fluid, i.e. the product of the mass flowrate and the specific heat normally remains constant throughout the heat exchange process. (It is this latter point that creates the major difference between direct-contact and non direct-contact heat exchanger theory for air and water.) The theory describing the thermal performance of non direct-contact heat exchangers is well established and is documented in many standard texts (50,51,52). A modification to the normal NTU method has been developed in the course of this work and is presented below to show a sequence of logic which will be referred to later in drawing analogies between the direct-contact and the non direct-contact case.

A diagram of a section of a non direct-contact counter-flow water-air heat exchanger is shown in Figure 7.9. The heat transfer rate across an element of heat exchanger surface is given by:

$$dq = U (t_w - t_{db}) dA \quad (7.35)$$

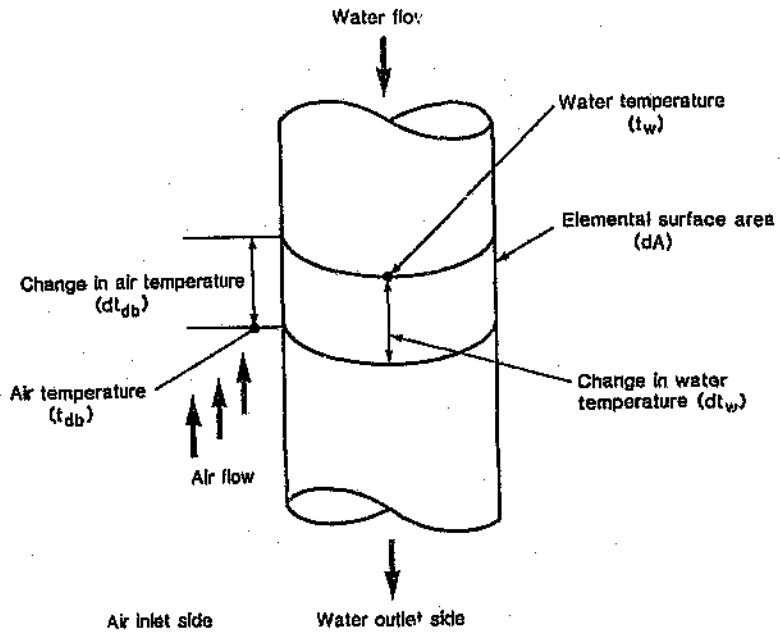


**Figure 7.9** Elemental section of a non direct-contact counterflow heat exchanger

The term,  $U$ , is the overall heat transfer coefficient which describes the combined effect of the thermal resistances in the water film adjacent to the separating surface, in the separating wall and in the air film adjacent to the wall surface. These resistances are described by thermal conductivity data, or, in the case of the film co-efficients, in terms of correlation equations for the Nusselt or Stanton numbers for forced convection situations.

The heat flow causes a change in the temperature of the air stream (and the water stream) and the change of energy state of the air stream across the elemental area may, in the absence of moisture transfer and changes in kinetic and potential energy, be described by:

$$dq_a = m_a c_a dt_{db} \quad (7.36)$$

Energy balances between the water and air streams across the counterflow heat exchanger from the air inlet side (water outlet side) to the section being considered, produce:

$$m_a c_a (t_{db} - t_{dbi}) = m_w c_w (t_w - t_{wo}) \quad (7.37)$$

An energy balance between the two streams across the entire heat exchanger produces:

$$m_a c_a (t_{dbo} - t_{dbi}) = m_w c_w (t_{wi} - t_{wo}) \quad (7.38)$$

These equations are normally combined to produce the familiar 'Effectiveness - NTU' equation(50) given below:

$$E = \frac{1 - e^{-NTU \left(1 - \frac{C_{min}}{C_{max}}\right)}}{1 - \left(\frac{C_{min}}{C_{max}}\right) e^{-NTU \left(1 - \frac{C_{min}}{C_{max}}\right)}} \quad (7.39)$$

This equation introduces the three so-called heat exchanger parameters.

$\frac{C_{min}}{C_{max}}$  Thermal capacity ratio, where  $C_{min}$  is the thermal capacity (W/K) of the fluid with the lower thermal capacity,  $C_{max}$  is that of the fluid with the higher thermal capacity.

NTU - Number of transfer units, which is the design characteristic or thermal 'size' of the heat exchanger given by  $NTU = UA/C_{min}$ .

E - Effectiveness, which is the ratio of the change in temperature of the fluid with the lower thermal capacity to the difference between the fluid inlet temperatures.

The familiar 'Effectiveness - NTU' approach is shown graphically in Figure 7.10. This form of the relationship is often clumsy in its application (by virtue of having to determine which fluid gives  $C_{min}$  and having to invert the factor  $C_{min}/C_{max}$  from time to time). More importantly, it is not suitable for the specific manipulation which is required in Section 4.2.1. Thus a new form of this relationship has been developed below.

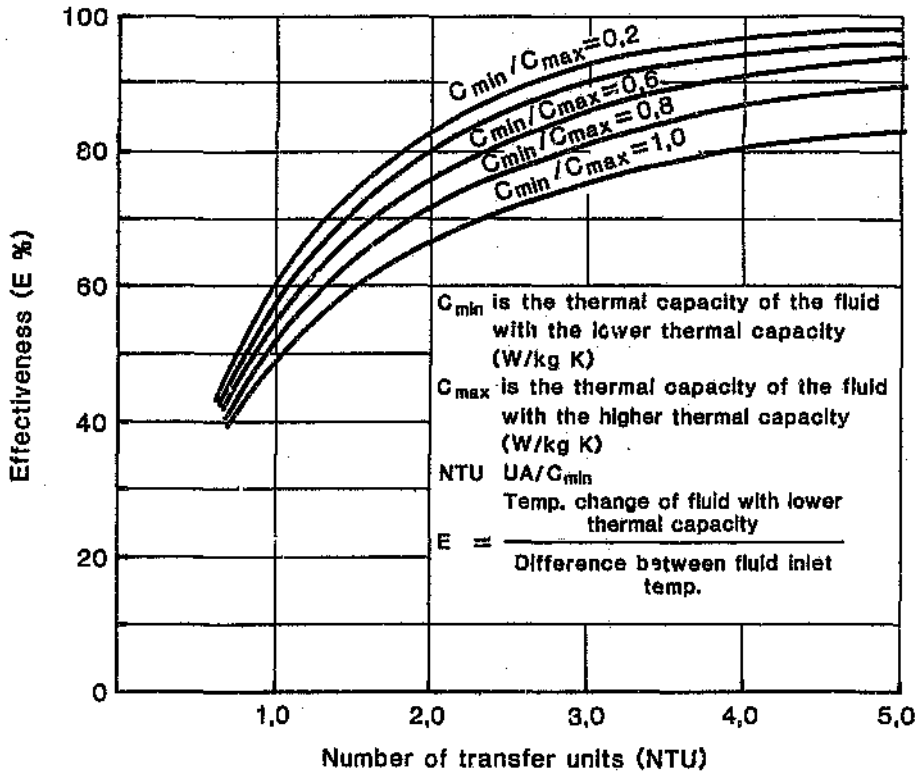


Figure 7.10 Performance of non direct-contact counter-flow heat exchangers (E vs NTU)

Combining Equations 7.35, 7.36 and 7.37 gives:

$$\frac{U}{m_a' c_a} dA = \frac{dt_{db}}{J_1 + J_2 t_{db}}$$

where

$$J_1 = t_{wo} - \frac{m_a' c_a}{m_w' c_w} t_{db1} \quad (7.40)$$

$$J_2 = \frac{m_a' c_a}{m_w' c_w} - 1$$

Integrating Equation 7.40 across the entire heat exchanger between the inlet and outlet air conditions and combining with Equation 7.38 yields:

$$\frac{t_w - t_{wo}}{t_w - t_{db1}} = \frac{1 - e^{-UA/m_a' c_a (1 - \frac{m_a' c_a}{m_w' c_w})}}{(\frac{m_w' c_w}{m_a' c_a}) - e^{-UA/m_a' c_a (1 - \frac{m_a' c_a}{m_w' c_w})}} \quad (7.41)$$

Writing Equation 7.41 in terms of the somewhat modified heat exchanger parameters gives:

$$E_w = \frac{1 - e^{-N(1-1/R)}}{R - e^{-N(1-1/R)}} \quad (7.42)$$

Equation 7.42 is shown plotted in Figure 7.11 and it is in this form that the relationship will be referred to in much more detail later.

The three new heat exchanger parameters are now described as:

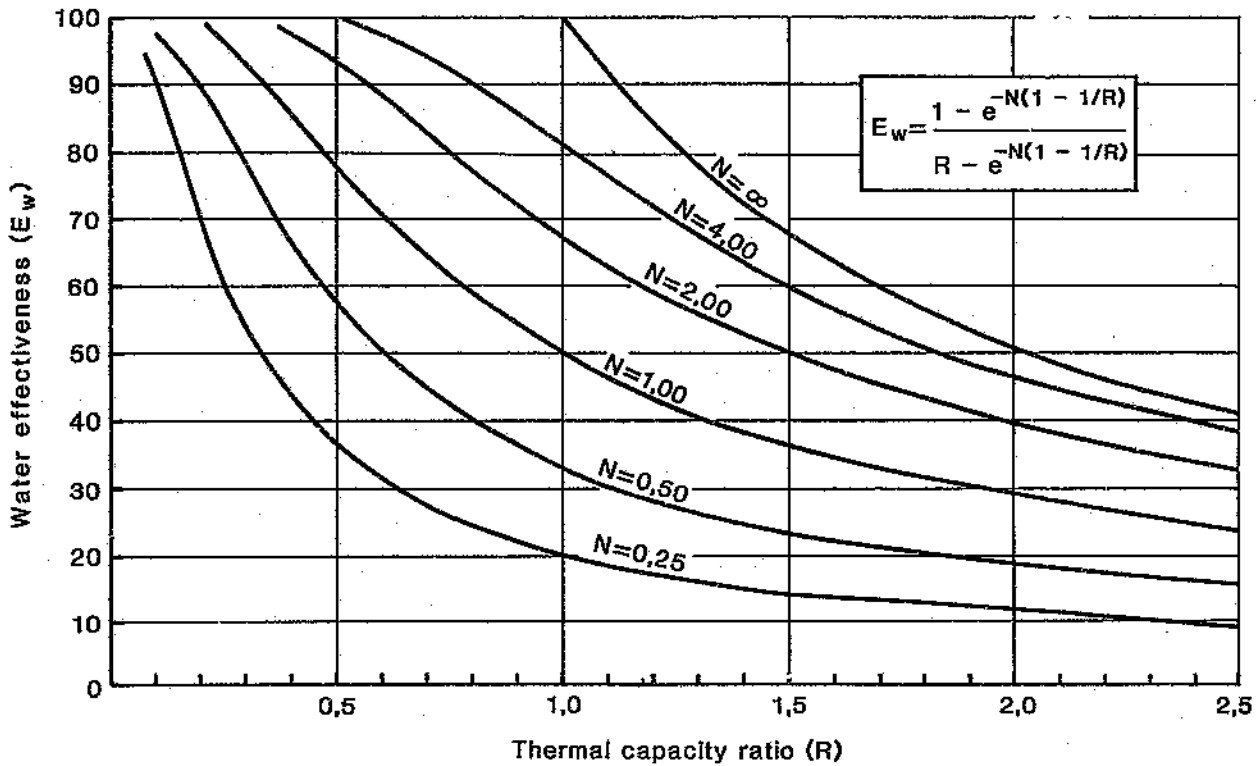


Figure 7.11 Performance of non direct-contact counterflow heat exchangers ( $E_w$  vs  $R$ )

- R - thermal capacity ratio, the ratio of the thermal capacity of the water stream to that of the air,  

$$R = \dot{m}_w c_w / \dot{m}_a c_a$$
- N - design characteristic or thermal size of the heat exchanger based on air flowrate,  $N = UA / \dot{m}_a c_a$
- $E_w$  - water effectiveness, the ratio of the change in temperature of the water to the difference between the inlet water and inlet air temperatures,  

$$E_w = (t_{wi} - t_{wo}) / (t_{wi} - t_{dbi})$$

The difference between Equation 7.41 and the normal 'Effectiveness - NTU' equation quoted in standard texts should be stressed. The thermal capacity ratio is usually defined so that it is always less than unity, with the numerator referring to the fluid with the smaller thermal capacity. In Equation 7.41 the thermal capacity ratio is given as the ratio of the thermal capacity of the water stream to that of the air stream, irrespective of which is the larger. The effectiveness (or efficiency) normally refers to the fluid with the lower thermal capacity. In Equation 7.41, the water efficiency is used under all circumstances. The Number of Transfer Units is normally based on the fluid with the lower thermal capacity. However, in this present application the design parameter N will always be based on the thermal capacity of the air stream.

#### 7.4.2 Development of a performance equation for the direct-contact case

The basis of this development is three equations which evolve from a consideration of an elemental surface of a direct-contact water-air heat exchanger as shown in Figure 7.12.

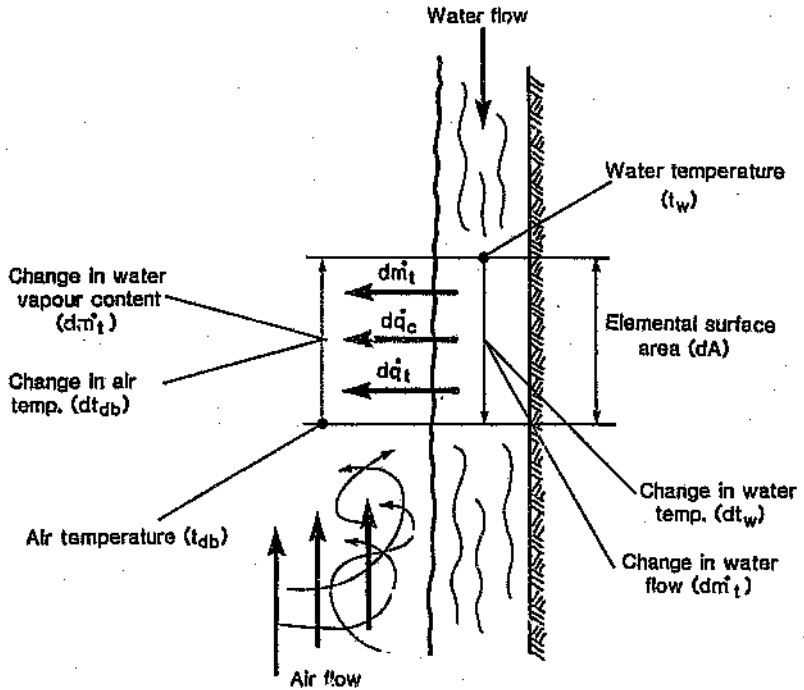


Figure 7.12 Elemental section of a direct-contact counterflow heat exchanger

The first equation describes the total heat transfer (sensible and latent) from the air-water interface and, as discussed earlier, this is best described as:

$$dq = h_c ( t_w - t_{db} + \lambda B' ) dA \quad (7.43)$$

The other two equations describe the change of energy state of the air and water streams due to the heat and mass transfer across the incremental area. The equation describing the change of energy content of the air stream is given as:

$$dq = m'_a di_a \quad (7.44)$$

The change of energy content of the water stream is given as:

$$dq = m'_w c_w dt_w + dm'_w c_w t_w \quad (7.45)$$

The essence of the development of an overall performance equation is the solution of these three equations simultaneously and their subsequent integration over the entire heat exchanger. In order to generate a solution (along the lines analogous to the non direct-contact heat exchanger) a number of simplifying assumptions must be made. It then becomes possible to manipulate the resulting functions algebraically, enabling the form of the overall performance equation and the correct grouping of the various parameters to evolve.

As seen earlier in Sections 7.2 and 7.3, the three basic equations can be simplified and rewritten as:

$$dq = \beta \frac{h_c}{C_{\text{air}}} (\Sigma_w - \Sigma_a) dA \quad (7.46)$$

$$dq = \alpha m_a d\Sigma \quad (7.47)$$

$$dq = \gamma m_w c_w dt_w \quad (7.48)$$

The logic in writing the equations in this form is that the parameters  $\alpha$ ,  $\beta$  and  $\gamma$  are reasonably constant over the range of air and water conditions being considered, and each has a value close to unity. It is also possible, with the equations in this form, to follow a similar sequence of logic to that set out in Section 7.4.1 for the simpler non direct-contact case.

Combining Equations 7.47 and 7.48 and integrating to create an energy balance between the air inlet / water outlet boundary and an intermediate point of a counter-flow heat exchanger, produces:

$$\alpha_i m_a (\Sigma_i - \Sigma_o) = \gamma_i m_w c_w (t_w - t_{wo}) \quad (7.49)$$

The subscript,  $i$ , in  $\alpha_i$  and  $\gamma_i$  refers to the fact that the energy balance has been taken between the air inlet and an intermediate position in the heat exchanger. In a similar manner an overall heat balance across the entire heat exchanger produces:

$$\alpha_o m_a (\Sigma_o - \Sigma_i) = \gamma_o m_w c_w (t_i - t_{wo}) \quad (7.50)$$

It is important to note that finite differences and not single point values are involved in Equations 7.49 and 7.50. In fact, these equations should be considered as defining the terms  $\alpha_1$ ,  $\alpha_0$ ,  $\gamma_1$  and  $\gamma_0$ .

Before progressing with the development of this logic it is necessary to make a last important definition. A pseudo-specific heat term,  $c_a^*$ , for saturated air based on sigma energy;

$$c_a^* = (\Sigma - a) / t_{wb} \quad (7.51)$$

where

$$a = \Sigma_0 \%$$

At the water surface condition, this pseudo-specific heat is given as:

$$\Sigma_w = a + c_{aw}^* t_w \quad (7.52)$$

The pseudo-specific heat term for saturated air depends only on the temperature and the barometric pressure. The constant,  $a$ , in Equation 7.51 is the value of the sigma energy content at 0 °C and is dependent on barometric pressure only. The terms may be calculated from the psychrometric equations given in Appendix A. The variation of the pseudo-specific heat over the range of conditions being considered is given in Figure 7.13.

Substituting Equation 7.52 into Equation 7.49, for  $t_w$ , and re-arranging produces:

$$\Sigma_w = a + c_{aw}^* t_{wb} + \left( \frac{\alpha}{\gamma} \right) \frac{m_a c_{aw}^*}{m_w c_w} (\Sigma - \Sigma_1) \quad (7.53)$$

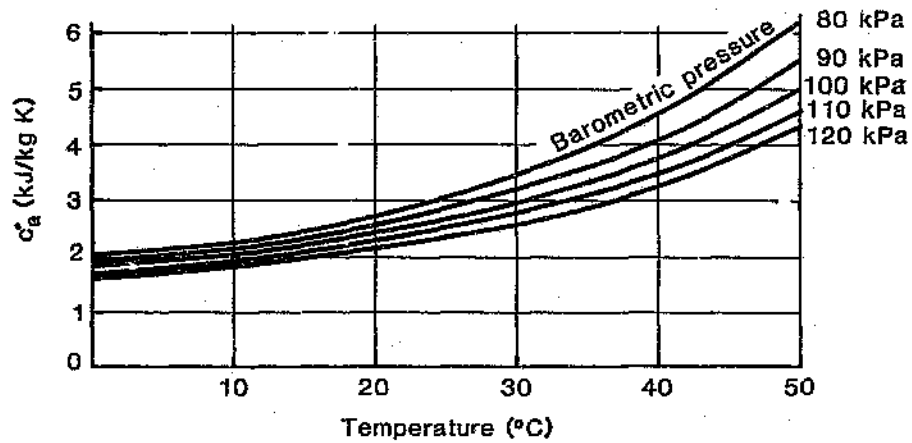


Figure 7.13 Values of the pseudo-specific heat term for different temperatures and pressures

Equating Equations 7.46 and 7.47 gives:

$$\frac{h_c dA}{m_a (\alpha/\beta) C_{\text{avaf}}^*} = \frac{d\Sigma}{(\Sigma_w - \Sigma)} \quad (7.54)$$

Substituting Equation 7.53 into Equation 7.54 gives:

$$\frac{h_c dA}{m_a (\alpha/\beta) C_{\text{avaf}}^*} = \frac{d\Sigma}{(J_3 + J_4 \Sigma)} \quad (7.55)$$

where

$$J_3 = a + C_{\text{aw}}^* t_{\text{wo}} - \left( \frac{\alpha}{\gamma} \right) \frac{m_a C_{\text{aw}}^*}{m_w C_w} \Sigma_1$$

$$J_4 = \left( \frac{\alpha}{\gamma} \right) \frac{m_a C_{\text{aw}}^*}{m_w C_w} - 1$$

To make the integration of Equation 7.55 analytically possible we now define  $(\alpha/\gamma)_1$ ,  $[(\alpha/\beta) C_{\text{avaf}}^*]$ ,  $C_{\text{aw}}^*$  as representative mean values of these terms over the limits of the integral. These mean representative values and the implications of this assumption are discussed later. At this stage the reader is asked to accept the validity of the use of these mean representative terms, obviously provided that correctly chosen values are utilized. It must also be noted that the value of the film coefficient,  $h_c$ , must remain constant for the integration to be possible. This also infers that a representative mean value of the film coefficient is used.

Integrating Equation 7.55 across the entire heat exchanger, between inlet and outlet air conditions (see Appendix O), yields:

$$E_w^* = \frac{1 - e^{-N^* (1 - 1/R^*)}}{(1 - J + JR^*) - e^{-N^* (1 - 1/R^*)}} \quad (7.57)$$

where

$$R^* = [ m_w' c_w ] / [ m_a' c_{aw}^* (\alpha/\gamma)_i ]$$

$$N^* = h_c A / [ m_a' (\alpha/\beta) c_{paf}^* ]$$

$$E_w^* = ( t_{wi} - t_{wo} ) / ( t_{wi} - ( \frac{C_{ai}^*}{C_{aw}^*} ) t_{wbi} )$$

$$J = (\alpha/\gamma)_i / (\alpha/\gamma)_o$$

Note that in the interests of simplicity the 'bar' notation, referring to representative mean values, has been dropped. However, it must be understood that the representative mean values are always implied when referring to the overall performance equation.

At this stage it is possible to make an initial statement of a performance hypothesis on the basis of Equation 7.57. However, the equation can only be expected to describe performance trends accurately if appropriate values of  $(\alpha/\gamma)_i$ ,  $[(\alpha/\beta) c_{paf}^*]$ ,  $C_{aw}^*$  are used to represent these parameters throughout the heat exchanger process (and if the film coefficient,  $h_c$ , remains fairly constant throughout the heat exchanger).

Note that the concept of the pseudo-specific heat as presented thus far is not really an assumption but rather a definition. The assumptions come later when a simple way of calculating this term from a knowledge of the inlet process conditions, is presented. The most important issue is that a single representative value will be used for a single set of process conditions.

Equation 7.57 is extremely useful in that it supplies an explanation of the grouping of the various terms and, as will be seen, this is an important achievement

of the present work.

Equation 7.57 represents the new performance equation in its full form. In fact, bearing in mind the definitions of the various terms like  $\alpha_1$ ,  $\gamma_1$ ,  $\beta$  and  $c_{aw}^*$  and the definition of representative mean values, the equation may be considered rigorous. However, it is still of limited practical use in its present form and attention is now turned to refining the equation and examining the selection of representative mean values of the various parameters.

#### 7.5 Refinement of performance equation and procedure for selecting parameter values

In determining appropriate values of the pseudo-specific heat  $c_{aw}^*$ ,  $[(\alpha/\beta) c_{avaf}^*]$ ,  $(\alpha/\gamma)_i$  and  $(\alpha/\gamma)_o$ , it is necessary to understand how these vary with water temperature, air temperature and barometric pressure. Clearly, of major importance is their variation across a heat exchanger for a specific set of process operating conditions.

In investigating these aspects use is again made of the computer simulator developed earlier. Recall that the simulator, which has proved to mimic the test heat exchangers very well, determines the heat and mass transfer rates from a knowledge of the  $h_c A$  term, the inlet temperature conditions and the flowrates. This is achieved by dividing the heat exchanger into small sections and then solving the applicable differential equations numerically and sequentially from inlet to outlet conditions. Thus, all the internal conditions as well as end states may be predicted for both hypothetical situations and for real test data.

### 7.5.1 Initial simplification of performance equation

An initial simplification, and perhaps an obvious one, applies to:

$$J = (\alpha/\gamma)_1 / (\alpha/\gamma)_0 \quad (7.58)$$

This term is a second order correction in the energy balance relationship to account for the fact that fully rigorous enthalpy balances are not used.

As seen from the development of the overall performance relationship, the infinitesimal differential values (or point values) of  $\alpha/\gamma$  have no relevance. Rather, it is the values relating to a finite section of the heat exchanger (from the air inlet boundary condition) that are applicable. For these finite differences and for any point within the heat exchanger:

$$(\alpha/\gamma)_1 = \dot{m}_w c_w (t_w - t_{w0}) / \dot{m}_a (\Sigma - \Sigma_1) \quad (7.59)$$

$$J = \frac{(t_w - t_{w0}) (\Sigma_0 - \Sigma_1)}{(t_w - t_{w0}) (\Sigma_a - \Sigma_1)} \quad (7.60)$$

The variation of the term  $J$  across and within the heat exchangers for each test has been determined through the use of the computer simulator and is given in Table 7.2. The term has been found, not surprisingly, to vary negligibly from unity, having an overall mean value of 0.997 (standard deviation = 0.008). It is thus proposed that a universal value of 1.000 be adopted.

However, it is of academic interest to note that the value is always greater than 1,0 for the cold water (condensation type) tests and less than 1,0 for the hot water (evaporation type) tests. The mean values are 1,003 and 0,990 respectively and although this is a clear distinction that can be made between the two types of tests, it is of little relevance because the heat exchanger effectiveness is only affected negligibly by the term, J.

Thus, the term in the overall performance equation that contains J may be modified by equating J to unity as follows:

$$(1 - J + JR^*) = R^* \quad (7.61)$$

Note that any small deviation of J from unity is, in any event, self-compensating, since the order of magnitude of  $R^*$  is approximately 1,0 and the differential is given as:

$$\frac{d(1 - J + JR^*)}{dJ} = R^* - 1 \quad (7.62)$$

The overall Equation 7.57 can then be written in a simpler form as:

$$E_w^* = \frac{1 - e^{-N^*(1 - 1/R^*)}}{R^* - e^{-N^*(1 - 1/R^*)}} \quad (7.63)$$

The similarity between this and Equation 7.41 (which evolved from the non-direct contact theory) is obvious,

with the so-called heat exchanger parameters now being given as:

$R^*$  - thermal capacity ratio, the ratio of the thermal capacity of the water stream to the equivalent thermal capacity of the air stream

$$R^* = \dot{m}_w c_w / [ \dot{m}_a (\alpha/\gamma)_t c_{aw}^* ] \quad (7.64)$$

$N^*$  - design characteristic or thermal size of direct-contact heat exchanger based on air flowrate

$$N^* = h_c A / [ \dot{m}_a (\alpha/\beta) c_{avaf}^* ] \quad (7.65)$$

$E_w^*$  - direct contact water effectiveness based on wet-bulb temperature and the pseudo-specific heat concept

$$E_w = (t_{w1} - t_{w0}) / (t_{w1} - \frac{c_{al}^*}{c_{aw}^*} t_{wbl}) \quad (7.66)$$

The overall performance equation may also be rearranged and written in terms of the more commonly used water efficiency, as:

$$\begin{aligned} E_w &= (t_{w1} - t_{w0}) / (t_{w1} - t_{wbl}) \quad (7.67) \\ &= \phi_1 \left[ \frac{1 - e^{-N^*} (1 - 1/R^*)}{R^* - e^{-N^*} (1 - 1/R^*)} \right] \end{aligned}$$

$$\text{where } \phi_1 = (t_{w1} - \frac{c_{al}^*}{c_{aw}^*} t_{wbl}) / (t_{w1} - t_{wbl})$$

### 7.5.2 Initial examination of parameters in performance equation for selected hypothetical conditions

Six hypothetical situations are initially examined. The conditions were chosen to cover the full range of temperature conditions as well as some typical water cooling duties. The specified conditions and results are summarized in Table 7.3 and the variations of each of the relevant parameters within the hypothetical heat exchanger are plotted in Figures 7.14 a-f.

A study of these figures clearly indicates that the terms  $(\alpha/\gamma)_i$  and  $[(\alpha/\beta) c_{avaf}^*]$  do not vary significantly across the heat exchanger for any one set of process conditions. The arithmetic mean values of the two terms are also shown in Figure 7.14 a-f. The fact that the variations on either side of these mean values are small indicates the probable acceptability of using single preselected values of these two terms in the practical application of the overall performance equation. This becomes fully apparent later.

The variation of the pseudo-specific heat term for air,  $c_{aw}$ , over the full range of conditions being considered in this study is given in Figure 7.13. The value varies from 1,6 to 6,2 kJ/kgK. With this wide variation it is clear that no single universal value may be used. However, the variation across a single heat exchanger for typical operating conditions would be considerably smaller and this is evident from Figures 7.14 a-f. The appropriate representative values of the pseudo-specific heat term for the six hypothetical runs have been calculated and are indicated in Table 7.3 and Figures 7.14 a-f. These values are determined through the solution of Equation 7.63 using the arithmetic mean values of  $(\alpha/\gamma)_i$  and  $[(\alpha/\beta) c_{avaf}^*]$ . Note that the

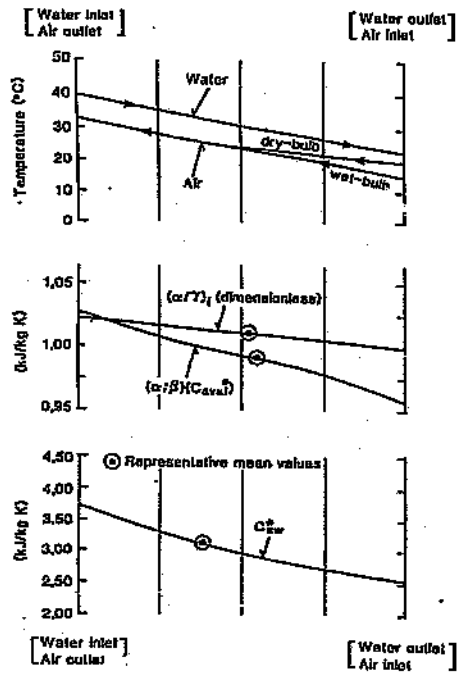


Figure 7.14.a Hypothetical calculation A

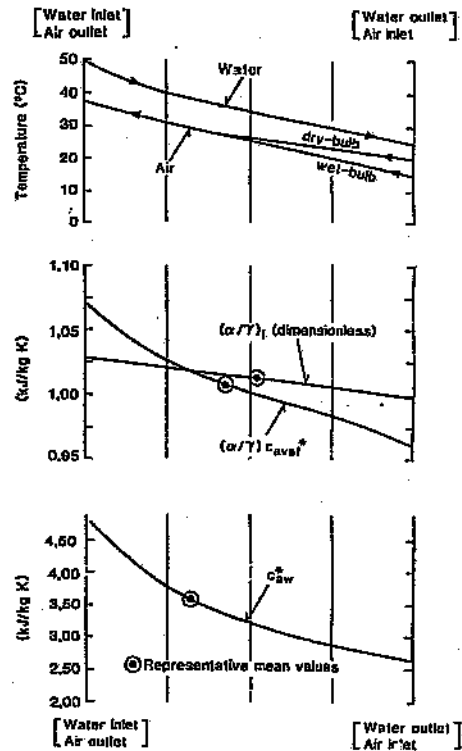


Figure 7.14.b Hypothetical calculation B

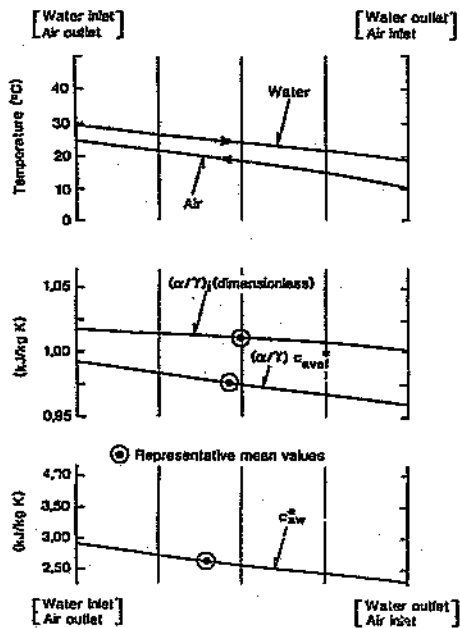


Figure 7.14.c Hypothetical calculation C

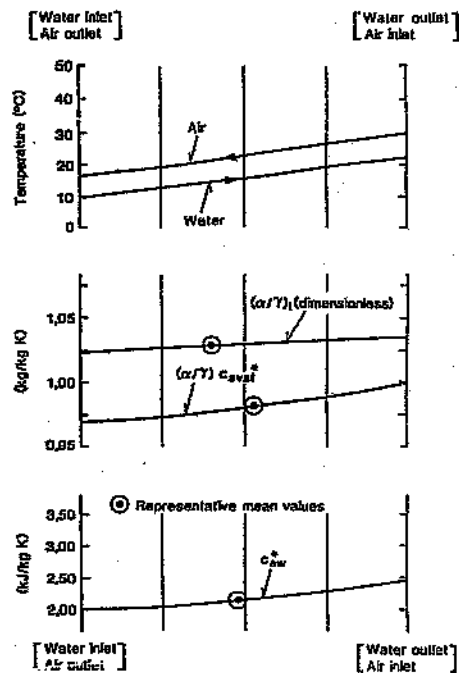


Figure 7.14.d Hypothetical calculation D

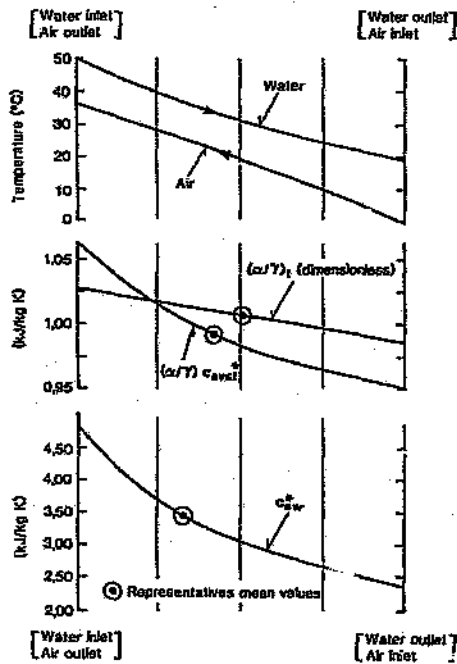


Figure 7.14.e Hypothetical calculation E

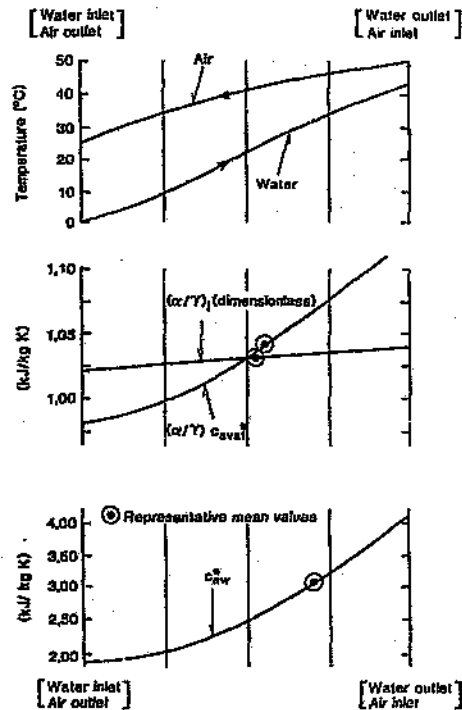


Figure 7.14.f Hypothetical calculation F

representative values of  $c_{aw}^*$  are roughly at the midpoint of the heat exchanger. This evidence indicates that the use of a single value of the pseudo-specific heat term would be possible for a single set of process conditions. Thus, the error in using a single representative value in integrating Equation 7.55 is probably acceptable. This becomes fully apparent later.

### 7.5.3 Examination of parameters in performance equation for the experimental data

For illustrative purposes Tests No. 42 and 58 have again been considered and the relevant parameters and their variations are shown in Figures 7.15 a-b. Also shown are the arithmetic values of  $(\alpha/\gamma)_i$  and  $[(\alpha/\beta) c_{avaf}^*]$  and the appropriate representative values of the pseudo-specific heat term.

Clearly the tentative conclusions drawn in Section 7.7.1 are supported by this information.

The values of the terms  $(\alpha/\gamma)_i$ ,  $[(\alpha/\beta) c_{avaf}^*]$  and  $c_{aw}^*$  have been examined for the full set of test data and each is considered in turn below.

#### Experimental values of $(\alpha/\gamma)_i$

The individual terms  $\alpha$  and  $\gamma$ , which are applicable to elemental points within the heat exchanger, were discussed in Section 7.3. The values of the ratio  $(\alpha/\gamma)$  are given in Figure 7.16. The clear distinction between water cooling and air cooling applications is of particular importance. Note also the representation of Test Nos 42 and 58 which have been included for illustrative purposes.

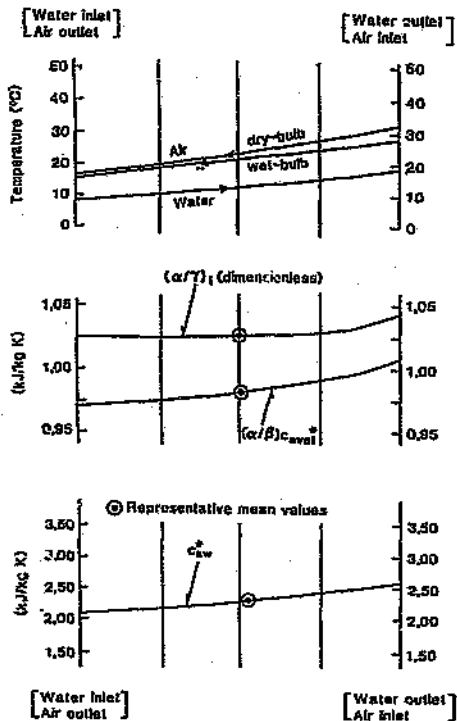


Figure 7.15.a Experimental data  
Test No. 42

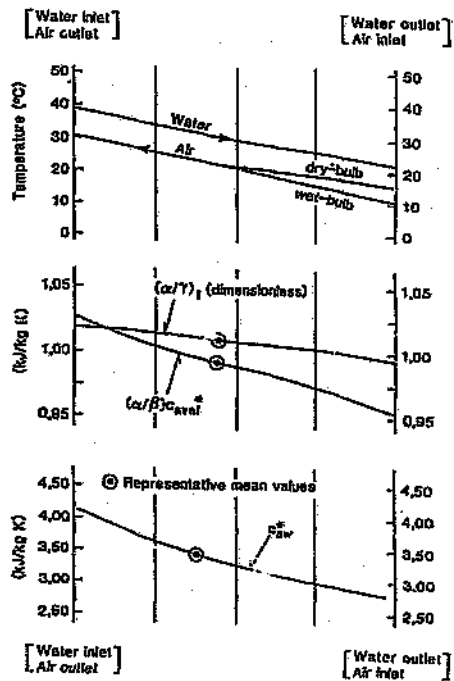


Figure 7.15.b Experimental data  
Test No. 58

The values of the ratio relating to a finite section is given by :

$$(\alpha/\gamma)_i = \frac{\dot{m}_w^i c_w (t_w - t_{wo})}{\dot{m}_a^i (\Sigma - \Sigma_i)} \quad (7.68)$$

From a practical point of view the value of this ratio can only really be examined with a complete set of heat exchanger data. The variation of the term  $(\alpha/\gamma)_i$  between inlet and outlet of the heat exchangers for each test is shown in Table 7.4 along with the arithmetic mean values. It should be noted that for the cold water tests the value of the term decreases between air inlet and outlet, and for the hot water tests this trend is reversed. For the cold water tests the variation in the value for any one test is not greater than 1,3 per cent. For the hot water tests the variation in the value is not greater than 2,6 per cent. Thus, the earlier conclusion is confirmed that  $(\alpha/\gamma)_i$  does not vary significantly for any one test. This logic can now be taken to its conclusion with an examination of all the test data. The database consisted of 10 values per test for each of the 160 tests and the relevant statistics are as follows:

Cold water tests: mean 1,03 (s.d. 0,6 %)  
 Hot water tests: mean 1,00 (s.d. 1,1 %)  
 All tests combined: mean 1,02 (s.d. 1,5 %).

The selection of single representative values is discussed later in combination with the selection of values for the other parameters. However, at this stage note that the preferred value for the cold water tests would be higher than that for the hot water

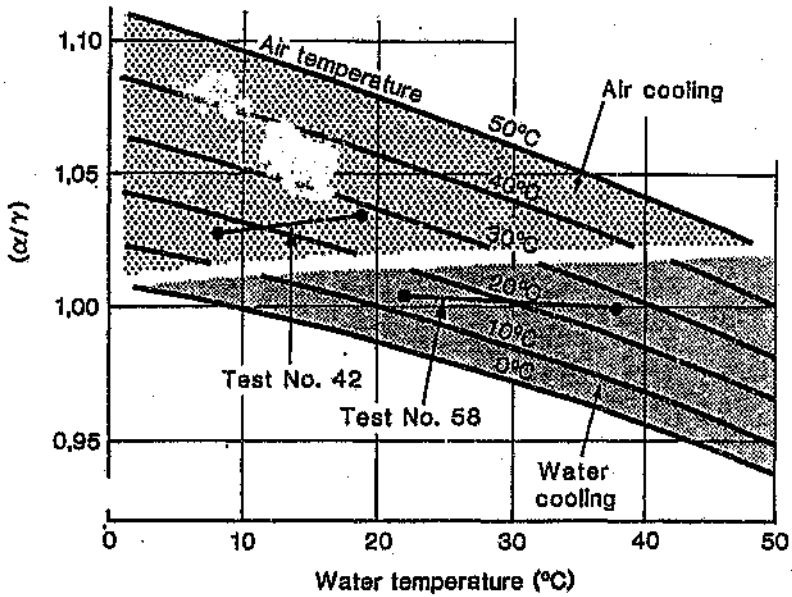


**Figure 7.16** Values of  $(\alpha/\gamma)$  for water in contact with saturated air, note for all practical purposes these values are independent of barometric pressure

tests. Note also that this is exactly what is indicated by the shaded areas depicted in Figure 7.16.

### Experimental values of $[(\alpha/\beta) C_{\text{avaf}}^*]$

The individual terms  $\alpha$  and  $\beta$  were discussed in Sections 7.2 and 7.3. The value of the ratio  $(\alpha/\beta)$  is dependent on the air condition, water temperature and barometric pressure. For saturated conditions the value of  $(\alpha/\beta)$  varies from 0.927 to 0.987, which is a smaller fractional variation than occurs in either of the individual terms  $\alpha$  or  $\beta$ . Thus the variations from unity in either term are self compensating to a certain extent since they are combined in a ratio. The variation of  $(\alpha/\beta)$  for saturated conditions is shown in Figure 7.17. However the values of  $(\alpha/\beta)$  are not, in themselves, of major importance, since it is the term  $[(\alpha/\beta) C_{\text{avaf}}^*]$  that is used in the overall equation.

Recall that by definition:

$$\alpha = \Delta i_a / \Delta \Sigma \quad (7.69)$$

$$\beta = \frac{C_{\text{avaf}}^* (t_w - t_{\text{db}} + \lambda B')}{(\Sigma_w - \Sigma_a)} \quad (7.70)$$

The combined term for an element of heat exchanger is given as:

$$(\alpha/\beta) C_{\text{avaf}}^* = \frac{[\Sigma_w - \Sigma_a]}{[\Delta \Sigma]} \frac{[\Delta i_a]}{[t_w - t_{\text{db}} + \lambda B']}] \quad (7.71)$$

This term is the product of two ratios combining the

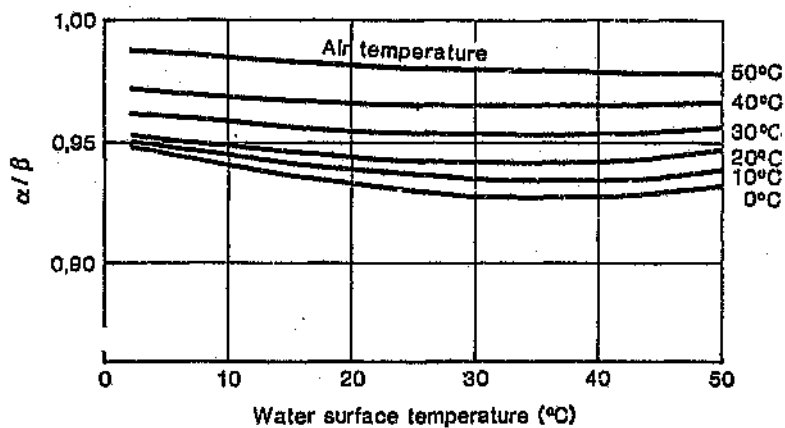


Figure 7.17 Values of the ratio  $\alpha/\beta$  for saturated air at 100 kPa

approximations for the total heat transfer driving force and that for the change of energy of the air stream. The values of this combined term are given in Figure 7.18 for saturated air.

The variation of the term between inlet and outlet and the arithmetic mean values are shown in Table 7.5 for each test. It should be noted that for the cold water tests the value of the term decreases between the air inlet and the air outlet, but for the hot water tests this trend is reversed. (In fact the slope of the lines of air temperature, water temperature and  $[(\alpha/\beta) c_{avaf}^*]$ , as drawn in Figures 7.14 and 7.15, are all similar.) For the cold water tests the variation of the value for any one test is not greater than six per cent. For the hot water tests the variation of the value is not greater than 11 per cent. Thus the earlier conclusion that  $[(\alpha/\beta) c_{avaf}^*]$  does not vary significantly for any one test is confirmed. (The acceptability of this will be fully confirmed later.)

The value of this term does not vary significantly when considered on a statistical basis for all tests over the full range of operating conditions. The database examined consisted of 10 values across the heat exchanger for each of the 160 tests. The relevant statistics are as follows:

Cold water tests: mean 0,988 (s.d. 1,5 %)  
 Hot water tests: mean 0,997 (s.d. 3,0 %)  
 All tests combined: mean 0,993 (s.d. 2,5 %).

The mean value of any one test does not vary by more than 5 per cent from unity and a universal value of unity can probably be used with acceptable accuracy

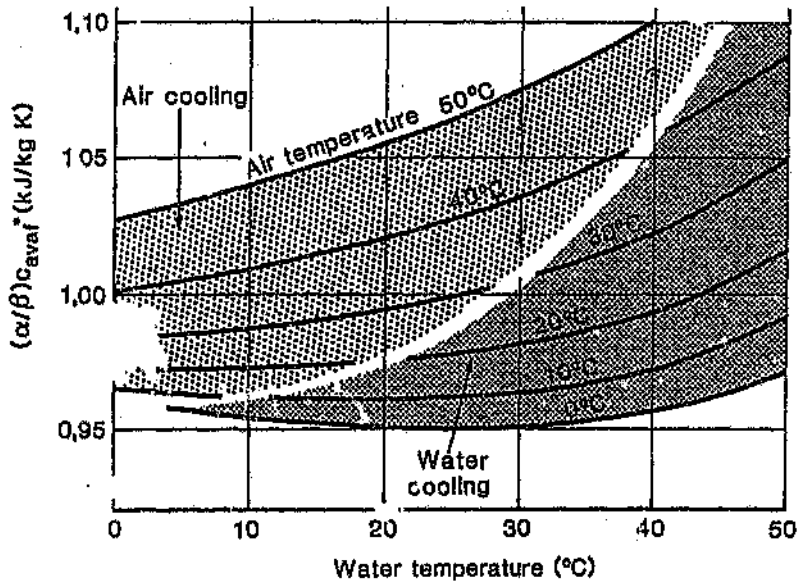


Figure 7.18 Values of  $(\alpha/\beta) c_{avaf}^*$  for saturated air at 100 kPa

(this is confirmed later). The mean values for all the cold water tests do not differ significantly from that of the hot water tests and there is no evidence that a differentiation can be made between cold water and hot water tests in the selection of appropriate values of  $[(\alpha/\beta) c_{avaf}^*]$ . This is further illustrated in Figure 7.18.

**Experimental values of the specific heat term for saturated air**

Recall that the pseudo-specific heat term for saturated air was defined in terms of sigma energy as:

$$\Sigma = a + c_a^* t_{wb} \quad (7.72)$$

The specific heat term of particular interest applies to saturated air at the water interface temperature. This is given as:

$$c_{aw}^* = (\Sigma_w - a) / t_w \quad (7.73)$$

The sigma energy content is shown plotted against temperature in Figure 7.19. Values of the pseudo-specific heat term may be depicted as the slope of a straight line on this plot. A typical water cooling duty from 45 °C to 35 °C at a wet-bulb temperature of 15 °C is depicted and certain key values of the pseudo-specific heat term shown. Since the term is applicable to the water surface temperature, the representative value can be expected to fall within the shaded area in Figure 7.19. This may also be illustrated using a plot of the

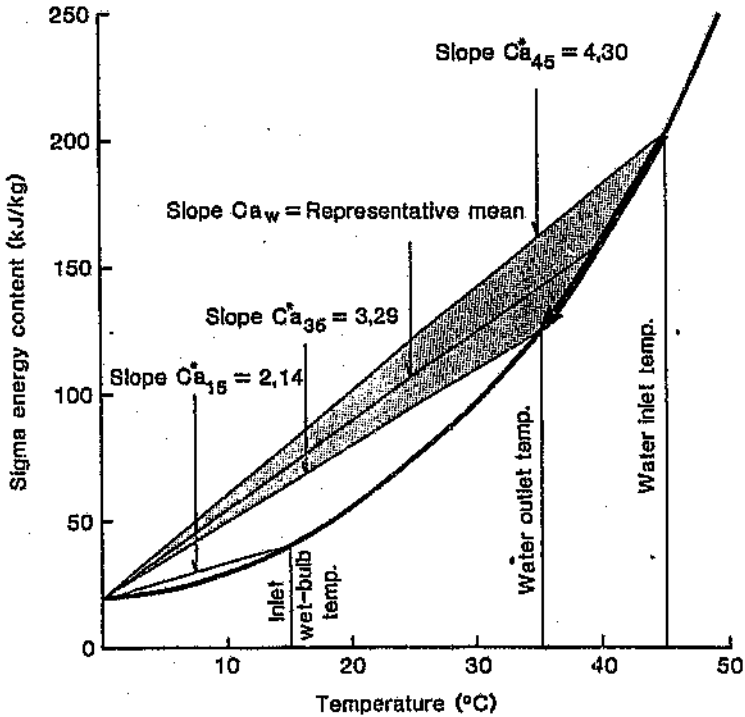
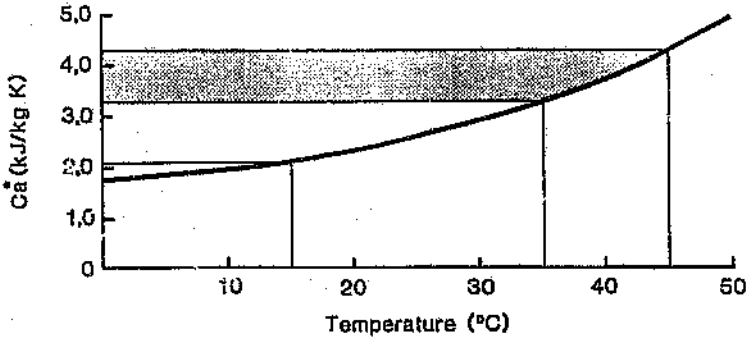


Figure 7.19 Plot of sigma energy content of air, depicting key values of the pseudo-specific heat term (100 kPa)

pseudo-specific heat term against temperature; this is also shown in Figure 7.19.

Turning now to the experimental data, for each of the tests, the arithmetic mean values across the heat exchanger of the terms  $(\alpha/\gamma)_i$  and  $[(\alpha/\beta) c_{avaf}^*]$  have been calculated. Based on these values, and through the solution of Equation 7.63, the appropriate representative value of the pseudo-specific heat term,  $c_{aw}$ , has been calculated for each test. Table 7.6 lists these representative values along with some of the basic test information. A careful study of this information in combination with Figure 7.13 reveals that the values of  $c_{aw}^*$  are all between the inlet and outlet water conditions. The set of data in Table 7.6 satisfy the overall performance equation (Equation 7.63) with no anomalies. It can be tentatively concluded from this that the assumptions made in integrating the basic equation (Equation 7.55) are acceptable.

However, for the performance equation to be of practical benefit the user must be able to predict performance from a knowledge of the input process conditions (and preferably the technique should not be iterative). This requires a procedure for determining the mean representative values of  $(\alpha/\gamma)_i$ ,  $[(\alpha/\beta) c_{avaf}^*]$  and  $c_{aw}^*$  without necessarily having a knowledge of the outlet conditions.

#### 7.5.4 Selection of appropriate sets of values of $(\alpha/\gamma)_i$ , $[(\alpha/\beta) c_{avaf}^*]$ and $c_{aw}^*$

In selecting the appropriate values of these terms to be used in practice, it must be stressed that the method must remain simple, from a practical point of view, without compromising the required accuracy. For

instance, tables and charts of values of these parameters for different sets of conditions are considered impractical.

Based on the evidence presented above and the large simulated data base used to check the overall equation (see Appendix P), it is apparent that the use of a single universal value of  $[(\alpha/\beta) c_{\text{avaf}}^*]$  would be acceptable. Obviously a value of unity is indicated. However, note that the units of this term are those of specific heat - kJ/kg K. It is anticipated that if a value of unity is used, its dimensionality would soon be lost to the user and confusion would be created in its application (note that the design characteristic  $N^*$  is dimensionless). The obvious solution is to assign  $[(\alpha/\beta) c_{\text{avaf}}^*]$  the value of the specific heat of pure air,  $c_a = 1,005$  kJ/kg K.

Also, based on this evidence it is apparent that the use of global values for the term  $(\alpha/\gamma)_1$  would be acceptable. For acceptable accuracy it was found that different values should be used for water cooling and air cooling applications. These values are:

$$\begin{aligned} (\alpha/\gamma)_1 &= 1,00 \text{ for water cooling} \\ &= 1,05 \text{ for air cooling} \end{aligned}$$

The appropriate value of the pseudo-specific heat term will be between its value at the water inlet temperature and its value at the air inlet wet-bulb temperature, thus:

$$c_{\text{aw}}^* = L c_{\text{aw}}^* + (1 - L) c_a^* \quad (7.74)$$

where

$$L = 0 \text{ to } 1$$

Values of  $L$  close to 1 will apply where the temperature change of the water (range) is small. This would be the case for large values of the ratio of the thermal capacity of the water stream to the air stream, and heat exchangers with a low value of the design characteristic. Smaller values of  $L$  would be applicable for low ratios of the thermal capacity of the water stream to the air stream and heat exchangers with a high value of the design characteristic. Thus, it is to be expected that the value of  $L$  could be predicted from a knowledge of the thermal capacity ratio and the design characteristic. To avoid using an iterative procedure in estimating  $L$ , an approximate thermal capacity ratio term is now introduced. Use is made of the parameter employed in Whillier's (19) work which is defined, between inlet water and inlet air conditions, as :

$$Z = \frac{\dot{m}_w C_w (t_{wi} - t_{ai})}{\dot{m}_a (\Sigma_{wi} - \Sigma_{ai})} \quad (7.75)$$

To enable the prediction of  $L$ , the following relationship is now examined :

$$L = f ( Z , N^* ) \quad (7.76)$$

Based on the universal values selected for  $[(\alpha/\beta) \text{ cavaf}^*]$  and  $(\alpha/\gamma)_1$ , a set of values of  $c_{aw}^*$  was calculated for each of the tests through the solution of Equation 7.63. Values of  $L$  were then calculated through Equation 7.74 and the appropriate relationship for Equation 7.76 determined (see Appendix Q). The relationship is shown graphically in Figure 7.20, and

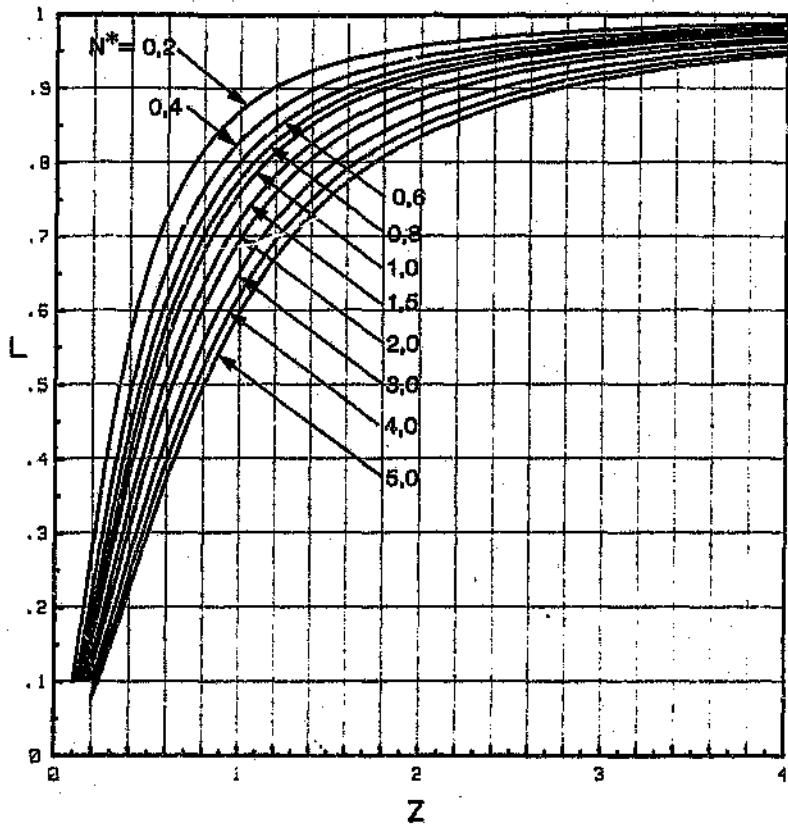


Figure 7.20 Value of  $L$  for varying water-air flow ratios and different values of the design characteristic  $N^*$

through Figure 7.20 and Equation 7.74 the representative value of  $C_{aw}^*$  may now be determined from a knowledge of the inlet process conditions and the design characteristics.

#### 7.5.5 Final specification of performance equation

It is now possible to make the final refinements to the performance equation and to specify the procedures related to its use.

The performance equation is given as:

$$E_w^* = \frac{1 - e^{-N^* (1 - 1/R^*)}}{R^* - e^{-N^* (1 - 1/R^*)}} \quad (7.77)$$

where

$$N^* = h_c A / (m_a^* c_a)$$

$$R^* = (m_w^* c_w) / (m_a^* c_{aw}^*) \quad : \text{ for water cooling}$$

$$= 0.95 (m_w^* c_w) / (m_a^* c_{aw}^*) \quad : \text{ for air cooling}$$

$$E_w^* = (t_{w1} - t_{w0}) / (t_{w1} - \frac{C_{al}^*}{C_{rw}^*} t_{wb1})$$

A procedure for using the equation is best described on the basis of solving the following problem:

The inlet flowrates and temperature conditions are specified for a certain direct-contact heat exchanger which is cooling water and is characterized by a known  $h_c A$  value. What is the outlet water temperature?

- (i) Determine the value of  $N^* = h_c A / \dot{m}_a c_{pa}$ .
- (ii) Determine the value of  $Z$  from Equation 7.75.
- (iii) From  $Z$  and  $N^*$  determine appropriate value of  $L$  from Figure 7.20. Then calculate  $c_{aw}^*$  from the inlet temperature conditions (Equation 7.74).
- (iv) Determine the thermal capacity ratio  $R^* = (\dot{m}_w c_w) / (\dot{m}_a c_{aw}^*)$ .
- (v) With the knowledge of  $N^*$  and  $R^*$  determine the water effectiveness through Equation 7.76.

Now that the basic method has been specified, the next obvious stage is to check its accuracy against the experimental data and the performance of the comprehensive theoretical model.

	Error in enthalpy approximation (term x) %					Error in sigma energy approximation (term y) %				
	mean	abs. mean	min	max	$\sigma$	mean	abs. mean	min	max	$\sigma$
Cold water tests	+2,0	2,0	+0,9	+3,1	0,5	-2,7	2,7	+4,0	-1,8	0,5
Hot water tests	+3,9	3,9	+2,0	+5,8	0,9	-1,4	1,6	-2,6	+1,9	0,6
All tests	+3,0	3,0	+0,9	+5,8	1,2	-2,0	2,1	-4,0	+1,9	0,8

Table 7.1 Comparison of simplified energy balance using enthalpy and that using sigma energy



Test number	Air in / water out boundary										Water in / Air out boundary		Mean
331	1.889	1.888	1.887	1.885	1.884	1.883	1.883	1.882	1.881	1.880	1.880	1.880	1.884
341	1.911	1.899	1.897	1.885	1.884	1.883	1.882	1.881	1.881	1.880	1.880	1.880	1.884
351	1.912	1.910	1.907	1.885	1.884	1.883	1.882	1.881	1.881	1.880	1.880	1.880	1.884
361	1.811	1.899	1.897	1.885	1.884	1.883	1.882	1.881	1.881	1.880	1.880	1.880	1.884
371	1.896	1.885	1.885	1.884	1.884	1.883	1.882	1.881	1.881	1.880	1.880	1.880	1.884
381	1.889	1.887	1.886	1.885	1.884	1.883	1.882	1.881	1.881	1.880	1.880	1.880	1.884
391	1.810	1.898	1.887	1.885	1.884	1.883	1.882	1.881	1.881	1.880	1.880	1.880	1.884
401	1.889	1.887	1.886	1.885	1.884	1.883	1.882	1.881	1.881	1.880	1.880	1.880	1.884
411	1.884	1.884	1.884	1.883	1.883	1.883	1.882	1.881	1.881	1.880	1.880	1.880	1.884
421	1.889	1.887	1.886	1.885	1.884	1.883	1.882	1.881	1.881	1.880	1.880	1.880	1.884
431	1.889	1.887	1.886	1.885	1.884	1.883	1.882	1.881	1.881	1.880	1.880	1.880	1.884
441	1.886	1.885	1.884	1.883	1.882	1.882	1.881	1.881	1.880	1.880	1.880	1.880	1.884
451	1.883	1.883	1.883	1.883	1.883	1.882	1.882	1.881	1.881	1.880	1.880	1.880	1.884
461	1.886	1.886	1.885	1.884	1.884	1.883	1.882	1.881	1.881	1.880	1.880	1.880	1.884
471	1.885	1.884	1.884	1.883	1.883	1.882	1.881	1.881	1.880	1.880	1.880	1.880	1.884
481	1.885	1.884	1.884	1.883	1.882	1.882	1.881	1.881	1.880	1.880	1.880	1.880	1.884
491	.978	.981	.984	.986	.989	.991	.993	.995	.998	1.000	1.000	1.000	.989
501	.977	.982	.986	.989	.991	.993	.995	.997	.999	1.000	1.000	1.000	.991
511	.975	.981	.986	.989	.992	.994	.996	.997	.999	1.000	1.000	1.000	.991
521	.975	.981	.985	.989	.991	.994	.996	.997	.999	1.000	1.000	1.000	.991
531	.979	.982	.984	.986	.988	.990	.992	.995	.997	1.000	1.000	1.000	.989
541	.978	.982	.985	.987	.990	.992	.994	.996	.998	1.000	1.000	1.000	.990
551	.974	.979	.983	.986	.989	.992	.994	.996	.998	1.000	1.000	1.000	.989
561	.975	.980	.984	.987	.990	.993	.995	.997	.998	1.000	1.000	1.000	.990
571	.981	.983	.985	.986	.988	.990	.992	.994	.997	1.000	1.000	1.000	.990
581	.980	.982	.985	.987	.989	.991	.993	.995	.998	1.000	1.000	1.000	.990
591	.978	.981	.985	.987	.990	.992	.994	.996	.998	1.000	1.000	1.000	.990
601	.976	.980	.984	.987	.989	.992	.994	.996	.998	1.000	1.000	1.000	.989
611	.981	.983	.985	.986	.988	.990	.992	.994	.996	1.000	1.000	1.000	.989
621	.981	.983	.985	.987	.989	.991	.993	.995	.997	1.000	1.000	1.000	.990
631	.977	.981	.984	.986	.989	.991	.993	.995	.998	1.000	1.000	1.000	.989
641	.976	.980	.983	.986	.989	.991	.993	.995	.998	1.000	1.000	1.000	.989

Table 7.2 (Cont) Variation of the term  $J$  across and within the heat exchangers for each test

Test number	Air in / water out boundary										Mean	Water in / Air out boundary									
651	1.010	1.008	1.007	1.006	1.005	1.004	1.003	1.002	1.001	1.000	1.000	1.000	1.000	1.000	1.000	1.000	1.000	1.000	1.000		
661	1.013	1.010	1.007	1.005	1.004	1.004	1.002	1.002	1.001	1.000	1.000	1.000	1.000	1.000	1.000	1.000	1.000	1.000	1.000		
671	1.011	1.008	1.005	1.003	1.002	1.001	1.001	1.001	1.000	1.000	1.000	1.000	1.000	1.000	1.000	1.000	1.000	1.000	1.000		
681	1.012	1.009	1.006	1.004	1.003	1.003	1.002	1.001	1.001	1.000	1.000	1.000	1.000	1.000	1.000	1.000	1.000	1.000	1.000		
691	1.006	1.006	1.005	1.005	1.004	1.004	1.003	1.002	1.002	1.001	1.000	1.000	1.000	1.000	1.000	1.000	1.000	1.000	1.000		
701	1.010	1.008	1.007	1.005	1.004	1.003	1.002	1.001	1.001	1.000	1.000	1.000	1.000	1.000	1.000	1.000	1.000	1.000	1.000		
711	1.010	1.008	1.006	1.004	1.003	1.002	1.001	1.001	1.001	1.000	1.000	1.000	1.000	1.000	1.000	1.000	1.000	1.000	1.000		
721	1.011	1.009	1.006	1.005	1.003	1.002	1.001	1.001	1.001	1.000	1.000	1.000	1.000	1.000	1.000	1.000	1.000	1.000	1.000		
731	1.004	1.004	1.004	1.004	1.003	1.003	1.002	1.002	1.001	1.000	1.000	1.000	1.000	1.000	1.000	1.000	1.000	1.000	1.000		
741	1.009	1.007	1.006	1.005	1.004	1.003	1.002	1.001	1.001	1.000	1.000	1.000	1.000	1.000	1.000	1.000	1.000	1.000	1.000		
751	1.011	1.008	1.007	1.005	1.004	1.003	1.002	1.001	1.001	1.000	1.000	1.000	1.000	1.000	1.000	1.000	1.000	1.000	1.000		
761	1.011	1.009	1.006	1.005	1.003	1.002	1.001	1.001	1.000	1.000	1.000	1.000	1.000	1.000	1.000	1.000	1.000	1.000	1.000		
771	1.003	1.003	1.003	1.003	1.003	1.002	1.002	1.001	1.001	1.000	1.000	1.000	1.000	1.000	1.000	1.000	1.000	1.000	1.000		
781	1.006	1.005	1.003	1.004	1.003	1.003	1.002	1.001	1.001	1.000	1.000	1.000	1.000	1.000	1.000	1.000	1.000	1.000	1.000		
791	1.007	1.006	1.005	1.004	1.003	1.002	1.002	1.001	1.001	1.000	1.000	1.000	1.000	1.000	1.000	1.000	1.000	1.000	1.000		
801	1.008	1.007	1.005	1.004	1.003	1.002	1.001	1.001	1.001	1.000	1.000	1.000	1.000	1.000	1.000	1.000	1.000	1.000	1.000		
811	.977	.981	.983	.986	.988	.991	.993	.995	.998	.998	1.000	1.000	1.000	1.000	1.000	1.000	1.000	1.000	1.000		
821	.973	.979	.984	.987	.990	.993	.995	.997	.998	.999	1.000	1.000	1.000	1.000	1.000	1.000	1.000	1.000	1.000		
831	.976	.983	.988	.991	.994	.996	.997	.998	.999	1.000	1.000	1.000	1.000	1.000	1.000	1.000	1.000	1.000	1.000		
841	.977	.984	.988	.991	.994	.996	.997	.998	.999	1.000	1.000	1.000	1.000	1.000	1.000	1.000	1.000	1.000	1.000		
851	.978	.981	.983	.985	.987	.989	.991	.994	.996	1.000	1.000	1.000	1.000	1.000	1.000	1.000	1.000	1.000	1.000		
861	.972	.977	.981	.984	.987	.990	.992	.995	.997	.998	1.000	1.000	1.000	1.000	1.000	1.000	1.000	1.000	1.000		
871	.973	.980	.984	.987	.990	.993	.995	.997	.998	1.000	1.000	1.000	1.000	1.000	1.000	1.000	1.000	1.000	1.000		
881	.975	.981	.985	.989	.992	.994	.996	.997	.999	1.000	1.000	1.000	1.000	1.000	1.000	1.000	1.000	1.000	1.000		
891	.980	.982	.983	.985	.987	.989	.991	.993	.996	1.000	1.000	1.000	1.000	1.000	1.000	1.000	1.000	1.000	1.000		
901	.973	.977	.980	.983	.985	.988	.991	.993	.996	1.000	1.000	1.000	1.000	1.000	1.000	1.000	1.000	1.000	1.000		
911	.973	.978	.982	.985	.988	.990	.993	.995	.997	1.000	1.000	1.000	1.000	1.000	1.000	1.000	1.000	1.000	1.000		
921	.974	.979	.984	.987	.990	.992	.994	.996	.998	1.000	1.000	1.000	1.000	1.000	1.000	1.000	1.000	1.000	1.000		
931	.980	.983	.984	.986	.987	.989	.991	.993	.996	1.000	1.000	1.000	1.000	1.000	1.000	1.000	1.000	1.000	1.000		
941	.976	.978	.981	.983	.985	.988	.990	.993	.996	1.000	1.000	1.000	1.000	1.000	1.000	1.000	1.000	1.000	1.000		
951	.974	.978	.981	.984	.986	.989	.992	.994	.997	1.000	1.000	1.000	1.000	1.000	1.000	1.000	1.000	1.000	1.000		
961	.975	.979	.983	.986	.989	.991	.993	.996	.998	1.000	1.000	1.000	1.000	1.000	1.000	1.000	1.000	1.000	1.000		

Table 7.2 (Cont)

Variation of the term J across  
and within the heat exchangers  
for each test



Test number	Air in / water out boundary										Meter in / Air out boundary	
	Mean											
1291	1.016	1.009	1.007	1.006	1.005	1.004	1.003	1.002	1.001	1.000	1.000	1.005
1301	1.012	1.010	1.007	1.005	1.004	1.003	1.002	1.001	1.000	1.000	1.000	1.004
1311	1.013	1.010	1.007	1.005	1.004	1.002	1.002	1.001	1.000	1.000	1.000	1.004
1321	1.011	1.008	1.006	1.004	1.003	1.002	1.001	1.001	1.000	1.000	1.000	1.004
1331	1.007	1.006	1.006	1.005	1.004	1.003	1.003	1.002	1.001	1.000	1.000	1.004
1341	1.011	1.009	1.007	1.006	1.004	1.003	1.002	1.001	1.001	1.000	1.000	1.004
1351	1.011	1.009	1.007	1.005	1.004	1.003	1.002	1.001	1.000	1.000	1.000	1.004
1361	1.010	1.008	1.006	1.005	1.003	1.002	1.002	1.001	1.000	1.000	1.000	1.004
1371	1.005	1.005	1.004	1.004	1.003	1.003	1.002	1.002	1.001	1.000	1.000	1.003
1381	1.009	1.008	1.007	1.005	1.004	1.003	1.002	1.001	1.001	1.000	1.000	1.004
1391	1.007	1.006	1.005	1.004	1.003	1.002	1.002	1.001	1.000	1.000	1.000	1.003
1401	1.008	1.007	1.005	1.004	1.003	1.002	1.002	1.001	1.000	1.000	1.000	1.003
1411	1.003	1.003	1.003	1.003	1.003	1.003	1.002	1.002	1.001	1.000	1.000	1.002
1421	1.008	1.007	1.006	1.005	1.004	1.003	1.002	1.002	1.001	1.000	1.000	1.004
1431	1.007	1.006	1.005	1.004	1.003	1.002	1.002	1.001	1.000	1.000	1.000	1.003
1441	1.007	1.006	1.005	1.004	1.003	1.002	1.002	1.001	1.000	1.000	1.000	1.003
1451	.988	.983	.986	.988	.990	.992	.994	.996	.998	1.000	1.000	.991
1461	.979	.984	.987	.988	.993	.995	.996	.998	.999	1.000	1.000	.992
1471	.978	.984	.988	.991	.994	.996	.997	.998	.999	1.000	1.000	.993
1481	.981	.986	.996	.993	.995	.997	.998	.999	.999	1.000	1.000	.994
1491	.981	.983	.985	.987	.989	.991	.993	.995	.997	1.000	1.000	.996
1501	.978	.982	.985	.988	.990	.992	.994	.996	.998	1.000	1.000	.998
1511	.977	.982	.986	.989	.991	.993	.995	.997	.999	1.000	1.000	.991
1521	.986	.985	.989	.991	.994	.995	.997	.998	.999	1.000	1.000	.993
1531	.982	.984	.986	.987	.989	.991	.993	.995	.997	1.000	1.000	.998
1541	.978	.982	.984	.987	.989	.991	.993	.995	.998	1.000	1.000	.998
1551	.976	.981	.984	.987	.990	.992	.994	.996	.998	1.000	1.000	.998
1561	.980	.985	.988	.991	.993	.995	.996	.998	.999	1.000	1.000	.992
1571	.984	.985	.987	.988	.990	.991	.992	.994	.997	1.000	1.000	.991
1581	.979	.982	.984	.986	.988	.990	.992	.995	.997	1.000	1.000	.998
1591	.977	.980	.983	.986	.989	.991	.993	.995	.998	1.000	1.000	.989
1601	.980	.984	.987	.990	.992	.994	.996	.997	.999	1.000	1.000	.992

Table 7.2 (Cont)

Variation of the term  $J$  across  
and within the heat exchangers  
for each test

Table 7.3 Performance of hypothetical heat exchanger under selected temperature conditions (barometric pressure 100 kPa)

Test number	$h_A$ (kW/K)	$h_y$ (kg/s)	$h_o$ (kg/s)	$t_{in}$ (°C)			$t_{wo}$ (°C)	$t_{out}$ (°C)			Duty (kW)	Average Values		$c_{av}$ (kJ/kgK) (2)	$E_w$	$E_R$	$E_N$	$E_{18}$	$E_{19}$
				$t_{wi}$	wb	db		wb	db	$t_{1/2}$ (1)		$(\alpha/\beta)_{c_{av}}$ (1)							
A	20	10	10	40	15	20	23,73	32,17	32,17	704	1,011	0,992	3,13	0,55	1,32	2,02	0,65	1,19	
B	20	10	10	50	15	20	25,32	37,69	37,69	1070	1,012	1,008	3,58	0,60	1,16	1,99	0,71	1,72	
C	20	10	10	30	10	10	19,07	24,85	24,85	467	1,012	0,976	2,66	0,48	1,56	2,05	0,55	1,13	
D	20	10	10	10	30	30	22,46	16,58	16,58	536	1,028	0,982	2,18	0,41	1,87	2,04	0,62	1,51	
E	20	10	0	50	0	0	23,43	35,91	35,91	1268	1,007	0,984	3,49	0,59	1,19	2,01	0,59	1,00	
F	20	10	10	0	50	50	43,59	26,32	26,32	1344	1,032	1,040	3,08	0,54	1,32	1,92	0,87	1,62	

Note 1. These are the arithmetic mean values for all the segments of the heat exchanger.

2. This value comes from the solution of Equation 7.63 using the mean values of  $(\alpha/\gamma)_i$  and  $(\alpha/\beta)_{c_{av}}$ .

3. This term is defined in Equation 7.57.





Test number	Air in / Water out boundary										Water in / Air out boundary									
	Mean																			
651	1.034	1.033	1.032	1.030	1.029	1.028	1.027	1.026	1.025	1.025	1.025	1.025	1.025	1.025	1.025	1.025	1.025	1.025	1.025	1.025
661	1.045	1.041	1.039	1.037	1.035	1.034	1.033	1.032	1.032	1.031	1.031	1.031	1.031	1.031	1.031	1.031	1.031	1.031	1.031	1.031
671	1.044	1.040	1.038	1.036	1.035	1.034	1.033	1.033	1.032	1.032	1.032	1.032	1.032	1.032	1.032	1.032	1.032	1.032	1.032	1.032
681	1.047	1.043	1.041	1.039	1.038	1.036	1.036	1.035	1.035	1.034	1.034	1.034	1.034	1.034	1.034	1.034	1.034	1.034	1.034	1.034
691	1.027	1.026	1.026	1.025	1.024	1.024	1.023	1.022	1.021	1.020	1.020	1.020	1.020	1.020	1.020	1.020	1.020	1.020	1.020	1.020
701	1.034	1.032	1.030	1.029	1.027	1.026	1.025	1.024	1.024	1.023	1.023	1.023	1.023	1.023	1.023	1.023	1.023	1.023	1.023	1.023
711	1.037	1.034	1.032	1.031	1.029	1.028	1.028	1.027	1.027	1.026	1.026	1.026	1.026	1.026	1.026	1.026	1.026	1.026	1.026	1.026
721	1.041	1.038	1.036	1.034	1.033	1.032	1.031	1.030	1.030	1.029	1.029	1.029	1.029	1.029	1.029	1.029	1.029	1.029	1.029	1.029
731	1.024	1.024	1.023	1.023	1.023	1.022	1.021	1.021	1.020	1.019	1.019	1.019	1.019	1.019	1.019	1.019	1.019	1.019	1.019	1.019
741	1.028	1.027	1.026	1.025	1.024	1.023	1.022	1.021	1.020	1.020	1.020	1.020	1.020	1.020	1.020	1.020	1.020	1.020	1.020	1.020
751	1.034	1.032	1.030	1.029	1.027	1.026	1.025	1.025	1.024	1.024	1.024	1.024	1.024	1.024	1.024	1.024	1.024	1.024	1.024	1.024
761	1.037	1.035	1.033	1.031	1.030	1.028	1.028	1.027	1.027	1.026	1.026	1.026	1.026	1.026	1.026	1.026	1.026	1.026	1.026	1.026
771	1.021	1.021	1.021	1.021	1.021	1.020	1.020	1.019	1.019	1.019	1.019	1.019	1.019	1.019	1.019	1.019	1.019	1.019	1.019	1.019
781	1.024	1.024	1.023	1.022	1.022	1.021	1.020	1.020	1.019	1.019	1.019	1.019	1.019	1.019	1.019	1.019	1.019	1.019	1.019	1.019
791	1.028	1.027	1.026	1.025	1.024	1.023	1.022	1.021	1.021	1.020	1.020	1.020	1.020	1.020	1.020	1.020	1.020	1.020	1.020	1.020
801	1.031	1.029	1.028	1.027	1.026	1.025	1.024	1.024	1.023	1.023	1.023	1.023	1.023	1.023	1.023	1.023	1.023	1.023	1.023	1.023
811	.999	1.002	1.005	1.008	1.011	1.013	1.015	1.017	1.020	1.022	1.022	1.022	1.022	1.022	1.022	1.022	1.022	1.022	1.022	1.022
821	.995	1.002	1.006	1.010	1.013	1.015	1.018	1.020	1.021	1.023	1.023	1.023	1.023	1.023	1.023	1.023	1.023	1.023	1.023	1.023
831	.993	1.001	1.005	1.009	1.011	1.013	1.015	1.016	1.017	1.018	1.018	1.018	1.018	1.018	1.018	1.018	1.018	1.018	1.018	1.018
841	.991	.998	1.003	1.006	1.009	1.010	1.012	1.013	1.014	1.015	1.015	1.015	1.015	1.015	1.015	1.015	1.015	1.015	1.015	1.015
851	1.004	1.006	1.008	1.011	1.013	1.015	1.017	1.019	1.022	1.026	1.026	1.026	1.026	1.026	1.026	1.026	1.026	1.026	1.026	1.026
861	.997	1.002	1.006	1.010	1.013	1.015	1.018	1.021	1.023	1.026	1.026	1.026	1.026	1.026	1.026	1.026	1.026	1.026	1.026	1.026
871	.995	1.002	1.006	1.010	1.013	1.015	1.017	1.019	1.021	1.023	1.023	1.023	1.023	1.023	1.023	1.023	1.023	1.023	1.023	1.023
881	.994	1.000	1.005	1.008	1.011	1.013	1.015	1.017	1.018	1.020	1.020	1.020	1.020	1.020	1.020	1.020	1.020	1.020	1.020	1.020
891	1.006	1.008	1.010	1.012	1.014	1.015	1.017	1.020	1.023	1.027	1.027	1.027	1.027	1.027	1.027	1.027	1.027	1.027	1.027	1.027
901	1.001	1.004	1.008	1.010	1.013	1.016	1.018	1.021	1.024	1.028	1.028	1.028	1.028	1.028	1.028	1.028	1.028	1.028	1.028	1.028
911	.998	1.003	1.007	1.010	1.013	1.015	1.018	1.020	1.023	1.025	1.025	1.025	1.025	1.025	1.025	1.025	1.025	1.025	1.025	1.025
921	.997	1.002	1.006	1.009	1.012	1.015	1.017	1.019	1.021	1.023	1.023	1.023	1.023	1.023	1.023	1.023	1.023	1.023	1.023	1.023
931	1.006	1.008	1.010	1.012	1.013	1.015	1.017	1.019	1.022	1.026	1.026	1.026	1.026	1.026	1.026	1.026	1.026	1.026	1.026	1.026
941	1.002	1.005	1.008	1.010	1.013	1.015	1.017	1.020	1.023	1.028	1.028	1.028	1.028	1.028	1.028	1.028	1.028	1.028	1.028	1.028
951	.996	1.002	1.005	1.008	1.011	1.014	1.016	1.019	1.022	1.025	1.025	1.025	1.025	1.025	1.025	1.025	1.025	1.025	1.025	1.025
961	.997	1.001	1.005	1.008	1.011	1.013	1.016	1.018	1.020	1.023	1.023	1.023	1.023	1.023	1.023	1.023	1.023	1.023	1.023	1.023

Table 7.4 (Cont) Variations of the term  $(\alpha/\gamma)$ ; across and within the heat exchangers for each test



Test number	Air in / Water out boundary										Water in / Air out boundary									
											Mean									
1291	1.038	1.037	1.035	1.034	1.033	1.032	1.031	1.030	1.029	1.028	1.033	1.032	1.031	1.031	1.030	1.029	1.028	1.027	1.026	1.025
1301	1.043	1.040	1.038	1.036	1.034	1.033	1.032	1.031	1.031	1.030	1.033	1.032	1.031	1.031	1.030	1.029	1.028	1.027	1.026	1.025
1311	1.047	1.044	1.041	1.039	1.038	1.036	1.035	1.035	1.034	1.034	1.036	1.035	1.035	1.034	1.034	1.033	1.032	1.031	1.030	1.029
1321	1.043	1.041	1.038	1.037	1.035	1.034	1.034	1.033	1.033	1.032	1.035	1.034	1.034	1.033	1.033	1.032	1.031	1.030	1.029	1.028
1331	1.038	1.029	1.028	1.028	1.027	1.026	1.025	1.024	1.024	1.023	1.026	1.025	1.025	1.024	1.024	1.023	1.022	1.021	1.020	1.019
1341	1.034	1.034	1.032	1.031	1.030	1.028	1.027	1.026	1.026	1.025	1.028	1.027	1.027	1.026	1.026	1.025	1.024	1.023	1.022	1.021
1351	1.040	1.038	1.035	1.034	1.032	1.031	1.030	1.029	1.029	1.028	1.031	1.030	1.030	1.029	1.029	1.028	1.027	1.026	1.025	1.024
1361	1.039	1.037	1.035	1.033	1.032	1.031	1.030	1.030	1.029	1.029	1.031	1.030	1.030	1.029	1.029	1.028	1.027	1.026	1.025	1.024
1371	1.025	1.025	1.024	1.024	1.023	1.023	1.022	1.022	1.021	1.021	1.024	1.023	1.022	1.022	1.021	1.021	1.020	1.019	1.018	1.017
1381	1.031	1.030	1.028	1.027	1.026	1.025	1.024	1.023	1.022	1.022	1.025	1.024	1.023	1.022	1.022	1.021	1.020	1.019	1.018	1.017
1391	1.030	1.029	1.028	1.026	1.025	1.025	1.024	1.023	1.023	1.022	1.025	1.024	1.023	1.023	1.022	1.021	1.020	1.019	1.018	1.017
1401	1.034	1.032	1.031	1.030	1.029	1.028	1.027	1.026	1.026	1.025	1.028	1.027	1.026	1.026	1.025	1.024	1.023	1.022	1.021	1.020
1411	1.022	1.022	1.022	1.022	1.022	1.021	1.021	1.020	1.019	1.019	1.022	1.021	1.021	1.020	1.019	1.018	1.017	1.016	1.015	1.014
1421	1.027	1.026	1.025	1.024	1.024	1.023	1.022	1.021	1.020	1.020	1.023	1.022	1.021	1.020	1.019	1.018	1.017	1.016	1.015	1.014
1431	1.028	1.027	1.026	1.025	1.024	1.023	1.022	1.022	1.021	1.021	1.024	1.023	1.022	1.021	1.021	1.020	1.019	1.018	1.017	1.016
1441	1.030	1.029	1.028	1.027	1.026	1.025	1.024	1.024	1.023	1.023	1.026	1.025	1.024	1.023	1.023	1.022	1.021	1.020	1.019	1.018
1451	.998	1.002	1.004	1.007	1.009	1.011	1.013	1.015	1.017	1.019	1.016	1.015	1.015	1.016	1.017	1.018	1.019	1.020	1.021	1.021
1461	.995	1.001	1.004	1.007	1.010	1.012	1.013	1.015	1.016	1.017	1.014	1.013	1.013	1.014	1.015	1.016	1.017	1.018	1.019	1.020
1471	.992	.990	1.003	1.006	1.008	1.010	1.012	1.013	1.014	1.015	1.011	1.010	1.010	1.011	1.012	1.013	1.014	1.015	1.016	1.017
1481	.992	.990	1.002	1.005	1.007	1.008	1.009	1.009	1.010	1.011	1.007	1.006	1.006	1.007	1.008	1.009	1.010	1.011	1.012	1.013
1491	1.002	1.004	1.006	1.008	1.010	1.012	1.014	1.016	1.019	1.021	1.015	1.014	1.014	1.015	1.016	1.017	1.018	1.019	1.020	1.021
1501	.998	1.002	1.005	1.008	1.010	1.013	1.015	1.017	1.019	1.020	1.013	1.012	1.012	1.013	1.014	1.015	1.016	1.017	1.018	1.019
1511	.994	1.000	1.004	1.007	1.009	1.012	1.014	1.015	1.017	1.018	1.011	1.010	1.010	1.011	1.012	1.013	1.014	1.015	1.016	1.017
1521	.994	.999	1.003	1.006	1.008	1.010	1.011	1.012	1.014	1.014	1.007	1.006	1.006	1.007	1.008	1.009	1.010	1.011	1.012	1.013
1531	1.005	1.007	1.009	1.010	1.012	1.013	1.015	1.017	1.020	1.023	1.014	1.013	1.013	1.014	1.015	1.016	1.017	1.018	1.019	1.020
1541	1.001	1.004	1.007	1.009	1.011	1.014	1.016	1.018	1.020	1.023	1.011	1.010	1.010	1.011	1.012	1.013	1.014	1.015	1.016	1.017
1551	.997	1.001	1.003	1.006	1.010	1.013	1.015	1.017	1.019	1.021	1.009	1.008	1.008	1.009	1.010	1.011	1.012	1.013	1.014	1.015
1561	.997	1.001	1.003	1.007	1.009	1.011	1.013	1.014	1.016	1.017	1.007	1.006	1.006	1.007	1.008	1.009	1.010	1.011	1.012	1.013
1571	1.007	1.009	1.010	1.012	1.013	1.015	1.016	1.018	1.020	1.024	1.012	1.011	1.011	1.012	1.013	1.014	1.015	1.016	1.017	1.018
1581	1.003	1.006	1.010	1.010	1.012	1.014	1.016	1.019	1.021	1.024	1.010	1.009	1.009	1.010	1.011	1.012	1.013	1.014	1.015	1.016
1591	.998	1.002	1.003	1.006	1.011	1.013	1.015	1.018	1.020	1.022	1.008	1.007	1.007	1.008	1.009	1.010	1.011	1.012	1.013	1.014
1601	.998	1.002	1.003	1.007	1.010	1.012	1.013	1.015	1.018	1.021	1.008	1.007	1.007	1.008	1.009	1.010	1.011	1.012	1.013	1.014

Table 7.4 (Cont) Variations of the term  $(\alpha/\gamma)$ , across and within the heat exchangers for each test

Test number	Air in / water out boundary											Water in / Air out boundary										
	Mean												Mean									
11	.978	.986	.984	.982	.981	.979	.977	.976	.974	.973	.971	.970	.968	.966	.965	.963	.961	.960	.958	.957	.955	.954
21	.989	.995	.991	.989	.987	.985	.983	.981	.979	.977	.975	.973	.971	.969	.967	.965	.963	.961	.959	.957	.955	.954
31	.981	.988	.994	.989	.984	.980	.977	.974	.972	.970	.968	.966	.964	.962	.960	.958	.956	.954	.952	.950	.948	.947
41	.977	.997	.990	.984	.979	.976	.973	.970	.968	.966	.964	.962	.960	.958	.956	.954	.952	.950	.948	.946	.944	.943
51	.994	.999	.998	.997	.996	.995	.994	.992	.991	.990	.989	.988	.987	.986	.985	.984	.983	.982	.981	.980	.979	.978
61	.967	.999	.996	.993	.990	.988	.986	.984	.982	.981	.980	.979	.978	.977	.976	.975	.974	.973	.972	.971	.970	.969
71	.982	.997	.992	.988	.985	.981	.978	.975	.973	.971	.970	.968	.966	.964	.962	.960	.958	.956	.954	.952	.950	.949
81	.978	.995	.989	.985	.981	.978	.975	.973	.971	.970	.968	.966	.964	.962	.960	.958	.956	.954	.952	.950	.948	.947
91	.997	.983	.981	.980	.979	.977	.976	.975	.973	.971	.970	.968	.966	.964	.962	.960	.958	.956	.954	.952	.950	.949
101	.965	.993	.991	.989	.987	.985	.983	.982	.980	.978	.977	.975	.974	.972	.971	.970	.968	.966	.964	.962	.960	.959
111	.981	.992	.989	.986	.983	.981	.979	.977	.975	.974	.972	.971	.969	.967	.965	.963	.961	.959	.957	.955	.953	.952
121	.987	.981	.997	.993	.990	.987	.984	.982	.980	.979	.977	.975	.973	.971	.969	.967	.965	.963	.961	.959	.957	.956
131	.991	.995	.994	.993	.992	.991	.990	.989	.988	.987	.986	.985	.984	.983	.982	.981	.980	.979	.978	.977	.976	.975
141	.987	.995	.993	.991	.989	.988	.986	.984	.982	.981	.980	.979	.978	.977	.976	.975	.974	.973	.972	.971	.970	.969
151	.984	.996	.993	.990	.987	.984	.982	.980	.978	.976	.975	.974	.973	.972	.971	.970	.969	.968	.967	.966	.965	.964
161	.982	.993	.990	.987	.984	.982	.980	.978	.976	.974	.973	.972	.971	.970	.969	.968	.967	.966	.965	.964	.963	.962
171	.989	.972	.976	.980	.984	.988	.991	.995	.999	1.003	1.002	1.001	1.000	1.000	1.000	1.000	1.000	1.000	1.000	1.000	1.000	1.000
181	1.019	.984	.994	1.004	1.007	1.015	1.022	1.029	1.037	1.044	1.051	1.058	1.065	1.071	1.077	1.083	1.089	1.095	1.101	1.107	1.113	1.119
191	1.029	.989	1.003	1.009	1.019	1.027	1.035	1.042	1.049	1.055	1.061	1.067	1.073	1.079	1.085	1.091	1.097	1.103	1.109	1.115	1.121	1.127
201	1.036	.995	1.005	1.017	1.027	1.036	1.044	1.051	1.057	1.062	1.067	1.072	1.077	1.082	1.087	1.092	1.097	1.102	1.107	1.112	1.117	1.122
211	.982	.968	.971	.974	.977	.980	.983	.987	.990	.993	.997	.999	.999	.999	.999	.999	.999	.999	.999	.999	.999	.999
221	1.006	.976	.984	.991	.998	1.005	1.007	1.014	1.021	1.028	1.036	1.043	1.050	1.057	1.064	1.071	1.078	1.085	1.092	1.099	1.106	1.113
231	1.018	.980	.991	1.001	1.006	1.014	1.022	1.030	1.037	1.045	1.053	1.061	1.069	1.077	1.085	1.093	1.101	1.109	1.117	1.125	1.133	1.141
241	1.025	.985	.998	1.004	1.014	1.023	1.031	1.039	1.046	1.053	1.060	1.068	1.075	1.083	1.091	1.099	1.107	1.115	1.123	1.131	1.139	1.147
251	.996	.973	.976	.979	.983	.987	.991	.995	1.000	1.004	1.010	1.016	1.022	1.028	1.034	1.040	1.046	1.052	1.058	1.064	1.070	1.076
261	.995	.970	.974	.982	.987	.993	.999	1.005	1.006	1.013	1.020	1.027	1.034	1.041	1.048	1.055	1.062	1.069	1.076	1.083	1.090	1.097
271	1.009	.976	.985	.993	1.001	1.009	1.011	1.018	1.025	1.033	1.041	1.049	1.057	1.065	1.073	1.081	1.089	1.097	1.105	1.113	1.121	1.129
281	1.014	.979	.989	.998	1.007	1.010	1.018	1.025	1.032	1.040	1.047	1.055	1.063	1.071	1.079	1.087	1.095	1.103	1.111	1.119	1.127	1.135
291	.981	.965	.968	.971	.974	.978	.982	.986	.990	.995	1.000	1.005	1.010	1.015	1.020	1.025	1.030	1.035	1.040	1.045	1.050	1.055
301	.991	.960	.973	.978	.983	.988	.994	1.000	1.006	1.008	1.015	1.020	1.025	1.030	1.035	1.040	1.045	1.050	1.055	1.060	1.065	1.070
311	1.001	.971	.978	.985	.992	.999	1.006	1.013	1.018	1.023	1.031	1.038	1.045	1.052	1.059	1.066	1.073	1.080	1.087	1.094	1.101	1.108
321	1.006	.972	.981	.989	.997	1.005	1.008	1.015	1.022	1.030	1.038	1.046	1.054	1.062	1.070	1.078	1.086	1.094	1.102	1.110	1.118	1.126

Table 7.5 Variation of the term  $[(\alpha/\delta) C_{over}^*]$  across and within the heat exchangers for each test





Test number	Air in / water out boundary										Water in / Air out boundary		Mean
971	.971	.986	.989	.996	.992	.988	.985	.982	.979	.976		.991	
981	.999	.992	.987	.982	.978	.974	.972	.969	.968	.966		.979	
991	.996	.989	.984	.979	.976	.974	.972	.971	.970	.969		.978	
1001	.999	.993	.987	.982	.979	.976	.973	.971	.970	.969		.980	
1011	1.014	1.019	1.005	1.001	.997	.993	.990	.986	.983	.980		.996	
1021	1.010	1.004	1.000	.995	.992	.988	.985	.983	.980	.978		.992	
1031	1.003	.997	.992	.988	.984	.981	.979	.976	.975	.973		.985	
1041	1.000	.995	.990	.986	.982	.979	.977	.975	.973	.972		.983	
1051	1.015	1.011	1.007	1.002	.998	.995	.991	.987	.984	.981		.997	
1061	1.003	.999	.994	.991	.987	.984	.981	.978	.976	.974		.987	
1071	1.002	.998	.995	.992	.989	.988	.986	.984	.982	.981		.990	
1081	.999	.995	.992	.989	.987	.985	.983	.982	.980	.979		.987	
1091	1.000	1.016	1.011	1.006	1.001	.997	.993	.989	.985	.981		1.000	
1101	1.000	1.004	1.000	.996	.993	.989	.986	.983	.981	.978		.992	
1111	1.003	.999	.995	.991	.988	.985	.982	.980	.978	.976		.988	
1121	.999	.995	.992	.989	.987	.985	.982	.981	.979	.978		.987	
1131	.972	.988	.988	.995	1.002	1.010	1.013	1.020	1.028	1.037		1.005	
1141	.983	.996	1.003	1.012	1.021	1.029	1.037	1.045	1.052	1.059		1.024	
1151	.994	1.000	1.015	1.025	1.033	1.040	1.047	1.052	1.057	1.062		1.033	
1161	.997	1.012	1.018	1.028	1.036	1.043	1.050	1.055	1.060	1.064		1.036	
1171	.961	.968	.974	.981	.988	.995	1.004	1.008	1.018	1.031		.993	
1181	.970	.980	.990	.999	1.003	1.011	1.019	1.028	1.038	1.048		1.009	
1191	.980	.992	1.002	1.007	1.014	1.022	1.029	1.036	1.043	1.050		1.017	
1201	.986	.999	1.010	1.014	1.023	1.030	1.038	1.044	1.051	1.057		1.025	
1211	.952	.958	.964	.970	.977	.984	.992	1.001	1.008	1.024		.983	
1221	.963	.971	.979	.987	.995	.999	1.007	1.017	1.027	1.040		.999	
1231	.971	.981	.990	.998	1.006	1.010	1.017	1.025	1.032	1.041		1.007	
1241	.979	.988	1.000	1.009	1.013	1.021	1.028	1.036	1.044	1.052		1.017	
1251	.948	.947	.954	.960	.967	.974	.981	.991	1.004	1.019		.974	
1261	.955	.963	.970	.977	.985	.993	.998	1.007	1.019	1.034		.990	
1271	.963	.972	.981	.988	.996	1.000	1.007	1.015	1.024	1.034		.998	
1281	.972	.982	.992	1.001	1.005	1.013	1.021	1.030	1.039	1.049		1.010	

Table 7.5 (Cont) Variation of the term  $[(c/B) C_{over}]$  across and within the heat exchangers for each test



Test number	Water flow rate kg/s	Air mass flow rate (dry) kg/s	Inlet water temperature °C	Inlet water temperature °C	Inlet water temperature °C	Inlet water temperature °C	Dry W	Q <sub>W</sub> kW	Q <sub>W</sub> /W <sub>0</sub>	Q <sub>W</sub> /W <sub>0</sub>	α <sub>W</sub> (square)	α <sub>W</sub> /beta <sub>W</sub> conv kg/kg K	Q <sub>W</sub> kg/kg K	Re	Pr	Ex
11	2.97	1.81	11.72	15.89	33.01	32.9	1.69	.23	1.05	1.09	2.33	2.02	.30	.11	.11	
21	5.89	2.17	6.81	12.91	33.89	32.9	2.15	.36	1.05	.99	2.19	4.97	1.06	.12	.12	
31	8.76	1.81	7.13	11.32	32.88	33.9	3.62	.34	1.04	.98	2.14	9.09	1.70	.09	.09	
41	12.63	1.79	7.36	16.62	32.78	166.3	3.82	.31	1.04	.98	2.13	12.67	2.19	.07	.07	
51	2.96	3.37	11.74	15.91	36.19	32.5	1.69	.27	1.04	.99	2.31	1.53	.24	.13	.13	
61	6.85	3.39	6.62	12.81	27.83	131.6	2.55	.42	1.04	.99	2.15	3.95	.76	.15	.15	
71	9.95	3.35	7.98	12.64	25.91	214.3	4.68	.52	1.04	.98	2.15	5.83	1.43	.14	.14	
81	13.77	3.32	7.35	11.94	29.77	232.8	5.60	.48	1.04	.98	2.14	6.82	1.81	.12	.12	
91	3.25	4.34	8.54	13.72	29.63	72.0	1.85	.32	1.04	1.00	2.20	1.37	.24	.15	.15	
101	5.98	4.65	6.87	12.88	24.99	152.6	3.18	.52	1.03	.98	2.14	2.31	.60	.19	.19	
111	9.35	4.67	7.61	12.39	26.81	213.5	5.86	.62	1.03	.98	2.15	3.63	1.23	.18	.18	
121	12.71	4.65	11.48	16.81	29.59	246.6	6.44	.49	1.03	.99	2.30	4.92	1.43	.15	.15	
131	2.99	6.47	8.37	13.49	26.86	64.7	1.23	.41	1.03	.99	2.18	.86	.19	.19	.19	
141	6.81	6.43	7.86	14.26	25.94	163.4	3.75	.62	1.03	.99	2.21	1.72	.59	.22	.22	
151	9.68	6.39	7.28	13.94	26.66	289.7	6.49	.71	1.03	.98	2.18	2.44	1.03	.22	.22	
161	11.95	6.52	6.86	13.47	25.43	274.2	9.74	.72	1.03	.98	2.19	3.41	1.37	.28	.28	
171	2.98	2.28	38.98	33.22	9.88	75.4	1.69	.22	.98	.99	3.93	1.46	.32	.17	.17	
181	5.92	2.17	43.86	35.88	16.94	287.9	2.60	.32	.99	1.02	4.35	2.64	.94	.21	.21	
191	8.94	2.15	42.23	35.94	16.88	263.2	3.19	.31	1.00	1.03	4.38	3.99	1.44	.18	.18	
201	11.92	2.14	42.43	36.95	18.66	288.3	3.60	.26	1.00	1.04	4.47	5.24	1.62	.15	.15	
211	2.96	3.74	38.75	32.13	9.35	85.9	1.78	.23	.98	.98	3.84	.88	.21	.28	.28	
221	5.94	3.69	43.18	33.26	16.39	258.7	2.41	.37	.99	1.01	4.21	1.62	.63	.26	.26	
231	9.83	3.66	42.38	32.67	16.38	384.4	4.60	.46	1.00	1.02	4.21	2.46	1.24	.26	.26	
241	11.92	3.69	42.52	34.88	9.97	446.0	8.49	.41	1.00	1.03	4.32	3.44	1.45	.23	.23	
251	2.98	5.28	43.48	34.22	16.87	122.2	1.99	.28	.98	.99	4.19	.58	.17	.24	.24	
261	6.84	5.23	41.35	36.88	18.12	276.9	2.94	.43	.99	1.00	3.95	1.24	.54	.29	.29	
271	9.16	5.13	41.54	36.78	11.71	431.1	5.38	.54	1.00	1.01	4.82	1.86	1.04	.31	.31	
281	11.84	5.32	41.48	31.46	11.42	317.9	6.85	.53	1.00	1.01	4.88	2.29	1.27	.28	.28	
291	2.85	7.15	41.57	36.78	9.32	148.4	1.21	.39	.98	.98	3.87	.46	.17	.38	.38	
301	5.97	7.95	41.48	29.36	18.52	316.1	3.38	.52	.99	.99	3.85	.93	.47	.34	.34	
311	9.83	6.98	41.58	29.66	11.49	467.6	5.33	.57	1.00	1.00	3.92	1.39	.79	.34	.34	
321	11.84	7.13	41.7	29.79	16.44	599.2	7.57	.59	1.00	1.01	3.98	1.76	1.06	.35	.35	

Table 7.6 Representative values of the terms in the overall performance equation for each test

test number	Water flow rate kg/s	Air mass flow rate (dry) kg/s	Inlet water temperature °C	Outlet water temperature °C	Inlet wet-bulb temperature °C	Wet bulb °C	Wet bulb °C	Wet bulb °C	Inlet (p/pa)at	Outlet (p/pa)at	Wet bulb °C	Wet bulb °C	Wet bulb °C	Wet bulb °C	Wet bulb °C	Wet bulb °C
351	2.82	1.68	9.84	26.67	33.38	131.2	2.51	.86	1.84	.99	2.39	2.58	1.35	.27		
349	5.75	1.87	9.47	15.79	32.28	182.2	4.40	.73	1.84	.98	2.22	5.61	2.41	.16		
351	8.98	1.78	9.26	13.87	32.99	171.9	5.86	.54	1.84	.97	2.19	9.66	2.91	.18		
361	11.94	1.77	9.94	13.81	32.11	156.5	4.47	.38	1.84	.98	2.28	12.76	2.59	.87		
371	2.85	3.33	9.81	23.25	31.28	184.9	3.68	1.24	1.83	1.00	2.59	1.39	1.11	.41		
391	5.77	3.35	8.92	13.75	29.77	217.4	6.19	1.84	1.83	.98	2.27	3.99	1.89	.26		
391	9.28	3.33	7.65	13.49	29.28	239.5	7.32	.77	1.83	.97	2.16	5.23	2.26	.17		
401	11.88	3.34	18.55	15.15	36.15	233.2	7.26	.59	1.83	.98	2.24	6.44	2.22	.13		
411	2.97	4.85	9.44	24.84	29.36	177.6	4.77	1.68	1.83	1.06	2.57	.94	.99	.52		
421	5.88	4.88	8.46	18.76	29.84	255.2	7.84	1.31	1.83	.98	2.31	2.18	1.63	.34		
431	9.32	4.82	7.66	15.84	27.51	293.6	10.25	1.84	1.83	.98	2.18	3.61	2.18	.23		
441	11.93	4.91	12.81	17.42	26.86	234.2	11.39	.98	1.83	.99	2.33	4.25	3.35	.28		
451	2.89	6.57	9.43	24.78	27.69	188.1	6.64	2.19	1.82	1.08	2.63	.68	1.81	.66		
461	5.91	6.60	7.95	26.27	26.85	386.1	11.82	1.82	1.82	.98	2.36	1.53	1.78	.46		
471	9.85	6.51	11.95	19.33	25.98	284.9	115.01	1.64	1.82	.99	2.35	2.42	2.46	.35		
481	12.84	6.58	12.29	18.89	25.93	292.9	116.63	1.38	1.82	.99	2.32	3.26	2.68	.27		
491	2.92	2.21	42.78	27.41	12.19	194.8	2.81	.98	1.88	1.81	3.98	1.41	1.26	.43		
501	5.72	2.14	39.33	29.74	12.89	239.3	4.79	.74	1.81	1.82	3.96	2.81	2.19	.38		
511	9.92	2.13	41.88	33.41	11.71	297.4	5.56	.53	1.88	1.84	4.27	4.83	2.39	.22		
521	11.56	2.12	41.99	36.48	12.87	288.9	3.85	.28	1.88	1.84	4.43	5.17	1.75	.15		
531	2.96	3.74	43.82	22.83	11.67	258.6	4.21	1.37	1.81	.99	3.58	.92	1.13	.56		
541	3.74	3.71	39.44	25.88	11.82	342.7	6.81	1.18	1.81	1.88	3.71	1.73	1.83	.42		
551	8.78	3.77	41.88	29.82	18.98	484.6	7.54	.77	1.88	1.82	4.18	2.37	1.95	.33		
561	11.63	3.68	42.83	33.35	11.93	442.9	6.22	.47	1.88	1.83	4.27	3.18	1.84	.24		
571	2.97	5.48	43.59	19.61	11.53	386.9	5.64	1.81	1.81	.98	3.54	.68	1.86	.67		
581	5.73	5.38	39.83	22.39	11.11	411.6	8.72	1.46	1.81	.99	3.47	1.37	1.63	.82		
591	8.78	8.35	38.56	25.63	11.62	491.5	10.42	1.18	1.81	1.88	3.65	1.83	1.94	.41		
601	11.45	5.48	41.93	28.93	11.72	595.3	9.87	.72	1.88	1.82	4.83	2.17	1.65	.33		
611	2.98	7.63	43.95	18.74	11.14	347.4	7.49	2.53	1.81	.97	3.12	.56	1.88	.75		
621	5.74	7.21	38.36	14.37	18.73	478.3	11.18	1.58	1.81	.99	3.28	1.81	1.57	.61		
631	8.88	7.89	39.69	23.93	11.81	633.2	14.47	1.58	1.81	1.88	3.58	1.44	2.84	.31		
641	11.58	6.96	41.81	27.17	11.88	737.4	12.92	1.62	1.81	1.81	3.92	1.77	1.63	.42		

Table 7.6 (Cont)

Representative values of the terms in the overall performance equation for each test

Test number	Water flow rate kg/s	Air mass flow rate (dry) kg/s	Inlet water temperature °C	Outlet water temperature °C	Inlet wet-bulb temperature °C	Duty kJ	h <sub>db</sub> W/K	Kwh/hr	calphs/gmass	Calphs/(hwt) cavst kJ/kg K	CHW kJ/kg K	Pa	Re	Gr
651	2.87	1.96	12.22	23.89	32.41	144.8	4.44	1.44	1.83	1.99	2.47	2.42	2.29	1.34
661	3.84	1.81	9.71	16.91	33.89	188.0	6.75	1.83	1.84	1.97	2.22	5.87	3.83	1.16
671	8.81	1.78	11.82	15.88	33.58	179.7	8.32	1.75	1.84	1.97	2.23	8.78	4.81	1.11
681	11.73	1.78	18.56	14.12	33.35	177.6	6.62	1.58	1.84	1.97	2.22	11.92	3.82	1.68
691	2.87	3.49	12.22	25.76	29.67	167.9	6.62	2.16	1.82	1.99	2.63	1.31	1.96	1.94
701	5.87	3.36	9.68	26.84	38.26	266.6	111.28	1.74	1.83	1.98	2.27	5.14	5.43	1.39
711	8.98	3.35	18.89	17.38	38.63	274.8	112.69	1.23	1.83	1.98	2.22	4.86	3.87	1.26
724	11.86	3.35	8.61	14.37	38.86	291.1	112.83	1.91	1.83	1.97	2.16	6.64	3.69	1.15
736	2.91	4.97	12.18	26.84	27.91	174.1	8.74	2.82	1.82	1.88	2.73	1.88	1.76	1.89
743	5.89	4.95	9.66	21.31	27.77	294.2	114.77	2.32	1.82	1.98	2.33	2.89	3.16	1.42
751	8.83	4.94	8.38	17.92	28.78	346.4	116.94	1.74	1.83	1.97	2.28	3.31	3.52	1.28
761	11.81	4.88	8.22	15.46	28.99	367.9	116.58	1.26	1.83	1.97	2.16	4.89	3.49	1.21
771	2.99	6.84	18.43	23.22	24.47	163.8	118.94	3.45	1.82	1.88	2.62	1.78	1.65	1.77
785	5.93	6.82	9.72	21.83	25.33	287.7	116.69	2.44	1.82	1.98	2.39	1.94	2.56	1.32
799	8.92	6.59	9.45	19.14	26.78	369.5	119.71	2.93	1.82	1.98	2.27	2.44	3.85	1.37
801	11.94	6.38	9.29	16.79	27.81	381.3	119.18	1.47	1.83	1.98	2.21	3.48	3.88	1.27
811	2.94	2.26	48.58	23.74	12.88	213.2	4.78	1.33	1.81	1.88	3.68	1.58	2.16	1.51
821	5.81	2.21	42.27	28.88	11.38	348.3	8.78	1.27	1.81	1.84	4.28	2.54	3.79	1.37
831	8.78	2.15	48.38	32.84	11.48	326.9	9.33	1.82	1.81	1.84	4.29	3.96	4.17	1.24
841	11.82	2.13	41.78	35.32	13.35	332.8	7.63	1.88	1.81	1.85	4.46	5.18	3.42	1.18
851	2.95	3.72	41.28	18.49	11.84	287.8	7.94	2.61	1.81	1.99	3.38	1.99	2.13	1.68
861	5.98	3.71	42.45	33.98	11.11	473.9	111.65	1.81	1.81	1.82	3.91	1.88	3.89	1.51
871	8.76	3.71	48.97	27.38	11.87	518.4	113.88	1.37	1.81	1.83	4.19	2.39	3.64	1.39
881	11.72	3.69	41.88	31.31	13.89	548.6	112.44	1.89	1.81	1.84	4.31	3.86	3.24	1.39
891	2.99	5.31	51.54	15.57	11.83	372.8	119.93	3.78	1.82	1.98	3.91	1.77	2.11	1.79
901	5.98	5.35	42.45	28.17	11.19	588.8	113.14	2.45	1.81	1.88	3.58	1.27	2.83	1.63
911	8.76	5.36	41.42	23.81	18.89	668.8	117.42	1.82	1.81	1.81	3.84	1.73	3.21	1.58
921	11.88	5.32	42.82	27.96	12.76	722.5	116.98	1.26	1.81	1.83	4.13	2.22	3.11	1.46
931	3.82	7.82	41.88	13.96	11.25	399.8	113.88	4.44	1.81	1.96	2.82	1.63	1.92	1.85
941	5.88	7.77	42.42	17.93	11.13	617.5	116.89	2.82	1.81	1.99	3.33	1.81	2.38	1.79
951	8.88	7.41	51.49	21.66	18.36	793.8	118.84	1.94	1.81	1.88	3.65	1.88	2.53	1.56
961	11.79	6.75	42.18	28.48	12.77	888.6	116.94	1.38	1.81	1.82	3.96	1.83	2.47	1.45

Table 7.6 (Cont)

Representative values of the terms in the overall performance equation for each test

Test number	Water flow rate kg/s	Air mass flow rate (dry) kg/s	Inlet water temperature °C	Outlet water temperature °C	Inlet wet-bulb temperature °C	Dry bulb °C	Wet bulb °C	Wet/dry	Latent/total	Latent/total convt kJ/kg K	CO <sub>2</sub> kJ/kg K	St	H	En	
971	1.94	9.57	28.29	33.51	131.8	2.37	.68	1.64	.99	2.38	2.51	1.23	.26	1	
981	3.79	1.92	8.77	18.69	32.93	188.7	3.89	.65	1.64	.98	2.23	5.47	2.67	.15	1
991	6.98	1.98	18.38	14.28	38.89	149.6	4.93	.52	1.63	.98	2.22	8.68	2.65	.11	1
1001	11.98	1.92	18.89	14.43	33.67	176.7	4.11	.34	1.64	.98	2.26	18.78	2.19	.98	1
1011	2.89	3.38	4.62	22.84	31.38	168.5	3.45	1.15	1.65	1.69	2.47	1.41	1.83	.39	1
1021	5.96	3.33	13.38	21.34	31.48	283.3	5.71	.91	1.63	.99	2.45	2.97	1.73	.26	1
1031	9.15	3.23	12.18	18.89	31.59	232.8	6.61	.69	1.63	.98	2.34	4.98	2.68	.17	1
1041	11.37	3.34	18.94	15.96	31.87	247.9	6.13	.51	1.64	.98	2.28	6.14	1.86	.13	1
1051	2.91	4.93	9.39	23.37	29.63	172.1	4.59	1.52	1.63	1.68	2.54	.95	.93	.58	1
1061	5.93	4.98	9.23	19.14	28.63	281.2	7.15	1.17	1.63	.99	2.33	2.88	1.46	.33	1
1071	8.93	4.91	13.12	17.75	28.47	176.8	8.43	.91	1.62	.99	2.38	3.39	1.74	.24	1
1081	11.81	4.92	13.43	16.23	28.93	192.2	7.98	.65	1.63	.99	2.31	4.23	1.63	.18	1
1091	3.84	6.85	18.12	25.81	28.82	194.1	8.69	2.18	1.62	1.68	2.66	.68	.98	.64	1
1101	5.97	6.62	17.33	21.49	27.82	259.7	8.82	1.42	1.63	.99	2.46	1.58	1.34	.42	1
1111	8.78	6.79	11.38	18.97	28.84	287.6	111.17	1.22	1.63	.99	2.36	2.27	1.69	.32	1
1121	11.85	6.88	11.57	16.83	25.68	268.6	118.77	.89	1.63	.99	2.31	3.83	1.61	.25	1
1131	2.98	2.15	41.26	28.28	12.68	185.4	2.33	.76	1.68	1.68	3.85	1.47	1.89	.39	1
1141	5.84	2.16	41.62	31.42	11.43	268.8	4.88	.62	1.68	1.62	4.16	2.71	1.84	.29	1
1151	8.98	2.13	48.96	33.91	12.67	275.8	4.74	.46	1.69	1.63	4.26	4.18	2.14	.21	1
1161	11.88	2.12	41.54	36.22	12.43	276.6	3.99	.29	1.68	1.64	4.38	5.33	1.81	.15	1
1171	2.97	3.67	42.75	24.44	18.96	233.3	3.31	1.87	1.68	.99	3.66	.92	.91	.51	1
1181	5.84	3.74	41.88	27.12	18.78	372.8	5.92	.94	1.68	1.61	3.98	1.67	1.57	.41	1
1191	8.94	3.69	46.41	30.27	12.81	396.2	6.61	.66	1.68	1.62	4.81	2.52	1.76	.38	1
1201	11.74	3.79	41.88	33.25	11.86	429.1	6.82	.45	1.68	1.63	4.22	3.14	1.58	.24	1
1211	2.98	5.33	42.76	26.64	18.66	283.9	4.66	1.53	1.61	.98	3.48	.68	.89	.62	1
1221	5.89	5.34	41.92	24.13	18.67	483.1	7.58	1.22	1.61	1.68	3.69	1.24	1.42	.58	1
1231	8.88	5.27	39.93	27.34	11.45	492.3	8.56	.88	1.68	1.61	3.81	1.87	1.61	.38	1
1241	11.78	5.35	41.43	36.58	11.68	585.8	8.21	.63	1.68	1.62	4.	2.24	1.51	.31	1
1251	3.88	7.86	42.85	17.88	18.58	338.8	6.81	2.28	1.61	.97	3.33	.56	.99	.73	1
1261	5.94	7.89	41.99	21.23	18.17	532.3	9.73	1.98	1.61	.99	3.49	1.88	1.39	.58	1
1271	8.98	7.84	39.38	28.19	11.88	591.5	111.61	1.22	1.61	1.68	3.61	1.47	1.65	.42	1
1281	11.74	7.18	41.78	27.75	11.32	713.8	111.35	.89	1.68	1.61	3.92	1.74	1.58	.48	1

Table 7.6 (Cont)

Representative values of the terms in the overall performance equation for each test

Test number	Water flow rate kg/s	Air mass flow rate (dry) kg/s	Inlet water temperature °C	Outlet water temperature °C	Inlet wet-bulb temperature °C	Duty kW	Wet bulb °C	Kwh/He	(alpha/gamma)	1/alpha/1/beta k/kg	DRW k/kg x	W	W <sub>0</sub>	Eff
1291	2.94	1.93	16.91	21.58	31.87	135.8	3.35	1.16	1.83	.98	2.41	2.37	1.87	.36
1367	5.87	1.92	9.32	16.48	32.45	179.7	6.33	.99	1.83	.97	2.27	3.39	3.39	.17
1311	8.84	1.92	9.93	13.96	32.52	186.8	6.36	.88	1.84	.97	2.18	6.51	3.51	.11
1321	11.81	1.87	12.88	15.43	32.68	188.6	6.68	.59	1.84	.98	2.28	11.19	3.65	.89
1331	2.93	3.39	16.95	23.21	39.65	186.3	5.44	1.76	1.85	.99	2.58	1.36	1.81	.49
1341	5.91	3.38	9.46	19.29	39.18	239.3	9.83	1.44	1.83	.98	2.27	3.13	2.74	.28
1351	8.86	3.36	9.97	16.46	39.87	278.9	18.38	1.88	1.83	.97	2.21	4.86	3.16	.19
1361	11.72	3.41	11.37	16.24	29.37	243.3	9.86	.78	1.83	.98	2.26	6.16	2.96	.18
1377	2.97	4.95	16.98	25.39	28.58	186.8	7.52	2.39	1.82	1.88	2.67	.92	1.52	.64
1381	5.94	4.93	9.37	28.75	28.15	298.2	11.89	1.89	1.83	.98	2.34	2.19	2.45	.46
1391	8.85	4.86	9.39	17.73	28.27	314.7	13.72	1.44	1.83	.98	2.23	3.33	2.88	.27
1481	11.88	4.85	16.98	16.92	28.31	381.3	13.34	1.83	1.83	.98	2.26	4.48	2.81	.21
1411	3.88	6.58	16.91	28.12	26.29	183.8	18.76	3.38	1.82	.88	2.73	.68	1.63	.78
1421	5.99	6.68	9.41	21.79	26.58	318.9	15.51	2.45	1.82	.98	2.41	1.53	2.48	.51
1431	8.93	6.57	9.84	18.73	26.88	339.9	18.58	1.94	1.82	.98	2.28	2.48	2.89	.36
1441	11.88	6.68	18.72	17.83	26.94	368.8	18.27	1.42	1.83	.98	2.27	3.23	2.83	.28
1451	2.92	2.15	36.58	23.31	12.13	187.4	4.31	1.48	1.81	1.88	3.46	1.63	2.82	.46
1461	5.93	2.14	36.92	28.86	11.87	229.1	6.38	.95	1.81	1.81	3.79	3.84	2.94	.38
1471	8.92	2.13	37.67	31.81	11.17	239.9	6.98	.65	1.81	1.82	3.96	4.41	3.21	.21
1481	11.88	2.08	34.83	39.79	11.39	212.8	6.38	.45	1.81	1.81	3.71	6.48	3.82	.15
1491	2.94	3.68	37.87	18.87	11.57	229.9	6.53	2.18	1.81	.98	3.18	1.84	1.88	.63
1581	5.97	3.79	37.38	24.89	11.88	342.9	9.28	1.44	1.81	1.88	3.39	1.88	2.58	.44
1511	8.94	3.78	38.83	27.36	11.17	415.1	18.65	1.86	1.81	1.81	3.83	2.82	2.84	.34
1521	11.91	3.68	34.78	28.87	11.67	348.1	18.29	.76	1.81	1.81	3.63	3.71	2.77	.24
1531	2.95	5.33	37.41	15.49	11.68	278.9	9.83	3.89	1.81	.97	2.96	.77	1.75	.75
1541	5.98	5.29	37.68	21.85	11.89	428.8	12.28	1.96	1.81	.99	3.46	1.58	2.34	.56
1551	8.95	5.39	38.29	24.28	11.11	543.5	14.38	1.47	1.81	1.81	3.67	1.91	2.68	.44
1561	11.89	5.34	34.21	25.29	11.67	439.7	14.78	1.12	1.81	1.88	3.58	2.44	2.75	.33
1571	2.94	7.11	37.51	14.34	12.84	271.8	11.94	4.18	1.81	.96	2.76	.82	1.75	.84
1581	5.98	7.89	31.77	18.38	11.85	495.8	11.52	2.54	1.81	.98	3.21	1.89	2.72	.65
1591	8.93	7.89	38.31	21.82	11.13	643.4	11.12	1.82	1.81	1.88	3.51	1.49	2.42	.53
1681	11.97	7.89	33.78	23.17	11.46	848.9	11.75	1.39	1.81	.99	3.37	2.88	2.52	.19

Table 7.6 (Cont). Representative values of the terms in the overall performance equation for each test

## 8. VERIFICATION OF THE SIMPLIFIED THEORETICAL MODEL (PERFORMANCE EQUATION) BY COMPARISON WITH THE COMPREHENSIVE THEORETICAL MODEL AND EXPERIMENTAL DATA.

### 8.1 Introduction

The basic manner in which the performance equation will be employed is to predict thermal duty from a knowledge of the inlet process conditions (flowrates and temperatures) and the overall design characteristics  $N^*$  (or overall transfer coefficient  $h_cA$ ). The basic procedure is defined in Section 7.5.5 and the accuracy is now examined by comparing predicted values of the water efficiency against the actual values.

### 8.2 Overall database

In order to thoroughly check the performance equation a large database of simulated conditions has been generated to supplement the experiment database. The computer simulator was run for a wide variety of flow conditions (water-air flow ratios from 0,75 to 4,0), for heat exchangers with widely differing design characteristics ( $N^*$  values from 1,0 to 4,0) over the full range of temperature and pressure conditions. Details are given in Appendix P. The overall database against which the simplified theoretical model or performance equation is to be verified thus comprises 160 experimental points and 490 simulated test points.

### 8.3 Comparison of actual performance against that predicted by performance equation

The accuracy of the performance equation has been examined by comparing the predicted values of the water efficiency against the actual values. The full data-base of 650 points is shown plotted in Figure 8.1. Also shown on Figure 8.1 is the line of identity. Clearly, the correlation is satisfactory for such a wide variety of process conditions and heat exchanger design characteristics.

The data have also been examined in independent groups and the following have been compared :

- . different experimental geometries
- . water cooling against air cooling processes
- . experimental test data against simulated test data
- . high water-air flow ratios against low water-air flow ratios

From this examination it has been concluded that there is no consistent trend apparent with regard to the deviation of the points from the line of identity. However, Figure 8.1 indicates an increase in the deviation at the higher water efficiencies. The explanation for this lies in the method of estimating the pseudo-specific heat. The inaccuracy in estimating the representative value of the pseudo-specific heat from a knowledge of the inlet conditions will inevitably increase as the temperature range of the water increases. This is because of the effect of the curvature of the sigma energy - temperature relationship is greater the wider the range in temperature.

Further work on the estimation of the value of the representative pseudo-specific heat will be beneficial at a later stage after further experience has been gained in the application of the method and a wider database is in existence.

In any event, Figure 8.1 clearly indicates that the method is both accurate and versatile.

### 8.3.1 Quantification of accuracy

The accuracy has been statistically quantified in terms of the difference between actual and predicted water efficiencies measured in percentage points. This information is summarized in Table 8.1 for all the 650 data points. The overall average absolute error of less than 1 percentage point in predicting the water efficiency is considered to be acceptable.

Table 8.1 Statistics related to the difference between actual and predicted water efficiency for entire database (values are given in percentage points)

	Absolute errors				Actual errors			
	ave.	s d*	min	max	ave.	s d	min	max
All tests	0,8	0,8	0,0	5,9	0,0	1,1	-3,1	+5,9
Cold water tests	0,5	0,5	0,0	3,1	-0,4	0,7	-3,1	+2,7
Hot water tests	1,0	1,0	0,0	5,9	+0,4	1,3	-2,3	+5,9

\* standard deviation

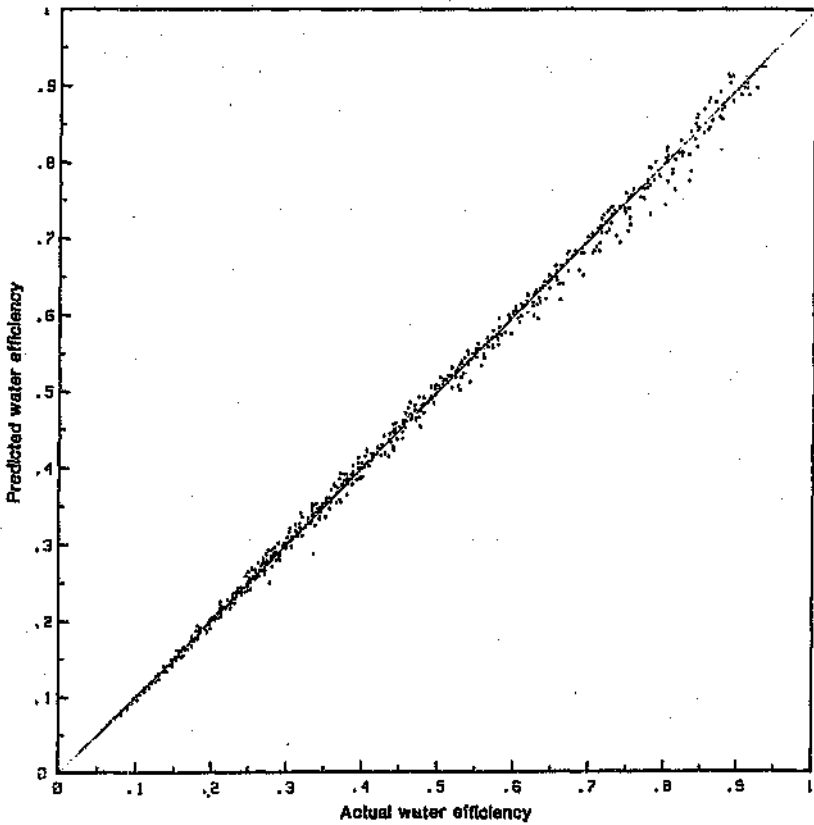


**Figure 8.1** Comparison of actual performance against predicted performance for full database (650 points)

## 9. DISCUSSION AND CONCLUSIONS

The main objective of this work is the development of an improved and simple method for the thermal analysis of direct contact water-air heat exchangers which may be used by the practicing field engineer. In addition to the main objective, a number of interesting points have emerged as secondary conclusions. This chapter is thus divided into two parts; the first part is directly related to the overall method of performance analysis and the second part to the other secondary conclusions.

### 9.1 Overall performance equation

#### 9.1.1. General philosophy

The approach adopted in solving this problem has been to develop simple equations to describe the change of energy state of the water and air streams as well as to describe the heat flow from an elemental wet area. The definition and introduction of a multiplying parameter into each of these three simple equations allows them each to describe the physical mechanisms exactly. These three equations are then algebraically manipulated to produce the overall performance equation and the accuracy of the original three equations is generally retained in the final equation. It is only once the final overall equation has been developed that some simplifications are introduced.

This tactic has been extremely valuable in identifying

the correct form of the overall equation and the relevant grouping of parameters. The more commonly used approach of starting with approximate equations would not have been successful in identifying the important issues and details would have been lost. This has been particularly true with regard to the new equation's ability to identify and account for the difference between water cooling and air cooling applications.

The essence of the new performance equation is embodied in four issues. First, the algebraic development of a performance equation in which it is not necessary to identify which fluid has the minimum thermal capacity.

Second, the use of sigma energy differences to describe the driving force for heat transfer from a wet surface (in place of enthalpy potential) as well as the change in energy state of the air stream.

Third, the definition and introduction of the pseudo-specific heat term based on sigma energy: the major difference between direct contact and non direct contact applications lies in the fact that the specific thermal capacity of the air stream varies significantly in direct contact units since it is dependent on moisture content, whereas it has a constant value in non direct contact units (assuming of course that no condensation occurs). The introduction of the pseudo-specific heat term based on sigma energy is of fundamental importance. (It should also be noted that the new method makes use of the specific thermal capacity of dry air as a reference value in the non-dimensional NTU term. This is the case for all thermal capacity ratios and is possible because of the first issue discussed above.)

Fourth, the use of the term  $(\alpha/\gamma)_i$  in combination

with the 'thermal capacity rate ratio': recall that

$$\dot{m}_w c_w \Delta t_w = (\alpha/\gamma)_i \dot{m}_a \Delta \Sigma \quad (9.1)$$

The term  $(\alpha/\gamma)_i$  has been introduced to account for the changes in mass flow due to condensation or evaporation (and the use of sigma energy). The term has a distinctly different value for water cooling and air cooling applications. This is clearly evident from Figure 7.16. It is through the definition and introduction of  $(\alpha/\gamma)_i$  that the method can account for the differences between condensation and evaporation processes.

### 9.1.2 Specification of performance equation

The method is now presented in its entirety, following which its application is discussed. (For the sake of convenience the equation and family of curves are repeated here.)

The overall performance equation is shown in Figure 9.1 and is given below:

$$E_w^* = \frac{1 - e^{-N^*} (1 - 1/R^*)}{R^* - e^{-N^*} (1 - 1/R^*)}$$

where

(9.2)

$$N^* = h_c A / (\dot{m}_a c_a)$$

$$R^* = (\dot{m}_w c_w) / (\dot{m}_a c_a^*) \quad : \text{ for water cooling}$$

$$= 0.85 (\dot{m}_w c_w) / (\dot{m}_a c_a^*) \quad : \text{ for air cooling}$$

$$E_w^* = (t_w - t_{w0}) / (t_w - \frac{c_{a1}^*}{c_{aw}^*} t_{wb1})$$

The values of the pseudo-specific heat term are determined from Figure 9.2. Thus the new method is entirely encapsulated in Figures 9.1 and 9.2.

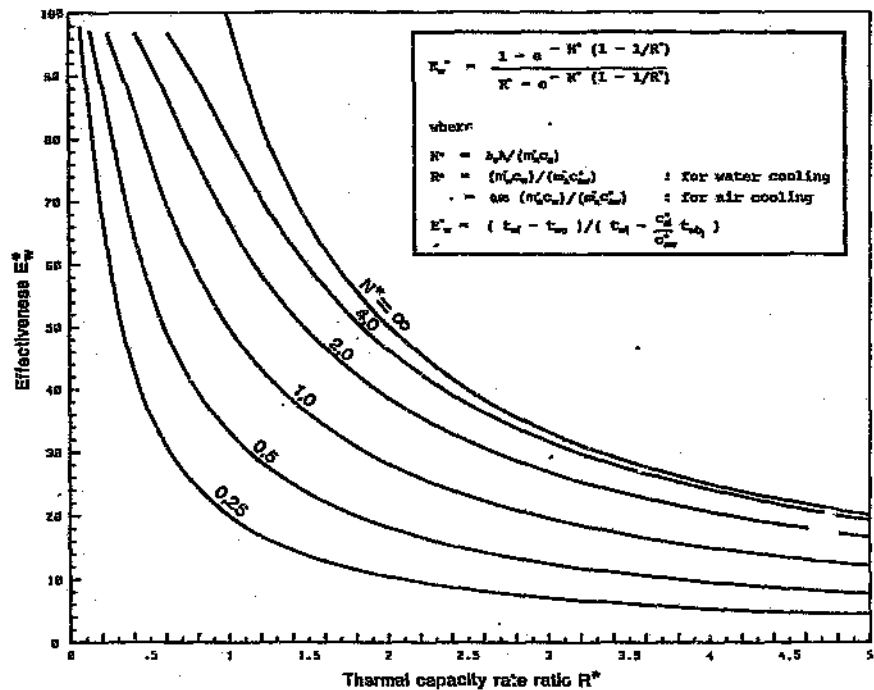


Figure 9.1 Graphical representation of overall performance equation

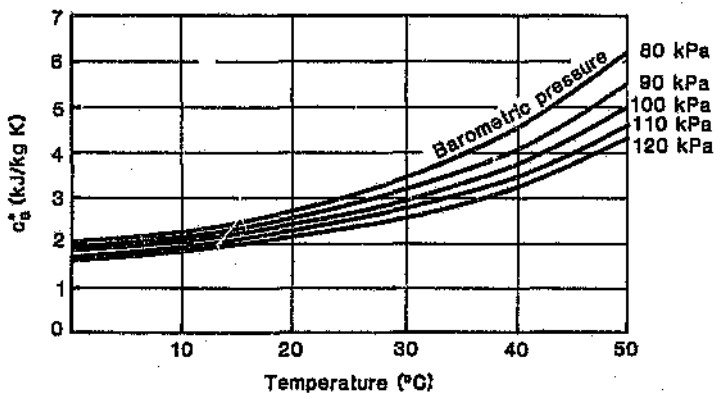
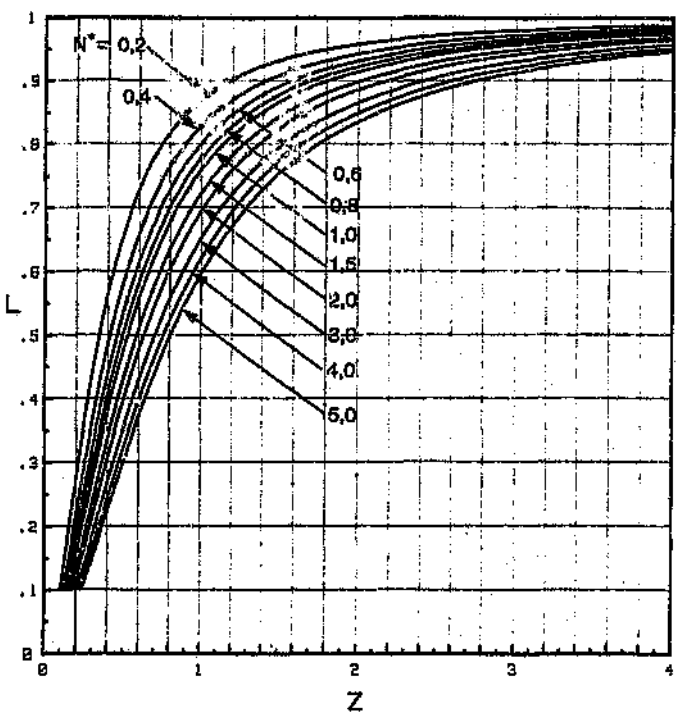


Figure 9.2 Determination of pseudo-specific heat term

### 9.1.3 Issues related to unification of heat exchanger theory

A unified heat exchanger theory has been developed in which the general approach used for direct contact heat exchangers is similar to that employed in conventional heat exchanger theory. The work described presents the complete development of a method which is directly analogous and generally consistent with the fundamental approach used in conventional heat exchanger theory, and one in which the algebraic form of the equation and the meaning of each of the parameters and their grouping can be understood.

It is in the use of the pseudo-specific heat term that a slight inconsistency arises when compared to conventional heat exchanger theory. To be exactly consistent, the pseudo-specific heat should in principle describe the change of energy state of the bulk air stream, whereas it describes the energy of saturated air at the surface temperature. Without this slight inconsistency with the normal theory, it is not possible to develop a performance equation of this nature with acceptable versatility and accuracy. As mentioned earlier, Jaber and Webb(23) reviewed numerous past attempts to apply the standard NTU method to cooling towers, and concluded that all the related definitions were flawed. This statement is basically a reflection of the problem of describing the specific thermal capacity of the air stream in direct contact units. The basic difference between direct contact and non direct contact applications is the fact that the specific thermal capacity varies significantly with changes in moisture content. It is this very real difference that necessitates the introduction of the inconsistency.

In a recent paper, Jaber and Webb(23) assert that

their definitions of NTU, effectiveness and 'capacity rate' ratio are the only correct and consistent interpretation of these heat exchanger terms for cooling towers. However it should be noted that the question of 'exact consistency' becomes a little subjective, since it depends on the interpretation of the basic conventional equations and their solution to produce the final overall equation, which may be arrived at through more than one sequence of logic. For example, Jaber and Webb define a pseudo mass flow rate of water which depends on the temperatures of the water within the tower and barometric pressure. (In achieving this, they introduce a term which is very similar in principle to the pseudo-specific heat for air defined in this thesis). Their 'capacity rate' ratio then becomes a ratio of two mass flow rates. It could be argued, that to be 'consistent' with conventional heat exchanger theory, a thermal capacity rate ratio should be used, in fact the very essence of the ratio is thermal capacities not mass capacities. The use of a mass rate capacity ratio obviously also affects the definition of the number of transfer units.

Notwithstanding, Jaber and Webb have captured the basic methodology of the normal heat exchanger procedures. However, the algebraic development of a performance equation in which it is not necessary to identify which fluid has the minimum thermal capacity is simply a progression from the normal NTU-effectiveness equation. The author submits that conventional heat exchanger theory itself could be simplified by representing the equations in this form. Without doubt, for direct contact processes this form of the equation solves many problems inherent in other methods. For example, with direct contact units it is possible for the minimum thermal capacity fluid to change over the length of the heat exchanger. The

current approach also allows the formulation of a single effectiveness term, an issue which complicates the approach proposed by Jaber and Webb(23).

Also associated with the performance equation, in which it is irrelevant which fluid has the lower thermal capacity, is an unambiguous definition of the basis of the NTU number. In previous work on cooling towers there have been many inconsistencies(23); some authors(97,99,101), make use of an NTU based on the air stream, while others(14,24,98,100) make use of an NTU based on the water stream.

The development of the performance equation in this thesis has concentrated on the counterflow configuration; however there is no reason why the same principles cannot be applied to any other configurations, such as the different crossflow configurations and parallel flow. Note that the starting point must be the transformation of the normal effectiveness-NTU equations into the preferred format. Recall that this format is independent of which fluid has the lower thermal capacity ratio. The effectiveness must be expressed as a water effectiveness and the thermal capacity ratio and the ratio of the thermal capacity of the water stream to that of the air stream. Take, for example, crossflow spray chambers which are often used in cooling mine ventilation air underground. These designs are basically a crossflow configuration with one fluid stream mixed and the other unmixed, the latter obviously being the water stream. For this configuration the normal NTU-effectiveness equation may be transposed to:

$$E_w = \frac{[1 - e^{-N} [1 - e^{-N R}]]}{R} \quad (9.3)$$

Also, for parallel flow heat exchangers the normal equation may be transposed to :

$$E_w = \frac{1 - e^{-N [ 1 + 1/R ]}}{1 + R} \quad (9.4)$$

In these equations, R is the ratio of the water thermal capacity to the air thermal capacity and N is based on air thermal capacity for all conditions.

The method is thus basically analogous to conventional heat exchanger theory and there would be some merit in extending this unification to include evaporative air and fluid coolers. Further work should also examine the F-log mean approach using sigma energy and an equivalent to Berman's (23,25) enthalpy correction factor.

#### 9.1.4 Extrapolation beyond range of operating conditions

Another important point for discussion is the extrapolation of the performance equation outside the range of conditions studied here. Because the equation is fundamentally sound, the general approach can be used for any conditions provided appropriate values are chosen for  $(\alpha/\gamma)_i$  and  $[(\alpha/\beta) C_{avaf}^*]$ . The 'universal' values selected earlier for  $(\alpha/\gamma)_i$  and  $[(\alpha/\beta) C_{avaf}^*]$  are applicable to the present range of conditions and it is likely that wide extrapolation would incur some error. Thus in using the equation for other operating conditions, it is necessary to choose the appropriate values of  $(\alpha/\gamma)_i$  and  $[(\alpha/\beta) C_{avaf}^*]$  for those conditions. This can be achieved through the use of Figures 7.16 and 7.18. For example, an air cooling duty application with cold water (say 5 °C) and air

hotter than 50 °C would indicate an appropriate value of  $(\alpha/\gamma)_i$  greater than 1,1 and a value of  $[(\alpha/\beta) c_{avaf}^*]$  of about 1,03. On the other hand, a water cooling application with water hotter than 50 °C and cold air (say 5 °C) would indicate an appropriate value of  $(\alpha/\gamma)_i$  less than 0,95 and a value of  $[(\alpha/\beta) c_{avaf}^*]$  of about 0,98.

It should be noted that unless extremely hot air is in contact with extremely hot water throughout the heat exchanger, it is unlikely that the appropriate value of  $[(\alpha/\beta) c_{avaf}^*]$  will be significantly different from the 1,005 kJ/kgK discussed earlier.

Figure 9.3 has been prepared as an aid in selecting appropriate values of  $(\alpha/\gamma)_i$ . The axes has been arranged so that a 'process line' which depends on the air-water flow ratio may be used to characterize the process.

#### 9.1.5 Equivalence with Merkel's method

Inherent in the new method is an equivalence to the Merkel or standard method. The description of thermal performance through Figure 9.1 may be directly compared to the standard method of representing the Merkel approach. The 'equivalence' becomes apparent when the axes in Figure 9.1 are transposed so that the value of the design characteristic,  $N^*$ , is given as the ordinate. This is shown in Figures 9.4, where Figure 9.4.a is simply a repeat of Figure 9.1 and Figure 9.4.b is the transposition.

The 'equivalent' of this for the Merkel method is shown in corresponding Figures 9.5 a and b. (Note, Figure 9.5.b is an exact replica of one of the CTI<sup>(59)</sup> sets

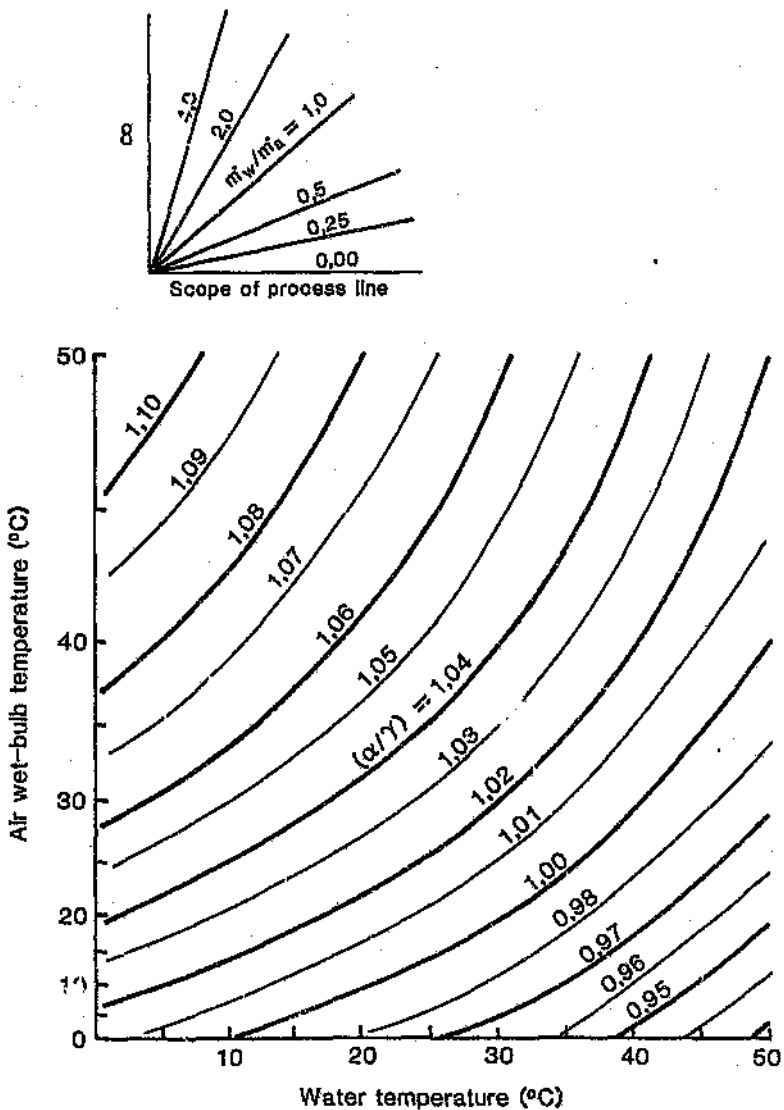


Figure 9.3 Graphical aid to determine value of  $(\alpha/\gamma)$

of curves with the specified 'Approach Temperatures' translated into water efficiencies.)

A comparison of Figures 9.4 and 9.5 illustrates the difference between the new approach and the standard Merkel approach. It must be noted that Figure 9.5 is only applicable for water cooling applications, for a single wet-bulb temperature, a single barometric pressure and a specific cooling range. On the other hand, the single Figure 9.4 (a or b) can be used for all wet-bulb temperatures (0 to 50 °C) for all barometric pressures (80 to 120 kPa), for all water temperatures (0 to 50 °C) and for both water cooling and air cooling applications.

This comparison clearly indicates the versatility of the new method. As a further illustration, note that in essence, the single Figure 9.4 (a or b) can be used to replace the more than 600 pages of curves published in the CTI manual.

#### **9.1.6 Matching design characteristics of direct contact heat exchangers**

There are two complementary issues involved in designing heat exchangers and rating their thermal performance. The first part is the description of the thermal performance in terms of the imposed process conditions and a value of the overall design characteristic. This first part has been the main subject of this thesis (summarized in Figure 9.1). Note however that this does not include a description of the design of the unit itself. The second part is the description of the design features related to the basic geometry and flow considerations which fix the nature and amount of contact surface provided, the relative velocity of the air

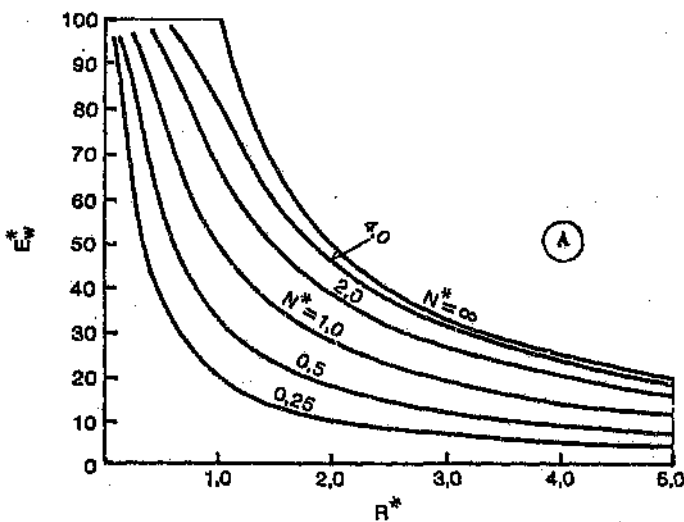
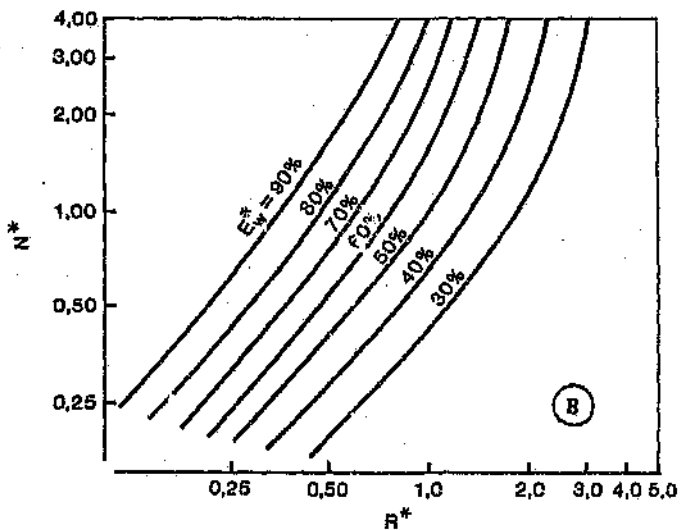


Figure 9.4 Representation of performance equation with axes transposed to show equivalence with CTI curves

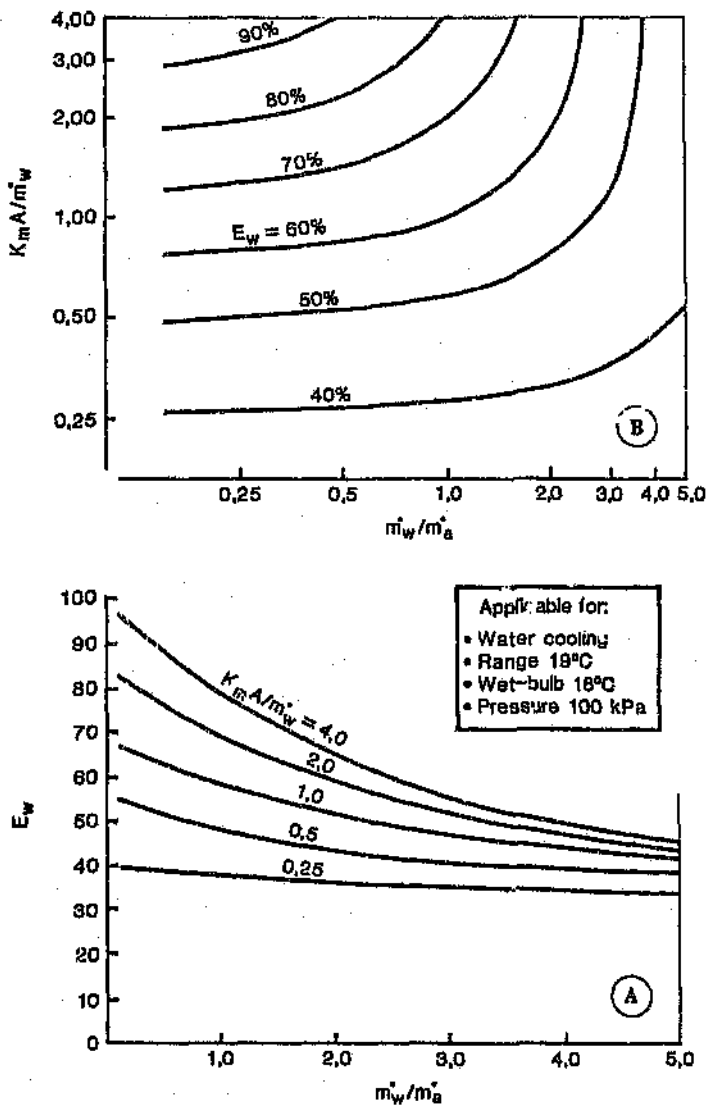


Figure 9.5 Representation of CFI curves with axes transposed to show equivalence with new performance equation

stream to the water surface and the thermodynamic properties of the fluid streams.

Because of the explicit nature of the algebraic solution that has been developed for the overall performance equation, it is now possible to examine how the two parts can be combined.

As discussed earlier, heat transfer and mass transfer data are usually correlated in similar relationships and through this similarity the mass transfer coefficient is described in terms of the heat transfer coefficient. Data on heat transfer coefficients are normally correlated through(96):

$$\text{Nu} = a \text{Re}^b \text{Pr}^z \quad (9.5)$$

Appendix J discusses the interpretation of this relationship for direct contact air-water heat exchangers in detail. In these applications, variations in Prandtl number do not play a significant role and essentially they may be dropped from this relationship. Accounting for this, and including a term for surface area, Equation 9.4 may be expanded to give:

$$\text{Nu.A} = \frac{h_c A d}{k_{\text{avf}}} = a_1 \left[ \frac{\rho_{\text{avo}} V d}{\mu_{\text{avf}}} \right]^b A \quad (9.6)$$

It will have been noted that the film coefficient and the surface area have been combined in a single overall term given as  $h_c A$ . This is because it is impossible to independently determine the value of the surface area

of water drops in the spray above and below the packing. Also, the wetted area of the packing would primarily depend on the packing geometry and, to some extent, the water flow rate. If, for a single geometry, the surface area is related to water flow rate alone (and assuming a rudimentary power function for this relationship) then this allows the equation to be re-written as below. Although this relationship is simplistic, it serves to illustrate the ability of the new equation to include a description of the design features.

$$\text{Nu.A} = \frac{h_c A d}{k_{avf}} = a_2 \left[ \frac{\rho_{avo} V d}{\mu_{avf}} \right]^b m_w^n \quad (9.7)$$

Rearranging this produces:

$$\frac{h_c A}{m_a c_a} = a_2 \left[ \frac{d}{A^*} \right]^{b-1} \frac{c_a k_{avf}}{\mu_{avf}^b} \left[ m_w^n \cdot m_a^m \right] \quad (9.8)$$

Note, the lefthand bracketed term contains both geometric and thermodynamic information and the righthand bracketed term contains the basic flow considerations.

It is normal practice to assume that the lefthand bracket does not vary significantly for most operating conditions (see Appendix J). Hence the following correlation (similar to that examined in Chapter 6) has been investigated:

$$N^* = \frac{h_c A}{m_a c_a} = a_3 m_w^n m_a^m \quad (9.9)$$

Introducing the thermal capacity rate ratio gives;

$$N^* = \phi R^{*n} \quad (9.10)$$

$$\phi = [ a_3 m_1^{m_1} (c_{aw}^*/c_w)^n ] \quad (9.11)$$

Substituting this into the overall performance equation gives :

$$E_w^* = \frac{1 - e^{-\phi R^{*n}} (1 - 1/R^*)}{R^* - e^{-\phi R^{*n}} (1 - 1/R^*)} \quad (9.12)$$

This equation thus allows the overall equation to include a description of the basic design features.

In examining Equation 9.9 further, curve fitting routines have been applied to the data related to the four packing geometries examined earlier. Values of the coefficients are given in Table 9.1.

Table 9.1 Values of coefficients in Equation 9.9 for the packing configurations

		$a_3$	$m_1$	$n$	$R^2$
12 mm Flute	0,6 m ht	0,92	0,29	0,48	0,89
12 mm Flute	1,2 m ht	2,04	0,11	0,40	0,90
19 mm Flute	0,6 m ht	0,95	0,18	0,44	0,93
19 mm Flute	1,2 m ht	1,56	0,19	0,39	0,96

So typically Equation 9.9 may be given as:

$$N^* = \phi R^{0.4} \quad (9.13)$$

$$\phi = [ a; m_a^{0.2} (c_{aw}^*/c_w)^{0.4} ] \quad (9.14)$$

It is likely that a particular configuration of design will display an approximately constant value of the index  $n$  in Equation 9.10. Thus it is possible to rate the thermal performance through a single characteristic,  $\phi$ . It should be noted that the design factor  $\phi$  is not a strong function of the process flow rates. It is independent of water flow rate and will only vary slightly with air flow rate (to the power of about 0,2). The design factor  $\phi$  is slightly dependent on temperature conditions through the pseudo-specific heat term; however this is not a strong function (to the power of about 0,4).

The experimental data for the four different packing configurations is shown plotted in Figure 9.6. It can be seen that the experimental points for each of the individual heat exchanger configurations generally fall on individual single lines. The deviation from the single lines are caused by experimental error, variations in air flow rate and differing temperature conditions. These latter two variations may be explained and accounted for through Equations 9.10 or 9.13.

Thus it is possible to characterise a single unit through a single line on a plot of  $E^*_w$  vs  $R^*$ . The

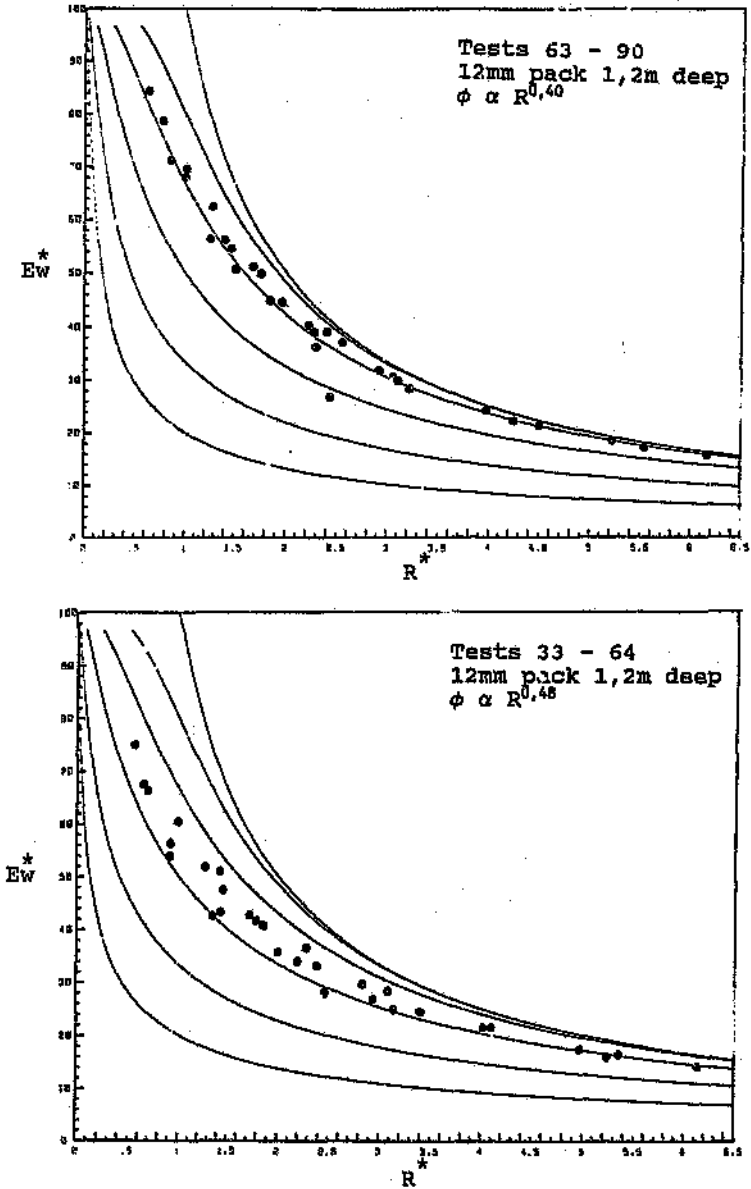


Figure 9.6 Experimental thermal characteristic of each packing geometry

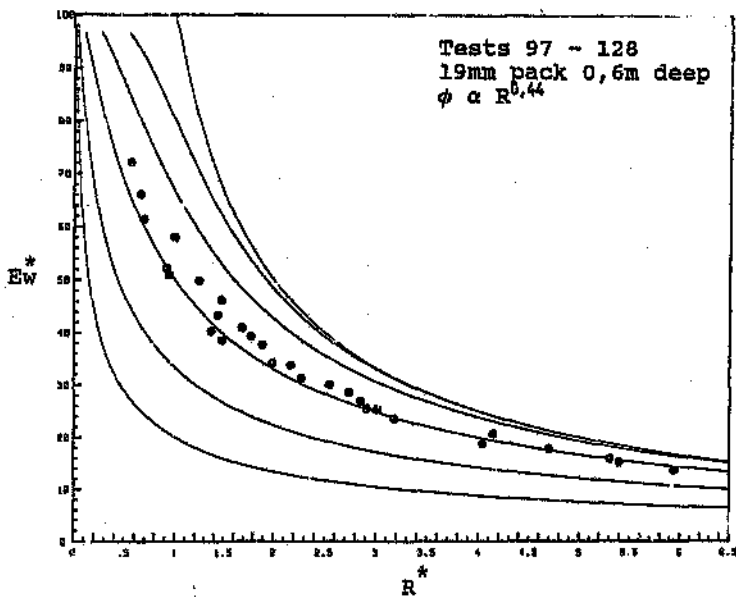
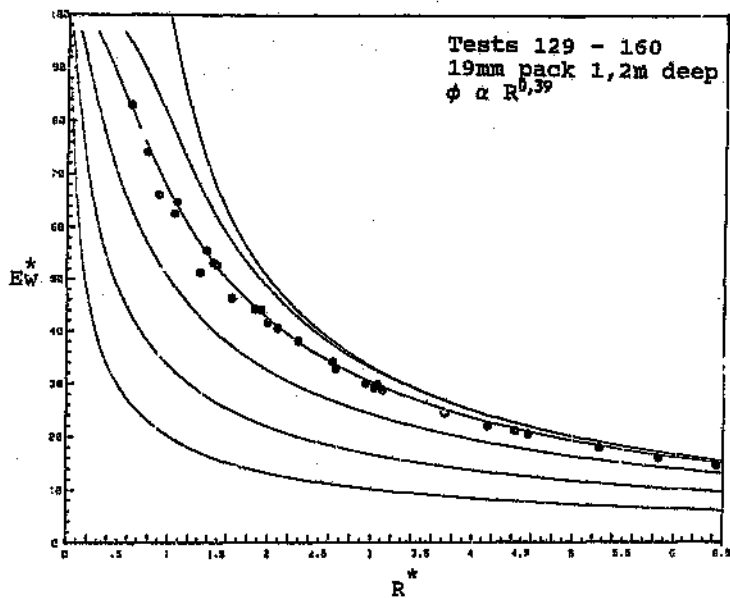


Figure 9.6 (Cont) Experimental thermal characteristic of each packing geometry

position of the line would vary slightly depending on air flow rate and prevailing temperature conditions, but these can be accounted for through Equation 9.10.

#### 9.1.7 Explanation of factor-of-merit method

Historically, the first step in the present sequence of logic was the original development of the so-called factor-of-merit method by Whillier(17,18,19). This approach, although entirely empirical, drew on a number of the fundamental definitions of conventional heat exchanger theory. The method in its original form was used widely in the mining industry and showed a remarkable versatility. However, a number of shortcomings have been revealed in its application and these have led to a number of serious disagreements between mining clients and cooling tower suppliers. The underlying reason is that the form of the performance equation was empirical. There was no algebraic development from heat transfer basics which could lead to a fundamental understanding of the form of the equation and the performance trends that it described. Furthermore, the accuracy was often questioned, particularly when the performance of water cooling and air cooling installations were being compared. An enhanced understanding of this approach and its limitations is now possible.

The essence of the factor-of-merit method is that a single characteristic may be used to describe the thermal performance of a heat exchanger. The characteristic is expressed in the form of a single curve relating effectiveness to a ratio of the thermal capacities of the water and air streams. The method described by Equation 9.1 is significantly different from the factor-of-merit approach in its definition of effectiveness and thermal capacity ratio. However, an analogy may be drawn to the reasoning presented in

Section 9.1.7 and this explains why it has been possible through the factor-of-merit method to roughly describe the thermal performance through a single relationship between effectiveness and a thermal capacity ratio. The inaccuracy in the factor-of-merit method stemmed from the simplistic definitions of effectiveness and thermal capacity ratio (which have now been refined). Furthermore, deviations from a single curve are to be expected for different temperature conditions and widely differing air flow ratios (as explained through Equation 9.10).

#### 9.1.8 Further research related to the overall performance equation

The method developed in this thesis is versatile, simple and directly analogous to conventional heat exchanger theory. It thus has the potential to become a widely accepted analysis tool. However, in order to facilitate this, it is anticipated that further work is required with respect to describing the design characteristics of various items of equipment along the lines given by Equation 9.8. The arguments, in terms of correlation, presented in Section 9.1.6 are simplistic and there is considerable scope for the development of a more sophisticated and fundamentally sound method of correlation of the mechanical design information. There are important improvements that can be made in this area.

#### 9.2 Additional specific conclusions

In addition to the overall performance equation, there are some interesting points which emerge as specific conclusions of this work.

### 9.2.1 Heat transfer at a wet surface

Merkel<sup>(12)</sup> developed a simplified equation to describe the total heat transfer from a wet surface in which the driving force is given by the difference between the enthalpy of saturated air at the wet-bulb temperature and the enthalpy of the film of saturated air at the wet surface temperature. This driving force has become known as the enthalpy potential and has been widely utilized for estimating heat flow from wet surfaces. Its use, however, involves a total of seven sequential approximations each of which individually may have errors of up to 10 per cent. The overall inaccuracy has been determined on a statistical basis for a total of more than 10 000 sets of conditions. The statistic distribution of these inaccuracies is presented in Figure 9.7.a (repeat of Figure 6.9). Note that the errors are not small and that the approximate values deviate significantly from the accurate value.

An improved simplified equation using sigma energy differences has been developed. This is given as:

$$\frac{h}{c_{p,air}} = \beta \left( \frac{h_o}{c_{p,air}} \right) [ \Sigma_w - \Sigma_a ] \quad (9.15)$$

The statistical distribution of the inaccuracy in this simplified equation with  $\beta = 1,1$ , is given in Figure 9.7.b (repeat of Figure 7.4).

Clearly, the accuracy of this new simplification is considerably better than that of the Merkel equation. Equation 9.14 should be considered as a statement of a much improved approximation for the total heat flow from a wet surface (in the absence of radiation).

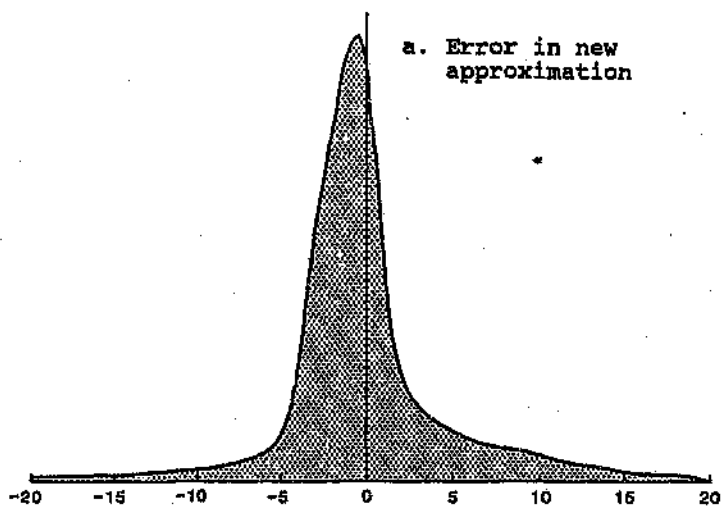
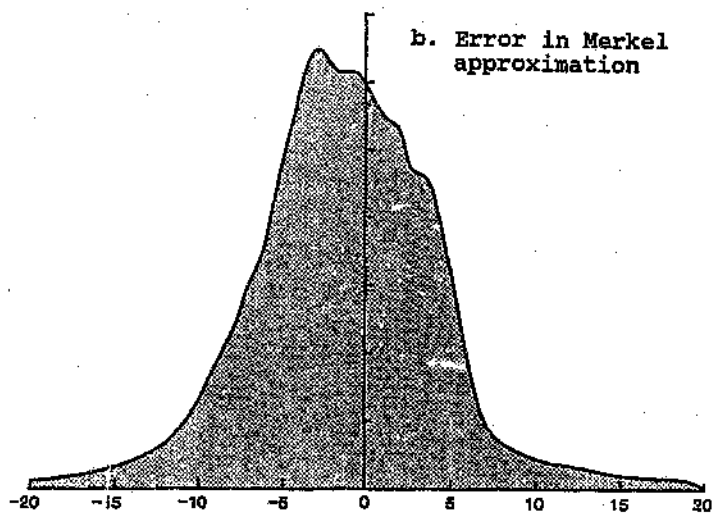


Figure 9.7 Errors in approximate equations for heat transfer from wet surface

### 9.2.2 Comparison of procedures for determining mass transfer

A study of the literature uncovered a surprising number of different approaches to quantifying mass transfer. Hence, this subject has been discussed in detail and a comparison made of the different published methods. The differences in the answers given are surprisingly high and can be as much as 16 per cent for the range of conditions under consideration. For higher temperatures, this difference can be even greater. This reflects poorly on the state of the art of convective mass transfer for the most common water-in-air evaporation and condensation processes.

### 9.2.3 Effect of radiation in direct contact heat exchangers

Arguments have been presented to justify neglecting the radiative heat transfer component in direct-contact heat exchangers. This component has been quantified by comparing it to the convective heat transfer. A wide variation in heat exchanger geometry was considered and it was shown that the ratio of the radiative component to the convective heat flow component will always be less than three per cent but normally of the order of 0,5 per cent. Note that the convective heat component itself is small, when compared to the total heat transfer.

### 9.2.4 Values of transport properties of water vapour - air mixtures

The thesis contains a comprehensive compilation of all the thermodynamic properties and equations related to the interaction of the air and water streams within

direct-contact heat exchangers. A considerable discussion has been presented with regard to a number of these parameters and in particular the diffusion coefficient for water vapour in air. A compilation of this nature is not readily available in any other single text.

#### 9.2.5 Heat and mass transfer analogy and value of the index, $z$

The literature indicates that the value of the index  $z$  in the heat and mass transfer analogy relationship [given by  $(Pr/Sc)^z$ ] depends on the geometry and flow situation. No single value of  $z$  is always correct (67).

Based on the present set of data, the opportunity existed to examine this issue from a fresh point of view, since the data contained information on both heat transfer measurements and mass transfer measurements. The value of  $z$  was calculated for each test and the subsequent statistical analysis indicated that the appropriate value of  $z$  is not significantly different from the value of 0,67. It was concluded that the value of  $z$  is not affected by the direction of mass transfer. Neither is it affected by the change in packing configuration. There was also no evidence that changes in Reynolds number, water flow or air velocity affected its value.

#### 9.2.6 Supersaturation of the air stream

The modelling of the supersaturation phenomena relies on the following assumptions:

- . Fog appears instantly with supersaturation.
- . Transfer coefficients remain unchanged with fogging.
- . Moist air and fog exist as a homogeneous mixture.
- . Fog droplets pass through heat exchanger packing together with the air stream but are captured in the demister.

Based on the above, the model was found to accurately predict the mass transfer rate for the tests in which fogging occurred. These were mostly the water cooling (evaporation) application. Where substantial supersaturation did occur, the fogged flow was typically about five per cent, but in some instances it was as high as nine per cent of the total mass transfer.

#### 9.2.7 Comparison of transfer coefficients for evaporation and condensation tests

The experimental programme was structured so that, for the same flow and geometry conditions, equivalent tests were done for cold water/hot air conditions and hot water/cold air conditions. This allowed the effects of these changes in temperature conditions and direction of mass transfer to be examined directly and in isolation to the flow and geometry variables. Comparisons were made by examining the ratio of the measured Nusselt numbers. This ratio was generally greater than unity and on an average basis the value of  $Nu_{\text{cold water}}$  was 7 per cent greater than  $Nu_{\text{hot water}}$ .

The values of the ratio  $Nu_{\text{cold/hot}}$  covered a wide range from 0,88 to 1,49; and this is probably an indication of the limitations of the simple heat and mass transfer analogy employed and of the basic logarithmic correction term used to account for the effect of mass transfer on the transfer coefficient.

Two further areas of research outside the scope of the present study are suggested. The first is an examination of the heat and mass transfer analogy and the correction term, on the basic premise that  $Nu_{\text{cold/hot}}$  should equal unity. The second is a study of the effect of water viscosity and surface tension on the formation of wet surface areas in packed towers.

#### 9.2.8 Comprehensive theoretical (computer) model

This research has included the development of a comprehensive computer model for the simulation of counter-flow direct-contact air-water heat exchangers. The program is successful in its ability to model real heat exchangers, and apart from heat and mass transfer criteria, takes account of the supersaturation or fogging of the air stream. The verified computer simulator can be considered as an independent product of this research and has the potential of being useful to other researchers in this field.

#### 9.2.9 Unique experimental database

Included in this research has been the generation of a unique experimental database on the performance of a suite of direct-contact heat exchangers. This information is unique in that identical situations were tested for evaporation and condensation conditions. The experimental error and the uncertainty in the results have been carefully quantified. This data also has the potential of being useful to other researchers in this field.

### 9.3 Concluding statement

Although, in recent times, the development of accurate computer models for direct-contact heat exchangers are gaining wider use, it must be noted that most of these developments are either related to research or are of a propriety nature and are held by a number of manufacturers. The end users or general field engineers do not have the specialist knowledge nor can they be expected to devote time to developing computer models. However, there is a great need to speak a common language.

The explicit performance equation developed here has the potential to achieve this since all that is required is a familiarity with normal heat exchanger conventions. The performance equation has a sound fundamental basis and has the potential to gain general acceptance. It has been examined against approximately 650 experimental and simulated sets of process conditions covering a wide range of conditions with both water cooling and air cooling applications and appears to be accurate and versatile.

In order to gain wide acceptance future verification is needed in engineering practice and further work is required with respect to describing the design characteristics of wide range of direct-contact heat exchangers.

## APPENDIX A      Equations used to evaluate the thermodynamic properties of moist air

### 1      Psychrometric properties

A knowledge of the various psychrometric properties of moist air is required in the modelling of thermal performance of water-air heat exchangers. Some of the psychrometric parameters are basic physical properties of air or water vapour and have been determined by measurement or by the application of fundamental procedures. Other psychrometric properties are evaluated from these basic parameters through the gas equation of state. Goff and Gratch's(40,41) work on calculating and tabulating accurate thermodynamic properties of moist air is generally considered the most accurate information available(10,21,29). However, the simplest approach is based on the ideal gas equation, Dalton's Law of partial pressures and the adiabatic saturation (or the thermodynamic wet-bulb) process. This is the approach followed in this thesis. Goff(41) stated that 'Dalton's Law must be regarded as an inaccurate conjecture based upon an unwarranted faith in the ultimate simplicity of nature'. While in principle his is probably true, in reality the numerical results obtained from the simple approach are not significantly different from those attained using the virial equation of state and other more accurate relationships. To illustrate this, consider the enthalpy of saturated air over the range of conditions being examined - the maximum error incurred in using the simple approach is less than 0,5 per cent (this is discussed in more detail later).

It would appear, then, that the simple approach is acceptable; however, perhaps a more important reason for its use is the need to be consistent with past work on cooling towers and be able to make direct comparisons with existing experimental correlations.

Equations to evaluate the various parameters are listed below. Most of this information is available in standard texts(10,21,29,42).

### 1.1 Water vapour pressure

The water vapour pressure of saturated air is a function of temperature only and may be described by a number of equations of varying complexity and accuracy(43,44). The relatively simple empirical equation(42,45) used here predicts the saturated vapour pressure to within 0,1 per cent of the tabulated values of Goff and Gratch(40, 41).

$$P_{vs} = 0,6105 e^{(17,27 t / (237,3 + t))} \quad (\text{kPa}) \quad (\text{A.1})$$

A consideration of the energy balance in the classical adiabatic saturation process (which defines the thermodynamic wet-bulb temperature) allows the actual water vapour pressure to be expressed in terms of the saturated vapour pressure, wet-bulb temperature, dry-bulb temperature and total pressure as :

$$P_v = \frac{P_{vs} (1555,6 - 2,465 t_{wb} + 1,005 t_{db}) - p \times 1,005 (t_{db} - t_{wb})}{1555,6 + 0,139 t_{db} - 1,599 t_{wb} - 0,14 (P_{vs} / p) (t_{db} - t_{wb})} \quad (\text{A.2})$$

The development of this relationship uses the equations for the enthalpy of water vapour, air and water given later. The saturated vapour pressure in Equation A.2 is calculated at the wet-bulb temperature.

## 1.2 Moisture content

The moisture content of the air may be evaluated from a knowledge of the water vapour pressure and the perfect gas laws. Two definitions of moisture content are applicable: first, the mass of water vapour per unit mass of air-water vapour mixture (the true specific humidity,  $W_v$ ) and, second, the mass of water vapour per unit mass of dry air (the apparent specific humidity,  $W$ ) (42).

$$W_v = 0,622 p_v / ( p - 0,378 p_v ) \quad (\text{kg/kg}) \quad (\text{A.3})$$

$$W = 0,622 p_v / ( P - p_v ) \quad (\text{kg/kg}) \quad (\text{A.4})$$

## 1.3 Density

Three definitions of density are relevant. First, the true density of air-water vapour mixtures, which is the mass of air-water vapour mixture per unit volume. Following Dalton's Law and the perfect gas relationship the true density is given as<sup>(42)</sup>:

$$\rho_{av} = \frac{( P - 0,378 p_v )}{( 0,287 ( 273,2 + t_{db} ) )} \quad (\text{kg/m}^3) \quad (\text{A.5})$$

Second, the density of the pure air, which is the mass of dry air per unit volume:

$$\rho_a = \frac{(p - p_v)}{(0,287 (273,2 + t_{db}))} \quad (\text{kg/m}^3) \quad (\text{A.6})$$

Third, the density of the pure water vapour, which is the mass of water vapour per unit volume:

$$\rho_v = \frac{p_v}{(0,461 (273,2 + t_{db}))} \quad (\text{kg/m}^3) \quad (\text{A.7})$$

#### 1.4 Enthalpy of water vapour

The enthalpy of water vapour can be obtained from standard tables(28). The water vapour in the air-water vapour mixture is in most cases in a superheated condition. However, it is fortunate, from the point of view of simplicity, that the enthalpy of water vapour is not strongly dependent on the degree of superheat and may be described with sufficient accuracy as a single function of temperature (see Figure A.1). This observation substantiates the assumption that water vapour behaves as a perfect gas. The enthalpy of water vapour may then be given as:

$$i_g = (2501 + 1,84 t) \times 10^3 \quad (\text{J/kg}) \quad (\text{A.8})$$

This equation is shown plotted with enthalpy(28) information for both saturated and superheated water vapour in Figure A.1. In studying this figure, note that, for the range of conditions being considered, the

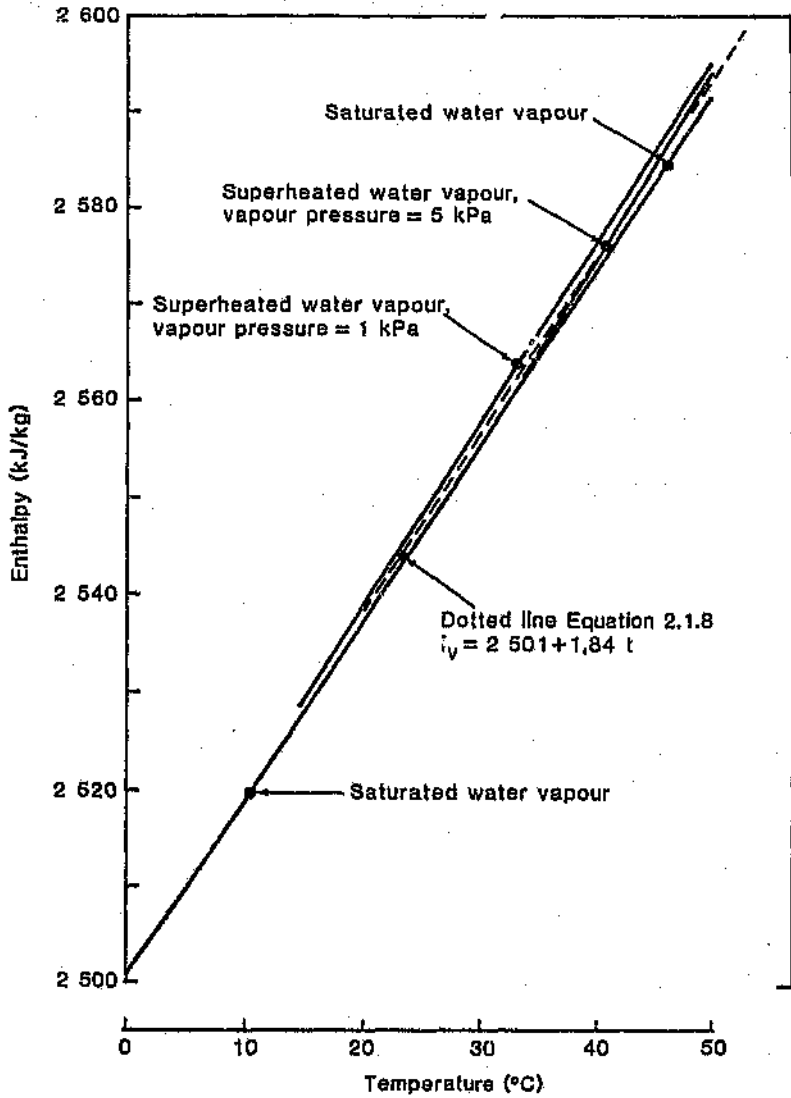


Figure A.1 Enthalpy of water vapour as a function of temperature

water vapour pressure has a minimum value of zero, a maximum value of 12 kPa and a typical value of 2 to 4 kPa.

The maximum error in using Equation A.8 would occur at 50 °C and would be between plus 1,5 and minus 2,0 kJ/kg depending on the degree of saturation. However Equation A.8 (fitted by the author) is considered an improvement over the equations suggested in many texts (10,11,21,29) which are fitted to the saturation conditions only.

The linearity of Equation A.8 infers a constant value of the thermal capacity or specific heat at constant pressure of water vapour. This is given as:

$$d i_g / dt = 1840 \quad (\text{J/kg K}) \quad (\text{A.9})$$

### 1.5 Thermal capacity or specific heat of air-water vapour mixtures

The thermal capacity or specific heat at constant pressure of pure air may be considered to be constant and have a value of 1005 J/kg K (this value changes by less than 0,1 per cent (28) over the range of conditions being considered). The thermal capacity of water vapour was discussed above and may be considered to have a constant value of 1840 J/kg K.

The thermal capacity of air-water vapour mixtures depends on the moisture content. The thermal capacity of moist air is usually quoted per unit mass of dry air (42). This is done for the convenience of calculation techniques used in normal air conditioning

work. However in itself, this definition is meaningless since it describes the thermal capacity of a gas per unit mass of another gas. A specific heat term defined in this manner would be incorrect when applied, for instance, in the empirical correlation equations (e.g. Equation 2.7) discussed in the text. It is important in this present work to make this differentiation, the reasons for which become evident in Chapter 6.

Thus, two different specific heat terms for moist air are applicable. First, the thermal capacity of air-water vapour mixtures per unit mass of dry air.

$$c_{\text{ava}} = 1005 + 1840 W \quad (\text{J/kg K}) \quad (\text{A.10})$$

Second, the true thermal capacity of moist air per unit mass of moist air.

$$c_{\text{av}} = c_{\text{ava}} (\rho_a / \rho_{\text{av}}) \quad (\text{J/kg K}) \quad (\text{A.11})$$

$$c_{\text{av}} = c_{\text{ava}} \left[ (p - p_v) / (p - 0,378 p_v) \right]$$

## 1.6 Enthalpy of air-water vapour mixtures

Following Dalton's Law, the enthalpy of an air-water vapour mixture is the sum of the enthalpies of the dry air and the water vapour. In the application used in this study, as is usually the case, the enthalpy is expressed per unit mass of dry air. This is given as:

$$i_a = 1005 t_{\text{db}} + W ( 2501 + 1,84 t_{\text{db}} ) \times 10^3 (\text{J/kg}) \quad (\text{A.12})$$

A number of sample calculations over the range of conditions being considered indicates that the difference in calculating the enthalpy through Equation A.12 and the more accurate routine advocated by Goff and Gratch(40,41) is less than 0,5 per cent.

### 1.7 Sigma heat content

The use of the concept of sigma heat content is of considerable value to the hypothesis presented in this thesis. The sigma heat content is expressed per unit mass of dry air and is defined as the enthalpy of the moist air minus the enthalpy of the water vapour content, calculated as if the water vapour was present as liquid water at the wet-bulb temperature. The concept of sigma heat content arises out of a consideration of the adiabatic saturation process, during which the sigma heat content of the moist air remains exactly constant (the enthalpy remains only approximately constant). This is discussed in detail in Chapter 7.

The thermal capacity of liquid water may be considered to have a constant value of 4187 J/kgK; this value changes by less than 0,5 per cent(28) over the range of temperatures being considered.

The sigma heat content of moist air per unit mass of dry air is given as:

$$\Sigma = i_a - 4187 t_{wb} \quad \text{(J/kg)} \quad \text{(A.13)}$$

Sigma heat content is a unique function of wet-bulb temperature (at any given barometric pressure). Although this is not clearly apparent from studying Equation A.13, it is in fact mathematically exact.

## 1.8 Latent heat of vapourization

The value of the latent heat of evaporation or condensation of water vapour can be found in standard<sup>(28)</sup> texts. The latent heat varies slightly with temperature and may be calculated from<sup>(42)</sup>:

$$\lambda = (2501 - 2,387 t) \times 10^3 \quad (\text{J/kg}) \quad (\text{A.14})$$

The value of the latent heat should be assessed at the surface temperature at which the evaporation or condensation takes place<sup>(46)</sup>.

## 2 Transport properties

A pre-requisite for calculating the total heat transfer from a wet surface into an air stream is a knowledge of the value of the transport properties of air-water vapour mixtures at different temperatures and water vapour content. Since empirical equations are used, the properties must be calculated on the same basis that led to the original correlation. All the correlation equations considered here make use of an average temperature condition (i.e. the average of the surface temperature and the bulk air stream temperature; this is referred to as the 'film' temperature). Furthermore, the air-water vapour mixture at this intermediate condition is considered to be saturated<sup>(25)</sup>.

### 2.1 Thermal conductivity

The kinetic theory of gases predicts that unless the pressures are extremely low, the thermal conductivity

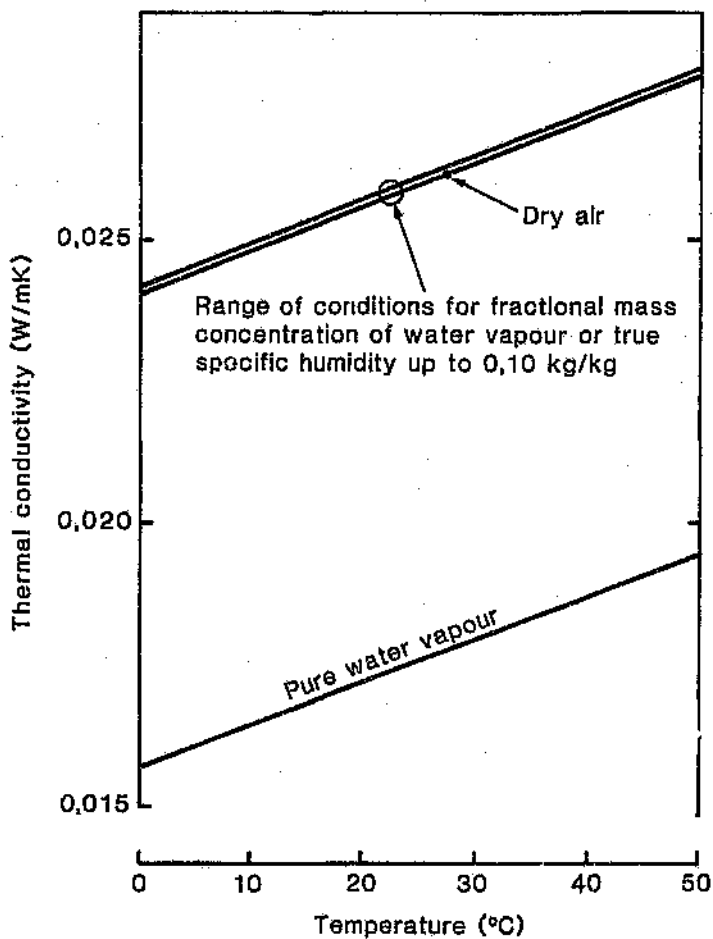


Figure A.2 Thermal conductivity of air-water vapour mixtures

of gases would not be affected by pressure changes(10,27,28). In reality, for the pressures under present consideration, the thermal conductivity of air increases by about one per cent per 100 kPa pressure change(26, 33). Thus, the variations in pressure from 80 to 120 kPa are expected to cause a change of less than 0,5 per cent in the thermal conductivity. This is regarded as insignificant and the thermal conductivity of the moisture is considered to be independent of pressure.

The variation of the thermal conductivity with temperature for both air and pure water vapour can be found in a number of standard texts(10,28,35). These trends are found plotted in Figure A.2 where it can be seen that the thermal conductivity varies in an approximately linear fashion with temperature.

The values for dry air are considerably higher than those for water vapour and one would expect some dependence on the composition of the mixture for moist air. However, the conductivity of the mixture is not linear with composition(35) and for the range of conditions presently being considered, where the maximum value of the mass fraction of water vapour is 0,10 (50 °C saturated air at 80 kPa), the thermal conductivity of moist air varies negligibly from that of dry air. Mason and Monchick(34,35) present data on the thermal conductivity of air-water vapour mixtures which is generally considered the most accurate available (used by ASHRAE and the US National Bureau of Standards). A curve fitting exercise based on this information has produced the following equation, which predicts the data to an accuracy of better than 0,5 per cent for the range of conditions being considered.

$$k = (2405 + 7,788 t) \times 10^{-5} \quad (\text{W/m K}) \quad (\text{A.15})$$

## 2.2 Dynamic viscosity

Again, as in the case of thermal conductivity, the kinetic theory of gases predicts that the viscosity would be independent of pressure. (Jacob<sup>(39)</sup> states that when this result was confirmed by experiments it became one of the strongest supports of the kinetic theory). In reality, it is generally accepted that for the range of pressures being considered, the viscosity is independent of pressure changes<sup>(28)</sup>. Ferry and Chilton<sup>(26)</sup> state that changes in viscosity with pressure are only significant for pressures exceeding 1000 kPa. The viscosity is thus not considered to be a function of pressure.

The variation of the viscosity with temperature for both air and pure water vapour can be found in a number of standard texts<sup>(10,28,35)</sup>. These trends are shown plotted in Figure A.3 where it can be seen that the viscosity varies almost linearly with temperature. The values of viscosity for dry air are considerably higher than those for water vapour and the viscosity of moist air has a dependence on composition. Mason and Monchick<sup>(35)</sup> present quasi-empirical data (they made empirical adjustments to the theoretical equations) for the full range of air-water vapour mixtures. A curve fitting exercise based on this information has produced the following equation, which predicts their data to an accuracy of better than 0.4 per cent for the range of conditions being considered.

$$\mu = K_4 + K_5 t \quad (\text{Ns/m}^2) \quad (\text{A.16})$$

where

$$K_4 = (1,722 - 0,387 W_v) \times 10^{-5}$$

$$K_5 = (4,736 - 1,481 W_v) \times 10^{-8}$$

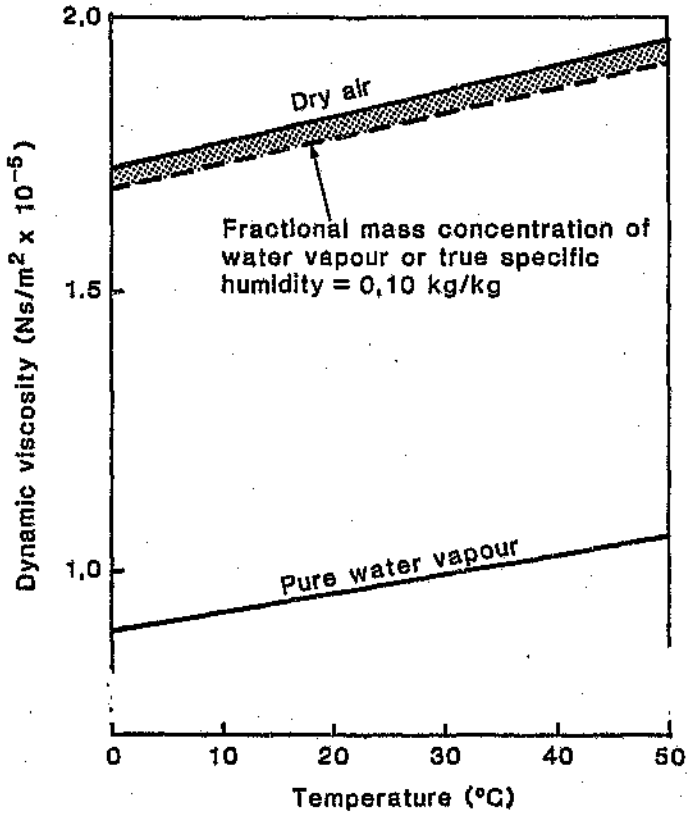


Figure A.3 Viscosity of air-water vapour mixtures

For the range of conditions presently under consideration the maximum value of the true specific humidity or the mass fraction of water vapour is 0,10 (50 °C saturated air at 80 kPa) and for this condition the viscosity does not vary by more than 2,5 per cent from that of dry air. However, Equation A.16 is used throughout this study to calculate the viscosity of moist air.

### 2.3 Diffusion coefficient of water vapour in air

Mason and Monchick(34,35) examined a considerable amount of experimental data and made empirical adjustments to the theoretical constants in the virial equation of state of real gases. They then recalculated the diffusion coefficient value and tabulated this information for temperatures up to 300 °C pressure of one atmosphere. These values are recommended by the US Bureau of Standards(35) and ASHRAE(10). Assuming the well accepted inverse relationship with pressure the following equation has been fitted (by the author) to this data and is used in this study:

$$D = 1,676 \times 10^{-7} T^{1,094} / p \quad (\text{m}^2/\text{s}) \quad (\text{A.17})$$